UNIVERSITAT DE BARCELONA

The Identification and the Functional Validation of Eye Development and Regeneration Genes in *Schmidtea Mediterranea*

Beatriz Calvo Lozano

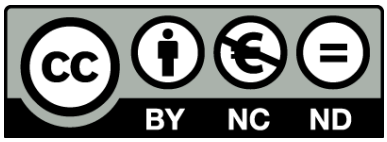

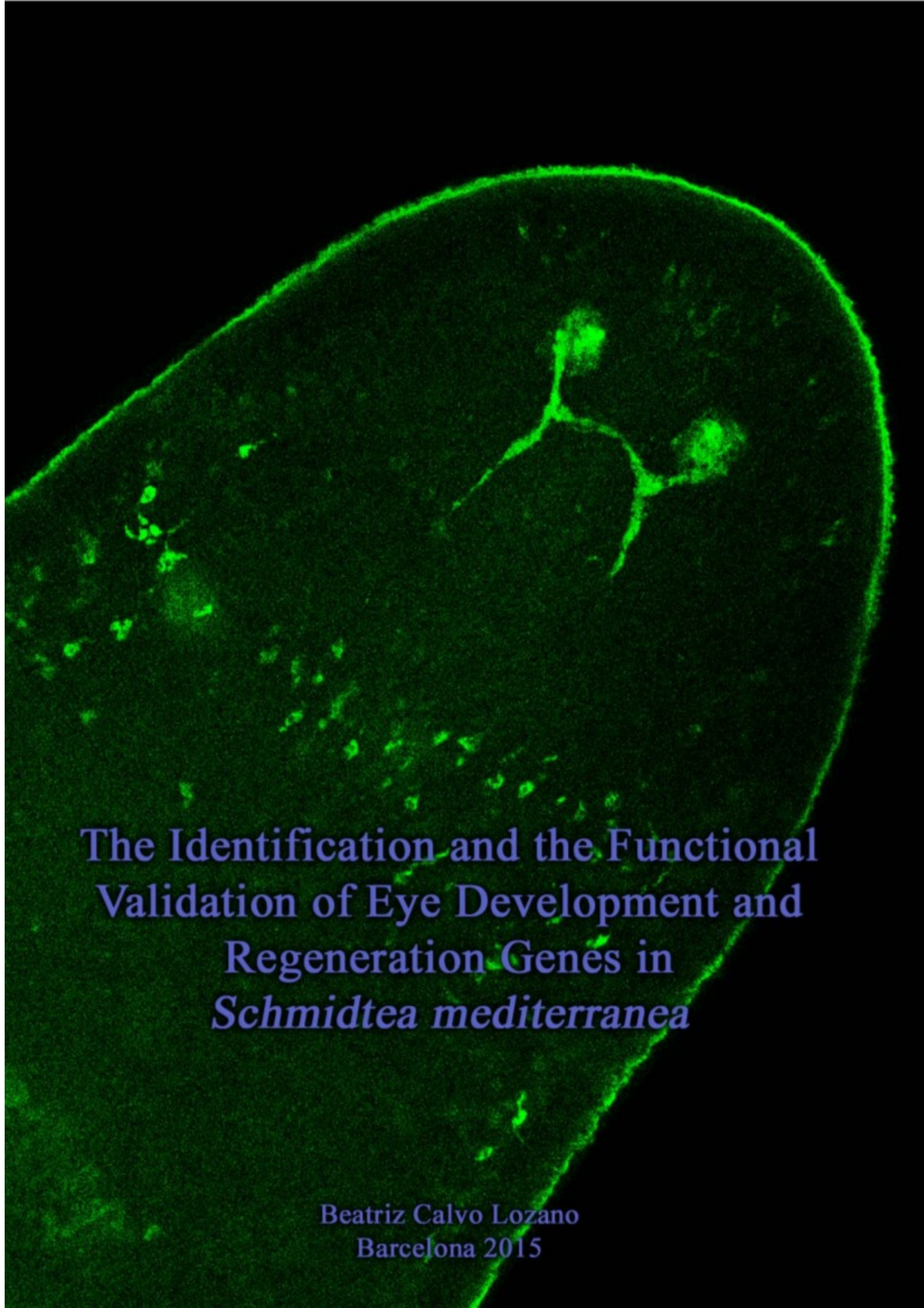

The Identification and the Functional Validation of Eye Development and Regeneration Genes in *Schmidtea mediterranea*

Beatriz Calvo Lozano

Barcelona 2015

Universitat de Barcelona
Biology Faculty - Genetic Department

GENETIC DEPARTMENT
GENETIC DOCTORAL PROGRAMME
BIOLOGY FACULTY
"UNIVERSITAT DE BARCELONA"
2009-2012

The Identification and the Functional Validation of Eye Development and Regeneration Genes in *Schmidtea mediterranea*

A thesis
submitted in partial fulfilment of the requirements of the degree
of
Doctor by the "Universitat de Barcelona"
by
Beatriz Calvo Lozano

Supervisor and Tutor

Prof. Emili Saló i Boix

Author

Beatriz Calvo Lozano

Barcelona, May 2015

I. Contents

IV. ABBREVIATIONS

AMD	age-related macular degeneration
BR	bacteriorhodopsin
cg	cerebral ganglion
CNS	central nervous system
d	days of regeneration
DHICA	5,6-dihydroxyindole-2-carboxylic acid
DiD	DiIC18(5)
DiI	1,1'-dioctadecyl-3,3,3'3'-tetramethylindocarbocyanine perchlorate
Dj	*Dugesia japonica*
EM	electron microscopy
ESTs	espressed sequence tags
FAD	flavin adenin dinucleotide
Fig.	figure
fr.2	second fragment of the same sequence
GPCR	G protein-coupled receptor
GST	Glutathione S-transferase
HR	halorhodopsin
IDO	indoleamine 2,3-dioxygenase
MTHF	5,10-methenyltetrahydrofolic acid
n	penetrance
NPC	nuclear pore complex
pc	pigment cells
r	rounds of injection
RA	Retinoic acid
RPE	retinal pigment epithelium
RGR	retinal pigment epithelium (RPE) G protein-coupled receptor
Smed	*Schmidtea mediterranea*
UB	University of Barcelona
1/10	one animal out of ten injected
7TM	7 transmembrane receptor
vs	versus
W/m^2	watts per square metre

1. INTRODUCTION

1.1 THE EYES OF *SCHMIDTEA MEDITERRANEA*

The nervous system is a precise and complex structure that enables living beings to carry out a variety of functions (de Castro et al., 2007). One of them, eyesight, provides an excellent model system for studies of patterning and cell fate determination within the central nervous system (CNS) (Cepko et al., 1996). The vertebrate eye comprises tissues originating from several embryonic lineages, including neuroectoderm, ectoderm, neural crest, and mesoderm. The coordinated development of these multiple tissue types is governed by intercellular interactions, which makes the eye an excellent model to study morphogenesis and inductive events during CNS development (Ha et al., 2012).

The relevance of the planarian eye as an invertebrate model to vertebrate systems is based on the homology found in molecular genetic studies between the photoreceptor neurons (rhabdomeric and ciliary) (Arendt, 2003), the conserved opsin signal transduction pathways (Gehring, 2012) and the common genes involved in eye development: *Sine oculis, Ovo, Pbx, Pax 6* and *Otx* (Pineda et al., 2000; Pineda et al., 2002; Lapan et al., 2012). Planarians are one of the simplest bilateral organisms that possess integrated neural networks similar to those of vertebrates (Cebriá et al., 2002a; Okamoto et al., 2005; Cowles et al., 2013). In addition, understanding the regenerative repair of eye damage, wich occurs naturally in these organisms, might help improve medical applications for retinal regeneration and also for the regeneration of other nerve tissues. Induced pluripotent stem cells (iPSCs) were differentiated into retinal cells by introducing the growth factors *oct3/4, sox2, c-myc* and *klf4,* in mouse embryo and adult fibroblasts (Takahashi et al., 2006; Hirami et al., 2009; Eiraku et al., 2011). Notably, mouse retinal neurons were transiently reprogrammed in vivo, modifying bone marrow stem cells (activating Wnt/β-catenin signalling) and fusing them with the damaged retina (Sanges et al., 2013). All this together makes *S. mediterranea* an appropriate and powerful model for studies of development, regeneration and stem cell biology.

1.2 Structure and function of planarian eyes

Planarians are free-living unsegmented and soft-bodied invertebrate flatworms that belong to the phylum Plathelminthes. Some of them, such as *Schmidtea mediterranea,* the subject of this study (Fig. 1.1, A), are able to regenerate any body part, such as entire eyes and replenish eye tissue throughout adulthood after an injury or fissioning (the anterior and posterior portions of the planarian separate at the post-pharyngeal region of the body) (Saló, 2006).

Biochemical electron microscopy and ocellar potential (OP) analysis of *S. mediterranea* has not previously been published and therefore many of its characteristics are based on experiments performed in other species. For example, light and electron microscopy studies of turbelarian eyes have revealed remarkable variation among species (Orii et al., 1998). *Polycelis* and *Pseudostomum quadriculatum* have multiple eyes, each of which is composed of a single photoreceptor cell. *Dugesia,* in contrast, has two pigment-cup ocelli composed of many photoreceptor and pigmented cells. Meanwhile, some taxa, such as *Otoplana intermedia,* have “Sehkolben”: eyes lacking pigment granules (Sopott-Ehlers, 1991). Light-sensitive organelles are usually microvilli but can also be cilia or a combination of microvilli and cilia, as in the polyclad larvae *Pseudoceros canadensis*, *Thysanozoon brocchi* and *Stylochus mediterraneus*. Furthermore, in *Convoluta*, *Polystoma intergerrimum* and *Nerilla antennata*, vacuole filled with platelets in the pigment cells serve as lenses (Sopott-Ehlers, 1991). Although each of these invertebrates has a central bilateral symmetric nervous system with a brain ganglia at the head end, they can be slightly different from species to species in terms of morphology, size and cell number (Cebriá, 2007).

In *S. mediterranea,* two nerve cords extend from the brain ventrally along the length of the body, with numerous smaller nerves branching off. A pair of dorsal eyes innervate the dorsomedial area of the brain (Fig. 1.1 C, G) (Okamoto et al., 2005; Saló, 2006; Cebriá, 2007). Several experiments including immunostaining, in situ hybridization carried out in *S. mediterranea* and electron micrographs, mainly performed in *Dugesia ryukyuensis* and *Dugesia japonica*, have revealed that the planarian eyes are formed by rabdomeric photoreceptor neurons enclosed by a cup-shaped cavity: the pigment cells (Fig. 1.1, 1.2) (Kishida, 1967; Sakai et al., 2000).

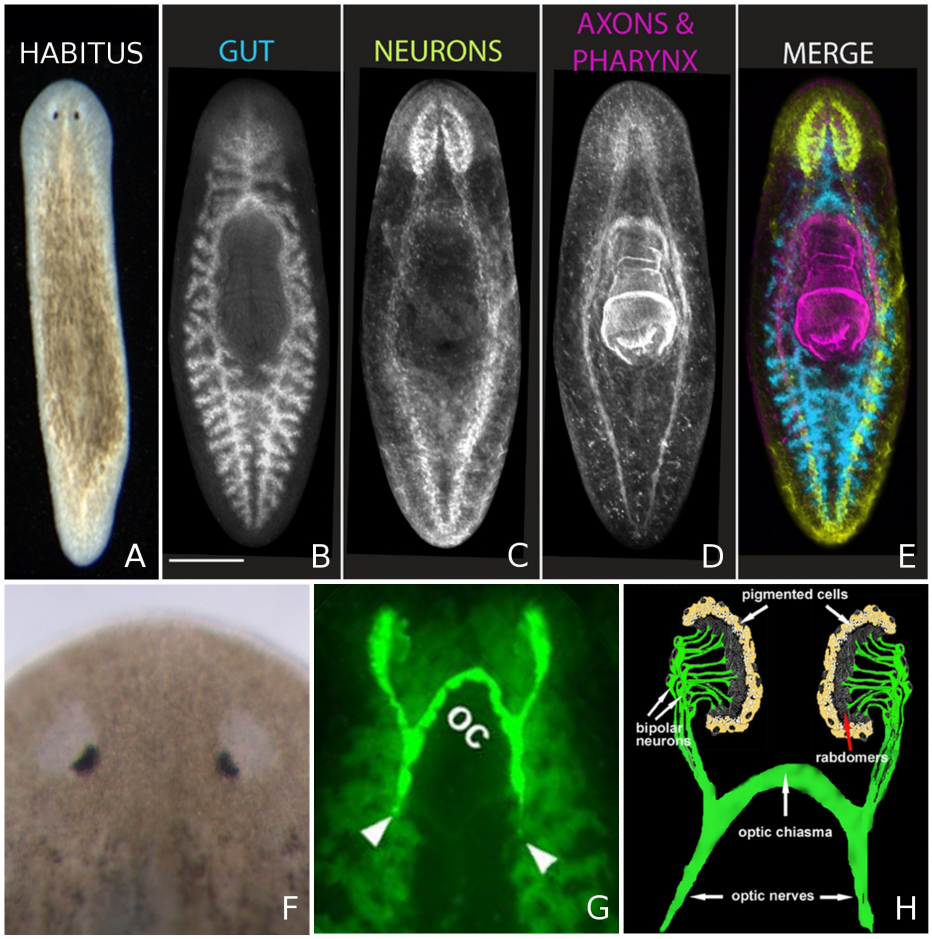

Figure 1.1 Immunostaining of internal anatomy and eyes of *S. mediterranea*. (A) *S. mediterranea* habitus. **(B)** Gut labelled with *Smed-porcn-1*. **(C)** Neurons labelled with *Smed-PC-2*. **(D)** Axons and pharynx labelled with anti-α- tubulin antibody). **(E)** Overlay of gut (blue), neurons (yellow), axons, and pharynx (magenta). **(F)** Eye: enlarged view. The black dots are the pigment cups, the hypopigmented skin surrounding the cups are the periglobular areas. **(G)** Double whole-mount immunostaining with an anti-phosphotyrosine antibody (light green) and the monoclonal antibody anti-arrestin (VC-1) that labels the cephalic ganglia and the visual axon projections, respectively. Connection points between cephalic ganglia and photoreceptors (white arrows) (oc: optic chiasm) **(H)** Schematic representation of the eye showing pigmented cells, bipolar neurons, optic chiasm and optic nerves. Scale bar: (B-E) 200 µm; A as in B. (Source (G) Cebriá, 2007; (B-E) Alvarado, 2012).

As in *Dugesia japonica*, the photoreceptors in *S. mediterranea* are probably of a microvilliar type (Tamamaki, 1990). However, the presence of cyclic nucleotide-gated (CNG) ion channels in the planarian genome raises the possibility of ciliary phototransduction (Zamanian et al., 2011). The photoreceptors consist of some 25 bipolar neurons: each contains a cell body, whose dentrites, called rhabdomere, are of microvilli, and long axons that project into the dorso-medial region of the brain (Fig. 1.2) (Alvarado et al., 1999; Sakai et al., 2000). The microvilli face the pigment cells forming an inverted “retina” (Fig. 1.2 a).

It has been suggested that the lamellate distal endings of the retinulae, are the site of the visual photopigment (Press, 1959). The photosensitive molecules responsible for detecting light are usually built of an apoprotein opsin, together with a chromophore. The retinoids, all-*trans* retinol, retinyl ester in oil-droplets and 11-*cis* retinal, extracted from *Dugesia japonica* have been suggested as the chromophore of the visual pigment in the eye (Azuma et al., 1992). Unexpectedly, the only *S. mediterranea* photopigment, *Smed-opsin*, published to date (GenBank: AF112361.1) has been found to be expressed in the photoreceptor cell bodies (Fig. 1.2) (Alvarado et al., 1999). However, in *Dugesia japonica, Dugesia dorotocephala, Notoplana koreana, Bdellocephala brunnea, Phagocata kawakatsui, Phagocata vivida and Polycelis auriclata,* a G-protein-coupled receptor with a seven-transmembrane-domain opsin, similar to the invertebrate *S. mediterranea* opsins, was localized on the membrane of rhabdomeres, in the microvilli of photoreceptive cells, inside the pigmented eye cups (Orii et al., 1998). The cell body and microvilli of rambomeric neurons seem to be strongly specialized, as in ciliary eyes.

Furthermore, the spectral sensitivity of the planarian photoreceptors, from measurements of the ocellar potential (OP), suggests the presence of a single rhodopsin-like pigment that absorbs maximally at approximately 508 nm in *Dugesia tigrina* (Brown et al., 1968a; Brown et al., 1968b), 475 nm (blue) in *Planarian lugubris,* 530 nm (green) in *Dendrocoelum lacteum* (Menzel, 1979) and around 500 nm in *Dugesia japonica* (Azuma et al., 1999).

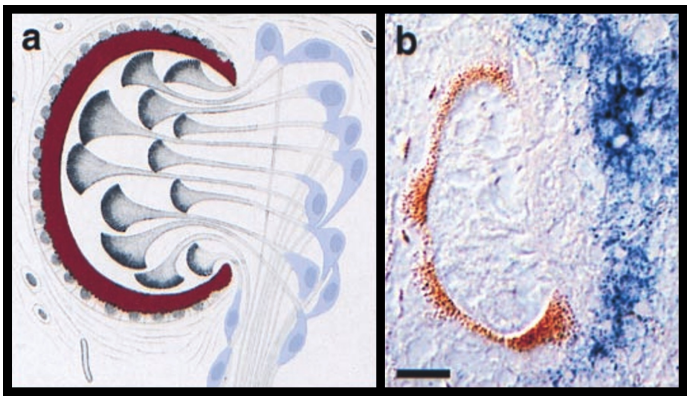

Figure 1.2 ***S. mediterranea* eye components. (A)** In red, the pigment cup; purple, the cell bodies of the light-sensing retinular cells: and dark grey, the rhabdomere structure that projects into the pigment cup. There are about 25 photosensory cells per photoreceptor. **(B)** Nomarski image of 4 µm plastic sections of an *S. mediterranea* in situ hybridized eye, labelled with *Smed-opsin* mRNA. Only cell bodies of the light-sensing photoreceptor cells are labeled with opsin mRNA, not the microvilli. In red, the pigment cup. The opsin used for this experiment (GenBank: AF112361.1) contains two overlapping regions, a Serpentine type 7TM GPCR chemoreceptor Srx (Region:7TM_GPCR_Srx; pfam10328) and a 7-transmembrane-domain receptor protein belonging to the rhodopsin family (Region: 7tm_1; pfam00001). Scale bars: B 10 µm. (Source: Alvarado et al., 1999).

The photoreceptor axons in *Dugesia japonica* project in three directions: towards the ipsilateral side of the brain, towards the contralateral side of the brain and towards the opposing eye. These innervations come from anterior or posterior regions in eye photoreceptors. The optic chiasm consists of contralateral axons and axons projecting from the opposite eye (Fig. 1.3) (Agata et al., 1998; Okamoto et al., 2005). Regional differences have also been detected in the *S. mediterranea* photoreceptor neurons and pigment cells. *Smed-actin-2* is only expressed in a subset of pigment cup cells (Fig 1.4,C); *smad6/7-2* and the prohormones *eye53-1*, *eye53-2, npp-12* and *mpl-2* are expressed in distinct domains of the photoreceptor neuron populations: *Smed-best-b* only in anterior photoreceptors and the kinase *Smed-pctaire* only in posterior photoreceptors (Fig 1.4) (Collins et al., 2010; González-Sastre et al., 2012; Lapan et al., 2012).

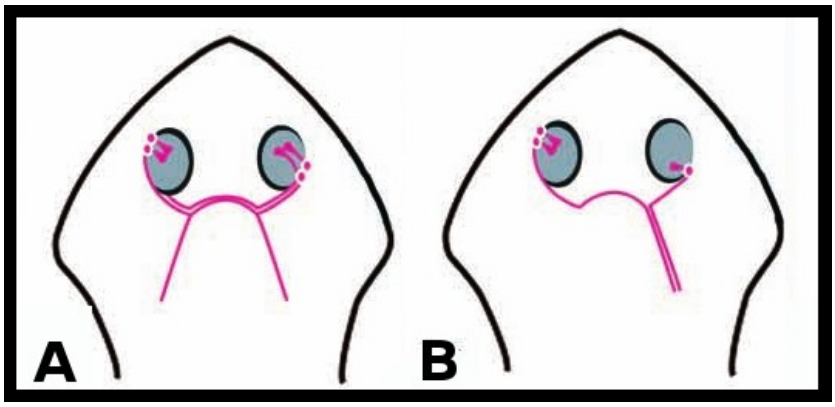

Figure 1.3 Schema of *Dugesia japonica* photoreceptors dyed with DiI and DiD. (A) Visual axons project in three directions: towards the ipsilateral side of the brain, the contralateral side of the brain and the opposing eye. These nerve cells innervate the dorsomedial area of the brain. **(B)** Anterior and posterior regional differences in eye photoreceptors. Posterior visual neurons have an ipsilateral projection, but anterior visual neurons project towards the contralateral side of the brain, demonstrating that the planarian has already developed regional differences in the eye. DiI and DiD are fluorescent lipophilic cationic indocarbocyanine dyes used as neuronal tracing due to their capacity to be retained in lipid bilayers (Source: Okamoto et al., 2005).

High-performance liquid chromatography (HPLC) showed that the pigment granules in pigment cup cells of *Dugesia ryukyuensis* are composed mainly of DHICA-derived eumelanin, as in many vertebrates (DHICA is 5,6-dihydroxyindole-2-carboxylic acid: an intermediate in melanin biosynthesis) (Hase et al., 2006). Pigment epithelial cells, lsuch as retinal pigment epithelial (RPE) cells in the human eye, might be essential for visual function such as light absorption, epithelial transport, spatial ion buffering, visual cycle, phagocytosis, secretion and immune modulation.

Even at the beginning of embryonic development, the functional differentiation of the photoreceptor layer and the RPE layer depend on each other (Strauss, 2005). The interactions between these tissues in humans are so critical that photoreceptors degenerate if the RPE is damaged or separated from them (Burke et al., 2005). Planarian RNAi with *Smed-sp6* and *Smed-dlx* for example, do not regenerate visible optic cups. These two conserved transcription factors are both expressed in the regenerating eye, specifically in the optic cups. At the same time, these flatworms present abnormal optic nerve projections into the brain and to the opposite eye, probably due to the physical absence of an optic cup (Lapan et al., 2011). Additionally, a high degree of similarity was found between the types of solute transporters expressed in the planarian optic pigment cells and vertebrate RPE, such as *glut-3* and *mct*-1 (Lapan et al., 2012). Moreover, there are morphological homologies with the vertebrate eye. The mouse ipsi-lateral or contralateral axons of (RGCs), the output neurons of the vertebrate retina, form the optic chiasm. Interestingly, in mice there are also two major RGC populations: (1) the Islet2-expressing contralateral projecting RGCs, which both produce and respond to Shh; and (2) the Zic2-expressing ipsilateral projecting RGCs (iRGCs), which lack Shh expression (Sánchez-Arrones et al., 2013).

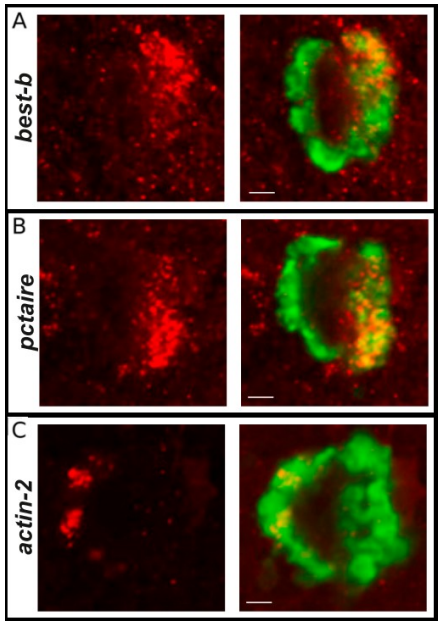

Figure 1.4 Regional differences within the photoreceptor neurons and pigment cell populations. Fluorescence in situ hybridization of 7-day blastemas with the genes *best-b*, *pctaire* and *actin-2* on the left-hand side (red) and co-expression with *tyrosinase* (in the pigment cup) or *opsin* (in the photoreceptor neurons) on the right-hand side (both in green). **(A)** *best-b* expressed in anterior photoreceptor neurons. **(B)** *pctaire* expressed in posterior photoreceptor neurons. **(C)** *actin-2* expressed in a subset of the optical photoreceptor cells. In all the images, the pigment cup is on the left and the cell bodies of photoreceptor neurons on the right-hand side. Scale bars: 10 μm. (Source: Lapan et al., 2012)

The capacity to capture light has been observed not only in the eye but in the skin of planarians; it is called “dermal light sense”. The eyeless green planarian *Castrada sp*. usually exhibits positive phototropic behaviour, but does not present a visual sensitivity curve with a maximum around λ = 530 nm, as is typically found in planarians with eyes such as *Mesostoma lingua, Fonticola vitta* or *Planaria lugubris*. It shows a dermal light sensitivity curve for red to violet radiation (Viaud, 1948). Although the photoreceptors responsible for its dermal light sense have not yet been identified, it is known that light has a stimulatory and an inhibitory effect on this flatworm. The inhibitory action of light varies as a function of intensity. On the average, *Castrada sp.* remains positive far longer in weak intensity and red light than it does due to the action of strong light and of green or violet rays. Furthermore, it has also been shown that in *Fonticola vitta* the speed in a positive direction increases with temperature, up to about 17º or 18° C, and decreases beyond that (Viaud, 1948; Parker et al., 1900). Furthermore, neurons possessing dense vesicles present a photoperiodic modulation of secreted melatonin and are found to be associated with the photoreceptors and with the control of asexual reproduction (fissioning) in *Dugesia dorotocephala* (Morita et al., 1987; Morita et al., 1988). Notably, fissioning in *D. dorotocephala* occurs only at night (Morita et al., 1993). Interestingly, it has been suggested that the rhodopsin-like proteins present in the tactile chemoreceptor auricles, of *Dugesia japonica,* are involved in the circadian rhythm, causing, for example, asexual fission. In contrast, the rhodopsin-like proteins in the microvilli of the eyes work, as photoreceptors for negative phototaxis behaviour (Asano, et al., 1998).

1.3 Regeneration and development of planarian eyes

Although a sexual species of *S. mediterranea* that lays cocoons exists, the *S. mediterranea* that is the subject of this study does not undergo embryonic development; it reproduces asexually. In this organism, cell differentiation and regeneration of tissues occur after fissioning, injury, starvation and cell turnover (aged differentiated cells) (Saló et al., 2009). Nevertheless, eye formation in sexual species that develop embryos (first cocoons, second hatchlings and third juveniles), such as *Schmidtea polychroa,* shows great similarities with adult planarian eye regeneration. The embryonic development of their visual organs has been divided into four major steps: (1) photoreceptor and pigment cell specification from a common precursor; (2) segregation of photoreceptor and pigment cells; (3) formation of the optic chiasm and pigment cup; and (4) modification of proportions and morphology of visual organs (Martín-Durán et al., 2012). *Schmidtea polychroa* embryos express *eya*, *six-1/2 and otxA* in the eyes, and lack expression of *pax6A*, *rax* and *dachshund* in the eye domain; similar to the case of the regeneration processes (Martín-Durán et al., 2012). Eye generation in embryos of the sexual *S. mediterranea* is regulated by transcription factors. *Ovo* is expressed in the eye primordium and eye progenitor, *six1/2* and *eya* in neural retina and pigment cells, and *Otx*, *Sp6-9*, *Dlx*, *Meis, SoxB, FoxQ2* and *Klf* in neural retina or pigment cells (Lapan et al., 2012). In *Dugesia japonica,* the first eye structures to appear on the second day after head amputation are a cluster of pigment cells and visual neurons on each side of the cephalic blastema. The second structures that appear on the third day are anti-arrestin (VC-1) positive axonal projections crossing the midline in a lateral orientation. On the fourth day, the VC-1 positive cells grow towards the cephalic ganglia (Inoue et al., 2004). It has been suggested that in *Dugesia japonica* two different cell types, the photoreceptors and the pigment cells, are differentiated from a common ancestor. This is based on the fact that the numbers of both types of cell in the eye are proportional to body length. Additionally, the ratio between the number of visual neurons and pigment cells (2:1) remains constant during cell turnover (aged differentiated cells), starvation, and regeneration (Takeda et al., 2009). Retinoic acid (RA), a vitamin A derivative, is known to be an active morphogen, directly regulating the expression of many genes that control the perception of positional information and the cell cycle. It is required for growth and development (embryonic anterior/posterior patterning and eye development) in vertebrates (Meiden, 1995; Duester, 2008). Interestingly, in *Girardia tigrina* and *S. mediterranea* RA (all-*trans*-RA) acts as a regulator of morphogenesis and neoblast proliferation. It inhibits the regeneration of the head part, causing a delay in the appearance of eye spots, but it has no effect on the tail end of the body (Romero et al., 2001; Ermakova et al., 2009).

Several eye-related planarian genes have been studied in recent years. Based on their mRNA expression patterns and their phenotypes after mRNA interference, these genes can be divided into four groups (Table 1.1, Table 1.2). (1) To date only two transcription factors, *Smed-six1-2* and *Smed-ovo*, both expressed in photoreceptor neurons and pigment cells, are known to inhibit the regeneration of cell types of the eye in 100% of the cases (Table 1.1) (Eckelt, 2011; Lapan et al., 2012). *Smed-eya* also inhibits eye regeneration completely but only in 40% of the cases. (2) A second group of genes are expressed in the eye and their loss of function causes a variety of defects in eye structures and functions, but they do not inhibit eye development completely. Good examples are *Smed-ops*, *Smed-otxA*, *Smed-tyrosinase*, *Smed-sp6-9*, *Smed-dlx* and *Smed-egfr-1*. (3) Genes such as *SmedBMP*, *Smed-slit*, *Djnou darake*, *DjWntA*, *Smed-βcatenin 1*, *Smed-netR*, *Smed-netrin2* or *Smed-roboA* are not expressed in the eye cells (Table 1.2). Nevertheless, they are critical for regeneration of the visual system in addition to that of other tissues in planarians. They might be responsible for general structural patterns such as dorsoventral or anteroposterior determination, or axon guidance that also affect eye development. (4) A fourth group of genes are found to be expressed only in the eyes or additionally in other parts of the planarian body, such as *Smed-Pax-6A*, *Smed-trpc1*, *Smed-plcb* or *Smed-pkc,* but interference with their mRNA does not cause eye regeneration defects (Table 1.2). (More than 100 additional genes with mRNA expression in the eye cells but which are not known to cuase eye development changes are not included in the tables (Lapan et al., 2012).)

Table 1.1 Summary of genes that affect regeneration of the visual system or have expression in visual cells in planarians. Only eye expression patterns have been specified except for genes without eye expression.

Group1: Genes with mRNA expression in eye cells and with complete eye development inhibition.

Planarian gene	Vertebrate homolog expression/ function	Expression of mRNA in planarian	Eye-related planarian RNAi phenotypes	References in Planarians
Dj/Gt/Smed-six1-2	Sine oculis, transcription factor	Photoreceptor cells, pigmented eye cells, eye precursor cells in blastema	Inhibition of eye regeneration	(Pineda et al., 2000; Pineda et al., 2001; Mannini et al., 2004)
Smed-ovo	Transcription factor	Photoreceptor neurons, pigmented eye cells and eye precursor cells	Inhibition of eye regeneration	(Lapan et al., 2012)
Dj/Smed-eya	Eye absent; transcription factor	Photoreceptor cells, pigmented eye cells and eye precursor cells in blastema	40% inhibition of eye regeneration	(Mannini et al., 2004; Salo et al., 2002; Pineda et al., 2000)

Group 2: Genes with mRNA expression in the eye cells but without complete eye regeneration inhibition.

Planarian gene	Vertebrate homolog expression/ function	Expression of mRNA in planarian	Eye-related planarian RNAi phenotypes	References in Planarians
Gt/Dj/Smed-opsin	Opsin ; phototransduction	Cel bodies of photoreceptors neurons	lost of negative phototaxis	(Alvarado et al., 1999; Pineda et al., 2000; Pineda et al., 2001; Saló, 2002)
Smed-otxA	Ortodenticle, transcription factor	Photoreceptor neurons	Inhibition of photorreceptor cells regeneration, reduced pigment cup aperture	(Lapan et al., 2011)
Smed-tyrosinase	melaning synthesis	Eye pigment cells	weakly pigmented optic cups	(Lapan et al., 2011)
Smed-sp6-9	transcription factor	Eye pigment cells	Do not regenerate visible optic cups, abnormal photoreceptor neuron	(Lapan et al., 2011)
Smed-dlx	transcription factor	Eye pigment cells	Do not regenerate visible optic cups, abnormal photoreceptor neuron	(Lapan et al., 2011)
Smed-soxB	transcription factor	Anterior photoreceptor neurons, eye progenitors	Small eye phenotypes	(Lapan et al., 2012)
Smed-foxQ2	transcription factor	Photoreceptor neurons, eye progenitors	Small eye phenotypes, closed pigment cup	(Lapan et al., 2012)
Smed-klf	transcription factor	Photoreceptor neurons, eye progenitors	Small eye phenotypes, circularized optic cup	(Lapan et al., 2012)
Smed-meis	transcription factor	Photoreceptor neurons, eye progenitors	Small eye phenotypes, elongated optic cup	(Lapan et al., 2012)
Smed-egfr-1	epidermal growth factor Receptor-1	Eye pigment cells	Decreased differentiation of eye pigment cells	(Fraguas et al., 2011)
Dj/Smed-eye53-1	prohormone	anterior photoreceptor neurons	Unable to respond properly to light	(Inoue et al., 2004; Collins et al., 2010)
Dj/smedeye53-2	prohormone	Posterior photoreceptors neurons	Unable to respond properly to light	(Collins et al., 2010)

Table 1.2 Summary of genes that affect regeneration of the visual system or have expression in visual cells in planarians. Only eye expression patterns have been specified, except for genes without eye expression.

Group 3: Genes without mRNA expression in the eye cells but influence eye development.

Planarian gene	Vertebrate homolog expression/ function	Expression of mRNA in planarian	Eye-related planarian RNAi phenotypes	References in Planarians
Dj-nou darake	FGF-receptor-like 1 (FGFRL1)	Head region	Ectopic eye and brain tisues	(Cebrià et al., 2002a)
DjWntA	Wnt-A	Posterior brain	Ectopic eyes	(Kobayashi et al., 2007)
Dj/Smed-BMP	Bone morphogenetic protein 2-4/ ventral determination	Dorsal midline	Dorsoventral eye duplication	(Orii et al., 1998; Orii et al., 2007; Molina et al., 2007; Reddien et al., 2007)
Smed-βcatenin 1	β catenin	Ubiquitous	Ectopic eyes	(Iglesias et al., 2008)
Smed-netrin2	netrin/DCC axon guiadance	Central nervous system	Defects in visual axon targeting and abnormal photophobic behaviour	(Cebrià, 2005)
Smed-netR	netrin/DCC axon guiadance	Central nervous system	Defects in visual axon targeting and abnormal photophobic behaviour	(Cebrià, 2005)
Smed-slit	Slit/ axon guidance	Dorsal and ventral midline	Cyclopic eye	(Cebria et al., 2007b)
Smed-roboA	Roundabout/ axon guidance	Central nervous system	Aberrant visual projections	(Cebria et al., 2007a)
Dj-CHC	Clathrin heavy chain	Ubiquitous	Projection of visual axons inhibition	(Inoue et al. 2007)
Smed-pbx	Transcription factor	Parenchyma, neoblast	Inhibition of eye progenitor regeneration	(Chen et al., 2013; Blassberg et al., 2013)
Dj-1020HH-1	Prohormone	Brain ganglia	Impaired negative phototaxis	(Inoue et al., 2004)

Group 4: Genes with mRNA expression in the eye cells but without any eye regeneration influence.

Planarian gene	Vertebrate homolog expression/ function	Expression of mRNA in planarian	Eye-related planarian RNAi phenotypes	References in Planarians
Dj/Gt/SmedPax6-A-B	Pax6; lens placode, optic vesicle	Low expr. in photoreceptor and pigmented eye cells	No phenotype	(Callaerts et al., 1999; Rossi et al., 2001; Pineda et al., 2001; Pineda et al., 2002)
Djβ-arrestin	Phototransduction	Photorreceptor neurons		(Umesono et al., 1999; Nakazawa et al., 2003)
DjTPH/Smed-tph	Tryptophan hydroxylase/syntesis of neurotransmiter serotonin	Eye pigment cells	No phenotype	(Nishimura et al., 2007; Fraguas et al., 2011)
Dj/Smed-synt	Synaptotagmin/synaptic transmiter release	Photoreceptors cell bodies		(Lapan et al., 2011)
Smed-mpl-2	Myomodulin prohormone-like-2	Posterior photoreceptors neurons		(Collins et al., 2010)
Smed-npp-12	Neuropeptide precursor-12	Anterior photoreceptor neurons		(Collins et al., 2010)
Dj-Inx4	Inexin 4	Photoreceptor cell bodies	No phenotype	(Nogi et al., 2005)
Dj-PHM	Peptidylglycine-hydroxylating-monooxygenase	Photoreceptors neurons		(Asada et al., 2005)
Djcyt-b_{561}	Cytochrome-b_{561}	Photoreceptor neurons		(Asada et al., 2005)

Models of eye cell regeneration are based on the existence of neoblasts. All the regions of the planarian body that can regenerate, contain somatic dividing cells (neoblasts). These are typically identified by the expression of cell cycle genes such as *Smed-wi-1* and *Smed-h2b*, via labelling with BrdU and due to its irradiation sensitivity (Guo et al., 2006; Dubois, 1949; Lapan et al., 2011). The latest "specialized neoblast model" proposed the existence of two major classes of neoblast; the sigma-class and the zeta-class. Zeta-neoblasts include specialized cells that give rise to an abundant postmitotic lineage, including epidermal cells, but are not required for regeneration. In contrast, sigma-neoblasts proliferate in response to injury, possess broad lineage capacity, and can give rise to zeta-neoblasts. Although these cell populations can-not be considered homogeneous, it has been suggested that eye cells come from the sigma neoblast population, and later specialize during regeneration to make photoreceptors and pigment cells (Fig. 1.5 A) (van Wolfswinkel et al., 2014; Reddien, 2013). The *S. mediterranea* eye-specific transcription factors *six1-2*, *eya* and *ovo* have been found to be expressed in neoblasts and in the blastema at the base of the wound, suggesting that they might be specifiers to all eye progenitor formation (Lapan et al., 2011; Lapan et al., 2012). Additional expression of *otxA* could specified photoreceptor neurons and additional expression of *sp6-9* and *dlx* specified pigment cells (Fig. 1.5 B) (Lapan et al., 2011; Lapan et al., 2012; Reddien, 2013).

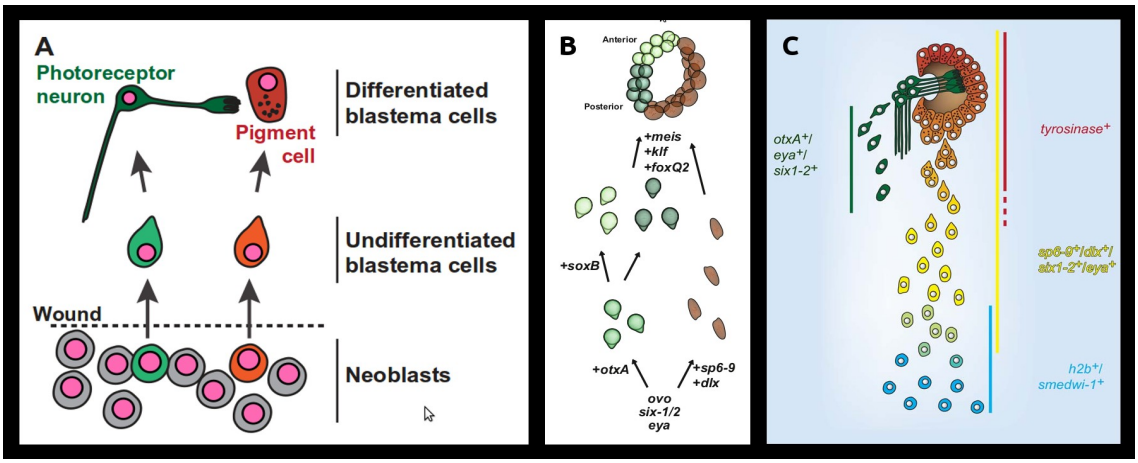

Figure 1.5 Models of *Schmidtea mediterranea* eye cell lineage during head regeneration. These three pictures represent the same eye cell lineage. Notice the simplification of the model proposed by the same author in **(A)** 2013, **(B)** 2012 and **(C)** 2011. Progenitors undergo changes in gene expression, including loss of neoblast markers (*2b+*, *smedwi-1+*) and activation of differentiation markers, as migration towards the eye primordium proceeds: *six1/2*, *ovo*, *dlx, sp6-9* and *eya*. Ultimately, terminally differentiating progenitors are incorporated into the eye, expressing tyrosinase (involved in melanin production). (Source: (A) (Reddien, 2013); (B) (Lapan et al., 2012); (C) (Lapan et al., 2011))

1.4 EYE SIGNALLING PATHWAYS

Comparative molecular genetics has shown that there is some degree of common ancestry between vertebrate and invertebrate visual systems (Arendt, 2003; Lapan et al., 2012). The morphological structures of the visual system have been identified in *S. mediterranea*, but the genetic components of visual processing, such as phototransduction, pigment biosynthesis, pigment transporters, microvillus structure, embryonic development and transcription factors, among others, are poorly understood (Reddien, 2013).

1.4.1 PHOTOTRANSDUCTION PATHWAY

Eyes can be categorized: as rhabdomeric or ciliary: according to the nature of the cellular elements that make up the photoreceptors (microvillus or cilium); by the kind of opsin molecule used for transduction of the light signal (binding 11-*cis* retinal or all-*trans* retinal); and by the signalling pathway used to convert a conformation change of the opsin molecule into a change in the electrical potential across the cell membrane (hiper-depolarization) (Fig.1.6) (Arendt, 2003; Fu et al., 2007; Hardie, 2001; Hardie et al., 2001; Graham, 2014).

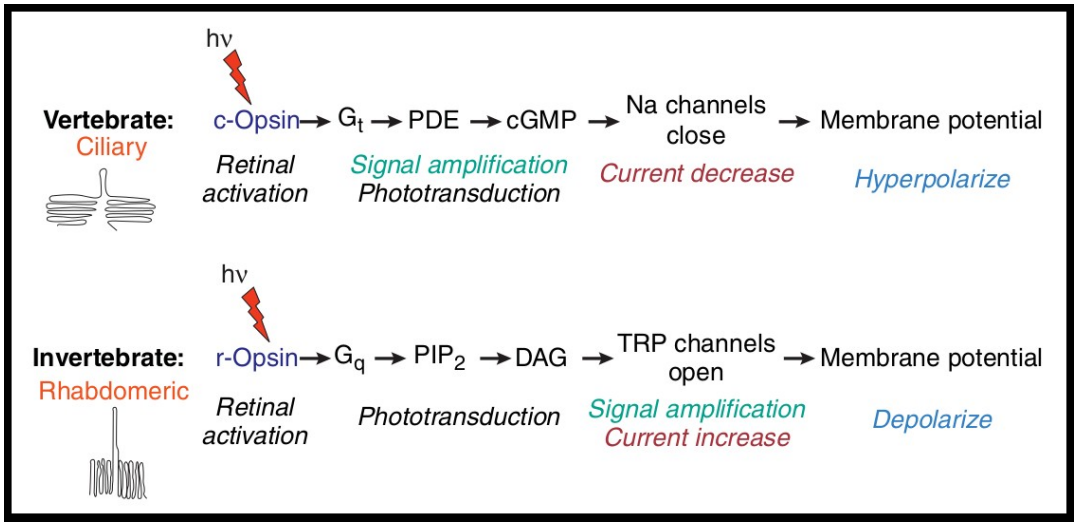

Figure 1.6 Schematic illustration showing the key differences between simplified representations of (top) canonical vertebrate ciliary phototransduction and (bottom) invertebrate rhabdomeric phototransduction, where hv represents incident photon energy. The two different opsin types (c-opsin and r-opsin) are contained in distinctly different types of neurons: ciliary and rhabdomeric. The opsins are coupled to different families of G proteins that act via different types of transduction cascades. Amplification occurs during phototransduction in ciliary receptors and during channel opening in rhabdomeric receptors. These cascades produce signals of different sign. G_t, transducin; PDE, phosphodiesterase; cGMP, cyclic guanosine monophosphate; G_q, guanine nucleotide-binding protein α15; PIP_2, phosphatidylinositol 4,5-bisphosphate; DAG, diacylglycerol. (Source: Fernald, 2006).

Opsin-based pigments are G protein-coupled receptors (GPCRs); rhodopsin is the best understood (Tsukamoto et al., 2010). However, there are various opsin-based pigments for vision and a wide variety of non-visual functions (Go-coupled opsin, Gs-coupled opsin, Gt-coupled opsin encephalopsin, neuropsin, Gq-coupled opsin, peropsin, retinal photoisomerase, melanopsin) (Tsukamoto et al., 2010; Terakita, 2012) (Fig. 1.7 B). Opsin-based pigments consist of a protein moiety (opsin) with seven -transmembrane alpha helices and a vitamin A derivative (retinal) as the chromophore (Fig. 1.7 A).

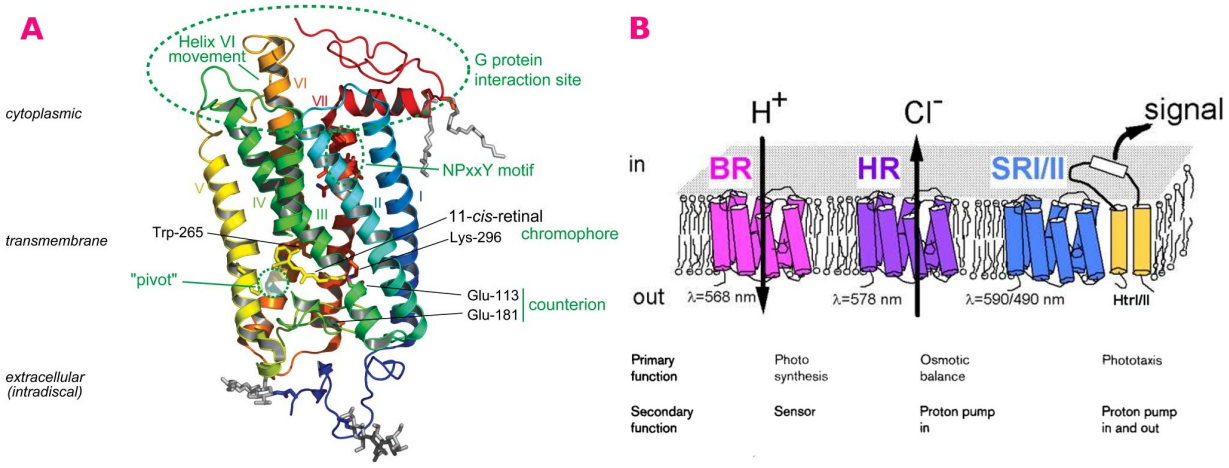

Figure 1.7 Crystalline structure of the dark state of bovine rhodopsin and schematic representation of the structure and function of the retinal rhodopsins from *Halobacterium salinarum*. (A) The structural model of bovine rhodopsin (PDB code 1U19). Some key residues and regions responsible for the rhodopsin characteristics are indicated. The retinal chromophore forms a covalent bond to Lys-296 via protonated Schiff base linkage. The proton on the Schiff base is necessary for visible light absorption but it is unstable within the opsin molecule. A negatively charged amino acid residue called the counterion is an essential amino acid residue necessary for opsin-based pigments to absorb visible light. The counterion position is closely related to whether an opsin-based pigment is bistable or monostable. Bistable pigments possess the counterion at position Glu-181; in contrast, monostable vertebrate visual pigments have the counterion at position Glu-113. Nevertheless, a bistable pigment parapinopsin, which is phylogenetically close to vertebrate visual pigments, has glutamic acids at both position 113 and position 181, but Glu-181 serves as a counterion at least in the photoproduct. The NPxxY' amino acid sequence motif is highly conserved among most opsins and other GPCRs but not in the photoisomerase retinochrome. A unique property of bistable pigments is that all-*trans*-retinal binds to a highly conserved amino acid residue, Trp-265, for example, in *Amphioxus*. A "pivot" region between the membrane-embedded domains of helices V and VI transmits retinal isomerization to the movement of the helices. This interaction is different in bistable and monostable pigments, resulting in different amplitudes of helix VI movement. **(B)** Bacteriorhodopsin (BR) transports protons into the cell, whereas halorhodopsin (HR) pumps chloride out of the cell. Sensory rhodopsin I (SRI) forms a complex with its transducer (halobacterial transducer I, Htrl). Formation of this complex triggers a signal transduction cascade that ultimately controls flagellar rotation. The secondary functions of the wild-type molecules include that of a photosensor for BR and a proton pump for HR and SRI. (Source: (A): Tsukamoto et al., 2010; (B): Oesterhelt et al., 1998)

During the visual cycle, vertebrate and invertebrate rhodopsin bind 11-*cis* retinal in the dark. Interestingly, in vertebrates, light isomerizes the retinal to the all-*trans* form, initiating conformational changes of protein moiety that lead to unstable photointermediate metarhodopsin II that releases all-*trans* retinal and forms a colourless opsin (i.e., it “bleaches” it). Rhodopsin regenerates by a slow process of renewal which takes days to complete, and requires the existence of an isomerizing enzyme and the presence of 11-*cis*-retinal. In contrast, in invertebrate squid and octopus rhodopsins, the photoproduct metarhodopsin is stable and can revert to the original dark state rapidly by subsequent light absorption, showing photoregeneration capacity. Therefore, these kinds of pigments are termed bistable (Fig. 1.8) (Tsukamoto et al., 2010).

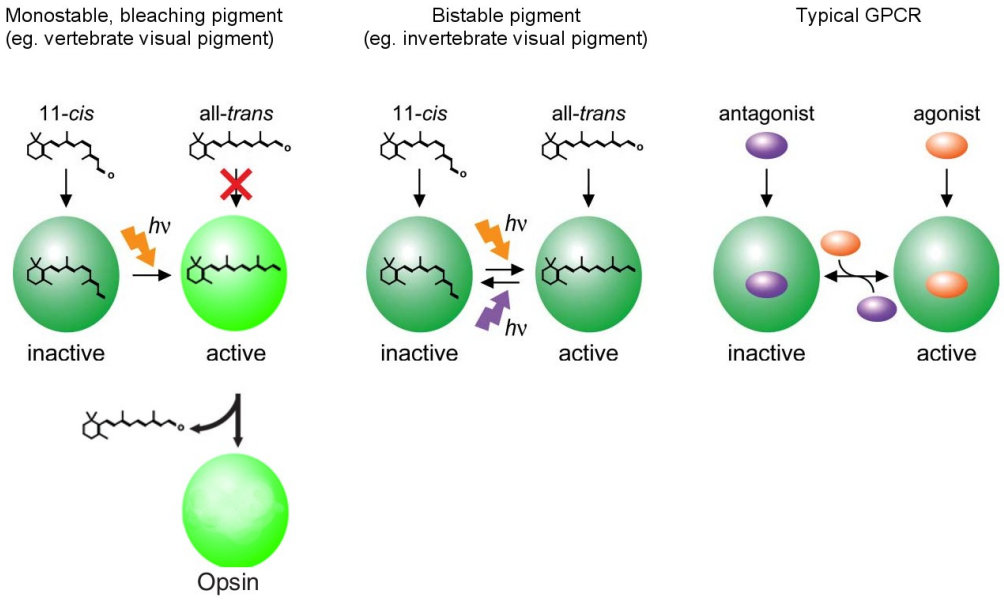

Figure 1.8 Photoreaction of monostable and bistable pigments and typical GPCR activation scheme. Monostable pigments can bind to 11-*cis*-retinal but not all-*trans*-retinal directly. Bistable pigments can bind to both 11-*cis* and all-*trans* retinal directly, and 11-*cis*-retinal and all-*trans*-retinal binding states are inter-convertible upon light absorption. The capacity of bistable pigments to bind to 11-*cis* and all-*trans* retinal is similar to the characteristics of typical GPCRs when they bind to antagonist and agonist. The inactive and active states of typical GPCRs are stabilized by the binding of antagonist and agonist, respectively. In general, addition of excess antagonist or agonist can exchange ligands bound to typical GPCRs, because there are no covalent bonds to ligands in typical GPCRs, as opposed to the case of monostable and bistable pigments (Source: modified from Tsukamoto et al., 2010).

Examples of bistable opsin-based pigments are Gt-Lamprey parapinopsin, Gq-squid rhodopsin, Gq-octopus rhodopsin, Gq-amphioxus melanopsin, Go-scallop scop 2, Go-amphioxus Amphiop2 and jumping spider peropsin. The amphioxus Go-coupled opsin-based pigments exhibit a reversible photoreaction showing a bistable nature. In addition, rhodopsin is one of the multiple genes that when mutated, causes retinitis pigmentosa (Dryja et al., 1990).

Amphioxus melanopsin is localized in putative non-visual photoreceptor cells with a rhabdomeric morphology and exhibits molecular properties almost identical to those of the invertebrate Gq-coupled rhodopsins, such as squid rhodopsin (Tsukamoto et al., 2010; Terakita, 2012). Melanopsin co-expresses with rhodopsin in *Xenopus* melanophores, suggesting a possible photoisomerase function (Miyashita et al., 2001). Nevertheless, in mammals, melanopsin is localized in intrinsically photosensitive RGC (ipRGCs). It is specialized in a wide variety of so-called non-image-forming light responses such as synchronization of circadian clocks to light/-dark cycles, regulation of pupil size, sleep propensity pineal melatonin production, regulation of body temperature, mood and aspects of arousal and concentration (Bailes et al., 2009).

Amphioxus peropsins bind preferentially to all-*trans*-retinal as a chromophore, and light isomerizes the chromophore to the 11-*cis* form, like retinochrome and retinal GPCR (RGR), suggesting a possible function of peropsin as a retinal-photoisomerase. Nevertheless, its 'NPxxY' amino acid sequence motif is conserved in most opsins and GPCRs but not in photoisomerases, implying that peropsin might drive G protein-mediated signalling (Tsukamoto et al., 2010; Terakita, 2012). Peropsin localizes in the apical face of the RPE, and most prominently in the microvilli that surround the outer photoreceptor segments of adult human and mouse retinas. It may also play a role in RPE physiology either by detecting light directly or by monitoring the concentration of retinoids or other photoreceptor-derived compounds (Sun et al., 1997).

Pinopsin, retinochrome, the photoisomerase RGR and cryptochromes are also members of the visual pigment family present in non-retinal tissues that have been hypothesized to play a role other than classical phototransduction. Pinopsin is localized in the outer segment of pinealocites in the pineal gland of chicken, and it is suggested that light-activated pinopsin is coupled to two types of G-protein α-subunits which trigger dual signal transduction pathways within a single cell (Matsushita et al., 2000). Retinochrome is a retinal chromoprotein present in the inner segments of cephalopod photoreceptors in a region adjacent to the rhabdoms that photoconverts all-*trans* retinal to 11-*cis* retinal. Although it is not a visual pigment, it may contribute to the visual mechanism by its co-operative relationship with cephalopod rhodopsin (Hara et al., 1972).

RGR is a vertebrate protein present in the intracellular membranes of both the RPE and Muller cells in the retina. It has the Lys 296 retinal attachment site, a histidine at the Glu113 site and binds to all-*trans* but not 11-*cis* retinal, absorbing both visible and ultraviolet light. It might act as a signal-transducing light receptor, participate in the visual cycle as retinal isomerases do, or function in both capacities (Hao et al., 1999; Hao et al., 1996).

Cryptochromes are proteins similar to photolyases that have reduced DNA repair activity or none at all, and have gained a novel role in signalling. They bind to two chromophores as a co-factors; a flavin (FAD) and a pterin (MTHF). They have the potential to sense not only light, but also redox state and the geomagnetic field. CRY mediates a rapid electrophysiological blue light response that is distinct from classical opsin-based phototransduction. In *Drosophila,* semireduced FAD is excited to other states by absorption of a photon, which then leads to a conformational change in the CRY protein (Chaves et al., 2011).

Other interesting opsins are bacteriorhodopsin (BR) and halorhodopsin (HR). Haloarchea possess a set of four related retinal proteins in their cell membrane: (BR), (HR), and two sensory rhodopsins (SRI and SRII) (Haupts, et al., 1999). HR, ubiquitous in haloarchaea, uses light energy to pump chloride but also bromide, iodide, and nitrate into the cell against their electrochemical gradients (Fig. 1.7, B). HR binds retinal covalently as a protonated Schiff base to its only lysine residue, Lys242 in helix G. The Schiff base absorbs green light with a maximum wavelength (λmax) of 578 nm. Photon absorption triggers a catalytic cycle via an all-*trans* to 13-*cis* isomerization of the retinal chromophore in less than 10 ps. An ongoing sequence of reactions leads to the net transport of one chloride per photon toward the cytosol. Despite the differences in ion specificity and transport, the transmembrane region of HR is structurally well conserved and shares 31% sequence identity with the BR from *Halobacterium salinarum*. Chloride and protons can be transported in both directions by and on the same molecule, HR. (Kolbe et al., 2000). BR associates into trimers (groups of three BR molecules) and converts the energy of green light (500–650 nm) into an electrochemical proton gradient, which in turn is used for ATP production by ATP synthases. Meanwhile HR is involved in maintaining the iso-osmolarity of the cytoplasm during cell growth by transporting chloride ions into the cell. SRI and SRII, in contrast, mediate phototactic behaviour, permitting the cell to avoid harmful blue and UV light and to accumulate in regions favourable for photosynthesis (Haupts et al., 1999).

1.4.2 Rhodopsin transport

There are many examples where genetic mutations that appear to interrupt the transport of molecules in photoreceptors leads to diseases causing vision loss; retinitis pigmentosa, Leber congenital amaurosis, Bardet-Biedl syndrome, Senior-Loken syndrome, Usher syndrome, and others. Some of these devastating diseases cause multiple organ failure that, in addition to vision loss, leads to deafness, developmental abnormalities such as mental retardation and life-threatening conditions such as kidney disease.

Blindness in Usher 1B (retinitis pigmentosa-dysacusis syndrome) patients probably results from defective ciliary transport of rhodopsin from myosin VIIa, the product of the human Usher syndrome 1B gene (Fig. 1.9 a-c) (Wolfrum et al., 2000).

Bardet–Biedl syndrome (BBS) is an oligogenic syndrome whose manifestations include retinal degeneration, renal abnormalities, obesity and polydactyly. It is caused by an intraflagellar transport deficit. In mouse, photoreceptor cells die due to defects in the transport of phototransduction proteins from the inner segments to the outer segments (Fig. 1.9 d) (Abd-El-Barr et al., 2007).

Although of the microvilliar type, in *Drosophila* photoreceptors, a transport mechanism takes place that is similar to that in ciliary photoreceptors. A dense microfilament web, the rhabdomere terminal web (RTW) extends into photoreceptor cytoplasm from the rhabdomere base; RTW microfilaments are oriented with their plus ends towards the rhabdomere base and block incursion of vesicles and proteins. Together with MyoV, Rab1 and Rab11 are required for Rhodopsin transport from ER to Golgi and from Golgi to the rhabdomere (Fig 1.9 e) (Li et al., 2007).

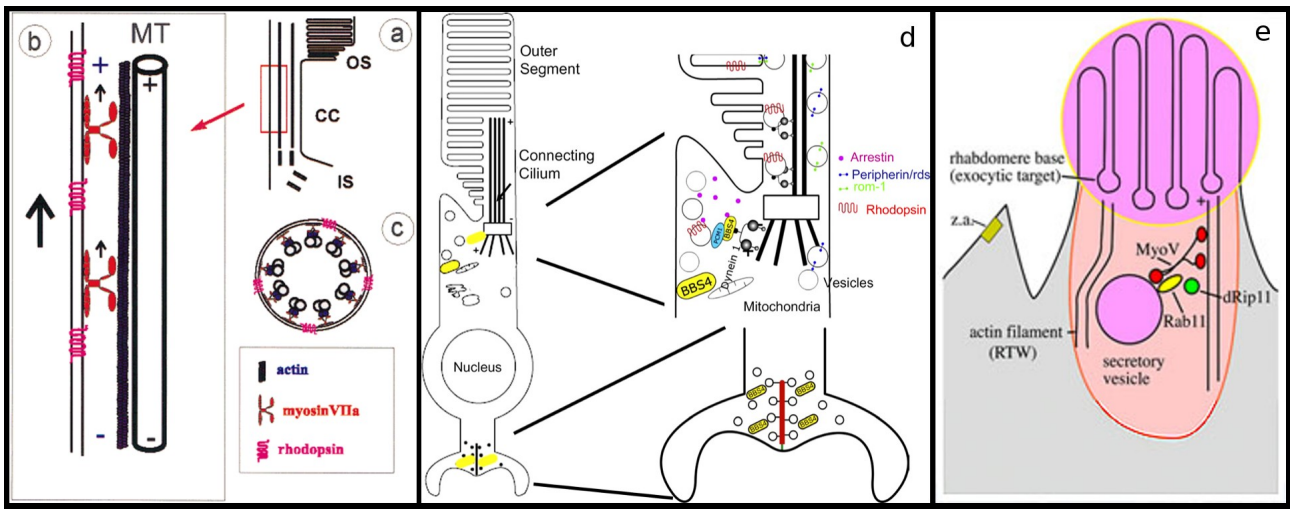

Figure 1. 9 Dynamics of protein transport models: (a-c) rhodopsin transport through the mouse rod connecting cilium, (d) BBS4 in the normal functioning of mammalian photoreceptors, (e) cytoplasm and apical transport in the *Drosophila* photoreceptor.

(a) Diagram of the ciliary joint between the inner segment (IS) and outer segment (OS). **(b)** Enlargement of the membrane and associated cytoskeleton compositions. Rhodopsin transport is probably driven by myosin VIIa moving along axonemal actin filaments (small arrows). Large arrows indicate the direction of the rhodopsin trafficking in the plasma membrane of the connecting cilium (CC). **(c)** Scheme of a transverse section through the connecting cilium. **(d)** Two distinctive roles for BBS4 have been proposed. The first involves the transport of phototransduction proteins, such as rhodopsin and arrestin to the outer segment (OS). The second involves synaptic transmission at the axon terminal from photoreceptors to the secondary neurons of the visual pathway. In addition to the transport of phototransduction proteins a second mechanism transports structural proteins, such as peripherin/rds and rom-1, but is BBS4-independent. **(e)** Secretory vesicles from the ER and Golgi are pulled through the rhabdomere terminal web (RTW) cytoplasm by a MyoV–Rab11–dRip11 complex to the exocytic plasma membrane target, the rhabdomere base (pink). MT, axonemal microtubule;+,-, polarity of cytoskeletal elements. (Source: (a,b,c) Wolfrum et al., 2000; (d) Abd-El-Barr et al., 2007; (e) Li et al., 2007)

1.4.3 ABC TRANSPORTER

In mice and humans 11-*cis*-retinal and all-*trans*-retinal are highly toxic due to their highly reactive aldehyde group; they have to be detoxified either by reduction to retinol or by sequestration within retinal-binding proteins. The ATP-binding cassette protein ABCA4 can transport toxic N-11-*cis*-retinylidene -phosphatidylethanolamine (PE) from the lumen to the cytoplasmic leaflet of photoreceptor disk membranes through the visual cycle (Fig. 1.10). It is almost exclusively expressed in the retina and localizes in outer segment disk edges of rod photoreceptors (Sun et al., 2000).

This transport across membranes together with chemical isomerization of N-11-*cis*-retinylidene-PE to its all-*trans* isomer and reduction to all-*trans*-retinol can prevent the accumulation of excess 11-*cis*-retinal and the potentially toxic bisretinoid compounds A2PE and its hydrolytic product A2E (Sparrow et al., 2012). These bisretinoid compounds accumulate as lipofuscin deposits in RPE cells upon the phagocytosis of outer segments and have been implicated in the pathology of a number of degenerative retinal diseases. These toxins have been found in ABCA4-deficient mice and individuals with autosomal recessive Stargardt macular degeneration. Mutations in ABCA4 cause lipofuscin accumulation and consequently atrophy of the central retina, and severe progressive loss of vision (Quazi et al., 2014). It is almost exclusively expressed in the retina where it localizes in the outer segment disk edges of rod photoreceptors (Sun et al., 2000).

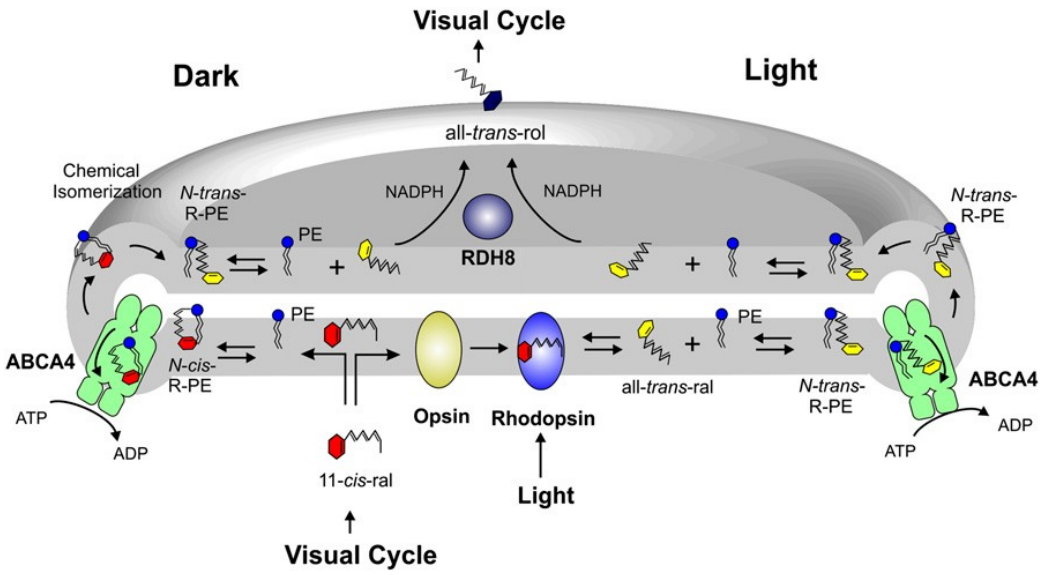

Figure 1.10 Reactions involved in the clearance of 11-*cis*- and all-*trans*-retinal from mammal photoreceptor disk membranes. Excess of 11-*cis*-retinaldehyde (11-*cis*-ral) is not required as the regeneration of rhodopsin (or cone opsin) reversibly reacts with PE to produce N-11-*cis*-retinylidene-PE (N-*cis*-R-PE), which is actively flipped by ABCA4 from the lumen to the cytoplasmic leaflet of disk membranes. N-*cis*-R-PE is isomerized to its all-*trans* isomer (N-*trans*-R-PE) which can also be transported by ABCA4. All-*trans*-retinal produced through mass action is reduced by RDH8 to produce all-*trans*-retinol (all-*trans*-rol) which enters the visual cycle in the RPE. All-*trans*-retinal produced from the bleaching of rhodopsin (or cone opsin) reversibly reacts with PE to form N-*trans*-R-PE, which can be flipped by ABCA4 to the cytoplasmic leaflet of discs, enabling all-*trans*-retinal to be reduced by RDH8 for enter into the visual cycle. N-*trans*/-*cis*-RPE: N-11-*trans*/*cis*-retinylidene-phosphatidylethanolamine; RDH8: retinol dehydrogenase 8; ABCA4: ATP-binding cassette transporter; RPE: retinal pigment epithelium. (Source: Quazi et al., 2014)

1.4.4 Pigment biosynthesis

Ommochromes, melanin and pteridines are the main contributors to body colouration, for example by insects. Body epidermis and eye colouration results from accumulation of different pigments: xanthommatin (ommochrome) and pteridines in the *Drosophila melanogaster* eye, melanin and sepiapterin (yellow pteridine) in the body of the scorpion fly, *Panorpa japonica,* and melanin in the cuticle and xanthommatin, sepialumazine (yellow pteridine), sepiapterin and uric acid in the epidermis of the silkworm, *Bombyx mori* (Kato et al., 2006). The brown, red or red-purple pigment ommochromes and the yellow xanthopterin contribute to the light brown body colour of *Dugesia ryukuensis* (Hase et al., 2006). Ommochromes are metabolites of tryptophan, via kynurenine and 3-hydroxykynurenine. They are responsible for a wide variety of colours, ranging from yellow through red and brown to black. It is present in the eyes of crustaceans and insects, but also in the chromatophores of cephalopods, and in spiders.

The Drosophila eye pigment mutants white, vermilion, scarlet, cinnabar, and cardinal have lesions in the tryptophan to xanthommatin (ommochrome) pathway, in the storage of xanthommatin or, most probably, in the transport of precursors into the compound eyes (Fig. 1.11) (Oxenkrug, 2010). The X-linked vermilion (v) mutants have deficient tryptophan 2,3-dioxygenase (TDO) activity (Beadle et al.,1936), which is the rate-limiting enzyme of tryptophan (TRY) conversion into kynurenine (KYN) in the pigmented eyes of Drosophila (Tearle, 1991). The deficient transmembrane transport of tryptophan underlies the impaired formation of KYN in the white (w) mutant of *D. melanogaste*r (Sullivan et al., 1975). This mutant is also deficient in the transport of guanine, the initial substrate for the biosynthesis of red pigments (drosopterins) (Sullivan et al., 1980; Oxenkrug, 2010).

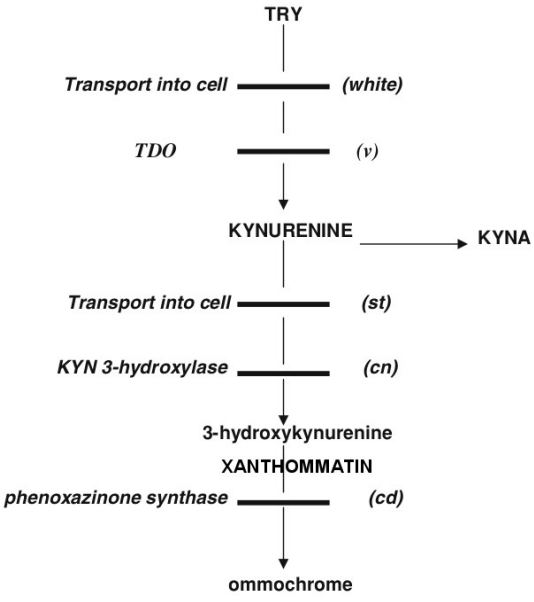

Figure 1.11 The kynurenine pathway of ommochrome metabolism in the eyes of *Drosophila melanogaster*. The vermilion mutant accumulates tryptophane; the cinnabar mutant accumulates kynurenine and kynurenic acid; and the enzyme Phenoxyazinone synthetase is probably defective in white mutants. TRY: tryptophan, TDO: TRY 2,3-dioxygenase, KYNA: kynurenic acid, v vermilion, st scarlet, cn cinnabar, cd cardinal. (Source: Oxenkrug, 2010).

Interestingly, the retinal blindness ceroid neuronal lipofuscinosis may be caused by the accumulation of the lipopigments ceroid and lipofuscin in human neurons (Khan et al., 2013). In the most common form of age-related macular degeneration (AMD), lipofuscin (the lipid-containing residue of outer segment phagocytosis and autophagy) also accumulates within the RPE cells in an inhomogeneous pattern (Fig. 1.12). This may be caused by the oxidative damage the RPE is exposed to with age. Lipofuscin may increase when it is fused with melanosomes that contains melanin, which is photooxidized with age. The highly oxygenated environment, exposition to high levels of visible light and the peroxidation the polyunsaturated fatty acids from photoreceptor outer segment membranes may undergo after phagocytosis, place the RPE at a high risk for oxidative damage (Burke et al., 2005).

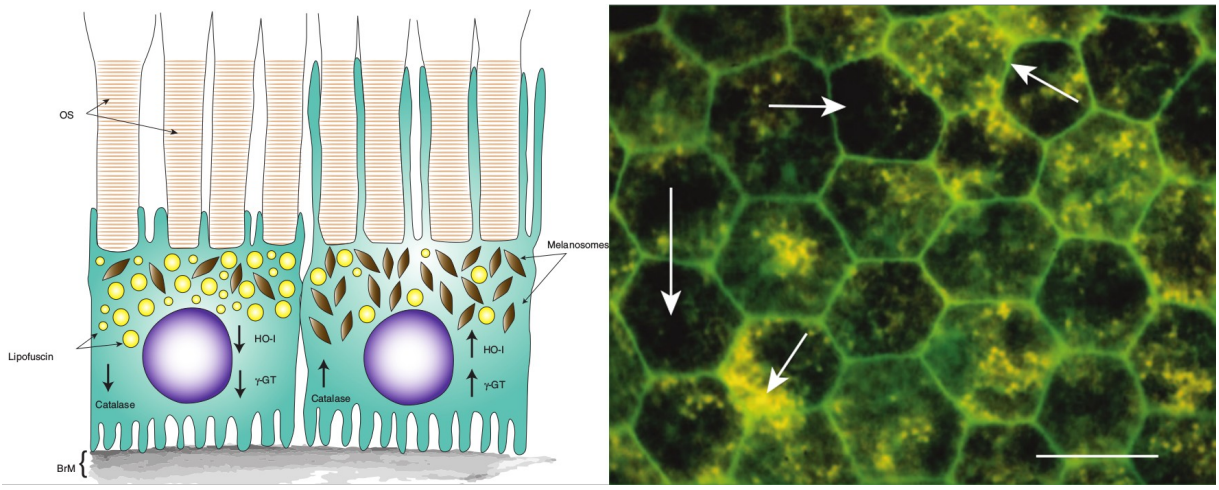

Figure 1.12 Lipofuscin distribution in human retinal pigment epithelium (RPE) cells. Left: RPE cells with differing properties, and their overlying photoreceptors. Melanosomes (brown granules), lipofuscin (yellow granules) and the antioxidant enzymes catalase, haem-oxygenase-1 (HO-1), and γ-glutamyltranspeptidase (γGT) are differently distributed among RPE cells. The apical domain of microvilli interacting with overlying photoreceptors can vary in length between cells. The Bruch's membrane (BrM), located on the basal side of the RPE, contacts the coroid from the opite side of the photoreceptor outer segments (OS). OS are embedded in RPE apical microvilli. **Right:** Whole mount of the human RPE, labelling actin (stained with fluorescein phalloidin) and granule content: brown pigment granules (large arrows), yellow lipofuscin granules (small arrows) and, actin microfilaments (green). Scale bar: 20 μm. (Source: Burke et al., 2005)

Besides ommochromes, it is known that melanin is widely distributed throughout the animal kingdom. However, melanin formation significantly differ from species to species. Insects use dopamine while vertebrates use dopa as the major precursor of melanin formation (Kato et al., 2006). In the pigment granules of pigment cup cells in the planaria *Dugesia ryukyuensis,* 5,6-dihydroxyindole-2-carboxylicacid (DHICA)-derived eumelanin has been found (Hase et al., 2006). In humans and mice melanogenesis, the synthesis of melanin from tyrosine, tyrosinase is responsible for the critical initial rate-limiting steps (Fig. 1.13, A).

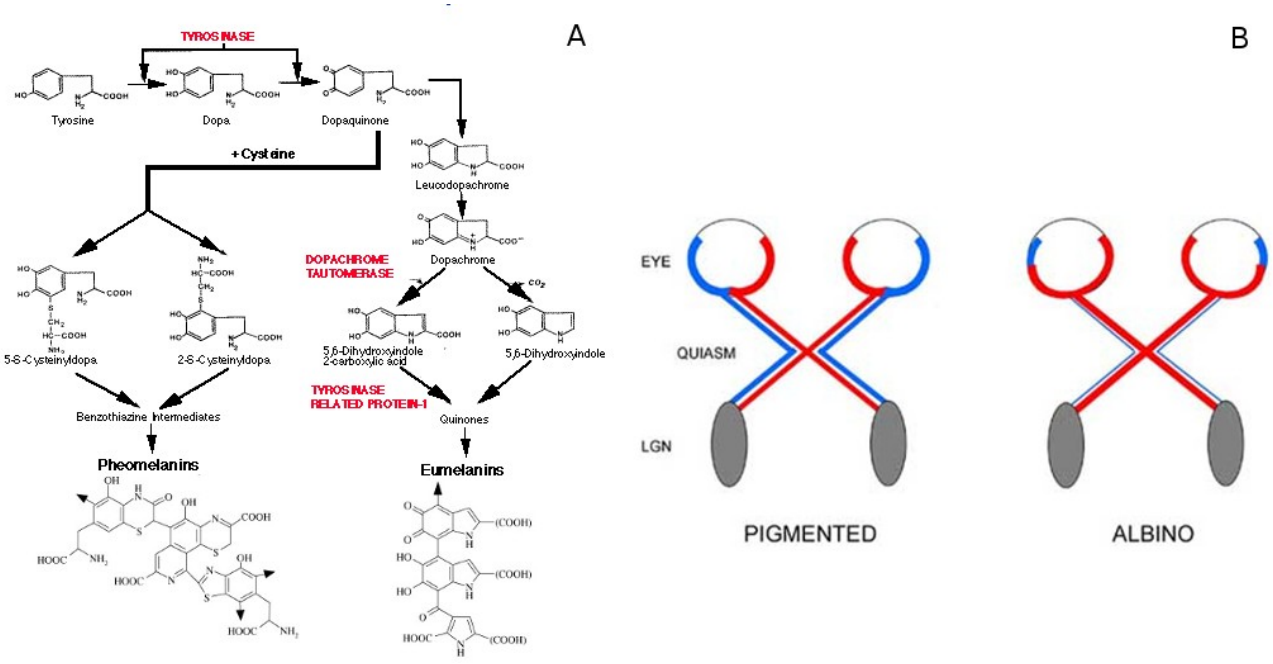

Figure 1.13 The melanin chemical pathway and schematic representation of visual pathways in a pigmented and an albino individual with frontalized eyes (e.g., a primate). (A) The enzyme tyrosinase is responsible for the critical initial rate-limiting steps in melanogenesis. **(B)** Left-hand drawing, a pigmented individual showing the presence of crossed and uncrossed retinal ganglion cell axonal projections going from the eye to the lateral geniculate nucleus (LGN) in the brain through the chiasm. Right-hand drawing, an analogous representation of an albino individual, showing a severe decrease in the uncrossed visual pathway and a corresponding increase in the crossed axonal fibres, caused by a tyrosinase transgene. (Source: A: modified from: http://www.didiersvt.com/cd_1s/html/c7/c7a3.htm ; B: Lavado et al., 2005)

Tyrosinase and melanin have been found in humans and mice skin melanocytes and retinal pigment epithelium. Whereas skin melanocytes produce melanosomes continuously, RPE cells are presumed to create melanosomes only pre-natally. Nevertheless, melanogenesis in RPE cells shares a common pathway with that in melanocytes. Tyrosinase and other melanizing proteins synthesize melanin in the melanosomal membrane, in vesicles, called premelanosomes (Biesemeier et al., 2010).

The absence of or defects in several human genes involved in the melanin pathway, such as tyrosinase, dopachrome tautomerase (TRP2), DHICA oxidase (TRP1), Hermansky-Pudlak syndrome (HPS) and ocular albinism (OA1), causes albinism. In addition to complete or partial hypopigmented skin, hair and eyes, this congenital disorder is characterized by the misrouting of retinal fibres at the optic chiasm (Fig. 1.13, B). Ipsilaterally destined temporal retinal fibres erroneously decussate and project contralaterally at the optic chiasm. The corresponding visual field is a partial mirror inversion of the representation in each hemisphere (Herrera et al., 2008). In addition, it has been shown that the visual photopigment rhodopsin is expressed in human epidermal melanocytes (HEMs) and contributes to solar ultraviolet radiation UVR phototransduction (Palczewski, 2006). This mechanism leads to pigment darkening within minutes (Wicks et al., 2011).

1.4.5 ATP-DEPENDENT PROCESSES (PHOSPHORYLATION)

The phototransduction process in mammals involves several proteins, such as visual pigments, arrestins, G proteins and cGMP-gated channels. In addition, the protein rhodopsin kinase (GRK1) interacts with photoisomerized rhodopsin (Rho*), deactivating the molecule and therefore the transducin-mediated (Gt) signalling, so that Rho* can be regenerated in processes that follow (Fig. 1.14). GRK1 binds to Rho* and phosphorylates Ser and Thr residues in the C-terminus. GRK1 accelerates inactivation of Rho* molecules which, in concert with regeneration leads to the normal rate of recovery of sensitivity (Maeda et al., 2003). Two genes encoding arrestin and GRK1 have been found to be mutated in Oguchi disease, a congenital stationary night blindness (Maeda et al., 2003).

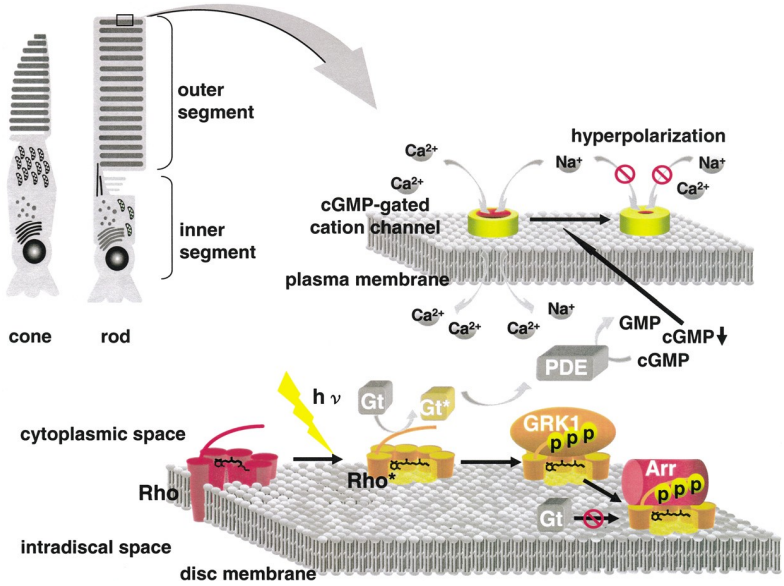

Figure 1.14 Molecular mechanisms of rhodopsin kinase (GRK1) activation. GRK1 is a membrane-associated enzyme that has a low affinity for rhodopsin (Rho). After photoactivation, due to conformational changes in the receptor, GRK1 forms a complex with Rho* by associating with the second and third cytoplasmic loops of the receptor. According to one model, GRK1 becomes activated, dissociates, and phosphorylates the C-terminal region of many Rho. According to another model, GRK1 remains bound and phosphorylates the nearby C-termini of Rho and Rho* at Ser334, Ser338 or Ser343. Phosphorylated Rho is capped by binding arrestin, which prevents any residual Gt activation by metarhodopsin (Meta II). Gt: transducin; Gt*: activated transducin; Arr: arrestin; PDE: phosphodiesterase. (Source: Maeda et al., 2003)

The kinase activity present in retinal outer segments (ROS) also catalyses the phosphorylation of other substrate proteins besides rhodopsin, such as protamines and histones (K˛hn et al., 1978). In the mammalian retinal photoreceptor a kinase, creatine kinase (CK), also catalyses the conversion of creatine and consumes adenosine triphosphate (ATP) to create phosphocreatine (PCr) and adenosine diphosphate (ADP) (Fig. 1.15). This reaction is reversible and the ATP synthase activity thus generates ATP from PCr and ADP (Hemmer et al., 1993). The CK/PCr system connects sites of ATP production (glycolysis and mitochondrial oxidative phosphorylation) with subcellular sites of ATP utilization (ATPases). The CK/PCr system has been found in polar cells such as photoreceptor cells, where diffusion limitations of ADP and ATP are particularly relevant (Walliman et al., 2011).

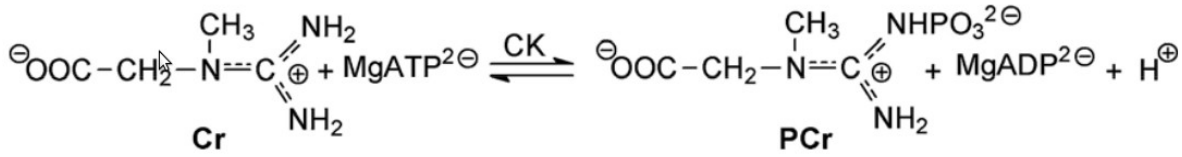

Figure 1.15 Reversible reaction catalysed by creatine kinase in the mammalian photoreceptor. Cr: creatine; PCr: phosphocreatine; CK: creatine kinase. (Source: Teixeira et al., 2012)

Due to the specialization of polarized neurons, the mammalian retinal photoreceptor rod outer segment (OS) is devoid of mitochondria. Nevertheless, processes requiring energy take place in the OS, such as the production, transport and recycling of photopigments, retinal chromophore isomerization from all-*trans* to 11-*cis* and the phagocytosis of 10% of the mass of each photoreceptor outer segment from the RPE as part of the diurnal schedule. The energy supply for these processes still remains controversial, because glycolysis does not seem sufficient. It has been proposed that the necessary energy may be supplied by oxidative phosphorylation (OXPHOS), by the versatile activity of phosphocreatine (PCr) as an ATP reservoir, by ATP transport, by ATP regeneration in situ and rapid buffering, or by one protein with both ATPase and ATP synthase activities (Calzia et al., 2013). The mechanism of energy supply in the rhabdomere of *S. mediterranea* is unknown.

Another substrate for a kinase enzyme is the protein Bardet–Biedl syndrome 5 (BBS5). In dark adapted rods, Arrestin 1 binds to BBS5. Light stimulates the activation of protein kinase C (PKC) which phosphorylates BBS5, in this way allowing the release of Arrestin 1 (Arr1). The detachment of Arrestin1 from BBS5 enables it to bind to rhodopsin (Fig. 1.16) (Smith et al., 2013).

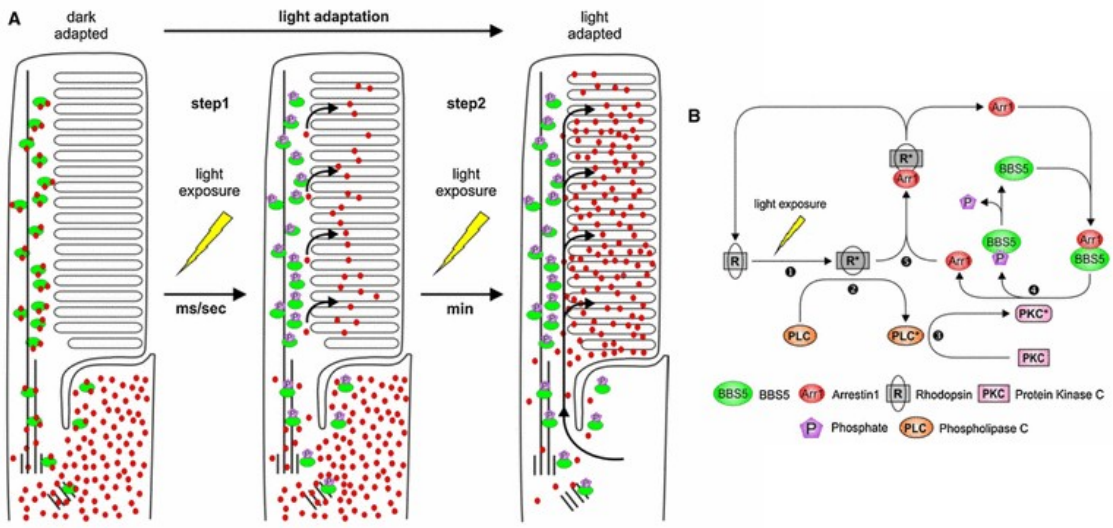

Figure 1.16 Model for the localization of the phospholipase C protein, kinase C (PKC) protein, Bardet–Biedl syndrome 5 (BBS5) and Arrestin 1 (Arr) in mouse rod photoreceptors. (A) In the dark, Arr1 (red dots) localizes in the inner segment, binds to BBS5 (green ovals) and moves along the axoneme. Upon light exposure, BBS5 is phosphorylated by PKC, releasing Arr1 into the OS disks and shutting down activated rhodopsin signalling. **(B)** Signal cascade in A: light activation of rhodopsin (R) (1), signalling through an undefined G-protein, leads to activation of phospholipase C (PLC) (2), and protein kinase C (PKC) (3), which phosphorylates BBS5 along the axoneme (4). Arr1 has a reduced affinity for phospho-BBS5 and can now diffuse throughout the OS and interact with activated rhodopsin (R*) (5). (Source: Smith et al., 2013)

Mutations in the mitochondrial F-type ATP synthase F0 subunit 6 gene (ATP6) causes, among other brain lesions, retinitis pigmentosa: a degenerative eye disease that causes severe vision impairment and often blindness (Schon et al., 2001). While energy metabolism in the vertebrate rod OS remains obscure (Calzia et al., 2013), the relation between photoreceptor cells and ATP synthases found in the archaea *Halobacterium salinarum* and in marine proteobacteria is much more clear (Bryant et al., 2006). Although the archaea *H. salinarum* is not photosynthetic, it has a mechanism for producing ATP by using sunlight to generate a proton gradient directly. Under anaerobic conditions, this archaea synthesizes a light-driven proton pump, (BR); a seven-membrane helical protein (Fig. 1.17) (Shibata et al., 2010). The protons exported from BR, flow into the cell through the ATPase, completing the circuit by building ATP (Oesterhelt, 1998; Haupts et al., 1999). The structure and function of ATP synthases/ATPase, as well as the type of ions they transport, are optimized in response to environmental conditions (Cross et al., 2004; Miranda-Astudillo, 2012). Therefore, it is not surprising that this protein has specialized in different cell types or organelles; A ATP synthase is present in archaea, F ATP synthase in bacteria, mitochondria, and chloroplasts, and V ATPase in eukaryotes (Miranda-Astudillo, 2012). Understanding the differences in the ATPase subunits would shed light on the functioning of energetic processes in planarian photoreceptors.

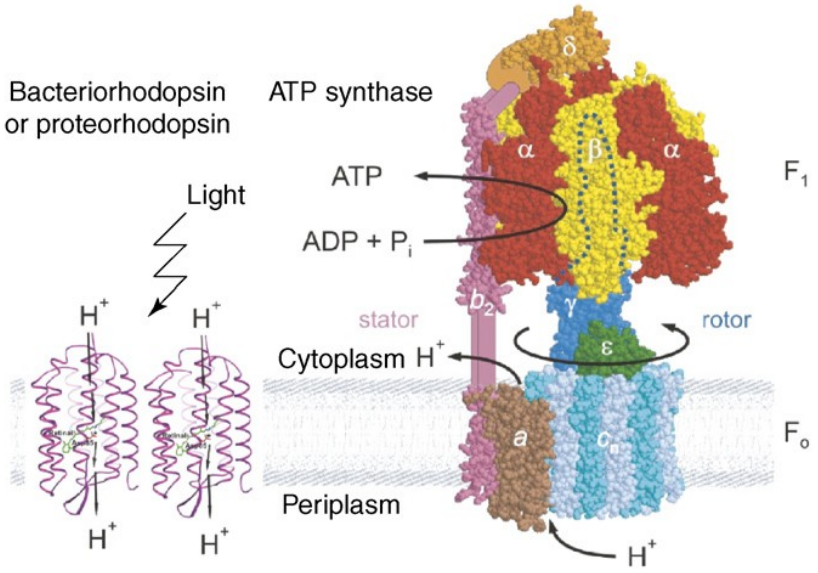

Figure 1.17 Chemiosmotic coupling between solar energy, bacteriorhodopsin, (BR) proteorhodopsin (PR) and phosphorylation by ATP synthase (chemical energy) in *Halobacterium salinarum* and marine proteobacteria. Absorption of light (500-650 nm) by retinal leads its isomerization causing a conformational change in PR or BR, which in turn leads to the expulsion of a proton into the periplasmic space. Translocation of protons to the cytoplasm is coupled to the synthesis and release of cytoplasmic ATP by ATP synthase. (Source: Bryant et al., 2006)

1.4.6 Structural proteins

The vertebrate photoreceptor outer segment contains the enzyme cascades responsible for phototransduction, while the inner segment houses the basic machinery required for cell metabolism. Between those compartments extensive bidirectional intracellular transport is necessary through the connecting cilium; a structure formed mainly of microtubules (Sedmak et al., 2010). Centrin proteins, which have four calcium-binding EF-hands (Salisbury, et al., 2002), are expressed in the connecting cilium in mammal photoreceptor cells and play an essential role in centriole (centrosome) duplication and separation during the cell cycle. In bovine, human and rat retina, centrin is localized at the connecting cilium of photoreceptor cells and in the centrosome of non-ciliated neuronal cells (Fig. 1.18) (Wolfrum et al., 1998). In addition, genes encoding proteins of the connecting cilium in photoreceptor cells have been identified as possible points of defects leading to the development of Usher syndrome: a disease which causes combined blindness and deafness and may lead to disorders in olfaction (Wolfrum et al., 1998).

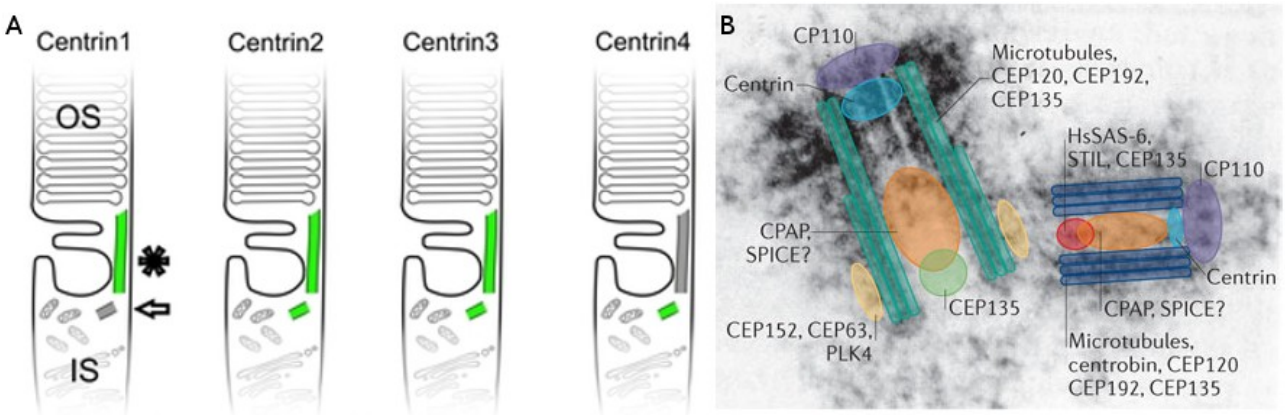

Figure 1. 18 Localization of four mammalian centrin isoforms in the compartments of the ciliary apparatus of photoreceptor cells and human centriolar and procentriolar proteins. (A) Graphic representation of Cen1p to 4p, differentially expressed in the the centriole/basal body and the connecting cilium. Centrins play an important role in centriole duplication. **(B)** Centrin is found towards the distal end of both procentriole and centriole, occupying a larger domain in the centriole. Polo-like kinase 4 (PLK4), spindle assembly abnormal protein 6 (HsSAS-6), centrosomal protein of 135 kDa (CEP135), spindle and centriole-associated protein (SPICE) (the question marks indicate position without accuracy), centriolar coiled-coil protein of 110 kDa (CP110), SCL/TAL1 interrupting locus (STIL). (Source: (A) http://www.ag-wolfrum.bio.uni-mainz.de/66_ENG_HTML.php; (B) Gˆnczy, 2012)

The *Drosophila* transport mechanisms through the rhabdomere actin microfilament web is similar to that one through the microtubule base connecting cilium in ciliary photoreceptors (Li et al., 2007). Microtubules (25 nm α-β-tubulin dimers) and microfilaments (5-7 nm actin proteins) are both assembled from highly conserved globular proteins that have nucleotide-binding and hydrolysing activity (Chang et al., 2004). They both share a plus end and a minus end; so unlike intermediate filaments (10 nm, vimentin, keratin, neurofilament proteins or nuclear lamins), microtubules and microfilaments are polar, which is the basis for cell motility and intracellular transport. Actin filaments (microfilaments) are present in mouse and human photoreceptor connecting cilium and in the microvilli of the RPE (Fig. 1.19) (El-Amraoui et al., 2005). In addition, it is well established that a dynamic and highly motile actin-based structure found at the growing end of a developing axon, known as a growth cone, facilitates the process of neural development (Medeiros et al., 2006).

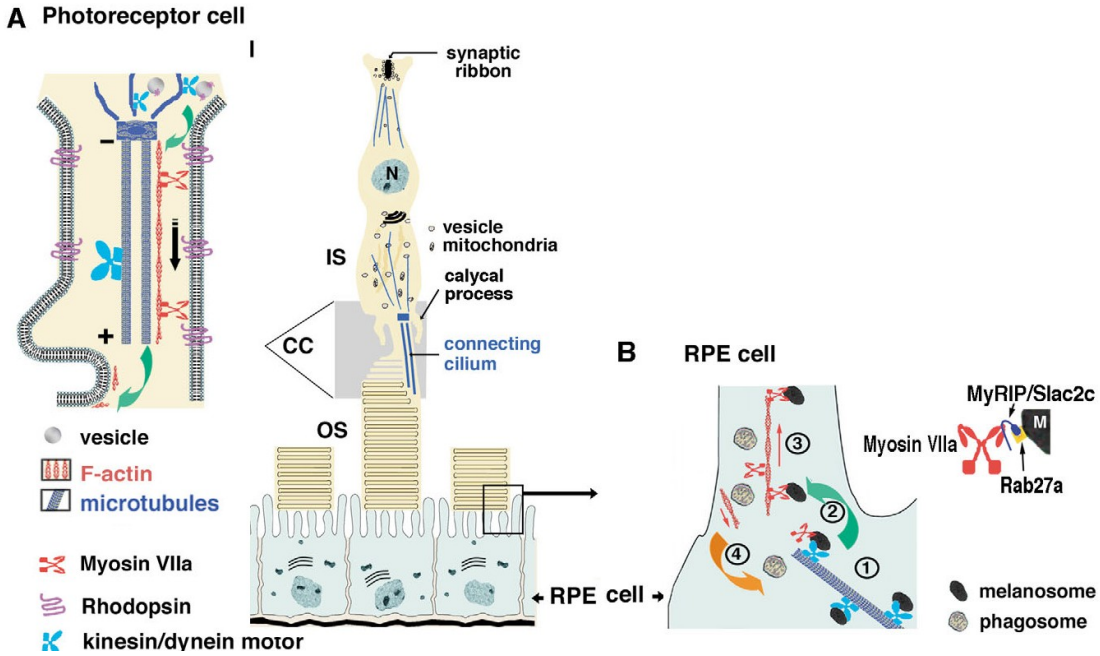

Figure 1.19 Photoreceptor and retinal pigment epithelial (RPE) cells with actin microfilaments. **(A)** At the tip of the photoreceptor inner segment actin microfilaments together with myosin VIIa may be involved in opsin transfer (green arrow) to the connecting cilium and its transport to the outer segments (OS). **(B)** In RPE cells, melanosomes (M) display fast, bidirectional microtubule-dependent long-range movements in the cell body driven by kinesin/dynein motor proteins (1). Upon reaching the plus end of the microtubule at the periphery, myosin VIIa may be involved in the transfer (green arrow) of these organelles towards the actin filaments (2). Rab27a, which is attached to the melanosome membrane, interacts with its effector, MyRIP/Slac2c, which in turn binds to myosin VIIa. Myosin VIIa then enables the retention and/or local movement of the melanosomes along the actin filaments of the microvilli (3). Myosin VIIa also plays a role in the transfer of phagosomes from the microvilli to the cell body (4; orange arrow). N, nucleus. (Source: El-Amraoui et al., 2005)

Defects associated with cilia function can lead to a significant number of human diseases (so-called ciliopathies) including reproductive problems, kidney defects, blindness, and respiratory problems (Obado et al., 2012). Although cilia do not have a membrane physically separating them from the rest of the cytoplasm, they form a selective barrier that concentrates certain proteins within the cilia but excludes others. The ciliary base contains a ciliary pore complex (CPC) whose molecular nature and selective mechanism are similar to the nuclear pore complex (NPC). A fundamental part of this selective diffusion barrier are the nucleoporins (Nups), located at the base of cilia in the region termed the transition zone, which have the same functionality as the NPC machinery in the nuclear envelope (Fig. 1.20, A-B) (Breslow et al., 2013). In the NPC, these proteins form the key framework for the correct placement of the Phenylalanine-Glycine repeat (FG) Nups throughout the central channel, and it is tempting to speculate that they perform a similar role in the ciliary barrier (Obado et al., 2012; Kee et al., 2012)

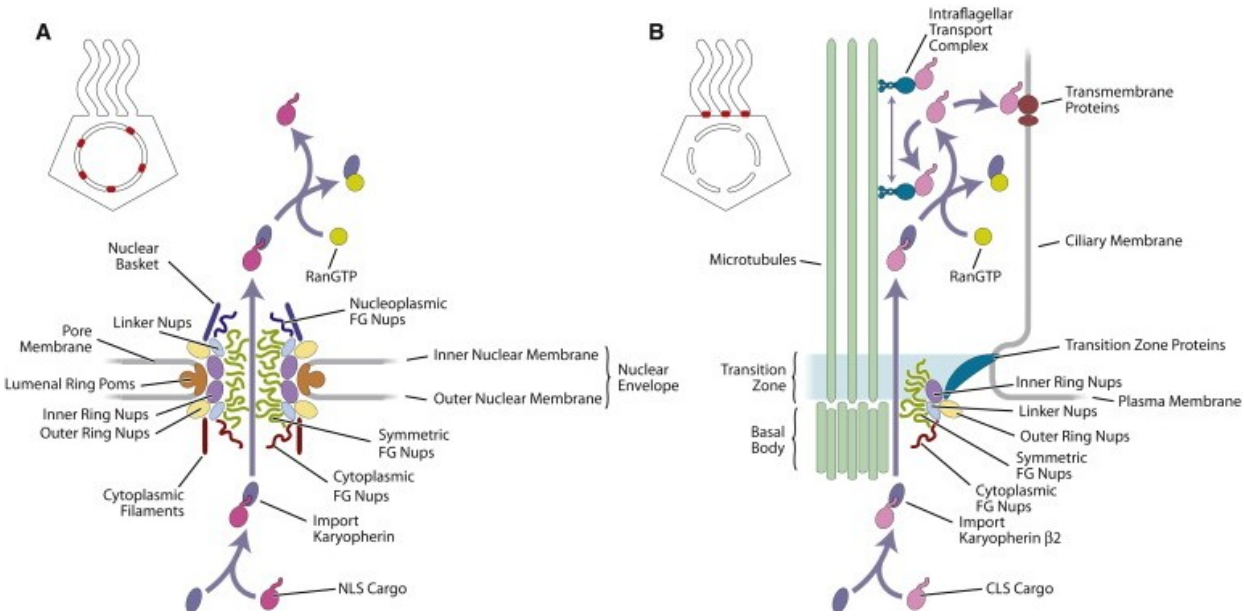

Figure 1.20 Structural and transport features of the nuclear and ciliary pore complexes. Highlights of the similarities between the nuclear pore complex (A) and the ciliary barrier (B) showing the hypothetical route of a cargo protein through each type of barrier. (Position of each shown in inset diagram of ciliated eukaryotic cell.) FG Nups (containing Phenylalanine-Glycine repeats) provide docking sites for transport factors called karyopherins, which bind nuclear or ciliary localization signals (NLSs and CLSs, respectively) containing cargo and facilitate nuclear and ciliary transport. So-called transition zone proteins in cilia connect the plasma membrane and the region between the microtubules and the basal body. The ciliary pore complex is thought to be located in this zone. (Source: Obado et al., 2012)

The Drosophila Ras–MAP kinase pathway removes two general barriers to photoreceptor differentiation: the protein Yan and the *tramtrack* gene (*ttk*) (Fig. 1.21). The first barrier, Yan, is an inhibitor of differentiation in both neuronal and non-neuronal tissues. As an MAP kinase substrate, Yan is capable of being phosphorylated and consequently degraded, permitting cell differentiation. The second barrier, the product of the *tramtrack* gene (*ttk*), specifically blocks neuronal differentiation. A product of the Ras–MAP kinase pathway, *phyllopod* (*phyl*) together with *seven in absentia* (*sina*), target *ttk* for degradation via the ubiquitin–proteasome pathway, thereby facilitating neuronal differentiation (Dickson, 1998).

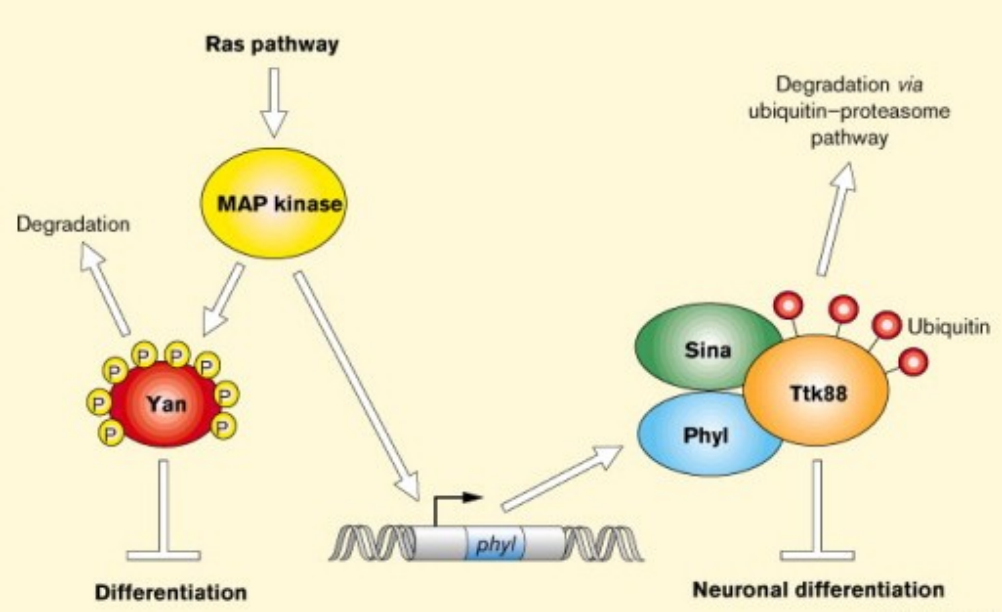

Figure 1.21 Model for the initial steps in Drosophila photoreceptor differentiation. Activation of the Ras–MAP kinase pathways leads to the phosphorylation of Yan and transcriptional activation of the *phyl* gene. Upon phosphorylation, Yan is degraded, allowing differentiation to occur. The Phyl protein then cooperates with Sina to target Ttk88 for degradation via the ubiquitin–proteasome pathway, thereby permitting neuronal differentiation (Dickson, 1998)

In summary, each single process of energy supply, transport, phototransduction and structure formation related to the eye organ requires specific key proteins. The aim of this study is to find them in this flatworm and elucidate whether they have different or the same functions as in other organisms.

2. OBJECTIVES

2.1 The principal aims of this thesis are:

a) to find genes involved in the regeneration and development of *S. mediterranea* eyes;

b) to study the function of selected genes during the regeneration process by interfering with their messenger RNA and analysing their mRNA expression patterns.

2.2 The specific aims of this thesis are:

1. to find in silico *S. mediterranea* DNA sequences in both public and tailor-made databases using the eye gene ontology;
2. to clone selected genes and characterize their messenger RNA expression patterns;
3. to determine the functional activity of the selected genes by observing external morphological changes after interfering with messenger RNA, followed by decapitation and regeneration;
4. to analyse the possible non-visible phenotypes of candidate genes with eye regeneration defects, using hybridization with specific neuronal markers.

3. Results and discussion

3.1 Selection of candidate genes

The capacity to convert light into chemical energy (i.e., ATP) or information (i.e., an intracellular signal) requires at least the activation of a photoreceptor containing one or more photoactive pigments called chromophores (Sancar, 2000). BR from *Halobacterium salinarum* is an example of a light-driven proton pump and HR from the same organism is able to pump chloride (Spudich, 2006). In contrast, the capture of light by the human retinal rhodopsins and cone-opsins stimulates transduction signals to the brain and forms images. The next structures found in nature to be associated with visual perception are the pigment cells. These can be seen as a simple spot, as in the *Euglena gracilis* stigma (Daiker et al., 2011), or as RPE in metazooans (Burke et al., 2005). The complexity of the rhabdomeric eye of *Gonodactylus smithii* enables it to sense ultraviolet, infrared and polarized light (Kleinlogel et al., 2008). The aim of this study was to find and analyse orthologues or new genes necessary to differentiate stem cells into specialized photoreceptors and genes involved in their signal cascades.

The sequences cloned here were obtained from three different sources: the NCBI, four distinct 454 pyrosequencing transcriptomes, and an eye-related Smed-Microarray.

Three sequences were extracted from the NCBI public database and 37 from the 454 Expressed Sequence Tags (EST). The ESTs obtained from *S. mediterranea* cDNA were processed by 4 individual 454 pyrosequencing approaches: the 454EST_Abril (Abril et al., 2010) database generated by our group at the University of Barcelona in 2010, and the Ilumina genome sequences generated by 3 European research groups: 454EST_Rajewsky, 454EST_Kerstin and 454EST_Aziz (Adamidi et al., 2011; Sandmann et al., 2011; Blythe et al., 2010). None of these four transcriptomes was specifically designed to find eye genes. Therefore, the gene search was based on gene ontology through the Blast2go approach. Word searching revealed long lists of opsins, photoreceptors, eye-related transcription factors, cryptochromes, and different enzyme genes that were picked out by hand. The majority of the gene names used were the acronyms of their Blast2go or Blastx-alignments homologues.

Meanwhile, 11 sequences from the Smed-Microarray database, constructed by Kay Eckelt, were also analysed in this study (doctoral thesis Eckelt, 2011, Universitat de Barcelona). The Smed-Microarray results and presented and discussed in section 3.9 below.

Cloned DNA sequences were used for in situ hybridization and RNAi experiments in fixed and living *S. mediterranea* flatworms (see the Material and methods section). Loss-of-function experiments and messenger RNA expression in *S. mediterranea* are a source of valuable information in the search for the functionality of a gene. In addition, the regeneration provoked after every RNAi, induced an embryon-like-stage, very useful for developing an understanding of differentiated cells.

3.2 Sequence Cloning

Two distinct methods were used to amplify DNA: TA and T7 cloning (see the Material and methods section). Both techniques require the use of at least two primer pairs: the sequence specific and the technique specific the T7-Universal primer or the M13 primer. Nevertheless, in some cases a third primer pair (the nested primer) was employed to improve the amount of PCR product. No differences were appreciated and following cloning was performed without a nested primer.

Although the TA method took longer, all the sequences inserted into the *E. coli* plasmid were successfully cloned. In contrast, 2 out of 40 sequences could not be amplified by the T7 method. This might be attributed to a mistaken DNA assembly in the 454 technique. This sequencing technology produced contigs that were the result of at least two sequencing reads and singletons of only one read. The singletons were sequencing reads with an average length of 327 bp (Abril et al., 2010).

Table 5 (List of eye-related gene sequence candidates*)* in Abril et al., 2010 shows some of the genes cloned in this study. Table 3.1, Table 3.2, Table 3.3, Table 3.4, Table 3.5 and Table 3.6 shows all the genes cloned; while in the Material and methods section, Table 5.1, Table 5.2, Table 5.3, Table 5.4 and Table 5.5, give the primers.

3.3 Functional study of candidate genes: interference with double-strain-mRNA (RNAi) and in situ hybridization

The chosen genes were divided into six groups. Five of them were formed depending on the putative protein functions: first opsins (Table 3.1), second those related to pigment biosynthesis (Table 3.2), third transcription factors (Table 3.3), fourth enzymes (Table 3.4) and finally transport and signalling proteins (Table 3.5). The rest of the genes belong to the Smed-Microarray selection. These genes were expressed at high levels in the anterior blastema of regenerating flatworms (Table 3.6). Full names, putative functions, homologue proteins, mRNA expression and RNAi phenotype of these genes can be found in the corresponding tables. The sequences *Smed-mrp1* and *Smed-mrp2* are fragments of the same gene. The sequences *Smed-white-sf1* and *Smed-white-sf2* also belong to a single gene.

The RNAi results were offered here as descriptive statistical analysis.

3.3.1 Phototaxis assay

The eyesight of RNAi flatworms tested with the Phototaxis assay were not conclusive enough to be taken into account. To be able to decide if a flatworm has completely or partially lost its sight, facts or evidence are required. Avoidance behaviour could not be demostrated. Either not enough mutant flatworms were available, or the software programs used were not prepared for this slippery organism. "*Trake*r" and "*Smart*" (*Panlab s.l.u*.) are good software programs for tracking, for example, maze of locomotor activity in mice; but they collapsed when trying to recognize and analyse the films of *S. mediterranea*. The outlines and body colour changes in *S. mediterranea* moving in three dimensions. In addition, their size combined with the light gradient necessary to provide the light conditions for the test prevented the capture of contrasted images. Although an attempt was made in the field to improve the quality of automated image analysis for planarians, the issue remains unsolved. "*ImagePlane*" (Flygare et al., 2013) covers the essential activities of: automatic determination of animal outline and size; automatic image thresholding; methods for counting labelled populations of cells; and quantification and sectorization of morphological changes induced by experimental manipulations. Nevertheless, no moving animals can be assessed with these algorithms. Furthermore, the "*Sensory Orientation Software*" (*SOS*) (Gomez-Marin et al., 2012), an image analysis system for tracking body posture and motion of single animals in two dimensions, has not been adapted to the three dimensional movement of the planarian *S. mediterranea*.

Table 3.1: Summary of experimental validation of putative opsin and other light sensor genes. The phenotypes here were found at least in one animal.

Smed gene	Name, proposed structure and function in other organism	E-value	mRNA expression	RNAi phenotype	Phenotype Penetrance %
Smed-rhodopsin1	Rhodopsin1, 7TM receptor protein (rhodopsin family), photoreception	5e-12 *Schistosoma mansoni* [flatworms]	Parenchyma	Hypopigmented reduced eye cups	20
Smed-rhodopsin2	Rhodopsin2, 7TM receptor (rhodopsin family), photoreception	9e-22 *Clonorchis sinensis* [flatworms]	Parenchyma	Underdeveloped eyes	30
Smed-rhodopsin10	Rhodopsin10, 7TM receptor protein (rhodopsin family), photoreception	3e-27 *Pediculus humanus corporis*	Parenchyma	Eye and skin pigmentation defects	20
Smed-rhodopsin4	Rhodopsin3, 7TM receptor protein (rhodopsin family), photoreception	7e-20 *Schistosoma mansoni* [flatworms]	Parenchyma	No phenotype	—
Smed-rhodopsin5	Rhodopsin5, 7TM receptor protein (rhodopsin family), photoreception	2e-20 *Todarodes pacificus* [cephalopods]	Parenchyma	No phenotype	—
Smed-rhodopsin7	Rhodopsin7, 7TM receptor protein (rhodopsin family), photoreception	3.0 *Anolis carolinensis* [lizards]	Parenchyma	No phenotype	—
Smed-rhodopsin8	Rhodopsin8, 7TM receptor protein (rhodopsin family), photoreception	2e-23 *Pediculus humanus corporis*	Parenchyma	No phenotype	—
Smed-rhodopsin9	Rhodopsin9, 7TM receptor protein (rhodopsin family), melatonin receptor	0.49 *Xenopus laevis* [frogs & toads]	Parenchyma	No phenotype	—
Smed-peropsin1	Peropsin1, 7TM receptor (rhodopsin family) , long wavelength phototoreception	6e-13 *Platynereis dumerilii* [segmented worms]	Parenchyma, photoreceptor cells	No phenotype	—
Smed-melanopsin3	Melanopsin-A-like, 7TM receptor (rhodopsin family), non-visual photoreception	2e-21 *Oreochromis niloticus* [bony fishes]	Eyes, tip of the head, pharynx, parenchyma	Eye and skin pigmentation defects	26
Smed-melanopsin2	Melanopsin2, 7TM receptor, short-wavelength (rhodopsin family), non-visual photoreception	7e-15 *Acanthopagrus butcheri* [bony fishes]	Parenchyma or no expression	Eye defects	30
Smed-melanopsin1	Melanopsin1, 7TM receptor (rhodopsin family), non-visual photoreception	2e-37 *Danio rerio* [bony fishes]	Cephalic ganglia, eyes	No phenotype	—
Smed-cry	Cryptochrom, FAD binding domain of DNA photolyase, photic entraiment	1e-103 *Amphimedon queenslandica* [sponges]	Parenchyma (Appendix)	Eye, skin pigmentation defects (Appendix)	16
Smed-blue-opsin	Blue opsin, 7TM protein (rhodopsin family), short-wavelength non-visual fotoreception	6e-12 *Gadus morhua* [bony fishes]	Parenchyma (Appendix)	No phenotype (Appendix)	—

Table 3.2: Summary of experimental validation of putative pigment biosyntesis related genes. The phenotypes here were found at least in one animal.

Smed gene	Name, proposed structure and function in other organism	E-value	mRNA expression	RNAi phenotype	Phenotype Penetrance %
Smed-white-sf1	White, ABC transporter, eye pigment precursor transporter	3e-57 *Drosophila melanogaster* [flies]	Intestine	Eye defects, regeneration defects	10
Smed-white-sf2	White, ABC transporter, eye pigment precursor transporter	1e-140 *Drosophila melanogaster* [flies]	Intestine	Eye defects	5
Smed-ver	Vermilion, tryptophan 2,3-dioxygenase, enzym for kynurenine (eye brown pigment) biosynthese	1e-126 *Drosophila ananassae* [flies]	Expanded ventral cg, pc	No phenotype	—
Smed-ncl	Neuronal ceroid lipofuscinosis, TLC transmembrane domain, retinal turnover, implicate in macula	1e-47 *Homo sapiens*	Parenchyma (Appendix)	Skin pigmentation defects (Appendix)	20

Table 3.3: Summary of experimental validation of putative transcription factors. The phenotypes here were found at least in one animal.

Smed gene	Name, proposed structure and function in other organism	E-value	mRNA expression	RNAi phenotype	Phenotype Penetrance %
Smed-exd (pbx)	Extra denticle, homeodomain of helix-turn-helix and 3 alpha helices, transcription factor (Abril et al., 2010) (Chen, 2013) (Blassberg, 2013)	0.0 *S. mediterranea*	Parenchyma not defined	Eye defects	32
Smed-mitf1	Microphthalmia-associated transcription factor, basic helix-loop-helix leucine zipper DNA-binding domain, melanocyte and osteoclast development	1e-06 *Drosophila melanogaster*	Parenchyma	No phenotype	—
Smed-mitf2	Microphthalmia-associated transcription factor, basic helix-loop-helix leucine zipper DNA-binding domain, melanocyte and osteoclast development	6e-05 *Pundamilia nyererei* [bony fishes]	Parenchyma	Eye defects, skin pigment defect	100
Smed-mitf3	Microphthalmia-associated transcription factor, basic helix-loop-helix leucine zipper DNA-binding domain, involved in melanocyte and osteoclast development	4e-04 *Aplysia californica*	Parenchyma	Eye defects, skin pigment defect	80
Smed-hox1	Homeobox 1, CASP C-terminal homeobox, transcription factor	9e-26 *Mus musculus*	Photoreceptors neurons, pharenchyma	Regeneration failed	100
Smed-hox2	Homeobox 2, homeobox domain, transcription factor	1e-46 *Danio rerio* [bony fishes]	Expanded cg, pc, defined around the intestine	Eye pigment cells defects	20
Smed-tlx	T-cell leukemia homeobox protein 3, homeobox domain, transcription factor	9e-42 *Capitella teleta* [segmented worms]	Parenchyma, defined around the intestine	No phenotype	—
Smed-hmt	Histone lysine methyltransferase, SET domain enhancer of zeste, epigenetic transcription factor	8e-75 *Schistosoma mansoni*	Distal eyes, intestine	No phenotype	—
Smed-yyl	Yin Yang 1, zinc finger double domain, transcriptional repressor protein	1e-56 *Daphnia pulex* [crustaceans]	Eyes, parenchyma	No phenotype	—
Smed-fox	Forkhead box, winged helix xfd-11, transcription factor	6e-51 *Nasonia vitripennis* [wasps &c.]	Parenchyma	No phenotype	—

Table 3.4: Summary of experimental validation of putative enzymes. The phenotypes here were found at least in one animal.

Smed gene	Name, proposed structure and function in other organism	E-value	mRNA expression	RNAi phenotype	Phenotype Penetrance %
Smed-tpr1	Tetratrico Peptide Repeat domain from tyrosine-hydroxilase. Catalyses the conversion of L-tyrosine to L-DOPA, which is the melanin synthesis initial step in melanocytes and retinal pigment epithelium (RPE) cells.	2e-115 *Mus musculus* [rodent]	Photoreceptor neurons, parenchyma	Head and pharynx fissioning	54
Smed-tpr2	Tetratrico Peptide Repeat domain from tyrosine-hydroxilase. Melanin synthesis in melanocytes and retinal pigment epithelium (RPE) cells.	2e-104 *Nasonia vitripennis* [wasp]	Parenchyma, cephalic ganglia	Head with one eye	9
Smed-kinase	Serine/threonine-protein kinase. Involved in rhodopsin phosphorilation and regulation of photoreceptor cell morphogenesis.	1e-149 *Schistosoma mansoni* [flatworm]	Photoreceptor neurons	Regeneration failed, death	100
Smed-VATP-syntase	Vacuolar ATP-syntase subunit C in retinitis pigmentose.	3e-75 *Homo sapiens* [primates]	Parenchyma around the intestine	Regeneration failed, early death	100

Table 3.5: Summary of experimental validation of putative transport and signaling related genes. The phenotypes here were found at least in one animal.

Smed gene	Name, proposed structure and function in other organism	E-value	mRNA expression	RNAi phenotype	Phenotype Penetrance %
Smed-dye	dead eye, Nic96 nucleoporin domain, nucleous transport	6e-16 *Oncorhynchus mykiss* [bony fishes]	Parenchyma around the intestine	Eye and regeneration defects	100
Smed-centrin	Centrin-1: EF hand motif, transport of the G-protein localiced in ciliarted cells like photoreceptors	5e-92 *Danio rerio* [bony fishes]	Parenchyma	Eye and regeneration defects	100
Smed-bbs	Bardet Biedl Syndrom, TRP tetratricopeptide repeat, transport protein across the photoreceptor-connecting cilium	1e-130 *Homo sapiens* [primates]	Parenchyma (Appendix)	No effect (Appendix)	—
Smed-ras	Rats sarcoma, six-stranded beta sheet and 5 alpha helices, signal transduction in photoreceptors	4e-98 *Drosophila melanogaster* [flies]	Parenchyma (Appendix)	No effect (Appendix)	—

Table 3.6: Summary of experimental Smed-microarray genes validation. The phenotypes here were found at least in one animal.

Smed gene	Name, proposed structure and function in other organism	E-value	mRNA expression	RNAi phenotype	Phenotype Penetrance %
Smed-mrp1	Multidrug resistance protein, ABC transporter for toxic reagents out of the cell (Toyoda et al., 2008)	2e-31 *Danio rerio*	Photoreceptors, parenchym	Eye defects	100
Smed-mrp2	Multidrug resistance-associated protein 1-like, ATP binding cassette, transmembrane ABC transporter	4e-50 *Ciona intestinalis*	Photoreceptors, distal part of the pharynx	Eye defects	100
Smed-fgfl	Nou darake 3, fibroblast growth factor, unknown funktion	0.0 *Schmidtea mediterranea* (Rink et al 2009)	Ubiquitous parenchym, pharynx	No effect	—
Smed-titin	Nou darake 3, fibroblast growth factor, unknown function	0.0 *Schmidtea mediterranea* (Rink et al 2009)	Ubiquitous parenchym, pharynx	No effect	—
Smed-fib	Fibropellin jagged, human growth factor like domain, EGF membran protein, signal transduction, nou- darake	1e-12 *Homo sapiens* [primates]	CNS: subepidermic nerve cords, cg, pharynx	No effect	—
Smed-duk3	Domain of unknown function	domain of unknown function	Dorsal and ventral lateral bands	No effect	—
Smed-duk5	Domain of unknown function	domain of unknown function	Pharynx, parenchym	No effect	—
Smed-duk6	Domain of unknown function	domain of unknown function	Cephalic ganglia, parenchym	No effect	—
Smed-duk10	Domain of unknown function	domain of unknown function	CNS without nerve cords	No effect	—
Smed-snap	Small nuclear RNA activating complex, Helix turn helix, Myb-like DNA-binding domain, transcription factor	0.009 *Macaca mulatta*	Ubiquitous parenchym (Appendix)	No effect (Appendix)	—
Smed-myb	Mind bomb, GRF zinc binding domain, DNA-binding protein, transcription factor	9e-36 *Strongylocentrotus purpuratus* [sea urchins]	Parenchym, cephalic ganglia (Appendix)	No effect (Appendix)	—

3.3.2 RNAi probes

RNA interference with *Smed-six* causes the loss of the capacity to regenerate the eyes after amputation of the head (Pineda et al., 2000; Lapan et al., 2011). It has been found that the penetrance and the lifespan of the phenotype of *Smed-six* hardly depends on the amount of RNA injected. Injections of 27ng/µL of *Smed-six* mRNA were more effective than 155 ng/µL. This might be caused by an increase in the RNA degradation pathway, stimulated by the presence of higher amounts of mRNA (Silverman, 2007; Houseley et al., 2009). On the other hand, the structure of mature eukaryotic mRNA includes the 5' cap, the 5' UTR, the coding region, the 3' UTR and the poly(A) tail. Because the cloning technique does not always permit us to amplify fully mature mRNA, it is probably more susceptible to being broken up by the action of enzymes, inducing at the same time the transcription of more exonucleases (Silverman, 2007).

The Figures 3.3.1, 3.3.2, 3.3.3 and 3.3.4 summarize the positive and the negative controls used in this study; *Smed-six* and *Jellyfish-gfp (GFP),* respectively. The Figure 3.3.4 shows the GFP controls for low dose injections, which did not show any regeneration difference compare with the normal GFP doses. No distinguishable regeneration was appreciated in the flatworms injected with the GFP mRNA and the regenerating wild type. Figures 3.3.2 and 3.3.3 summarize the most significant time points of the control (GFP) injections, where differences could be observed, despite the fact that each experiment has its own control.

Even though several methods of photographing living planarians have been tested (Stevenson et al., 2010), there is no standardized technique. The approaches used to produce photographs have been changed during the course of this thesis in order to improve the quality of the images.

Differences in the colour of the planarian skin and background affected on the adjustment of the microscope, always trying to get the best contrast.

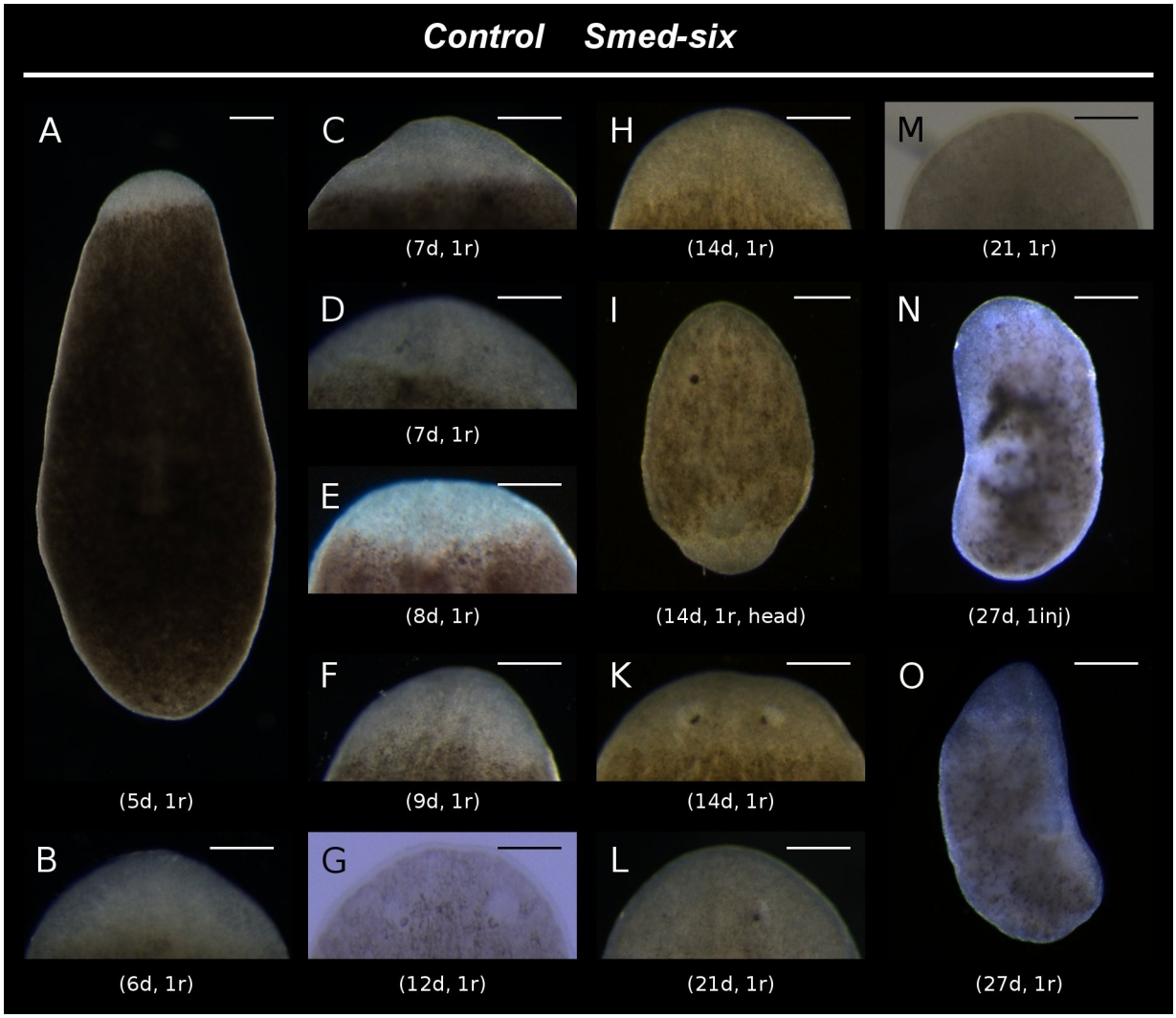

Figure 3.3.1 ***Smed-six*** **RNA interference**. The amount of mRNA injected determined the eye phenotype penetrance. Flatworms injected with 27 ng/µL *Smed-six* mRNA did not develop eyes, even after 27 days of regeneration. In order to maintain planarians alive for 27 days, they were fed. Each photograph contains the image of a different individual. In **A, B, C, E, F, H, M and O,** the eyes did not develop. **(D)** Slow recovery of the eyes. **(G)** Eyes developed with hypopigmented optic cups. **(I)** Only one eye remained during head morphogenesis. **(K)** Eyes too small. **(L)** Small and non-symmetric eyes. **(N)** One eye is reduced in size and pigmentation defects can be observed. Penetrance in: A, B, C, E, F, H, M, O n=20/20; D n=20/30; G n=1/30; I n=1/30; K n=7/30; L n=1/30; N n= 1/30. Scale bars: 150 µm.

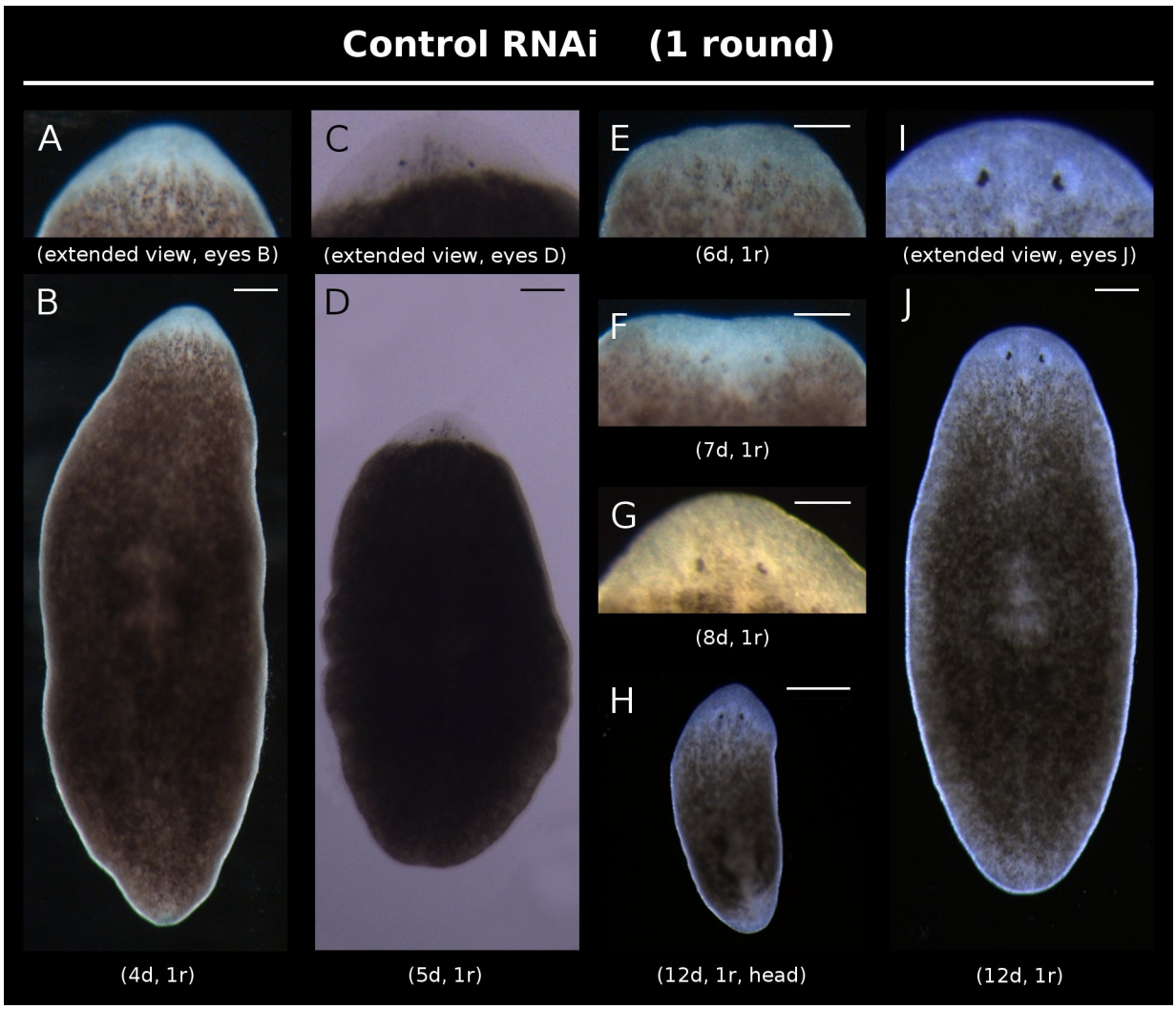

Figure 3.3.2 ***Schmidtea mediterranea*** **after one round of injections of** ***Jellyfish-gfp*** **mRNA, used as the negative control**. These photographs show the most significant stages, where differences in the eyes or the skin pigmentation can be appreciated. **(A and B)** Planarians without eyes on the fourth day of regeneration. **(C-J)** Progressively, the eyes regenerate until reaching normal size. **(F, G)** After 7 or 8 days, the eyes are complete built. **(H)** The decapitated head maintains the eye structures. Penetrance in: B n=4/50; D n= 50/50; E n= 50/50; F n= 50/50; G n= 50/50; H n= 50/50; J n= 50/50. Scale bars: 150 μm.

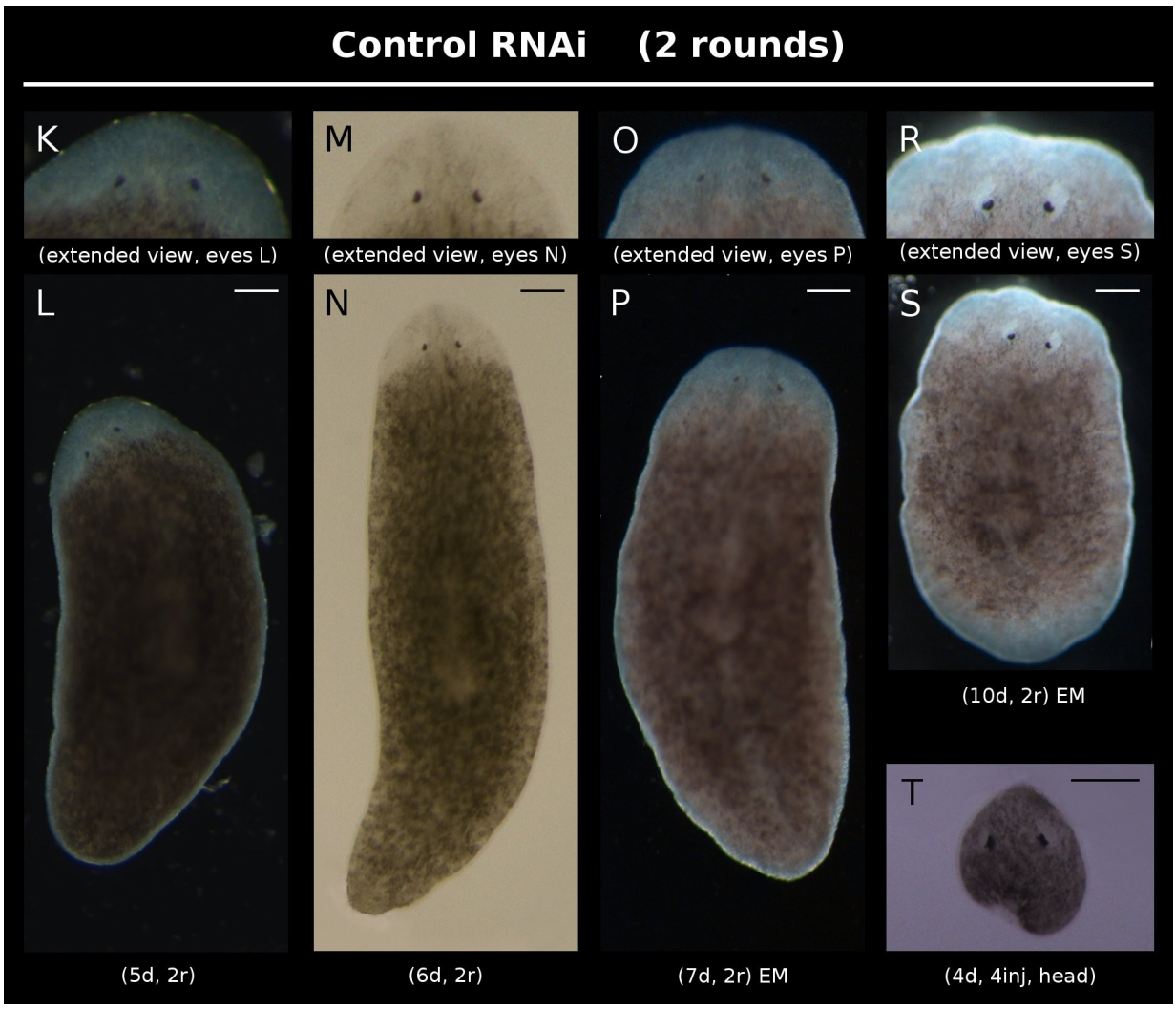

Figure 3.3.3. *Schmidtea mediterranea* after two rounds and four single injections of *Jellyfish-gfp* mRNA, used as the negative control. These photographs are the most significant stages, where differences in the eyes or the skin pigmentation can be appreciated. **(L)** Four-day regenerated body after 2 rounds of injection. **(T)** Four-day regenerated head, amputated after 4 single injections. Penetrance of: L n=26/50; N n= 40/40; P n= 5/5; S n= 5/5; T n= 5/5. Scale bars: 150 μm.

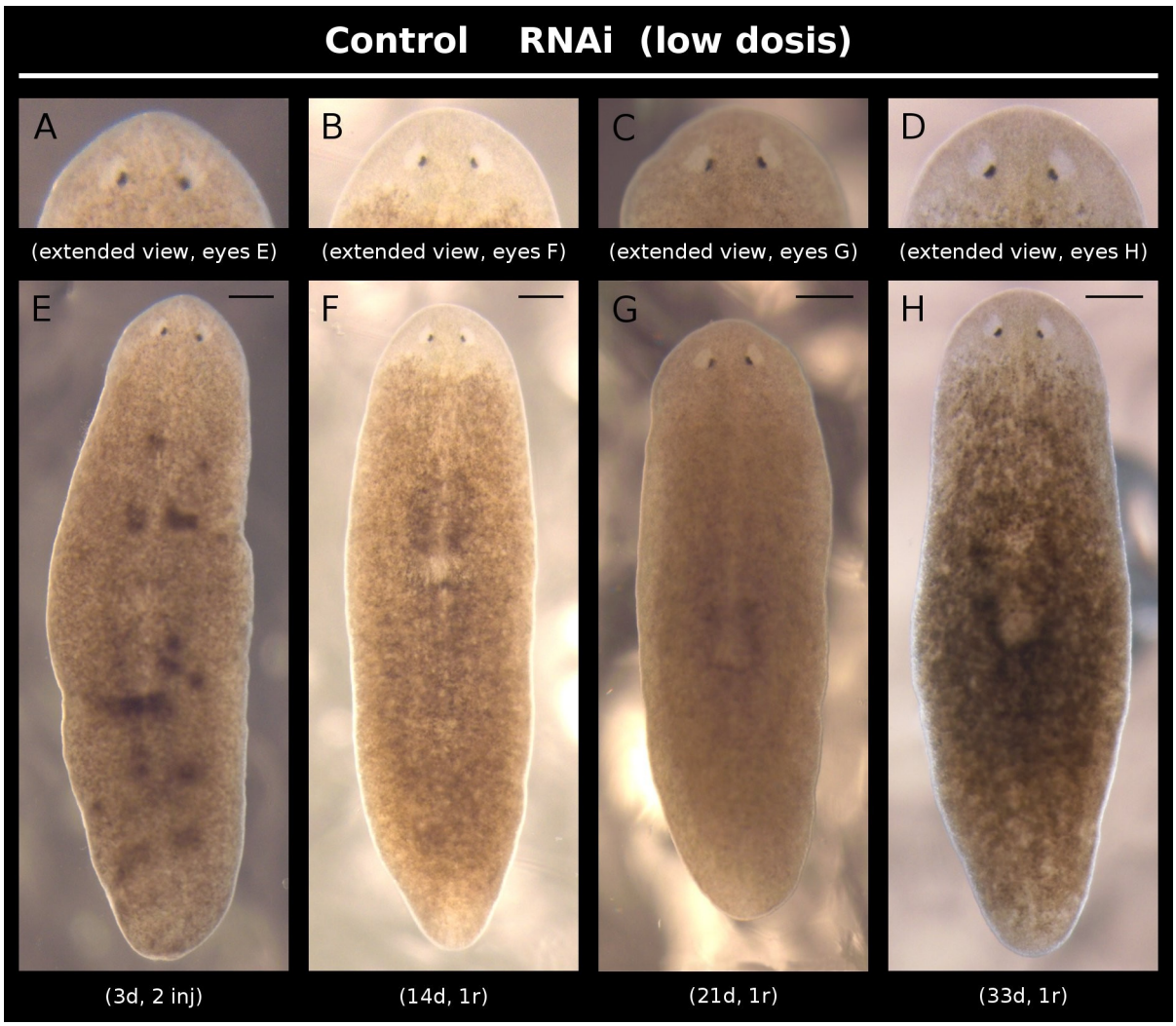

Figure 3.3.4. *Schmidtea mediterranea* after a low dose injections of *Jellyfish-gfp* mRNA, used here as a additional control. The eyes developed in every case as in intact planarians. The doses injected varied between 45 ng/μL and 90 ng/μL. **(E)** This flatworm was injected twice with 87 ng/μL mRNA and was not decapitated. Skin pigment spots were found in this control. **(F, G, H)** 45-55ng/μL was injected. Penetrance in: (E) n=5/5; (F) n=5/5; (G) n= 5/5; (H) 5/5. Every flatworm was placed over a coverslip on ice to be photographed. Scale bars: 150 μm.

3.3.3 In situ probes

Due to the fast and strong labelling of the photoreceptors during the in situ experiments, S*med-eye 53.1* was used as the in situ control. Figure 3.3.5 summarizes expression differences observed after injection of distinct amounts of riboprobe. Some relevant information can be hidden even in apparently clean in situ experiments. Body position can also improve the signal view. By the Figure 3.3.5, the in situ “a” hides two lateral body lines. But the pigment cells were very well delimited compare with the rest of the labelled tissues. This could also be attributed to different developing of the photographs or the physiological stage of every individual. The position of the pharynx in the in situ “c” revealed more clearly the pharynx as a tube, in which the skin is folded. Although the in situ “b” seems to have more background, it contains all the information. All three in situ experiments were useful as controls, because the eyes were well labelled in each of them. *Smed-slit* was also used as a control (Fig. 3.9.4). The developing time is also a key factor in order to reduce background.

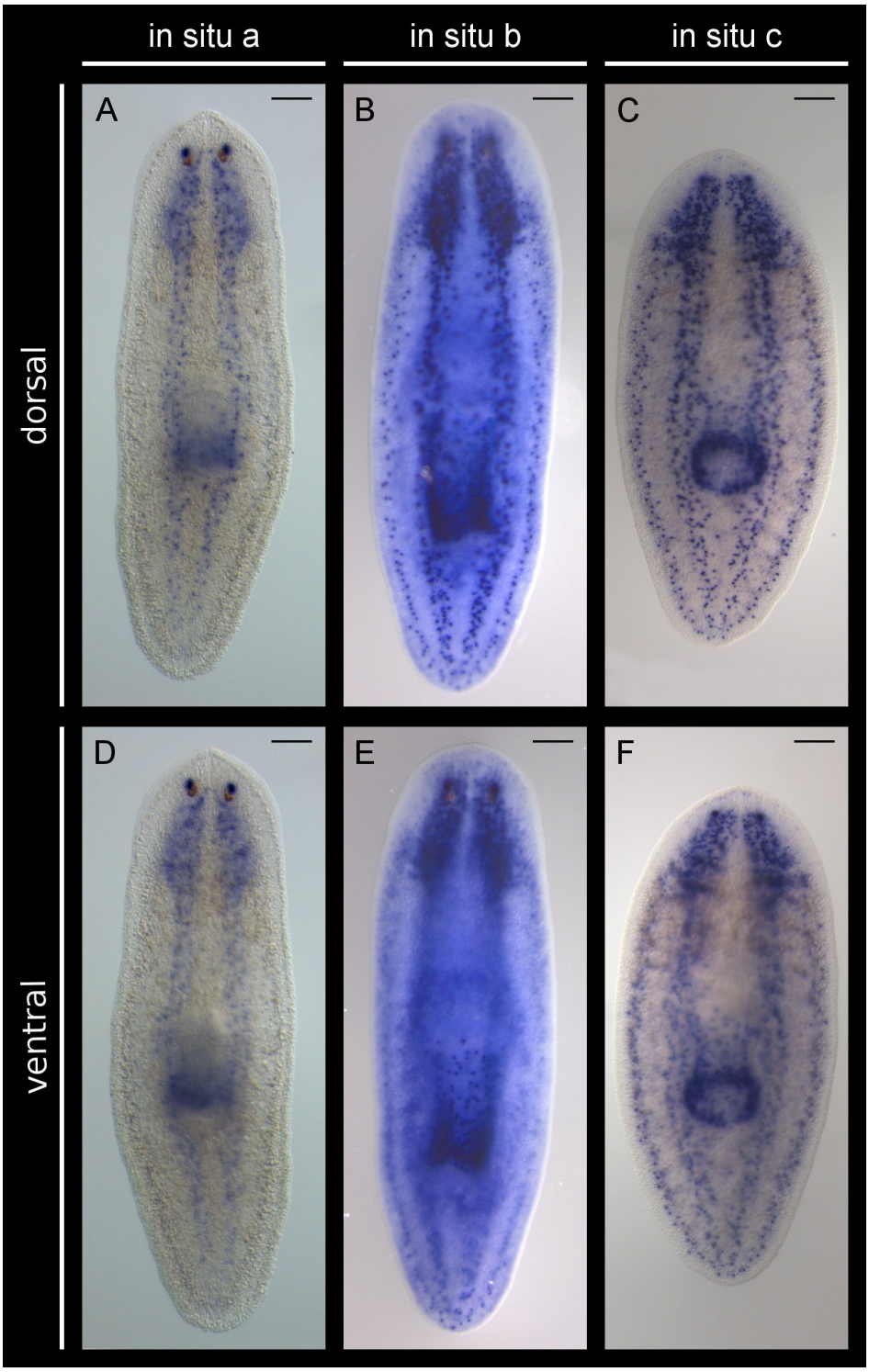

Figure 3.3.5. In situ hybridizations of *Smed-eye53.1* (DIG-labelled antisense mRNA probes, NBT/BCIP developed). The same flatworms are dorsally placed in the upper photographs and ventrally placed in the lower ones. **(A, D)** Hybridization performed with 300 ng/µL. *Smed-eye 53.1* mRNA is expressed in the photoreceptor cells, brain lobes, nerve cords and pharynx. The ventral placement of the flatworm in A and D highlights the ventral eye cell position by the sharpness of their labelling. **(B, E)** With a more concentrated probe, 620 ng/µL, two new lines of cells parallel to the ventral cords appear. There was more background in this experiment but at the same time additional information. The dorsally located ventral cords appeare diffused in E. **(C, F)** This in situ experiment had less background by using 400 ng/µL mRNA. The brain lobes, the ventral cords and the lines surrounding the body can be discriminated as single points. The end of the pharynx appears in C and F as a circle because of its position. Although the photoreceptor cells in C and F are well labelled, it is much easier to differentiate them from the rest of the labelled tissues in A and D. Scale bars: 200 µm.

3.4 Gene expression analysis and functional study of putative opsin-genes

The first part of this in silico search focused on cryptochromes and rhodopsins. To find cryptochrome and rhodopsin protein homologues in the *S. mediterranea* transcriptome 454, an in silico blast2go search was conducted throughout the 454 database. Several key words were used: opsin, phototransduction related, photoreceptor and 7-transmembrane (G-protein coupled receptor). As a result, 14 DNA sequences were screened and classified into three groups.

The first group consists of 8 rhodopsins, whose animal orthologues are involved in forming visual images, temperature discrimination (Shen et al., 2011), nematocyst discharge (in Hydra) (Plachetzki et al., 2012) and phototaxis. The second group is formed by *Smed-peropsin1* and *Smed-blue opsin* (in the Appendix 3). Their orthologues are capable of sensing light of long and short wavelengths. *Smed-melanopsin1*, *Smed-melanopsin2*, *Smed-melanopsin3* and *Smed-cryptochrom* (in the Appendix 3), which putatively act as photoreceptors regulating certain non-image forming photo responses in vertebrates, make up the third group (Nagashima et al., 2005).

Table 3.1 summarizes the full names, putative functions, expression patterns, phenotypes and phenotype penetrances of the opsin genes studied here. Loss-of-function of the *Smed-rhodosin1*, *Smed-rhodosin2*, *Smed-rhodosin10*, *Smed-melanopsin2* and *Smed-melanopsin3* genes produced mutants that failed to regenerate the eyes. Nevertheless, these mutations did not show complete penetrance. Two genes, *Smed-peropsin1* and *Smed-melanopsin1,* showed expression in the eyes and in the cephalic ganglia respectively. Nevertheless, neither *Smed-peropsin1* (in the Appendix 3) nor *Smed-melanopsin1* showed eye defects. Furthermore, *Smed-cry* loss-of-function produced hypopigmented skin (in the Appendix 3). Interestingly, most of the opsin genes were apparently expressed throughout the parenchyma.

It has been suggested that the normal role of retinoids, active metabolites of the carotenoid vitamin A, is in patterning vertebrate embryogenesis through the Hox genes (Marshall et al., 1996; Cunningham et al., 2015). Since RA (all-trans-RA) was found to be a regulator of planarian morphogenesis (Romero et al., 2001; Ermakova et al., 2009), the apoproteins containing other pigments that convert light into chemical energy or an intracellular signal, might be relevant to *S. mediterranea* development. Pigments acting as chromophores are carotenoids (retinal, lutein), bilins (phycocyanobilin); chlorophylls (cyclic tetrapyrroles), flavins (flavin adenine dinucleotide (FAD) and flavin mononucleotide (FMN)) and pterins (5,10-methenyltetrahydrofolate (MTHF)) (Sancar, 2000). Those present in the phytochromes of plants, algae, diatoms, fungi and some bacteria (Gehring, 2012) were not included in this study.

3.4.1 Rhodopsins

Eight rhodopsins, selected from the 454 *S. mediterranea* transcriptome database, that present high homology with rhodopsins from other organisms, are summarized in Table 3.1. After one round of RNA interference, followed by amputation of the head, regeneration deficiencies were found in three rhodopsins. The phenotypes observed in *Smed-rhodosin1*, *Smed-rhodosin2* and *Smed-rhodosin10* RNAi animals were the following: hypopigmented, underdeveloped and absent eye cups (Fig. 3.4.1). The expression of these three genes has unspecific parenchymal patterns (Fig. 3.4.2).

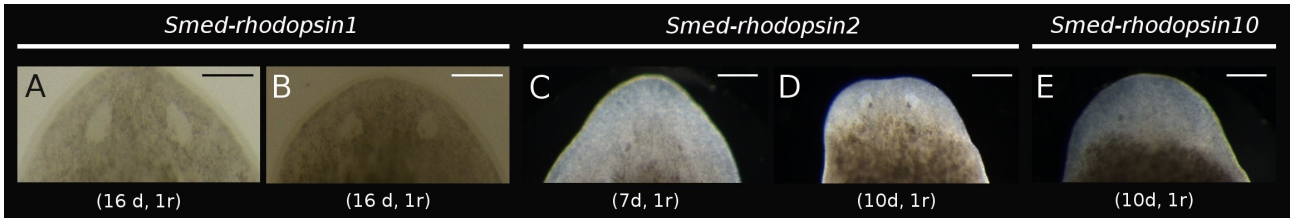

Figure 3.4.1. Eye regeneration defects of *Smed-rhodopsin1*, *Smed-rhodopsin2* and *Smed-rhodopsin10* RNAi flatworms after 7, 10 and 16 days of regeneration. The images show the heads of decapitated bodies days after regeneration started. Penetrance: **(A)** hypopigmented eye cups, n=1/10; **(B)** underdeveloped and hypopigmented eye cups, n=1/10; **(C)** less developed eyes, n=2/10; **(D)** less developed eyes, n=1/10; **(E)** absence of one pigment cup and periglobular area n=2/10. Controls are in Figure 3.3.2. Scale bars: 150 µm.

RNAi of animals injected with the other five opsins, *Smed-rhodosin4*, *Smed-rhodosin5, Smed-rhodosin7, Smed-rhodosin8* and *Smed-rhodosin9,* regenerated as the controls (Fig 3.3.2 and 3.3.3). The mRNA of *Smed-rhodopsin1, Smed-rhodopsin2, Smed-rhodopsin4, Smed-rhodopsin7, Smed-rhodopsin8, Smed-rhodopsin9*, and *Smed-rhodopsin10* were broadly expressed in the parenchyma of intact flatworms (Fig. 3.4.2). Nevertheless, *Smed-rhodopsin5* expression was restricted to the stomach branches, and the mRNA of *Smed-rhodopsin10* additionally had cephalic ganglia expression.

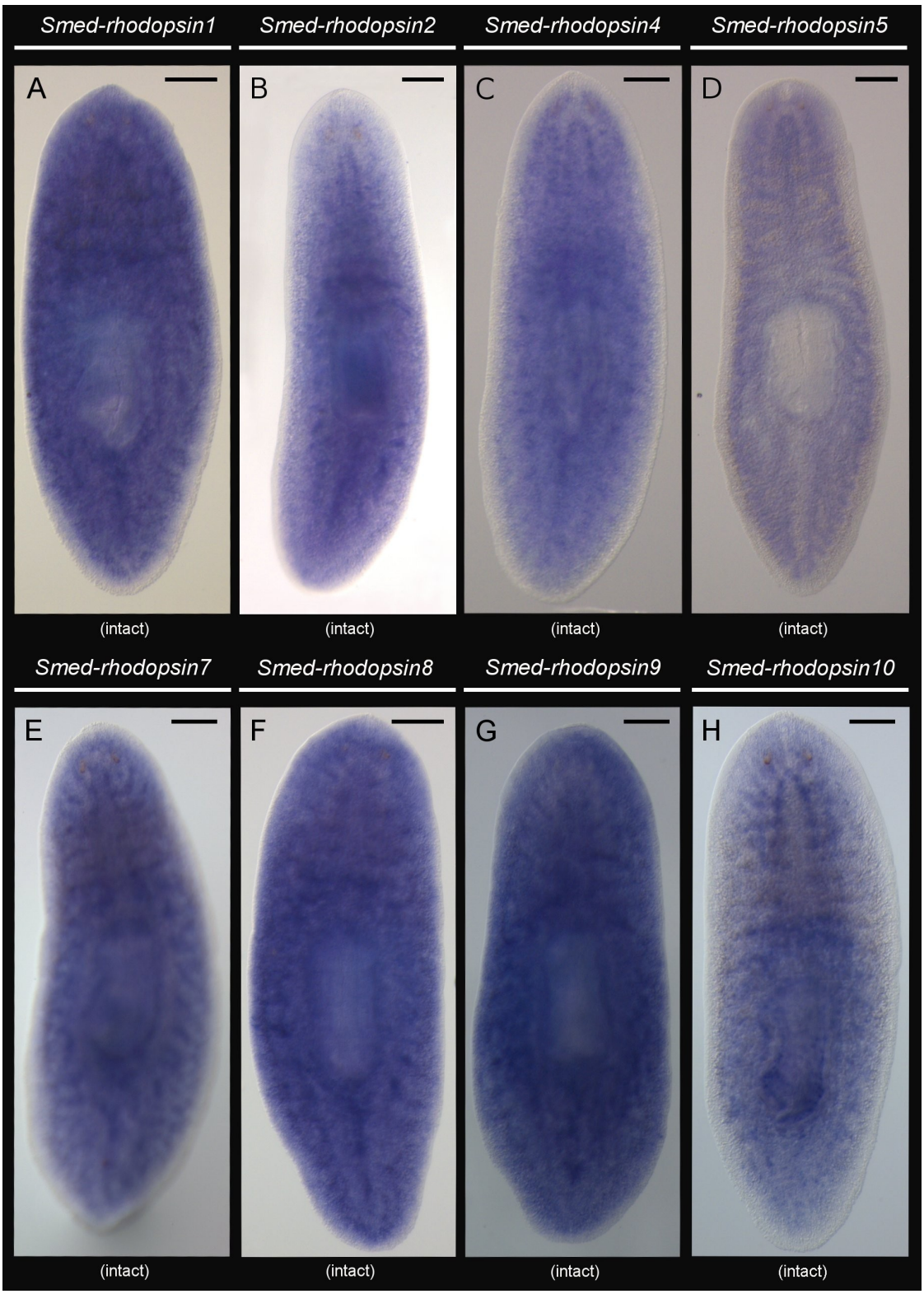

Figure 3.4.2. In situ hybridization of rhodopsin genes with enriched expression in the parenchymal tissue (DIG-labelled antisense mRNA probes, NBT/BCIP developed). **(A-H)** In situ hybridization of putative rhodopsin transcripts. The mRNA of *Smed-rhodopsin1, Smed-rhodopsin2, Smed-rhodopsin4, Smed-rhodopsin7, Smed-rhodopsin8, Smed-rhodopsin9*, and *Smed-rhodopsin10* are broadly expressed in the parenchyma of intact flatworms. *Smed-rhodopsin5* expression is restricted to the stomach branches. The mRNA of *Smed-rhodopsin10* additionally has cephalic ganglia expression. Controls are in Fig. 3.3.5. Scale bars: 200 µm.

Rhodopsin is a C-opsin present in the ciliary photoreceptors of animals. Nevertheless, in squid retina, the anti-rhodopsin antibody stained rhabdomeric microvilli (Katagiri et al., 2001). Rhodopsin is a seven-transmembrane-domain opsin apoprotein linked to 11-cis-retinylidene via a lysine residue in the helix 7 (Sakma, 2002). Light between 470 and -510 nm provokes conformational changes of the chromophore that allows the opsin to interact with a G-protein (transducin), and to trigger the phototransduction cascade, ultimately giving rise to a change in receptor membrane potential and consequently visual photoreception. The majority of inherited retinal diseases are caused by defects in photoreceptor-specific genes (Dryja, 2001). Good examples are retinoschisis (splitting of the retina), achromatopsia (the inability to perceive colour, decreased vision and, light sensitivity), Leber congenital amaurosis (severe visual impairment) and retinitis pigmentosa (severe vision impairment and often blindness) (Boye et al., 2012). *Smed-rhodopsin1*, *Smed-rhodopsin2* and *Smed-rhodopsin10* might be photoreceptors that are necessary for the structural formation of the *S. mediterranea* eye. However, their expression patterns indicate further functionalities, such as those of the melanopsins responsible for photoentrainment. It has to be taken into account that rhodopsins and melanopsins are structurally very similar and 6 sequences of 47 rhodopsins were identified as melanopsins in planarians (Zamanian et al., 2011). This possibility has to be further investigated.

3.4.2 Peropsins

Smed-peropsin1 DNA is highly homologous with the Peropsin1 of *Platynereis dumerilii,* which belongs to the rhodopsin family and is responsible for long wavelength photoreception. Table 3.1 summarizes the full name, putative function, expression pattern, phenotype and phenotype penetrance of the peropsin gene. The eyes of planarians injected with *Smed-peropsin1* mRNA regenerated as the controls (data not shown) (controls Fig. 3.3.2). Nevertheless, *Smed-peropsin1* is strongly expressed near or in the photoreceptor cells (Fig. 3.4.3). Moreover, its RNA is broadly expressed throughout the parenchyma of whole flatworms, but not in the pharynx (Fig. 3.4.3).

The in situ signal observed in the eyes in the Figure 3.4.3 is mixed with a strong pharenchymal signal, suggesting a light sensing functionality together with the existence of activity outside the eyes; this protein might have double functionality. Although the absence of a signal in the pharynx indicates a clean in situ result, nevertheless, some background signal might be mixed in here.

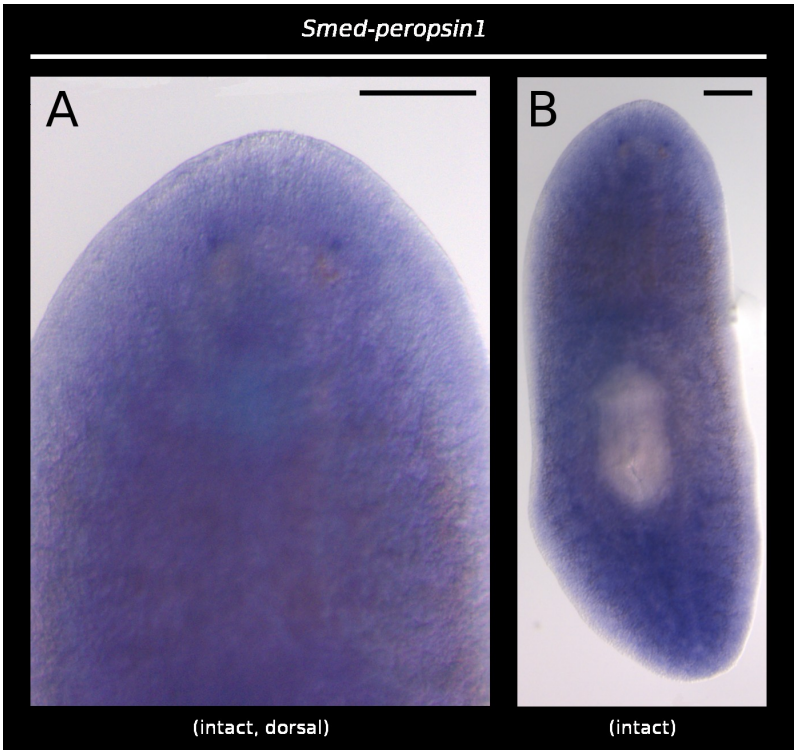

Figure 3.4.3. Whole-mount in situ hybridization showing the expression patterns of *Smed-peropsin1* in intact planarians (DIG-labelled antisense mRNA probes, NBT/BCIP developed). The head region of B is magnified to the upper left in A. *Smed-peropsin1* mRNA was expressed in the photoreceptor cells and broadly throughout the parenchyma of whole flatworms, but not in the pharynx. Controls are in Fig. 3.3.5. Scale bar: 200 µm.

Peropsin was previously called RPE-derived rhodopsin homologue (retinal pigment epithelium) and was first identified in humans (Rrh). It shows significant similarity to visual pigments, approximately 27% identity, but it is clearly distinct from known visual pigments. It is localized in the apical face of the RPE, in the microvilli that surround the photoreceptor outer segments of adult human and mouse retinas (Sun et al., 1997; Peirson et al., 2004). Several opsin-based molecules have been identified as photoisomerases, which catalyse the regeneration of photosensory opsins by converting the all-*trans* retinal to produce the chromophore 11-*cis* retinal in the process known as the "visual cycle" (Wald, 1968). Peropsin mRNA expression was found in cells of the pineal gland, retina, and brain tissue of chick. It has also been associated with both melatonin biosynthesis and circadian entrainment and is regulated on a circadian basis (Bailey et al., 2004).

Peropsin from the jumping spider *Hasarius adansoni* can form a photosensitive pigment in vivo, but in addition, it can function as a non-visual photoisomerase. This is based on evidence that the pigment binds to all-*trans* retinal as a chromophore in the dark state, and all-*trans* to 11-*cis* isomerization takes place upon absorption of light (Nagata et al., 2010). In addition to sharing its bistable nature with light-sensing rhodopsins, the spider peropsin, as well as the other peropsin homologues, contains the 'NPXXY' motif in the seventh transmembrane domain. This sequence is considered to play important roles in coupling with G proteins, suggesting that peropsins may also act as light-sensing GPCRs (Nagata et al., 2010).

In the principal eye of the jumping spider *Hasarius adansoni*, peropsin was localized in non-visual cells and was distributed particularly in the distal region of the retina (Nagata et al., 2010).

3.4.3 Melanopsins

Three melanopsins, *Smed-melanopsin1, Smed-melanopsin2* and *Smed-melanopsin3,* all highly homologous with melanopsins from other organisms responsible for non-visual photoreception were studied here. They are summarized in Table 3.1 with their full names, putative functions, expression patterns, phenotypes and phenotype penetrances.

One and two rounds of *Smed-melanopsin2* and *Smed-melanopsin3* RNAi followed by head amputation, showed eye regeneration and skin pigmentation defects from the eighth day of regeneration (Fig. 3.4.4). These phenotypes showed low penetrance. Fused pigment cups, only one cup or asymmetrical cups were found in *Smed-melanopsin3.* Small, too big, asymmetrical and absent pigment cups were also found in *Smed-melanopsin2* RNAi animals. Furthermore, both RNAi genes generated animals with special skin pigmentation, forming similar spots or dark areas surrounding the central nerve system, with the rest of the skin hypopigmented. Confocal microscopy of the specimen in Figure 3.4.4 B, injected with *Smed-melanopsin3* RNAi and stained with the VC1 antibody (Figure 3.4.5 B, C), demonstrated that not only the pigment cells regenerated abnormally. A straight projection of the contralateral fibres were also observed, probably due to a misrouting of retinal fibres at the optic chiasm. *Smed-melanopsin3* might induce axon guidance for some of the photoreceptor cells that erroneously decussate and project contralaterally at the optic chiasm, as indicated by the observed lack of *Smed-melanopsin3* after RNAi. *Smed-melanopsin3* expression in the eyes cannot be ruled out, although it is spread around the tip of the head and also in the pharynx and surroundings (Fig. 3.4.6). Nevertheless, *Smed-melanopsin2* presents no or very low expression.

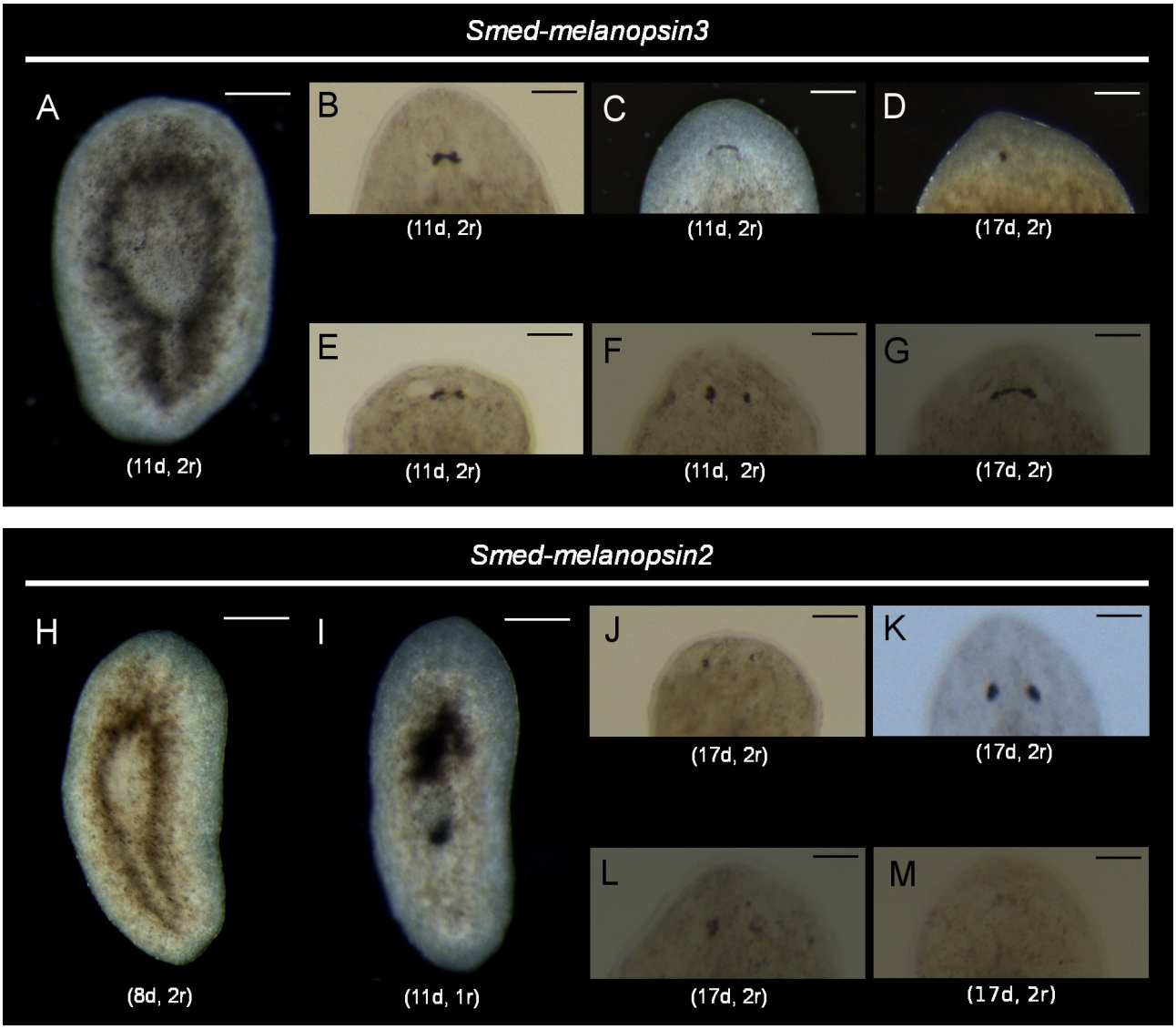

Figure 3.4.4. *Smed-melanopsin3* and *Smed-melanopsin2* (RNAi) affected eye development and skin pigmentation. Bodies and heads are visualized on days 8, 11 and 17 of regeneration after decapitation. **(A)** No pigment cups developed and there was abnormal skin pigmentation with an oval pattern. **(B)** The pigment cups were incorrectly positioned and fused to each other in a mid point between the eyes. **(C)** Fused optic cups in a line. **(D)** Only one eye developed. **(E)** The periglobular area was underdeveloped in one eye, there was a mid location of the optic cups with a small degree of fusion. **(F)** Asymmetric optic cups, located in the middle of the periglobular area. **(G)** Fused pigment cups. **(H)** Skin pigmentation defect, CNS patterned, no eyes developed. **(I)** Skin pigmentation concentrated in two central dorsal areas. **(J)** Small non symmetric eye cups. **(K**) Large pigment cups. **(L)** Non-symmetric pigment cups with no periglobular area defined. **(M)** Pigment cups shown as small shadows in the middle of the head. Penetrance in: (A) n=1/ 50; (B) n= 1/50; (C) n= 1/50; (D) n=2/50; (E) n=2/50; (F) n=2/50; (G) n= 4/50; (H) n=1/20; (I) n=1/20; (J) n=1/20; (K) n=1/20; (L) n=1/20; (M) n= 1/20. If not specified, the photographs are decapitated bodies after some days of regeneration. Controls are in Figures 3.3.2 and 3.3.3. Scale bars: 150 µm.

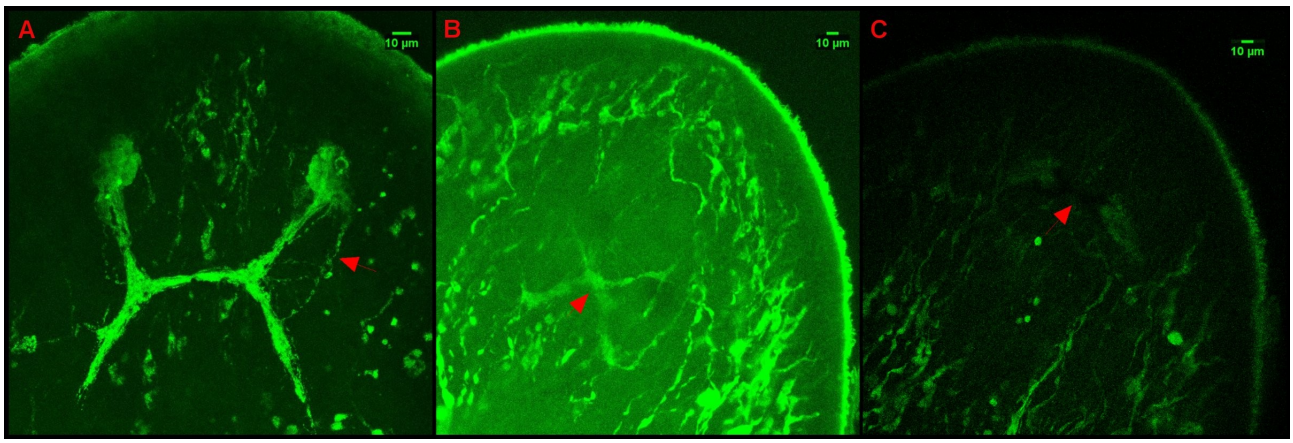

Figure 3.4.5: Confocal image of *Smed-melanopsin3* RNAi hybridized with the anti-arrestin antibody (VC1) in an immunofluorescence assay. (A) Control *Jelyfish*-GFP RNAi. The rhabdomeres, the axons and the optic chiasm of photoreceptor cells are labelled. It is difficult to decide whether the right eye has some misrouted axons (red arrow) or if this is a signal for a different structure. **(B)** *Smed-melanopsin3* RNAi after 11 days of regeneration presenting an abnormal optic chiasm. This phenotype might be caused by a systematic misrouting of chiasmatic fibres in favour of the crossed projection (red arrow), given it an X shape. **(C)** The same confocal series as inB. Here, a different stack of sections were taken, where the fused pigment cups (red arrow) and a part of the photoreceptor bodies can be seen. In addition to the eyes, other structures are also labelled with VC1 in every image; they might also be neurons. Scale bars: 10 µm.

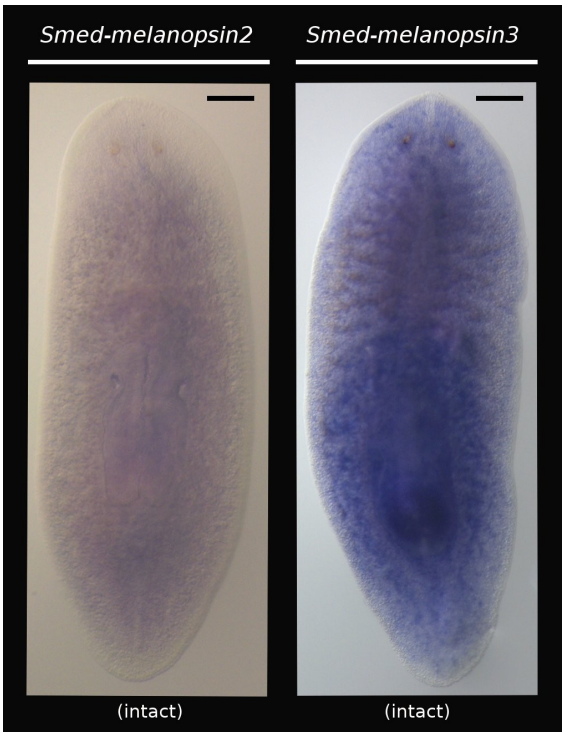

Figure 3.4.6. Whole-mount in situ hybridization showing the expression patterns of the indicated genes in intact planarians (DIG-labelled antisense mRNA probes, NBT/BCIP developed). (Left) No expression pattern was found by *Smed-melanopsin2* mRNA hybridization. **(Right)** *Smed-melanopsin3* hybridization present around the eyes and the tip of the head but also in the pharynx and surroundings. Scale bars: 200 µm.

Smed-melanopsin1 RNAi presented the same phenotype as the control (data not shown) (controls in Fig. 3.3.2 and Fig.3.3.3). However, *Smed-melanopsin1* mRNA expression is found in single cells located in the eyes, possibly in the cephalic ganglia and also in an oval pattern around to the pharynx. (Fig. 3.4.7).

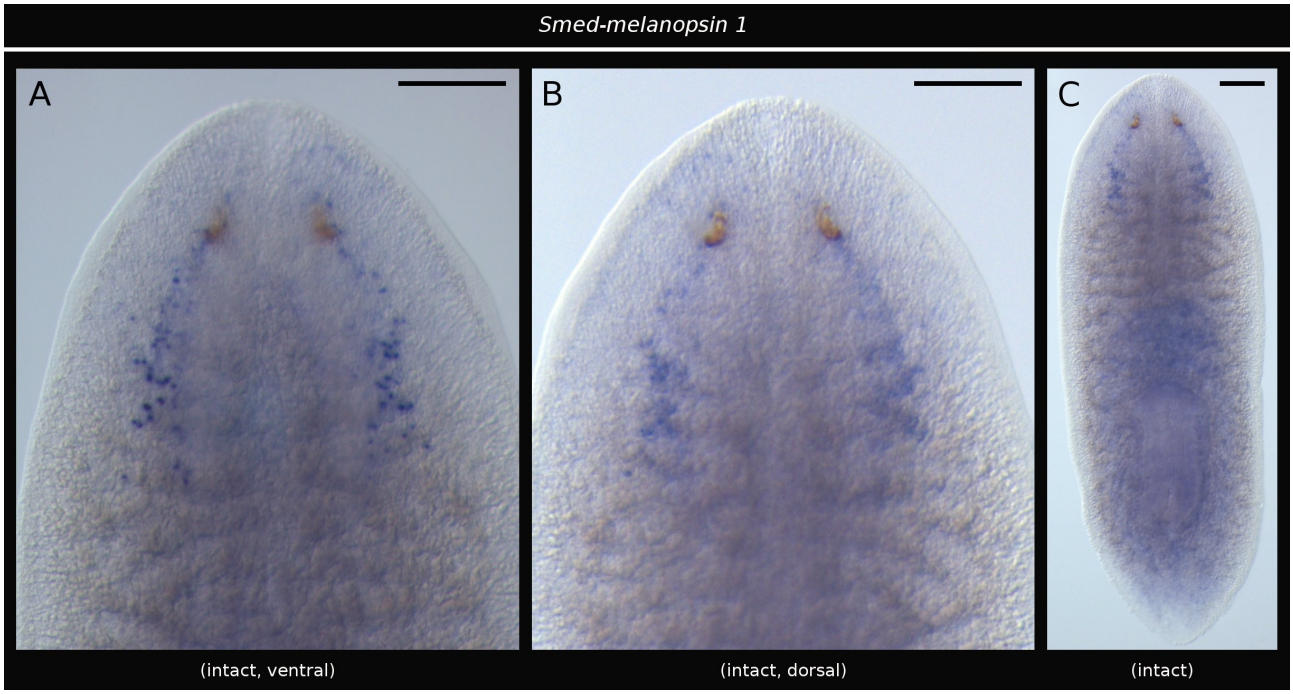

Figure 3.4.7. Whole-mount in situ hybridization showing the expression pattern of *Smed-melanopsin1* in an intact planarian (DIG-labeled antisense mRNA probe, NBT/BCIP developed). A and B are the magnified photograph of the head in C. **(A-C)** *Smed-melanopsin1* mRNA was detected in the cells surrounding the eyes, possibly the ventral cephalic ganglia, and also in an oval pattern around the pharynx. Scale bars: 200 µm.

The expression pattern found in *Smed-melanopsin1* mRNA might correspond to neuronal cells that send signals to a circadian oscillator within the brain, like the mammalian hypothalamic suprachiasmatic nuclei (SCN). Mammal oscillators can be found in multiple cell types and tissues (Bailes et al., 2009). However, the melanopsin protein is expressed only in the retina, and only in 1%-2% of RGR within rodents, primates, and humans (Hattar et al., 2002). In mice lacking all their rods and cones, induction of sleep by light rhythms is entirely dependent on melanopsin-(OPN4), with this protein located in the photosensitive RGC (pRGCs) (Lupi et al., 2008). The *X. laevis* Opn4 melanopsin, expressed in dermal melanophores, responds to light by dispersing melanosomes (pigment granules) and moreover presents peripheral clock characteristics (Isoldi et al., 2005; Bluhm et al., 2012).

The expression of melanopsin and clock genes in *X. laevis* dermal melanophores is modulated by melatonin; a molecule that is directly related to the biological clock machinery (Bluhm et al., 2012). Interestingly, melatonin is endogenously synthesized in planarians in a circadian manner (Morita et al., 1987; Itoh et al., 1999) and furthermore, inhibits the regeneration of the anterior end of the animal by suppressing the mitotic activity of the neoblasts (Ermakova et al., 2009; Romero et al., 2001).

Melanopsin expression is detected early in the mouse retina at embryonic day (E)10.5 (Tarttelin et al., 2003), following the appearance of RGC at (E)9. In mice, pRGCs undergo substantial postnatal changes in cell number, morphology and physiology (Sekaran et al., 2005), just like the general ganglion cell population (Young, 1984). pRGCs are overproduced at birth and subsequently reduced to their adult numbers (Sekaran et al., 2005). Interestingly, the domain of expression of optic cup and photoreceptor progenitors proposed in the "*Model for cell state changes in pigment cup regeneration*" by Lapan, 2011 (Fig. 1.5 C), is highly similar to the expression pattern observed in *Smed-melanopsin1* mRNA in situ. *Smed-melanopsin1* could initially induced, the formation of the RGC and be also involved in a circadian photoreception, just as the rhodopsin-like cells are in the auricles of *Dugesia japonica* (Asano, et al., 1998). In mammal cells containing melanopsin, the pRGCs synchronize circadian clocks to light-dark cycles and regulate the pupil size, sleep propensity and pineal melatonin production. In humans, there is evidence that this system regulates body temperature, mood and aspects of arousal and concentration (Bailes et al., 2009). These kinds of functions would be difficult to detect in planarians. Nevertheless, the eye and skin pigmentation defects in *Smed-melanopsin2* and *Smed-melanopsin3* RNAi planarians suggest they they have functions in two different tissues; these might also include photoreception. Furthermore, both mRNA patterns fit with the melanopsin found in non-mammalian vertebrates, where this photoreceptor is found in a wider subset of retinal cells, as well as in photosensitive structures outside the retina, such as the iris muscle of the eye, deep brain regions, the pineal gland, and the skin (Bellingham et al., 2006; Provencio et al., 1998). Multiple patterns of tissue expression have already been observed in other opsins such as Opn3 and TMT. In zebrafish, the teleost multiple tissue (TMT) opsin is the candidate that mediates circadian oscillations of genes from isolated organs and cell lines. Surprisingly, the heart and kidney of zebrafish can be entrained by light after being isolated and maintained in vitro (Whitmore et al., 2000). The TMT protein is a 402 amino acid protein that contains all of the essential features of an opsin photopigment, including a lysine residue at position 296; but nonetheless, it has a tyrosine instead of a glutamate at the Schiff base counterion. It has only been isolated from teleost fish, where it is expressed in the liver, kidney and heart, as well as the eye and the brain (Moutsaki et al., 2003).

I now consider the importance of axon projection at the optic chiasm in other species. In primates, the nasal retinal axons cross in the midline at the optic chiasm, while temporal retinal axons extend ipsilaterally, projecting toward the lateral geniculate nucleus and to the visual cortex. This pattern is critical for binocular vision, stereopsis and depth perception in vertebrates. In albino humans, ipsilaterally destined temporal retinal fibres (made up of RGC) erroneously decussate and project contralaterally at the optic chiasm. This leads to difficulty with depth perception in the affected humans (Herrera et al., 2008). Here it must be remembered that in some human albinos the fovea is absent and the macular region is underdeveloped. It suggests a general nervous system deficit (Elschnig, 1913). Similar aberrant contralateral projections have been shown in mice embryos lacking the winged helix transcription factor Foxd1. These mutants had both retinal development and chiasm morphogenesis disruption (Herrera et al., 2004).

The crossing of optic fibres appeared in evolution with the lenticular eye (simple eyes provided with a converging lens) and corrected the lateral inversion produced in the two middle sections of the mental images in vertebrates, due to the functional mechanism of the double dark chamber (Ramón, 1898). In lower animals the decussation is total, so that there is no overlap of information. The percentage of fibres that remain uncrossed varies between species depending upon how lateral the eyes are placed in the head. This partial decussation of optic fibres at the chiasm forms the basis for normal binocular vision (Neveu et al., 2007). Studying the orientation of every single optic chiasm fibre in *S. mediterranea* would provide valuable information regarding its kind of vision.

There have long been hints that opsins are present outside the eye. Opsins have been found in *Xenopus* skin melanophores (Provencio et al., 1998), in mouse and human neural tissue (Panda et al., 2003), in the laden cells near the stinging cells of hydra and jellyfish (Plachetzki et al., 2007), in the cilia of octopus skin (Ramirez, 2011b), in the mollusc tentacles called chitons (Ramirez et al., 2011a), in urchin spines (Ullrich-L¸ter et al., 2011), in the chordotonal neurons of the *Drosophila* larvae head, acting as temperature sensors (Shen et al., 2011), in the *Drosophila* antennal ear (Senthilan et al., 2012), and in both the cells that generate bioluminescence in the comb jelly *Mnemiopsis leidyi,* and in its sensory organ that helps it stay oriented in the water (Schnitzler et al., 2012). Some opsin functions outside the eyes are already known. Four good examples are: the sensitivity to mechanical stimuli found in the cilia of octopus skin (Ramirez, 2011b) and in the *Drosophila* antennal ear (Senthilan et al., 2012), temperature sensors in the *Drosophila* larvae (Shen et al., 2011) and melanosome dispersion in *Xenopus* melanophoren (Provencio et al., 1998). Other functions, such as monitoring how much the jellyfish is glowing, have not yet been demonstrated (Schnitzler et al., 2012).

In addition, BR and HR are both present in the haloarchaea *Halobacterium salinarum,* and both use light energy to pump protons, chloride and also bromide, iodide, and nitrate into the cell against their electrochemical gradients (Oesterhelt et al., 1998; Kolbe et al., 2000).

This study has shown that opsin sequences are also found to be abundant in the flatworm *S. mediterranea* across the whole body but are less present in the eyes. This assumption might indicate that planarian opsins have been selected into a different niche, for example the skin; acting as part of the dermal light sense (Parker et al., 1900; Yoshida et al., 1966); a characteristic observed in eyeless planarians such as *Castrada,* or blind ones such as *Mesostoma lingua, Fonticola vitta* and *Planaria lugubris* (Viaud, 1948). Another newly discovered rhodopsin niche is the phyllosphere environment of terrestrial plants. Microbial rhodopsins have been found in the leaves of soybean (*Glycine max*), tamarisk (*Tamarix nilotica*), clover (*Trifolium repens*), rice (*Oryza sativa*), and Arabidopsis thaliana. Curiously, they were absent from both agricultural and forest soils. Whether this microbial community exibits commensalism or mutualism is unknown (Atamna-Ismaeel et al., 2012).

Interestingly, a wide variety of organisms do not need traditional eyes to make use of the versatile heptahelical membrane protein, opsin. These molecules can act as light-driven pumps but also sense more than light. Whether the planarian opsins can be classified in any of these groups, should be a matter of further investigations. As Marla Ina Arnone and Craig Montell predicted, researchers are just beginning to appreciate all that opsins can do (Pennisi, 2013).

3.5 Gene expression analysis and functional study of putative genes related to pigment-biosynthesis

Further searches were preformed to find genes related to eye pigment biosynthesis. This reaction takes place in the visual apparatus of many organisms. These genes might influence pigment and photoreceptor cell development in *S. mediterranea,* as the RPE and the neural retina does, co-differentiating during vertebrate eye development (Strauss, 2005). Here the three DNA sequences selected from the 454 database, *Smed-white, Smed-ver* and *Smed-ncl,* presented a high degree of homology with an ABC transporter, a tryptophan 2,3-dioxygenase and a lipopigment-trafficking protein respectively. Table 3.2 summarizesthe full names, putative functions, expression patterns, phenotypes and phenotype penetrances of the three genes.

RNAi of the ABC transporter *Smed-white* influences eye regeneration and morphogenesis, and also affects eye and skin pigmentation. The loss-of-function of the *Smed-ncl,* a gene that is putatively implicated in lipopigment trafficking, modified the skin pigmentation in the posterior part of the body (in the Appendix 3). *Smed-ver* RNA in contrast, presents eye and brain expression patterns. Unexpectedly, interference with *Smed-ver* RNA automatically ejected the pharynx after injection, similarly to *Smed-white-sf2* RNAi.

3.5.1 *Smed-white* fragments: *Smed-white-sf1* and *Smed-white-sf2*

The ABC transporter gene *Smed-white* has a high degree of homology with the white gene from Drosophila; an eye pigment precursor transporter. One round of injections of *Smed-white-sf1* RNA in *S. mediterranea* before decapitation caused a mortality of 14% after 10 days of regeneration. Furthermore, ~8% of the flatworms failed to regenerate eyes (Fig. 3.5.1). Several visible eye phenotypes were observed; weakly pigmented, non-symmetric, fused and in some cases with an absence of pigment eye cups (Fig. 3.5.1, A, B, C, F). Apart from skin pigmentation defects (Fig. 3.5.1, A), pigment cups surrounded by a small periglobular area were also observed in long-term regenerating flatworms (Fig. 3.5.1, G). Moreover other phenotypes were also produced, for example a blastema that did not regenerate (Fig. 3.5.1, F) and locally hypopigmented tails, probably produced by spontaneous fissioning (Fig. 3.5.1, I).

Interestingly, a second round of injections increased to about 14% the number of flatworms with weak (Fig.3.5.2, A-D) and hypopigmented eye cups (Fig.3.5.2, E-H). In addition, the periglobular areas were more pigmented than in the controls (Fig. 3.3.3).

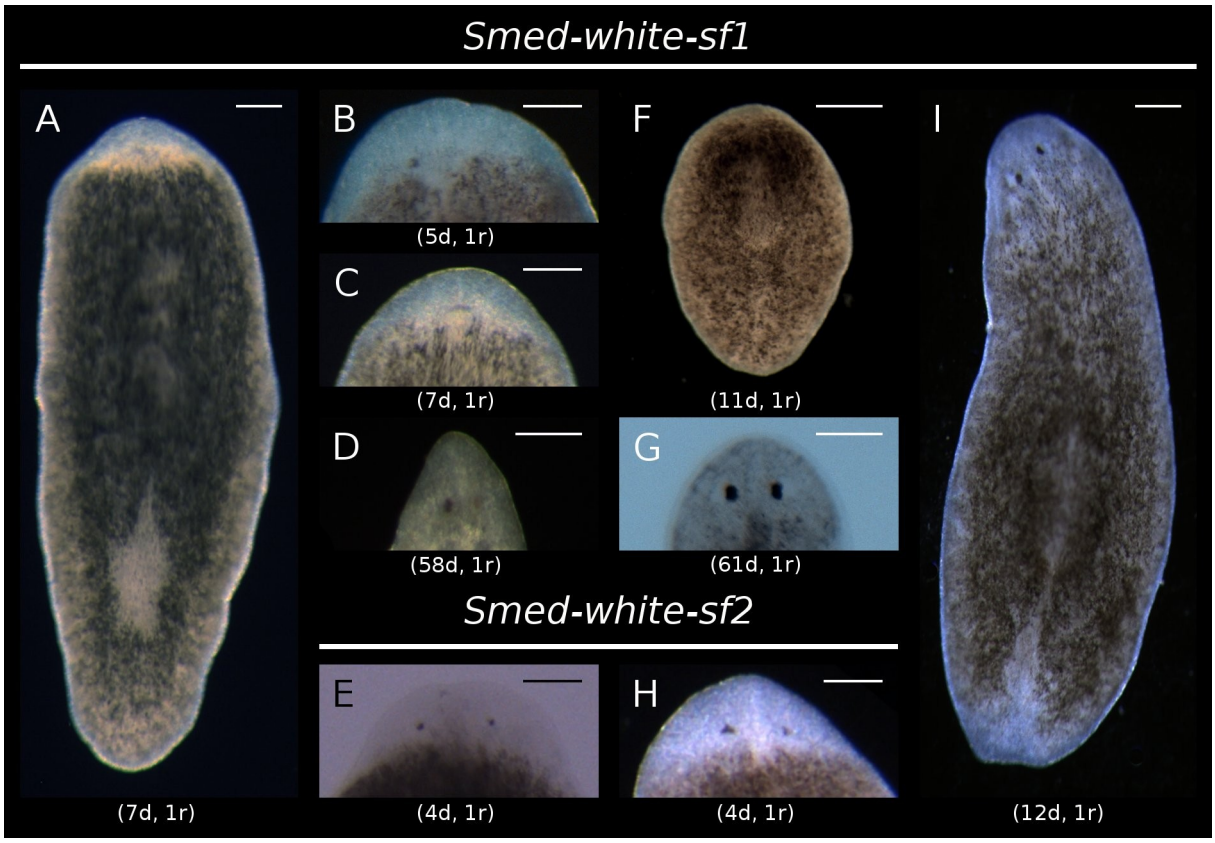

Figure 3.5.1 RNA interference with two different fragments of the white gen: *Smed-white-sf1* and *Smed-white-sf2*. Eye phenotypes after one round of injection and 4, 5, 7, 11, 12, 58 and 61 days of regeneration. **(A)** Absence of pigment cup and skin pigment defects in the tail area. **(B)** Asymmetric pigment cups. **(C)** Fused pigment cups. **(D**) Survivor after 58 days with abnormally developed eyes. **(F)** Non-regenerated blastema. **(G)** Large pigment cups in small periglobular area. **(I)** Possible tail fissioning. *Smed-white-sf2* RNAi: **(E)** with eye spots as controls and **(H)** with asymmetric pigment cups. Penetrance in (A) n=5/107; (B) n=15/107; (C) n=1/107; (D) n=1/107; (E) n=21/22; (F) n= 1/107; (G) n=1/107; (H) n=1/22; (I) n=10/107. 73/107 flatworms developed as controls and 15/107 died. Controls Fig. 3.3.2. Scale bars: 200 µm.

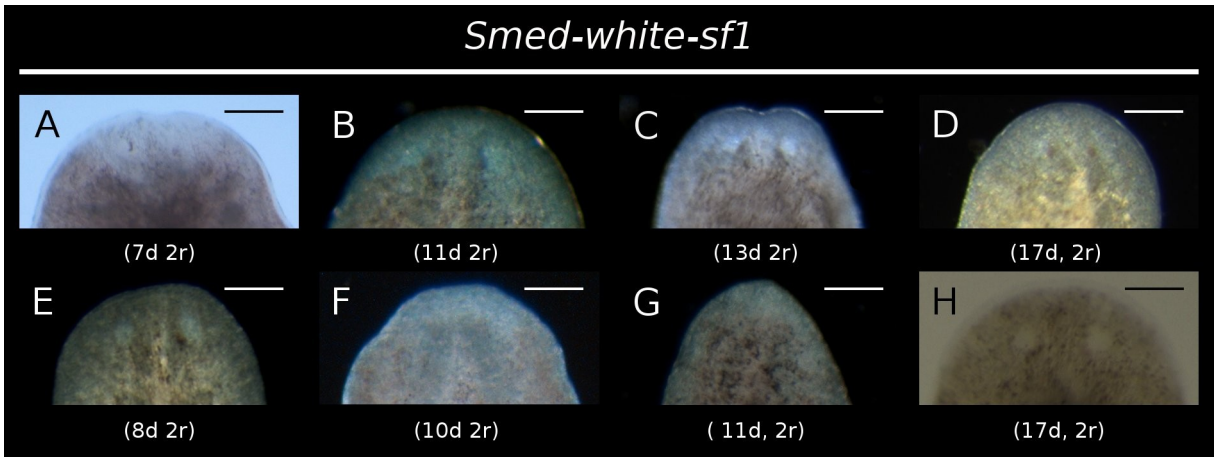

Figure 3.5.2 Heads of flatworms injected with *Smed-white-sf1* mRNA, after 2 rounds of injection and 7, 8, 10, 11, 13 and 17 days of regeneration. (A-D) Weak pigmented eye cups. **(E-H)** Underdeveloped eye cups. Penetrance in (A) n= 2/41; (B) n= 1/41; (C) n=1/41; (D) n=1/41; (E) n=1/41; (F) n=4/41; (G) n=4/41; (H) n=2/41. The specimens in A and F were visualized with electron microscopy. Controls are in Figure 3.3.3. Scale bars: 200 µm.

Nevertheless, modifying the standard order of the cutting steps (not cutting or cutting before the injection) and changing the injection doses, added new phenotypes. Hypopigmented eye and skin (Fig. 3.5.3 A, B, C, D), fused pigment cups that regenerated into two separated cups after 33 days (Fig. 3.5.3, E-M) and heterogeneous pigmentation (half orange) in the pigment cups were observed (Fig. 3.5.3, I, N).

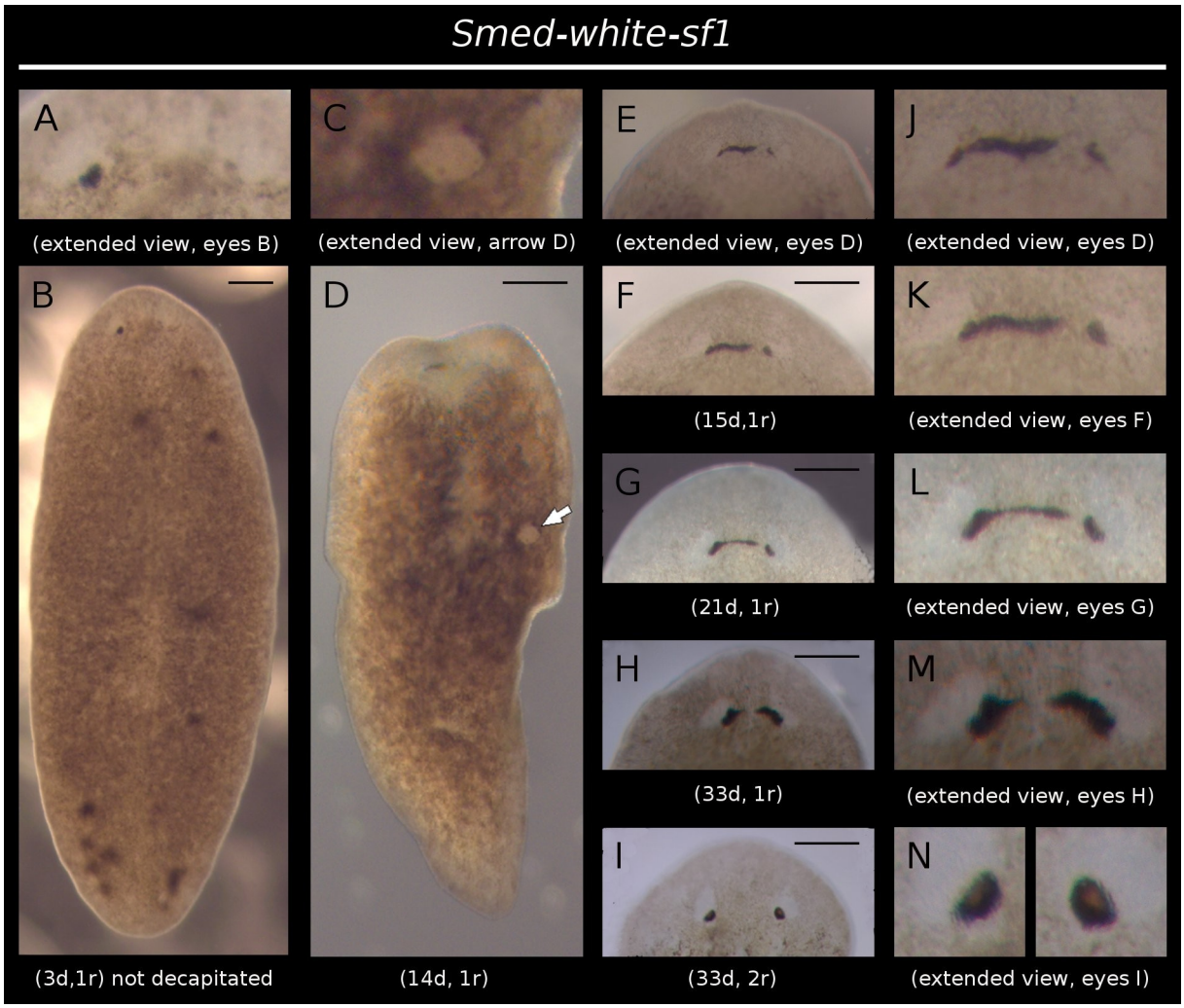

Figure 3.5.3. Phenotypes by low dose injections of one or two rounds of *Smed-white-sf1* mRNA. The doses injected varied in the range 45-270 ng/µL. **(B)** Without decapitation and one single injection (3 x 0.32 µl of a 270 ng/µL solution) one pigment cup disappeared and skin pigment appeared irregular. The morphogenesis also seemed to be affected. **(C-H)** The same animal photographed at different time points. The animal was decapitated after injection of 45-55ng/µL. **(F-H)** The fused eyes regenerated into two separated pigment cups after 33 days. **(I, N)** The pigmentation of the cups seemed to be unevenly distributed. Penetrance in: (B) n= 2/35; (D) n = 3/125; (F-H) n = 1/125; I n=1/155. Controls are in Figure 3.3.4. Scale bars: B, 200 µm; D, 200 µm; F-H, 150 µm.

The in situ hybridization in both intact and in regenerating flatworms (time course: 3 hours, 1, 2, 3 and 6 days) with both *Smed-white-sf1* and *Smed-white-sf2* mRNA showed expression in the gut branches, with no differences in the regenerating areas (Fig. 3.5.4).

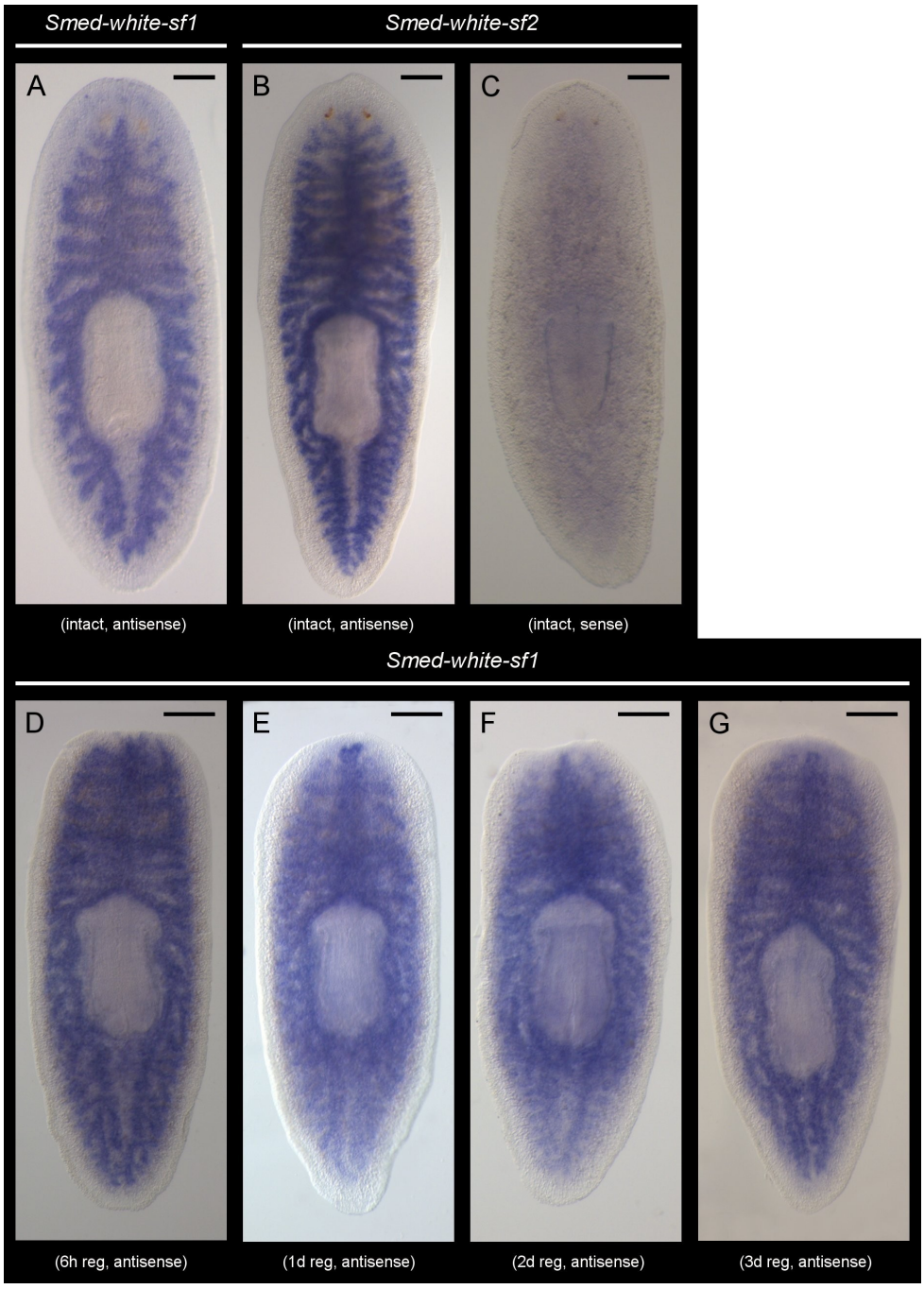

Figure 3.5.4. Whole-mount in situ hybridization showing the same expression patterns with two fragments of the same gene, *Smed-white-sf1* and *Smed-white-sf2*, in intact and in regenerating flatworms (DIG-labelled antisense mRNA probes, NBT/BCIP developed). (A) *Smed-white-sf1* mRNA was detected in the gut cells. **(B, C)** *Smed-white-sf2* antisense and sense mRNA hybridization respectively. The sense RNA strand was used here as the negative control. **(D-G)** Time course of *Smed-white-sf1* antisense mRNA after 6 hours,1, 2 and 3 days of regeneration. sf1= sequence fragment 1; sf2 = sequence fragment 2. Controls Fig. 3.3.4. Scale bars: 200 μm.

To demonstrate changes in the fine structure of the eye cells in *Smed-white-sf1*, the eye region was examined using an immunofluorescence assay and electron microscopy (Fig. 3.5.5; Fig. 3.5.6; Fig.3.5.7).

To measure changes in the photoreceptors, provoked by the *Smed-white* mutations, VC1 was used. This is an antibody that binds to arrestin, a molecule usually found in the inner and outer segment of rod and cone photoreceptors (see Introduction 1.4.2 and 1.4.5) and that in planarians binds to the rhabdomeres. The photoreceptors in *Smed-white* RNAi were reduced in size and near the tip of the head (Fig. 3.5.5, A).

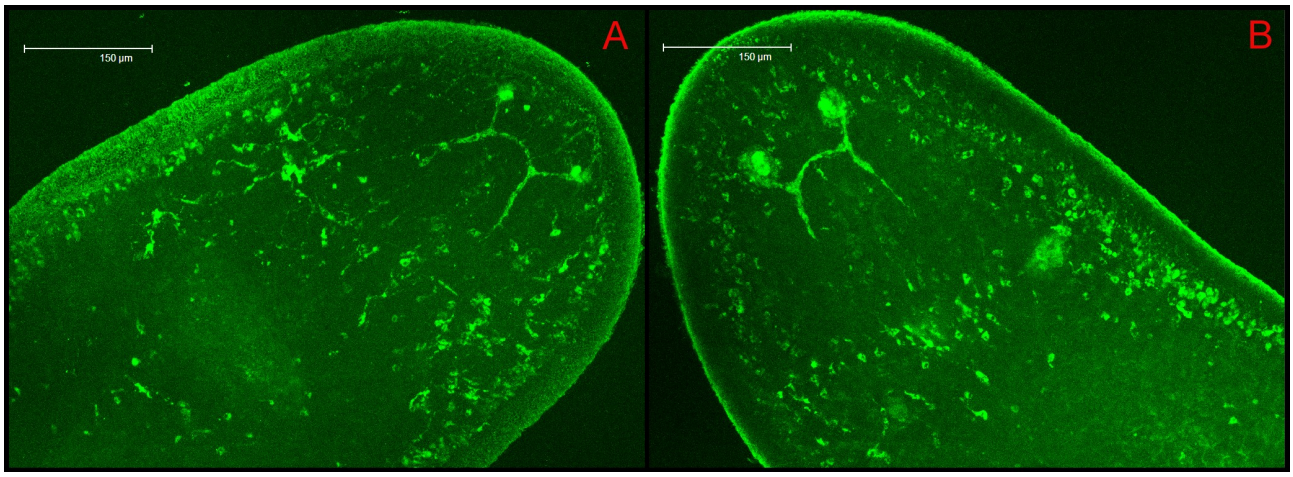

Figure 3.5.5 Confocal images of immunofluorescence *Smed-white* RNAi labelled with the anti-arrestin antibody (VC1). The staining was performed after 2 rounds of injections and 10 days of regeneration. **(B)** Control *Jelyfish*-GFP RNAi. The rhabdomeres, axons and optic chiasm of the photoreceptor cells are labelled. **(A)** The rhabdomeres seem to be underdeveloped, probably due to the absence of pigment cups (living flatworm Fig. 3.5.2 F). In addition to the eyes, other structures are also labelled with VC1; they might also be neurons. Scale bars: 150 µm.

The histological analysis of the *S. mediterranea eye* with electron microscopy showed for the first time the rhabdomeres (control) (Fig. 3.5.6), which as expected were very similar to their homologues in other planarians (i.e. *Dugesia tigrina*) (Press, 1959). The rhabdomeres inserted into the pigment cup have a tubular character, but it is not clear if they are grouped as drawn in Fig. 1.1. In addition, two different rhabdomere colour sections, one dark and bright, can be appreciated (Fig.3.5.6 D; Fig. 3.5.7 A, C). Several sorts of “pigment capsules” were also present (Fig.3.5.7 A, B), thus questioning the existence of other pigments in addition to melanin, such as ommochromes or pteridines (Kato et al., 2006; Hase et al., 2006). Nevertheless, the histological analysis of *Smed-white-sf1* was far from satisfactory, due to the fact that the eye pigment cell layer can only be seen as a cup-shaped pigment pile, after pigment formation. Therefore, it was not possible to identified reduced photoreceptors surrounded by hypopigmented or non-regenerated cups.

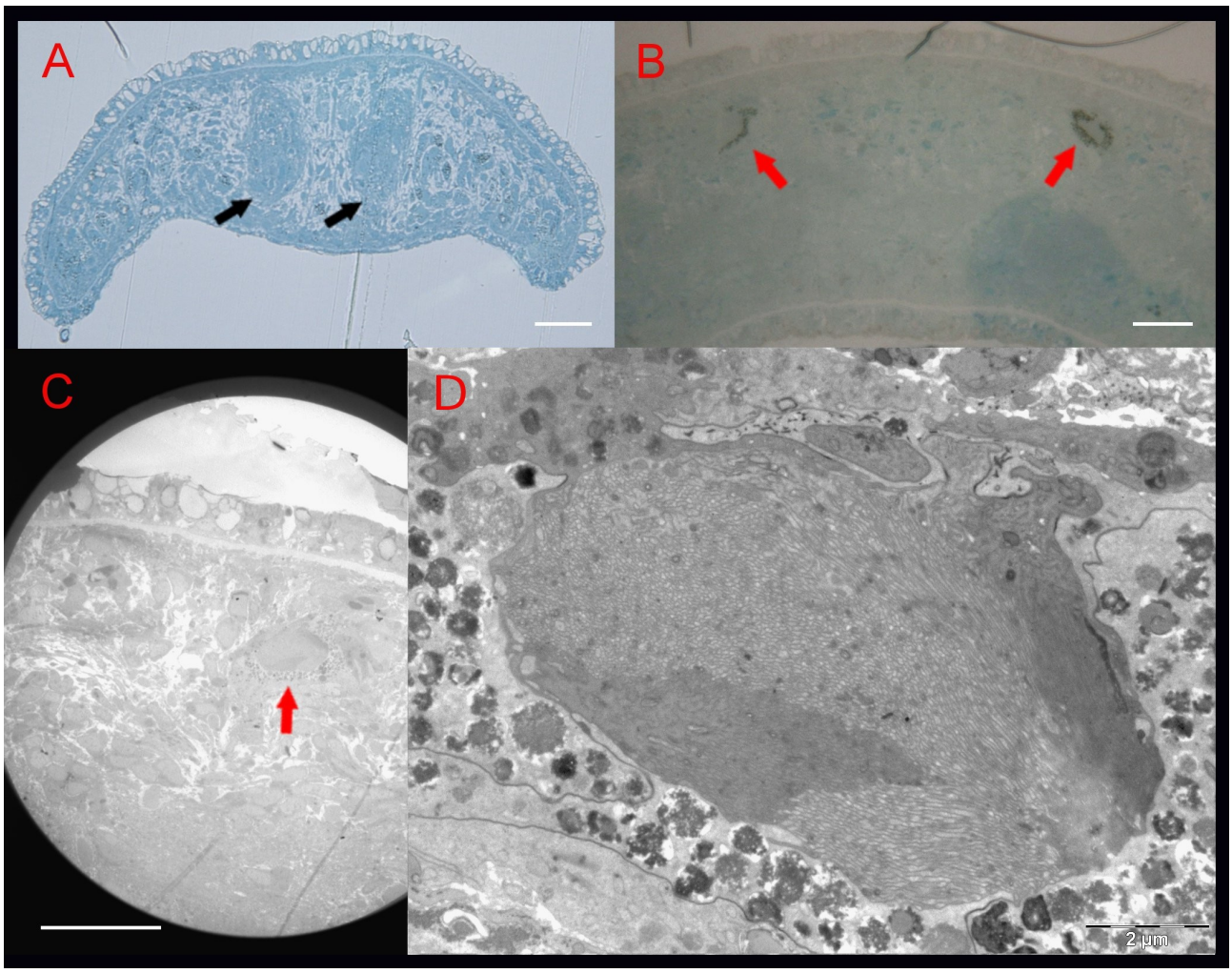

Figure 3.5.6: Electron micrograph of *S. mediterranea,* injected with GFP mRNA: eye and surroundings. **(A,B)** Light micrographs of transversal sections stained with methylene blue showing the mid location of the gut cavities in A (arrows) and the pigment cells of the eyes (red arrows) near the body edge (white line) in B. **(C)** Body section containing the eye (red arrow). Notice the distance to the epidermis. **(D)** Complete section of the eye, including pigment cells surrounding the rhabdomere. Scale bars: A, 40 µm; (B,C) 20 µm; D 2 µm.

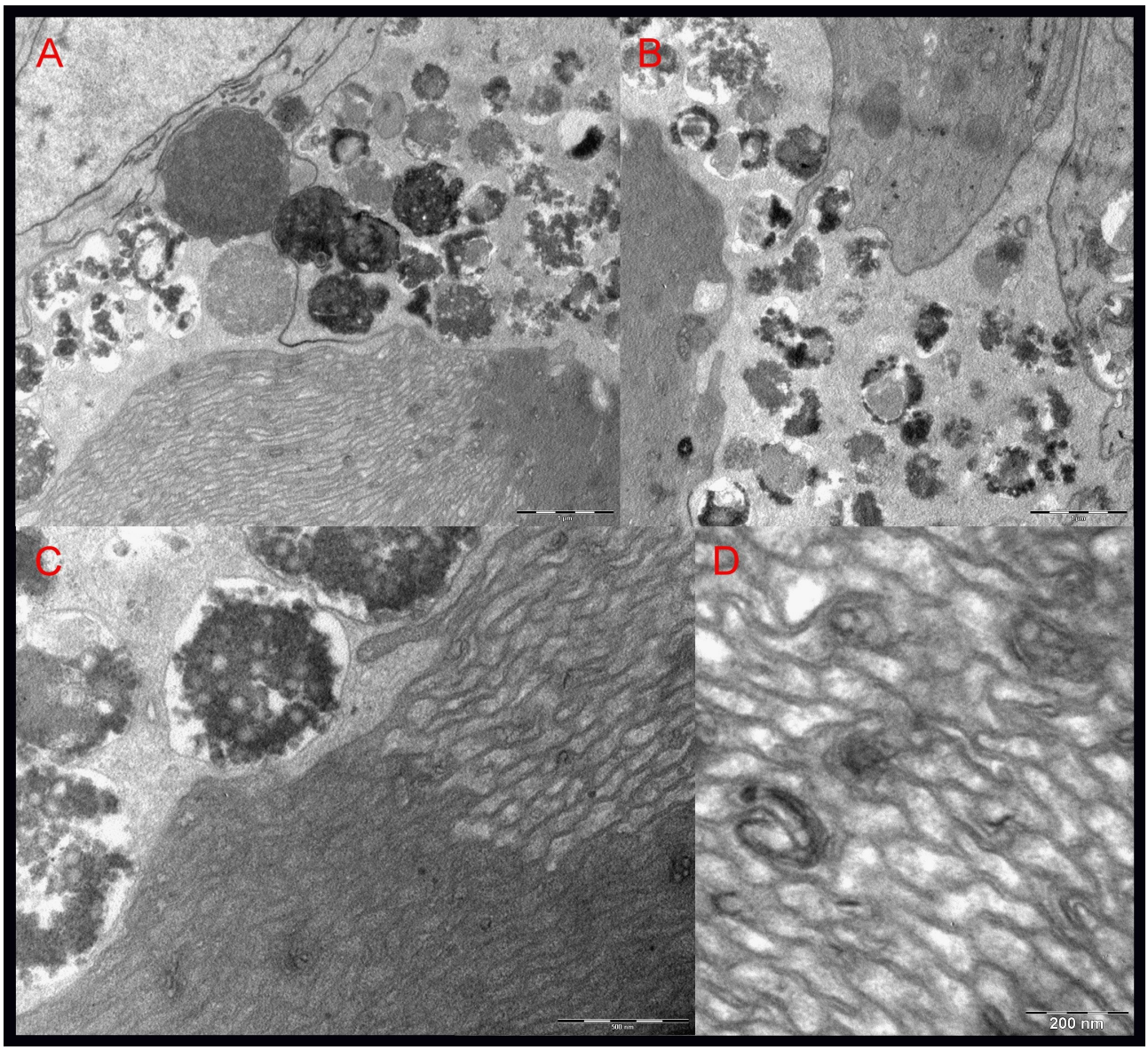

Figure 3.5.7 Electron micrographs of the *S. mediterranea* eye, details from Figure 3.5.6, D. (A) Pigment cells next to the rhabdomeres. **(B)** Pigment granule that seems heterogeneously built. **(C)** Transition areas of the rhabdomeres in two different states. The rhabdomeres in the dark area seem to be filled. **(D)** Detail of neuron membranes from the rhabdomeres. Scale bars: A, B 1 µm; C 500 nm; D 200 nm.

The *Smed-white-sf2* (white second fragment) RNAi caused 73 flatworms out of 107 to develop as the controls (Fig. 3.5.1, E) (controls Fig. 3.3.2). Nevertheless, asymmetric pigment cups were also observed (Fig. 3.5.1, H). Moreover, 34 flatworms out of 107 died after a few days. Furthermore, in order to find new phenotypes, 3600 ng/µL mRNA was injected. This caused an immediate ejection of the pharynx, as in *Smed-tpr1* RNAi (Fig. 3.7.1), and slow destruction of the body over the following days (data not shown).

The gene fragments *Smed-white-sf1 and Smed-white-sf2* both have an ABC transporter structure. ABC transporters are constituted minimally of two distinct types of domain, two transmembrane domains (TMD) and two nucleotide-binding domains (NBD). These regions can be found in the same protein or in two different ones. The sequence and architecture of TMDs is variable. The TMD of *D. melanogaster* consists of six alpha-helices that recognize a variety of substrates and undergo conformational changes to transport substrates across the membrane. The NBD domain binds ATP at the interface of the dimer. This protein transports, among others things, pigment precursors against a concentration gradient at the expense of ATP hydrolysis (Challoner et al., 1999). In humans, the gene ABCR, an ATP-binding cassette, is associated with AMD in Stargard eye disease (Dryja et al., 1998, Allikmets et al., 1997).

Interestingly, pharynx autotomy was only provoled by *Smed-white-sf2* fragment RNAi*,* and only after the injection of a considerable amount of RNA. This phenotype was also observed after treatment with the chemical sodium azide (Adler et al., 2014) and after the injection of the two pigment-related genes *Smed-ver* and *Smed-tpr1,* studied here. After pharynx ejection resulting from *Smed-white-sf2* RNAi, tissues were destroyed, but not by *Smed-tpr1,* in which normal regeneration resumed after some tissue destruction (Fig. 3.7.1). The absence of *Smed-white-sf2* RNA molecules might induce the accumulation of small peptides such as guanine and tryptophan, key pigment synthesis components, that could be capable, when present in sufficient quantities, to initiate a neuronal reaction like the evisceration autotomy observed in the sea cucumber *Thyone briareus* (see section 3.7.1 below).

Orange-yellow flecks, as shown in *Smed-white-sf1* (Fig. 3.5.3 I, N), distributed around the macula and the mid-periphery, also appear in Stargardt disease. They are caused by the progressive bilateral atrophy of the macular RPE and neuroepithelium (Dryja et al., 1998). A similar phenotype to that observed in G. *morsitans* white mutants was seen in *Smed-white-sf1* RNAi (Fig. 3.5.1, 3.5.2, 3.5.3). The white mutants of the tsetse fly *Glossina morsitans submorsitans* have a altered distribution of the eye pigment (xanthommatin and pteridines). The defective white gene cannot transport 3-hydroxykynurenine, the pigment precursor of the later stages of the xanthommatin pathway from tryptophan (Challoner et al.,1997). In addition, in *D. melanogaster* white mutants, eye colouration is affected (Morgan, 1910; Mackenzie et al., 1999). Here, the transport of guanine, a precursor of red pigment biosynthesis (drosopterins) (Sullivan et al., 1980) and tryptophan, precursor of brown pigments (ommochromes) (Summers et al., 1982), were defective.

Furthermore, bacterial ABC transporters have a wide range of physiological functions, such as the import of nutrients and export of antibiotics and toxins (Garmory et al., 2004). Considering the gut branches also reach eyes and skin, the protein transporter activity might be restricted to pigment precursors. Whether the eye pigment or the skin pigment precursors are the same or can be transported by the same ABC transporter, as it may recognize a variety of substrates, should be studied. Nevertheless, using quantitative RT-PCR and in situ RNA hybridization, Reed et al. identified xanthommatin as an ommochrome pigment found in red wing scales of the butterfly *Vanessa cardui* and described transcription patterns of the vermilion, cinnabar, and white genes in developing wings (Reed et al., 2005. Furthermore Oxenkrug, suggested that the slow rate of kynurenine formation from tryptophan, may be associated with prolongation of the life-span in *Drosophila melanogaster* eye-colour (white and vermilion) mutants (Oxenkrug, 2010), ascribing this a new effect to this protein pathway.

The reduction of photoreceptor cells after *Smed-white* RNAi shown in the Figure 3.5.5, suggests underdeveloped growth that might be caused by the pigment cup reduction. Both cell types appear in conjunction, depending on each other, in every eye in the animal kingdom: from insects and mollusca to higher vertebrates. When the communication between the developing RPE and the developing neuronal retina is interrupted, the RPE is able to form a multilayered retina-like structure by itself (Strauss, 2005).

3.5.2. *Smed-ver* (vermilion)

The *Smed-ver* DNA sequence shows high homology with the Drosophila vermilion gene that codes for tryptophan 2,3-dioxygenase. The full name, putative function, expression pattern, phenotype and phenotype penetrance of *Smed-ver* summarized in Table 3.2. After injection of 500 ng/µl *Smed-ver* RNA, all the flatworms ejected the pharynx a few minutes later, followed by skin and body destruction (data not shown). A similar pharynx autotomy phenotype had been observed after injection of *Smed-white-sf2* and *Smed-tpr1* (Fig. 3.7.2 E-H)*;* both are pigment-related genes (xantomatin transport and melanin synthesis respectivel). In addition, *Smed-ver* is specifically expressed in some cells that resemble the cephalic ganglia, but are more spread out on both sides and the tip of the head (Fig.3.5.8). Unlike the cerebral ganglion, these cells are both ventrally and dorsally located (Fig.3.5.8 A, B).

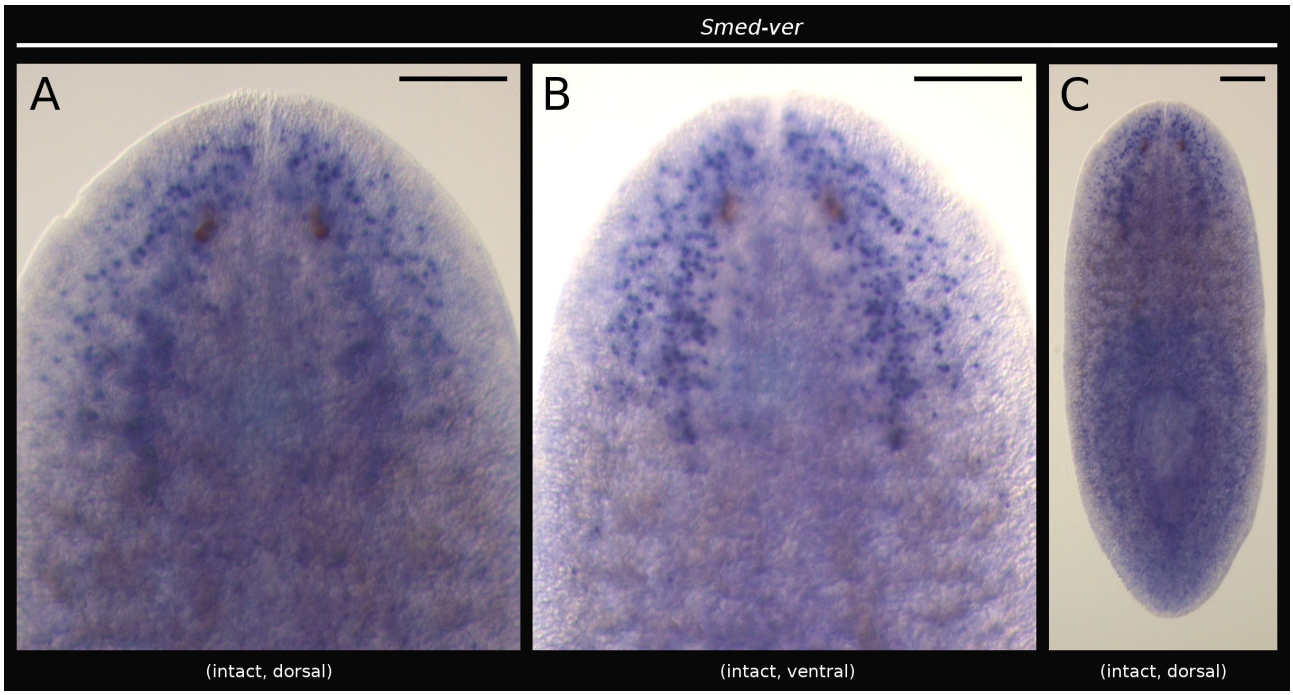

Figure 3.5.8 Whole-mount in situ hybridization showing the expression pattern of *Smed-ver* in intact flatworms (DIG-labelled antisense mRNA probes, NBT/BCIP developed). The head of C is dorsally and ventrally magnified in A and B. *Smed-ver* RNA was detected in a pattern that resembles the cerebral ganglia, but is more extended to the sides, surrounding the eyes and at the tip of the head. Unlike the cerebral ganglion, these cells are both ventrally and dorsally locate. It is also expressed in an oval pattern around and in the pharynx. Scale bars: 500 µm.

The *Smed-ver* gene encodes a tryptophan 2,3-dioxygenase or indoleamine 2,3-dioxygenase (IDO). The enzyme catalyses the first and rate-limiting step in the ommochrome synthesis, and the initial conversion of tryptophan to formylkynurenine. It is required for the normal brown colour, a composite of red and brown pigments, in the *Drosophila melanogaster* eye (Searles et al.,1990). The sex-linked, recessive vermilion-eye colour mutants of *D. melanogaster* are characterized phenotypically by the lack of brown eye pigment. Moreover, in the butterfly *Vanessa cardui,* vermilion was found to be transcribed throughout the fifth-instar wing discs, with higher levels being observed in the epidermis between the wing veins (Shapard et al., 1960).

Furthermore, IDO, mediates antiviral as well as antibacterial and antiparasitic effects by nearly complete depletion of the essential amino acid tryptophan at the local site of inflammation and in dentritic cells in mice (Obojes et al., 2005). Interestingly, in the human eye cataractous lens and during lens ageing, tryptophan can be oxidized by a non-enzymatic mechanism. Oxidation products such as kynurenines accumulate and react with proteins to form yellow-brown pigments causing covalent cross linking. These products pass through cell membranes and could thus diffuse through the cortex of the lens (Staniszewska et al., 2005). Furthermore, IDO can generate toxic metabolites produced within the kynurenine pathway, for example N-formyl-kynurenine, 3-hydroxy-kynurenine and antranilic acid (Obojes et al., 2005). Thus, the role of IDO in vivo is ambivalent and may depend on additional factors that are present during specific immune responses (Wirleitner et al., 2003).

The cerebral ganglion-like pattern of these cells and the labeling with an eye gene, *vermilion*, indicates the possibility of these cells being neurons. As *Smed-melanopsin1,* an opsin gene, and the rhodopsin-like cells in the auricles of *Dugesia japonica* (Asano, et al., 1998) have similar expression patterns, these cells might be photoreceptors, RGCs, responsible for negative phototaxis behaviour and circadian rhythm in *S. mediterranea.* These cells might synchronize circadian clocks to light-dark cycles and regulate melatonin production; a molecule that is endogenously synthesized in planarians in a circadian manner (Morita et al., 1987, Itoh et al., 1999). Morita et al. described melatonin-synthesizing cells located in the planarian head; presumably in close association with the photoreceptor system, in the apical portion of the photoreceptor cell (Morita et al., 1988).

Since fissioning of decapitated *Dugesia dorotocephala* is suppressed by continuous treatment with melatonin (Morita et al., 1993), the lack of *Smed-ver* might affect the amount of the essential amino acid tryptophan and influence the melatonin balance in *S. mediterranea* and consequently this ejection process. Originating in the circadian rhythm, these cells might be involved in asexual fission (Asano, et al., 1998) or even in other kinds of fission such as the pharynx autotomy observed in *Smed-ver* in this study.

The extreme reaction to by the *Smed-ver* mRNA injection together with the specific mRNA expression closely associated with the photoreceptor system (Fig.3.5.8) suggest the possibility of strong central neuronal activity, capable of provoking the pharynx autotomy. The chemical sodium azide causes the amputation of the pharynx in planarians (Adler et al., 2014), and the evisceration autotomy in the sea cucumber *Thyone briareus* is caused by nervous stimulation from a small peptide, potentially a neuropeptide (~150 MW), of unknown character. Whether the *Smed-ver* RNAi follows the same mechanism should be studied.

3.6 GENE EXPRESSION ANALYSIS AND FUNCTIONAL STUDY OF PUTATIVE TRANSCRIPTION FACTORS

Ten DNA sequences, *Smed-hox1, Smed-hox2, Smed-exd, Smed-yy1, Smed-hmt, Smed-fox, Smed-tlx, Smed-mitf1, Smed-mitf2* and *Smed-mitf3,* from the *S. mediterranea* transcriptome were identified as transcriptions factors in silico through the Blast2GO and Pfam approaches. Table 3.3 summarizes the full names, putative functions, expression patterns, phenotypes and phenotype penetrances of these genes. RNAi and in situ hybridization experiments were performed to identified putative functions and RNA expression patterns. Two genes, *Smed-hox2* and *Smed-exd,* that had expression patterns in the brain also presented eye regeneration defects after RNAi. Furthermore, *Smed-hox1,* with expression in the photoreceptor cells, did not regenerate the blastema. In addition, although the genes *Smed-yy1* and *Smed-hmt* had expression in the photoreceptor cells, no visible phenotype could be observed, either in the eyes or in any other parts of the body. Although *Smed-mitf2* and *Smed-mitf3* had low parenchymal expression, they presented eye and skin pigmentation defects.As well as having no visible phenotypes, *Smed-mitf1*, *Smed-fox* and *Smed-tlx* displayed broad and diffuse expression throughout the entire planarian body and pharynx.

3.6.1 *Smed-exd* /*Smed-pbx* (extradenticle/pre-B-cell leukaemia homeobox)

Smed-exd is found to have a high degree of homology with helix-turn-helix homeodomain proteins. Table 3.3 summarizes the full name, putative function, expression pattern, phenotype and phenotype penetrance of this gene. Furthermore, the *Smed-exd* DNA sequence, analysed in this study, extracted from the 454EST_Abril database (Abril et al., 2010), corresponds to *Smed-pbx* which appeared later (Chen et al., 2013; Blassberg et al., 2013) also referred to in the Table 3.3. Unlike this study, those two publications named this gene *Smed-pbx.* Figure. 3.6.1 shows the eye defects and the underdeveloped heads observed in *S. mediterranea* after the doubled-stranded mRNA injections conducted in this study. No pigment cups, no periglobular areas and not even a head developed after 12 days.

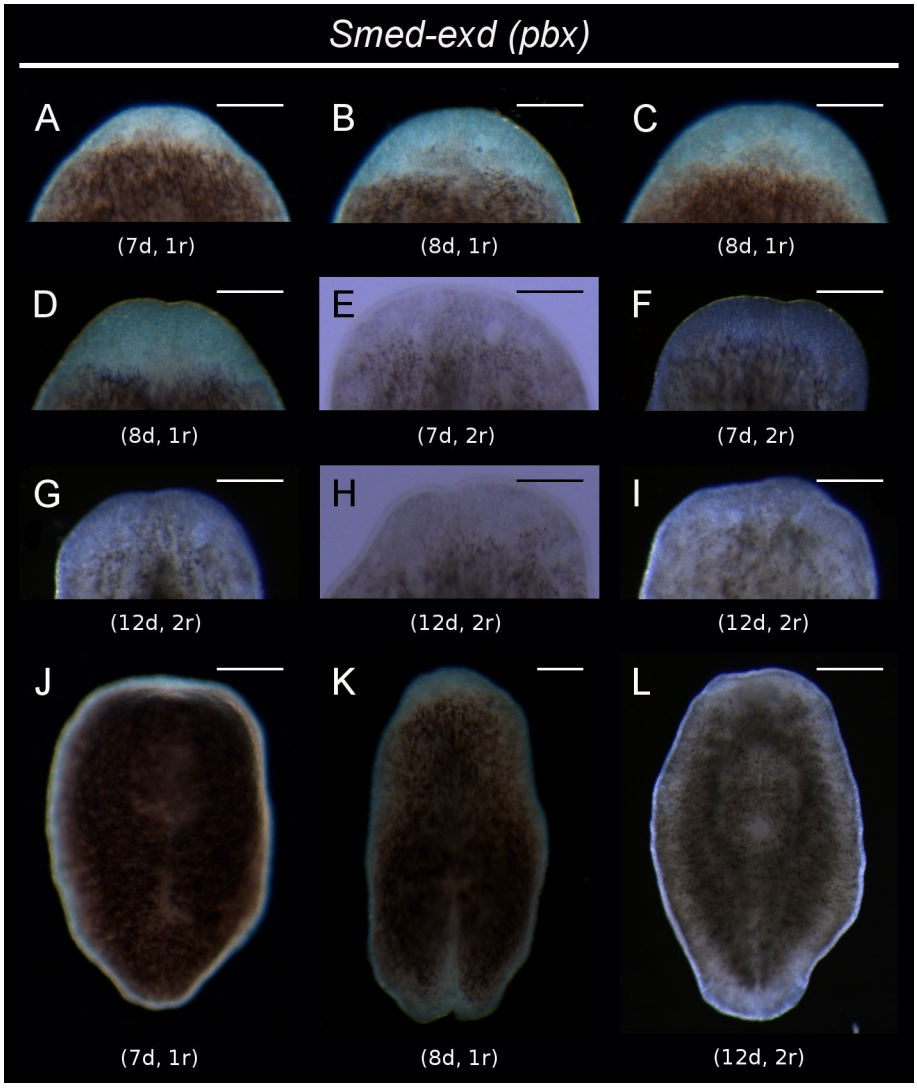

Figure 3.6.1. *Smed-exd (-pbx)* RNAi animals failed to regenerate eyes and blastemas. After injection of 110 ng/µL *Smed-exd* dsRNA 3 or 6 single times and 7 days of regeneration: **(A)** inability to regenerate the eyes; and **(J)** inability to regenerate the blastema. After one round of injection, a cut and 8 days of regeneration, four different phenotypes appeared: **(B)** pigmented cups too small; **(C)** absence of pigment cup but periglobular area present; **(D)** absence of periglobular area and pigment cups; **(K)** tail with transversal fission prints. After a second round, amputation and 7 days: **(E)** only the periglobular area developed; **(F)** the eyes did not regenerate. The same phenotypes remained after 12 days: **(G)** only one periglobular area was formed; **(H)** no eyes appeared, **(I)** only periglobular area developed that was too small developed; and **(L)** blastema did not grow. Penetrance in: A n=10/10; B n=4/10; C n= 1/10; D n=2/10; E n= 2/10; F n= 3/10; G n= 3/8; H n= 1/8; I n= 3/8; J n=2/10; K n=1/10; L n=2/ 10. The death rate was 2/10 after 12 days. The controls are in fig. 3.3.2 and fig. 3.3.3. If not specified, the photographs are decapitated bodies after the indicated number of days of regeneration. Scale bars: (A-I, K) 200 µm; (J, L) 100 µm.

Fluorescent labelling of the eyes in *Smed-exd* RNAi flatworms with anti-arrestin antibody and labelling with eye progenitor markers (otxA, eya) demonstrated that the photoreceptor cells and the optic chiasm disappeared after 8 days of regeneration (Fig. 3.6.2; Chen et al., 2013). This suggests that the *Smed-exd* is required for eye progenitor formation during regeneration, and ultimately for formation of photoreceptor neurons and pigmented optic cups (Chen et al., 2013).

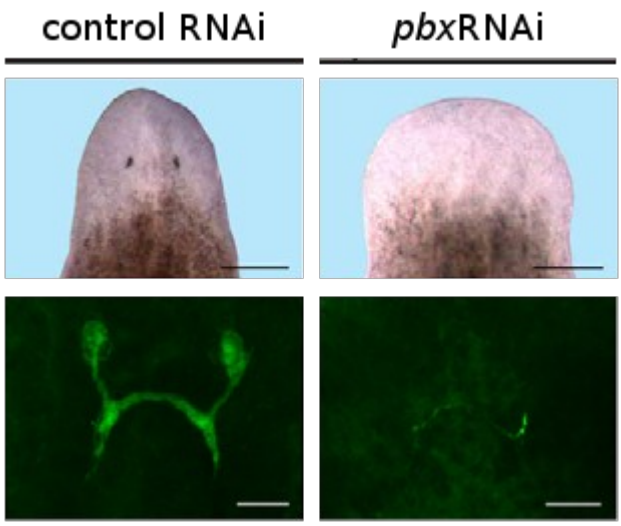

Figure 3.6.2 Eye regeneration defects observed in *S. mediterranea pbx* RNAi after 8 days of regeneration. Upper left: control RNAi, fed with *C. elegans* unc-22. The degree of development of the eye cups can be seen. **Upper right:** *pbx* RNAi without eye cups. **Lower left:** confocal image of a immunostained flatworm with axons and bodies of photoreceptor neurons are labelled with the α-ARRESTIN (α-ARR) antibody. **Lower right:** photoreceptor neurons could not be labelled with (α-ARR) due to its absence. Scale bars: RNAi, 200 µm; confocal images, 50 µm. (Source: Chen et al., 2013)

The *Smed-exd* expression pattern in *S. mediterranea* also includes the brain lobes; but in addition, an extended diffuse expression throughout the entire planarian body and pharynx is observed (Fig. 3.6.3).

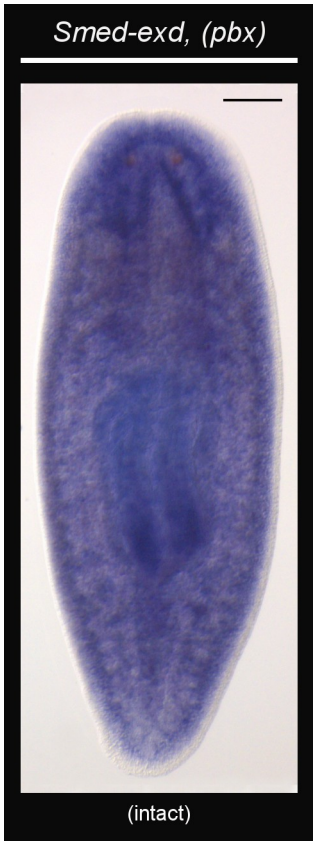

Figure 3.6.3. Whole-mount in situ hybridization showing the expression pattern of Smed-exd in an intact animal (DIG-labelled antisense mRNA probes, NBT/BCIP developed). *Smed-exd* also presentes broad expression throughout the body, including the pharynx and the brain lobes. In situ control Figure 3.3.5. Scale bar: 200 µm.

Three alpha helices connected by short loop regions build the helix-turn-helix homeobox domain of *Smed-exd* which in turn, is a common DNA and RNA binding domain found in transcription factors. EXD is the best-described example of how proteins, acting as cofactors, cooperatively interact with homeotic proteins to increase their specificity to DNA binding (Rauskolb et al., 1995). In *Drosophila melanogaster, Dm\exd* mutants, the observed phenotypes were: between others, defective neuroanatomy and ectopic eyes, among others (Pfeifer et al., 1990; Pai et al., 1998).

Furthermore, extradenticle is a homologue of the human proto-oncogene *pbx1* (Rauskolb et al., 1993) and together with the homotorax (*hth)* gene is essential for axon patterning in the embryonic brain (Nagao et al., 2000). *Drosophila melanogaster Dm\exd* is expressed in developing brain neurons, visual anlage, visual primordium, optic lobe and, central brain primordium in embryonic stages and also maternally (Nagao et al., 2000). Irradiation and fluorescence-activated cell sorting (FACS) experiments suggested that some *Smed-exd* expression might occur in neoblasts. They give rise to many newly forming blastema cells where they can regulate the expression of pole markers and formation of eye progenitors (Chen et al., 2013).

3.6.2 *Smed-mitf-1*, *Smed-mitf-2* and *Smed-mitf-3* (microphthalmia-associated transcription factor).

Two sequences, *Smed-mitf1* and *Smed-mitf3,* extracted from the *S. mediterranea* NCBI data-base, and one, *Smed-mitf2,* from the 454 sequencing approach (see Material and methods, section 5.2) have high homology with microphthalmia-associated transcription factor (Mitf). Table 3.3 summarizes the full names, putative functions, expression patterns, phenotypes and the phenotype penetrances of these genes. RNAi animals injected with *Smed-mitf2, Smed-mitf3* and a mixture of *Smed-mitf1,-2,-3* (1:1:1) presented severe eye and skin hypopigmentation, even 12 days after the first cut (Fig. 3.6.4). The in situ experiments in contrast, showed weak expression on all three genes in the parenchymal cells (Fig. 3.6.5).

Each of the three sequences has a basic helix-loop-helix zipper DNA-binding domain (bHLH). The motif is characterized by two α-helices connected by a loop. In general, one helix is smaller than the other and due to the flexibility of the loop, allows for dimerization by folding and packing up against the other helix. The larger helix typically contains the DNA-binding regions. bHLH proteins typically bind to a consensus sequence called an E-box, CANNTG (Chaudhary et al., 1999). Human MITF undergoes alternative splicing that results in MITF expression in a different cell lineage (Simmons et al., 2013). MITF is involved in the differentiation and development of melanocytes (Levy et al., 2006) and in osteoclast development (Hershey et al. 2004) and it also up-regulates both OCA2 (oculocutaneous albinism type 2) and SLC45A2 (solute carrier family 45 member 2), which are required for melanin synthesis enzymes such as tyrosinase (TYR) in humans (Law et al., 2012).

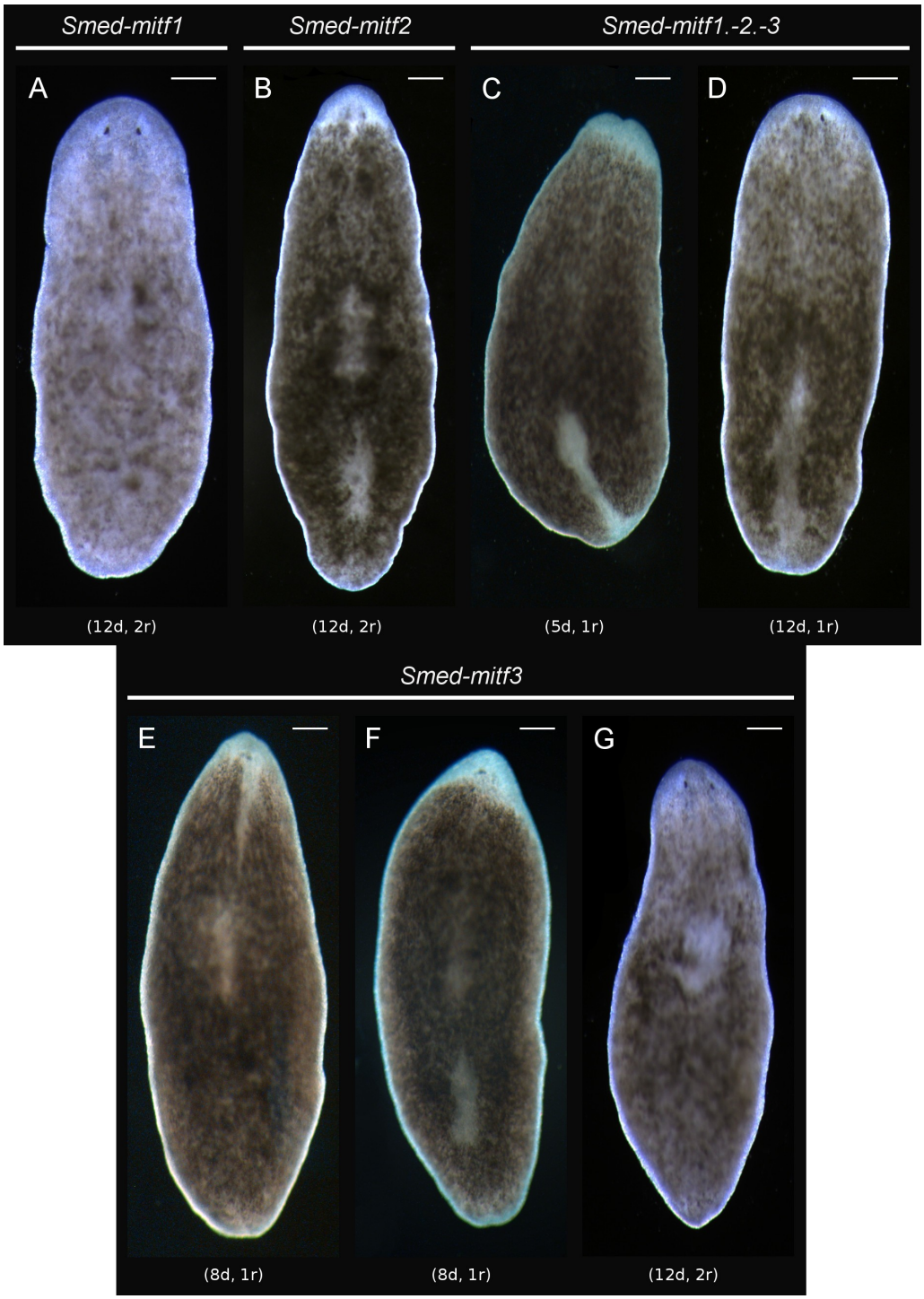

Figure 3.6.4. RNAi of *Smed-mitf1*, *Smed-mitf2*, *Smed-mitf3 and Smed-mitf1,-2,-3* together. (A) Eye and skin pigmentation seem to be as in the controls. **(B)** Pigment cups and skin pigment defects. **(C, D)** Injection with a mix of *Smed-mitf1, -2, -3*, together 1:1:1 affected eye and skin pigmentation development and might also induce spontaneous tail fissioning. **(E, F, G)** *Smed-mitf3* RNAi affected the eye symmetry and eye and skin pigmentation. Penetrance in: A n= 10/10; B n=10/10; C n=10/10; D n=10/10; E n=1/10; F n= 1/10; G n= 8/10. The controls are in Figures 3.3.2 and 3.3.3. Scale bars: (A-G) 200 µm.

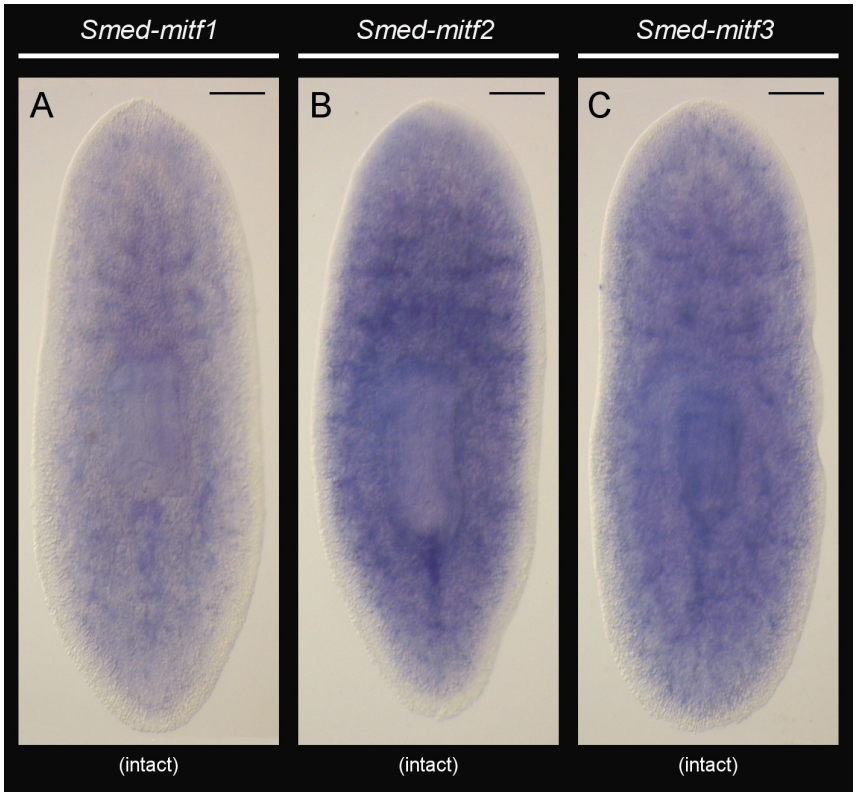

Figure 3.6.5. Whole-mount in situ hybridization showing the expression patterns of *Smed-mitf1*, *Smed-mitf2* and *Smed-mitf3* in intact animals (DIG-labelled antisense mRNA probes, NBT/BCIP developed). As expected, the three sequences have the same expression pattern. All three are expressed in the parenchymal cells, with *Smed-mitf1* being especially weak**.** In situ controls Figure 3.3.5. Scale bars: 200 μm.

The phenotypes observed by *Smed-mitf2* and, *Smed-mitf3* RNAi correlate with those in MITF mice and human mutants. Mitf knockout mice undergo many, affects in several different cell types, but mainly pigment cells, resulting in deafness, bone loss, small eyes, and poorly pigmented eyes and skin (Moore, 1995). Nevertheless, mouse Mitf is strongly expressed in the RPE pigment granules (Nakayama et al. 1998), unlike *Smed-mitf1*, *Smed-mitf2* and *Smed-mitf3* that spread widely throughout the body (Fig. 3.6.5). This expression agrees with the melanocytic cell lineage distribution in skin tissue suggested by Simmons (Simmons et al., 2013). Heterozygous mutations in human MITF cause auditory-pigmentary syndromes, such as Waardenburg syndrome type 2 (WS). The humans WS phenotype is characterized by hypopigmentary defects of the hair, skin and iris (hypoplastic iride) and structural eye defects (dystopia canthorum). Iris heterochromia might be partial in only one eye (Yang et al., 2013). Nonetheless, injection of *Smed-mift1* mRNA did not affect the development of the eyes or other parts of the body, not even after the second round of injections (Fig. 3.6.4 A). It is worth noting that minor skin and eye pigmentary defects or slight eye displacements, such as those seen in human MITF mutants (Yang et al., 2013), might go unnoticed in planarians and they cannot be accurately measured. The midline tail hypopigmentation observed by some *Smed-mitf1,-2,-3 animals*, might be caused by spontaneous tail fission (Fig. 3.6.4 C, D). This phenotype could also have another origin; this issue will be the subject of further research.

3.6.3 *Smed-hox1* and *Smed-hox2*

Smed-hox1 and *Smed-hox2* are both found to have high homology with the homeobox domain and might function as transcription factors. Their full names, putative functions, expression patterns, phenotypes and phenotype penetrances are summarized in Table 3.3. After RNAi and head amputation, *Smed-hox1* animals did not regenerate the head and *Smed-hox2* animals did not completely regenerate the eyes (fig 3.6.6 D, E). Both *Smed-hox1* as *Smed-hox2* presented eye and brain lobes expression patterns (Fig. 3.6.6 A, B, F, G). In addition, *Smed-hox2* had a brain expression pattern (Fig. 3.6.6 C), similar to that observed in *Smed-ver* (Fig. 3.5.8). Furthermore, the RNA expression spread throughout the parenchyma and the pharynx (Fig. 3.6.6 C, G). Part of the signal in Fig. 3.6.6 D, could be background.

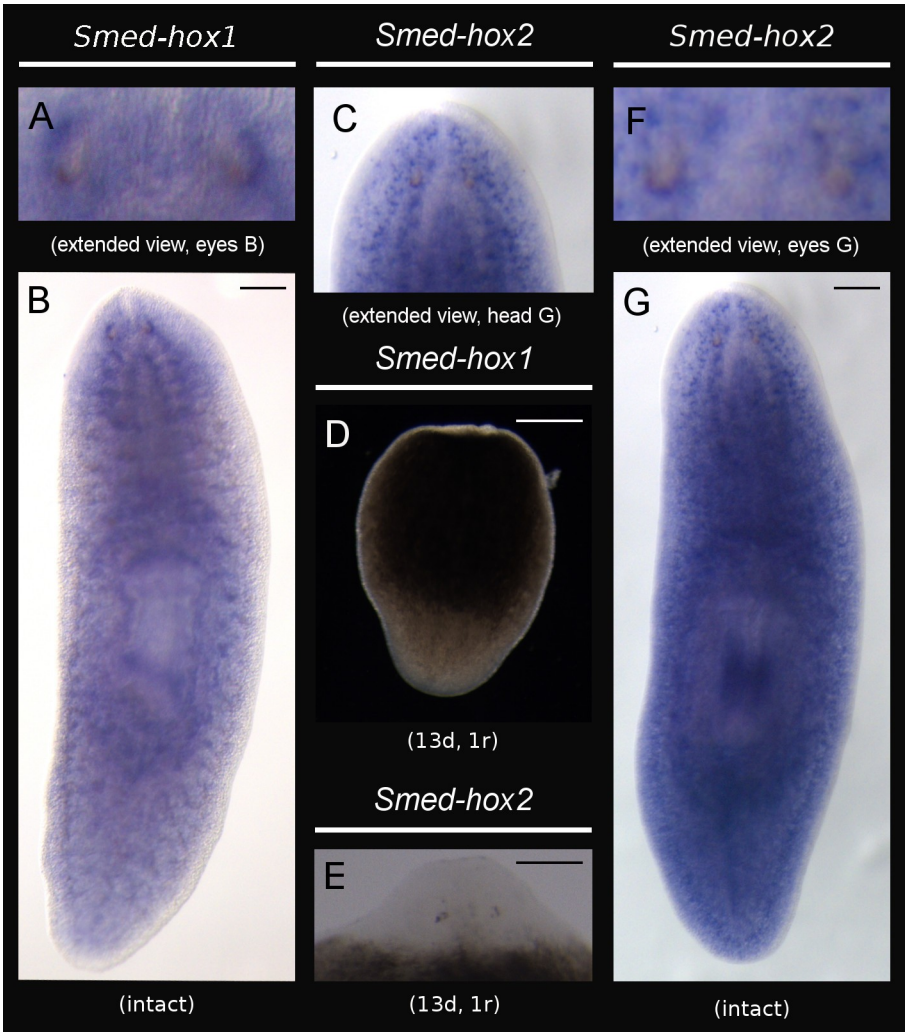

Figure 3.6.6 RNAi and whole-mount in situ hybridization of *Smed-hox1* and *Smed-hox2*. (D) *Smed-hox1* RNAi inhibited blastema regeneration. **(A, B)** *Smed-hox1* mRNA was expressed in the photoreceptor cells, brain and parenchymal cells. **(E)** *Smed-hox2* induced underdeveloped eyes. **(C, F, G)** *Smed-hox2* mRNA expression was detected around the photoreceptors and brain lobes, in the tip of the head and spread throughout the parenchymal cells. Penetrance in: D n= 5/5; E n=1/5. The RNAi controls are in Figs. 3.3.2 and 3.3.3. In situ control Figure. 3.3.5. Scale bars: (D) 100 µm; (B, G, E) 200 µm.

Although *Smed-hox1* and *Smed-hox2* genes both have an homeobox domain with a helix-turn-helix (HTH) structure, *Smed-hox1* also has a caspase CASP C-terminal region. Proteins with a CASP C-domain are Golgi membrane proteins, which are thought to play a role in vesicle transport. Furthermore, increased retinal expression of caspase-1 pro-enzyme may be a common marker of photoreceptor degeneration, because the caspases, a family of cysteine proteases, have been implicated in the regulation of apoptotic cell death in a variety of systems (Samardzija et al., 2006). Nevertheless, previous studies indicate that several genes encoding proteins with a homeodomain structure are required for proper retinal development. Mutations in homeobox genes can produce easily visible phenotypic changes. As an example, the homeobox gene *pax3* can causes Waarthenburg syndrome in humans, which presents, among other symptoms, iris pigmentary abnormality (heterochromia iridium) and hair and skin hypopigmentation (Waardenburg, 1951). Meanwhile, mutations in the *pax6* gene are known to cause two common disorders in humans: Peter's anomaly (thinning and clouding of the cornea) and aniridia. In the heterozygous condition, aniridia causes the absence of the iris in human and a panacular condition with macular and optic nerve hypoplasia, cataracts and corneal change. In the homozygous condition, in contrast, it results in the failure of the entire eye formation and, severe brain damage, as well as death prior to birth (Hingorani et al., 2012). Defects in the *pax6* gene also cause aniridia-like ocular defects, eyelessness or underdeveloped eyes in mice as well as in *Drosophila* (Ghering et al., 1999; Gehring, 2001; Davis, 2008). Notably, the *S. mediterranea* homeobox genes *otxA* and *six1/2* are also required for optic cup regeneration (Lapan et al., 2011). *Girardia tigrina six* is also essential for maintenance of the differentiated state of photoreceptor cells (Pineda et al., 2000). In addition, mutations in the human, *pax3* and MITF result in hair, skin and also eye hypopigmentation (Waardenburg, 1951; Yang et al., 2013). Remarkably, the eye and brain expression of *Smed-hox1* and *Smed-hox2* mRNA in *S. mediterranea* (Fig 3.6.6, A, B, C, F, G) might be similar to the expression patterns of other homeobox-containing genes such as *rax*, *pax6*, *six3* and *otx2*. In situ hybridization of *rax* RNA has shown that it is initially expressed in the region of the forebrain, where optic vesicles are formed, and in the ventricular zone of the developing mouse retina later in development (Furukawa, 1997). Although in the *S. mediterranea* brain neither structures has been found, similar patterns of expression have been identified in lineage-specified pigment cup cells (Lapan et al., 2011). Furthermore, in mouse, *pax6* (Walther et al., 1991), *six3* (Oliver et al., 1995) and *otx2* (Simeone, et al., 1993) are known to be expressed early in development in a region including the anlagen of the eye.

3.6.4 *Smed-tlx* (T-cell leukaemia homeobox gene: also called NR2E1)

Smed-tlx shows a high degree of homology with homeobox-domain proteins, especially with the transcription factor T-cell leukaemia homeobox-protein:. Its full name, putative function, expression pattern, phenotype and phenotype penetrance are summarized in Table 3.3. Loss-of-function of *Smed-tlx* RNAi did not provoke any visible regeneration differences in flatworms compared with to controls (data not shown) (controls Figures 3.3.2, and 3.3.3). Parenchymal mRNA hybridization did not provide any additional information as to its putative functionality (Fig. 3.6.7).

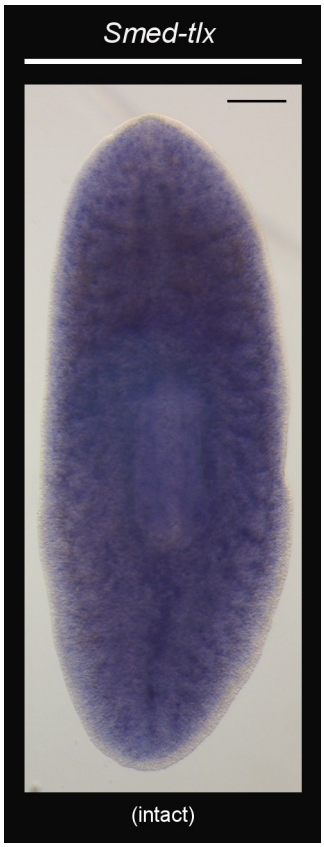

Figure 3.6.7 Whole-mount in situ hybridization showing the expression pattern of *Smed-tlx* in an intact animals (DIG-labelled antisense mRNA probes, NBT/BCIP developed). *Smed-tlx* displays broad diffuse expression throughout the entire planarian body and pharynx. In situ control Figure 3.3.5. Scale bar: 200 µm.

The homeobox gene *Smed-tlx,* provided with an HTH structure, is a member of the tailless class of orphan nuclear receptors: a super family of transcription factors characterized by a DNA-binding domain (DBD) and a ligand-binding domain (LBD) (Mangelsdorf et al., 1995). Expression of mice *Tlx* is localized in the neural retina, optic stalk, and forebrain. *Tlx* is a key component of retinal development and vision and an upstream regulator ofthe *Pax2* signalling cascade. *Tlx* mice mutant suffer progressive retinal and optic nerve degeneration with associated blindness, leading to reduced brain size and thin cerebral cortex (Ruth et al., 2000). Moreover, TLX interacts with the corepressor atrophin1 *(Atn1*), directly regulates the expression of *Pten* and its target *cyclin D1,* modulates the phospholipase C and mitogen-activated protein kinase (MAPK) pathways. TLX is required for coordinating retina-specific proliferation and differentiation programmes to prevent retinal dystrophy (Zhang et al., 2006). In addition, the human TLX3 is important in specifying cell fate in autonomic nervous system (ANS) differentiation, neuron migration and fate specification resulting in the sudden infant death syndrome (SIDS), which is characterized by the unexpected death of one-year-old infants (Weese-Mayer et al., 2004).

3.6.5 *Smed-hmt* (histone lysine methyltransferase)

Smed-hmt shares high homology with the SET domain enhancer of zeste. It is an epigenetic transcription factor that codes for the histone lysine methyltransferase in *Schistosoma mansoni.* Table 3.3 summarizes the full name, putative function, expression pattern, phenotype and phenotype penetrance of *Smed-hmt. S. mediterranea Smed-hmt* RNAi did not show any visible phenotype, even in the eyes; although its RNA is expressed in the distal part of the photoreceptor cells (Fig.3.6.8).

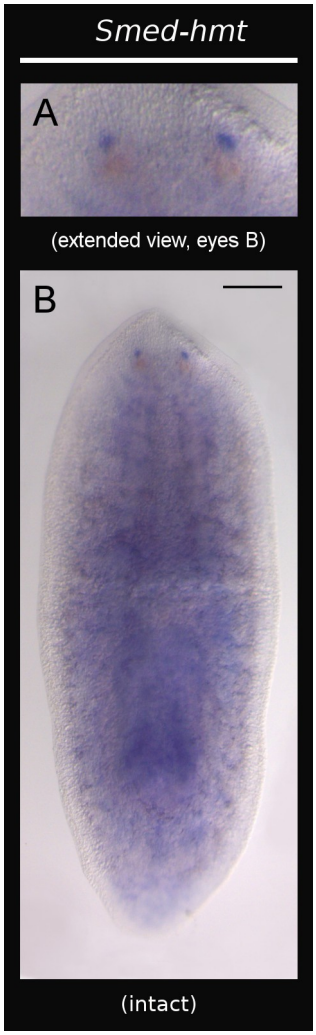

Figure 3.6.8 Expression pattern of *Smed-htm* DIG-labelled antisense mRNA probes in an intact animal (NBT/BCIP development). *Smed-htm* mRNA expression is enriched in the distal part of the photoreceptor cells. In situ control Figure 3.3.5. Scale bar: 200 µm.

Smed-hmt has a SET domain (β-strands) which provides the histone lysine methyltransferase activity of this protein. Histone lysine methyltransferase specifically monometilates and dimethylates 'Lys-4' of histone H3. H3 'Lys-4' methylation represents a specific tag for epigenetic transcriptional activation. The histone H3 K9 lysine methyltransferase (G9a) is essential for proper differentiation of post-mitotic cells and the integrity of retinal progenitor cells in the mouse retina. The mouse G9a KO mutant retina exhibits severe morphological defects, including photoreceptor rosette formation, partial loss of the outer nuclear layer, elevated cell death, and persistent cell proliferation. Moreover, Kimiko Katoh suggested that methylation mediated by G9a serves as an epigenetic memory in the differentiated state because G9a deletion in differentiating photoreceptor cells results in retinal degeneration (Kimiko Katoh et al., 2012). The *Drosophila* messenger RNA of dG9a is ubiquitously distributed due to its maternal contribution at stage 4 and stronger expression in the CNS and the neuroectoderm at stage 9 (Stabell et al., 2006). The photoreceptor cell expression of *Smed-hmt,* however, is a promising development for the retinal differentiation function in *S. mediterranea* (Fig.3.6.8), which should be researched further.

3.6.6 *Smed-yy1* (Yin Yang 1)

Smed-yy1 presents a high degree of homology with the double zinc-finger domain of the transcriptional repressor protein YinYang. Table 3.3 summarizes the full name, putative function, expression pattern, phenotype and phenotype penetrance of *Smed-yy1*. No visible phenotype was observed in *Smed-yy1* silenced flatworms (data not shown); nonetheless, the expression pattern in the eyes and throughout the parenchyma in *S. mediterranea* suggests a regulatory function in developmental eye genes (Fig. 3.6.9).

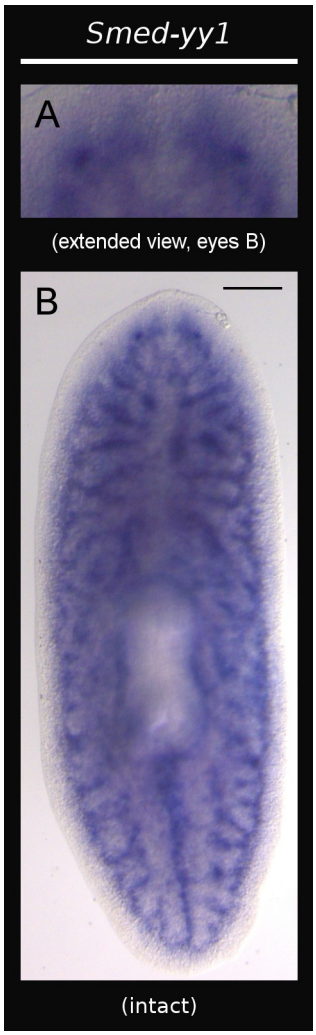

Figure 3.6.9. Expression pattern of *Smed-yy1* in an intact animal (DIG-labelled antisense mRNA probes, NBT/BCIP developed). *Smed-yy1* mRNA is found in the photoreceptor cells (A) and in cells delimiting the gut branches (B), but not in the pharynx. In situ control Figure 3.3.5. Scale bar; 200 μm.

Smed-yy1 has a double zinc-finger domain. YY1 is a bifunctional zinc-finger protein that serves as a repressor or activator of a variety of promoters. The DNA binding transcription factor Yin Yang 1 (YY1) is a powerful regulator of development, essential for early embryogenesis and adult tissue formation. In *Drosophila melanogaster,* YY1 is an orthologue of *pho* (pleiohomeotic): one of the transcription factors that binds the polycomb DNA response element (Vella et al., 2012). *Xenopus* YY1 regulates the *slug* gene expression and is necessary for neural ectoderm differentiation, have been detected in the nuclei of this germ cell layer. The downregulation of YY1 affects antero-posterior neural patterning and produces small eyes in *Xenopus* embryos (Morgan et al., 2004). Furthermore, mouse YY1 interacts with a class II PcG polycomb gene *Ring1/Ring1A* but not with *Pax 6.* Mouse YY1 deletion alters structures of the anterior segment of the eye, displaying the absence of a lens chamber, the failure of corneal endothelium development and lens epithelial defects (Lorente et al., 2006). YY1 also functions as an activator for the expression of the *Msx2* homeobox gene. In chicken MSX2 is involved in craniofacial morphogenesis including cranial neural crest cell apoptosis and the formation of the eye (Holme et al., 2000). In addition, the patterns of expression of YY1 in E10 and E12 mice embryos were restricted to the forebrain, midbrain, hindbrain and tail bud, albeit low levels of YY1 were also detected throughout the E10 embryo (Tan et al., 2002).

3.6.7 *Smed-fox* (fork-head box)

Smed-fox has a high degree of homology with the winged helix xfd structure of the forkhead homeobox protein; a transcription factor. Table 3.3 summarizes the full name, putative function, expression pattern, phenotype and phenotype penetrance of *Smed-fox.* The *Smed-fox* RNAi flatworms developed as the controls did (data not shown) (controls Figures 3.3.2, and 3.3.3). Moreover, the widespread parenchymal expression of its mRNA means it cannot be ruled out from the eyes (Fig.3.6.10).

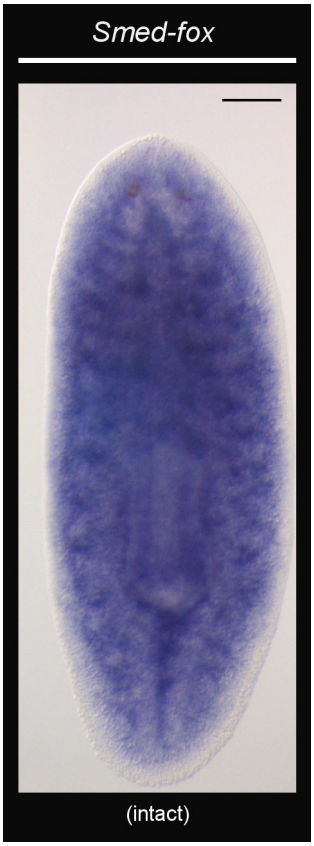

Figure 3.6.10. Whole-mount in situ hybridization showing the expression pattern of *Smed-fox* in an intact animal (DIG-labelled antisense mRNA probes, NBT/BCIP developed). *Smed-fox* displays broad diffuse expression throughout the entire planarian body and pharynx. In situ control Figure 3.3.5. Scale bar: 200 µm.

Smed-fox has a fork-head domain or "winged helix" consisting of four helices and two-stranded beta-sheets. The proteins consisting of about 110 amino acids are found in transcription factors that bind to DNA (Kaufmann et al., 1996). Several fork-head genes are important determinants of retinal cell fate and are present in developing retinal tissue in vertebrates; for example, human FOXC1, mouse *Foxd1*, *Foxn4* and *Foxg1*, *Xenopus foxn3* and zebrafish *foxl1* (Moose et al., 2009).

In humans, mutations in FOXC1 lead to Axenfeld-Rieger (AR) eyes, teeth and abdominal-region malformations. This autosomal disorder shows iris hypoplasia (adhesions of the iris and the cornea caused by an inadequate number of cells), hypertelorism (increased distance between the eye orbits), corneal opacity, abnormal pupillary function and position of the pupil (corectopia), and the progressive blinding condition glaucoma that occurs in approximately half of patients with AR malformations (Murphy et al., 2004). Additionally, inactivation of mouse *Foxd1* gene results in abnormal optic chiasm formation as well as forebrain anomalies that affect the binocular vision. Mouse *Foxd1* is expressed in RGCs of the temporal retina (Hatini et al., 1994; Herrera et al., 2004). Mouse *Foxg1* plays a dual role in eye development, initially in the control of eye morphogenesis by regulating gene expression in the retinal epithelium, and subsequently in axon guidance of RGCs.

Foxg1 mutant mice never develop an optic stalk; the most ventral of the structures to be derived from the optic vesicle during eye development. Instead, the optic stalk tissue is replaced by the neural retina. (Huh et al., 1999; Xuan et al., 1995). In *Foxg1*-/- eyes, RGC axon navigation is perturbed. Furthermore, the proportion of RGCs that contribute to the ipsilateral optic tract is significantly increased compared to wild-type RGCs (Pratt et al., 2004). The *Xenopus foxn3* knockout exhibits small eyes (Schuff et al., 2007).

Foxn4 knockout mice have a reduced number of amacrine and horizontal cells in the differentiated retina. Nevertheless, over-expression of Foxn4 results in an abundance of amacrine cells with no alteration in the horizontal cell subtype (Li et al., 2004). In mice, *Foxn4* is expressed throughout the proliferating ventricular zone (germinal neuroepithelium in foetal brain) and in the retina at stage E13.5 (Gouge et al., 2001). Zebrafish *foxl1* morphants showed aberrations in eye size, improper retinal layer formation and increases in the number of apoptotic cells (microophthalmic phenotype) together with degenerated brains; and over-expression of *foxl1* produced very small or no eyes (Nakada et al., 2006).

Five other forkhead genes, *DjFoxA, DjFoxG, DjFoxD, Smed-FoxD* and *Smed-FoxA,* have already been tested in planarians (Koinuma et al., 2000; Koinuma et al., 2003; Scimone et al., 2014; Vogg et al., 2014; Adler et al., 2014). RNAi has only been performed with *Smed-FoxD and Smed-FoxA,* genes which affect eye and pharynx regeneration, respectively; in addition *Smed-FoxA* produced dorsal lesions at the pharynx level. Nevertheless, their expression patterns suggest that *DjFoxG and DjFoxD* might also affect eye regeneration as a consequence of the anterior regeneration pole influence. Animals injected with *Smed-FoxD* dsRNA regenerated normally-sized anterior blastemas with one eye or smaller blastemas with no eyes. Furthermore, the animals showed a medially collapsed or a very small brain together with failure to regenerate a new midline and to properly pattern the anterior blastema, consistent with a role of the anterior pole in organizing patterns of the regenerating head (Scimone et al., 2014; Vogg et al., 2014). *Smed-FoxD* is expressed in a cluster of cells at the anterior-most tip of the regenerating head, the anterior regeneration pole (Vogg et al., 2014), and following injury, FoxD expression is induced in a restricted midline region of the animal (Scimone et al., 2014). Moreover, in *Dugesia japonica* and in *S. mediterranea,* the *DjFoxA* and *Smed-FoxA* genes are expressed in the pharynx, which suggests it participates in pharynx formation (Koinuma et al., 2000; Adler et al., 2014). In contrast, *DjFoxG* is expressed in the body and brain, with strong expression in the mesenchyme surrounding the gut; whereas *DjFoxD,* is expressed in the mid-apex of the head, between the two lobes of the brain in the mid-anterior blastema (Koinuma et al., 2003), similar to *Smed-FoxD* expression.

None of the phenotypes observed in vertebrate knockouts of FOXC1, *Foxd1*, *Foxn4*, *Foxg1*, *foxn3* and *foxl1* or planarian *FoxA*, *FoxG* and *FoxD*, could be found in *Smed-fox* mutants. Malformations such as a reduction of RGC number, as found by *Foxg1*-mutant mice (Pratt et al., 2004) or a decreased number of amacrine and horizontal cells as found in *Foxn4*-knockouts mice (Li et al., 2004) cannot be detected in planarians, because these cell types have not been identified in this flatworm. Neuronal cell markers that are specific to retinal ganglion, amacrine and horizontal cells might be necessary to test their existence and be able to measure this kind of transformations.

3.7 Gene expression analysis and functional study of putative enzymes

Smed-tpr1, Smed-tpr2, *Smed-kinase* and *Smed-VATP* synthase share high homology with a group of enzymes with functions relevant to photoreception processes, such as melanin synthesis, rhodopsin phosphorylation and photoreceptor energy supply. Their full names, putative functions, expression patterns, phenotypes and phenotype penetrances are summarized in Table 3.4. RNAi and in situ experiments were performed to elucidate their functionalities. S*med-tpr1* RNAi induced head fissioning and pharynx ejection; unlike *Smed-tpr2* RNAi which offered little evidence of affecting eye morphogenesis in a regenerating head. In addition, *Smed-tpr1* is expressed in the eyes and *Smed-tpr2* in the brain and probably also in the eyes. Interference with *Smed-VATP* synthase produced eyeless animals, among other anomalies, such as destruction of all tissues. *Smed-kinase,* an enzyme that needs energy to phosphorylate rhodopsin, is also lethal and its mRNA is expressed in photoreceptors. Specific evidences are presented and explained below.

3.7.1 *Smed-tpr1* and *Smed-tpr2*

Smed-tpr1 and *Smed-tpr2* shows a high degree of homology with the tetratrico peptide domain of tyrosine hydroxylase; an enzyme involved in the melanin synthesis. Table 3.4 summarizes their full names, putative functions, expression patterns, phenotypes and phenotype penetrances. The in situ hybridization showed *Smed-tpr1* mRNA expression in photoreceptors and *Smed-tpr2* in brain lobes and photoreceptors, indicating a relation between every each of these genes and eye tissue (Fig. 3.7.2). However, *Smed-tpr2* developed as the controls did (data not shown, controls Figure 3.3.2) except for one decapitated head that presented one less-developed eye cup (Appendix, Fig. 7.3.9). Unexpectedly, skin disruption, pharynx ejection and head fission appeared immediately after *Smed-tpr1* mRNA injection, followed by normal regeneration (Fig. 3.7.1). In order to eliminate the chemicals used for the RNA probe synthesis as a possible toxicity source, various concentrations of putative or, toxic effectors, DNAse, EtOH, phenol (upper phase), chloroform, methanol, and phenol/chloroform were tested on intact animals. Only phenol chloroform mixed in H_2O miliQ (1:10) produced bubbles in the flatworm skin; but never pharynx ejection.

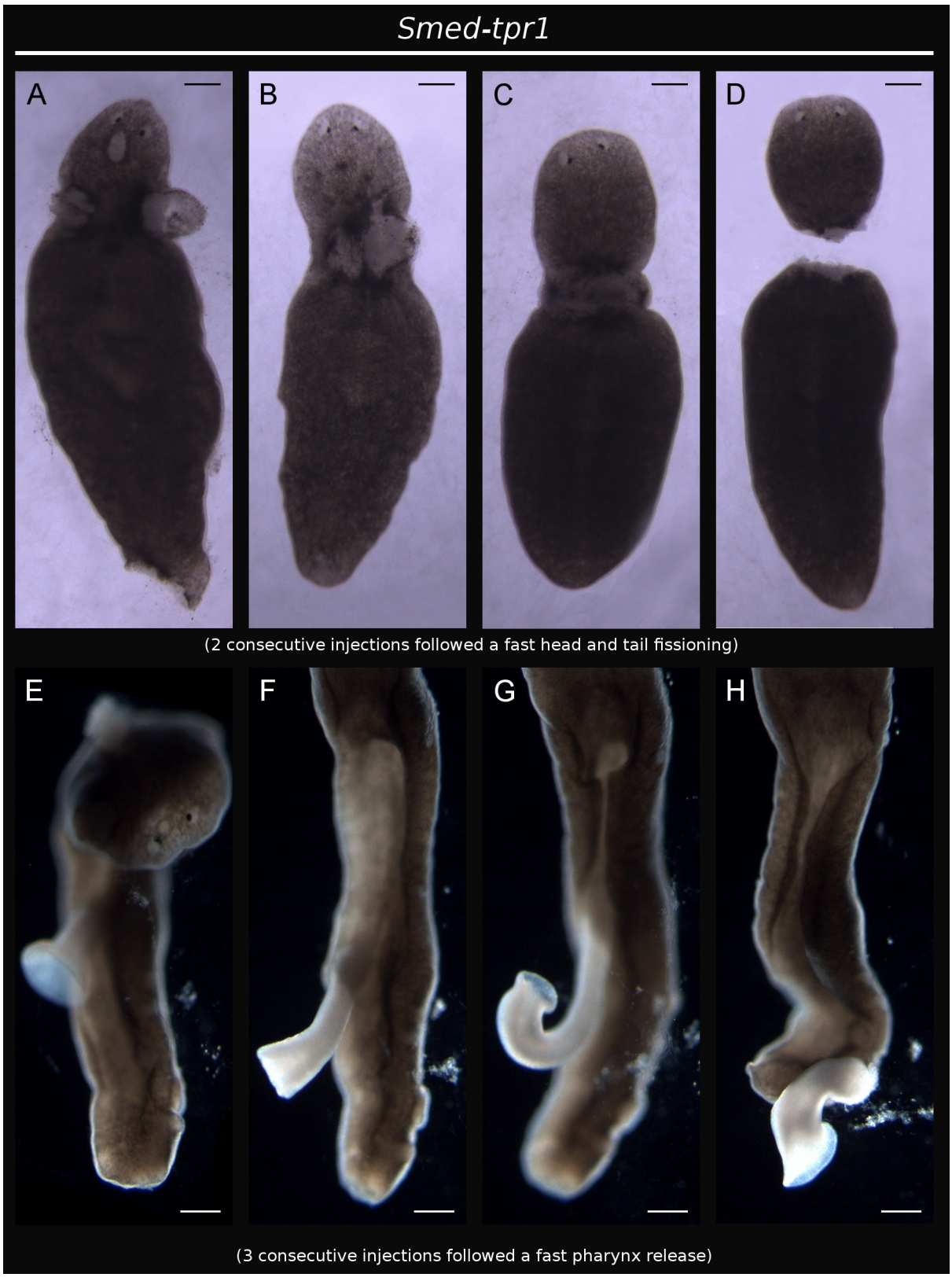

Figure 3.7.1 Phenotypes observed after the injection of *Smed-tpr1* mRNA. (A) Initiation of head and tail fissioning. Bubbles appeared at the dorsal part of the head between the eyes. **(B)** Initiation of head fissioning. The body elongated at the tip and the pigmentation looks darker at the wound edge. **(C)** Muscular contraction takes place in the wound area. (**D)** Detachment of the fissioning parts. **(E)** Initiation of the pharynx elongation, expulsion of dorsal internal tissues and skin pigmentation defects between the eyes. **(F-H)** Pharynx ejection. Penetrance in: **(A-D)** n=4/11; (E-H) n=2/11. Controls in Figure 3.3.2. Scale bars: 200 μm.

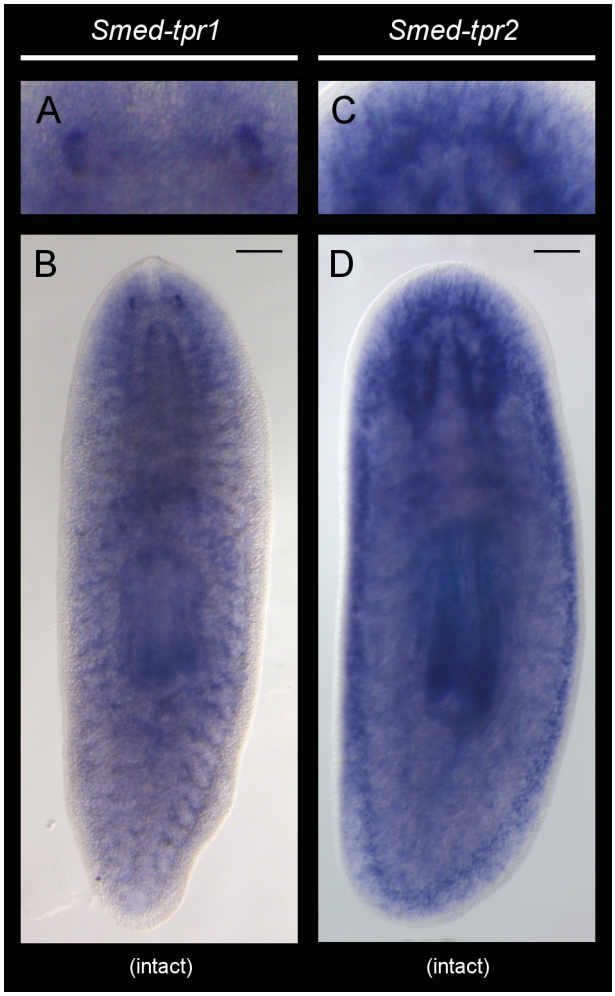

Figure 3.7.2 In situ hybridizations of *Smed-tpr1 and Smed-tpr2* DIG-labelled antisense mRNA probes (NBT/BCIP developed). (A, B) Expression of *Smed-tpr1* in the eyes; possibly the photoreceptors. The parenchymal tissue is also labelled. **(A)** Close-up of B. **(C, D)** *Smed-tpr2* is expressed in the eyes and along the external border of the brain lobes. The pharynx and the parenchymal cells are also labelled; **(C)** Close-up of eyes in D. Controls in Figure 3.3.5. Scale bars: 200 µm.

Smed-tpr1 and *Smed-tpr2* are tyrosine hydroxylases belonging to the 14-3-3 protein family. 14-3-3 proteins can be considered evolved members of the tetratrico peptide repeat (TPR) superfamily, which generally have 9-10 alpha helices. Tyrosine hydroxylase catalyzes the reaction in which L-tyrosine is hydroxylated in the meta position to produce L-3,4-dihydroxyphenylalanine (L-DOPA). Oculocutaneous albinism type 1 (OCA1) results from mutations in the tyrosinase gene (Tyr) (Oetting et al., 2003). This enzyme catalyzes the reaction between tyrosine and DOPA and between DOPA and dopaquinone; the initial steps in melanin synthesis in mice melanocytes and RPE cells (Beermann et al., 1992; Gimenez et al., 2003).

A similar pharynx ejection as that induced in the *Smed-tpr1* RNAi has been observed in two genes tested in this study, also related to pigment synthesis (*Smed-white-sf2, Smed-ver*), and by brief selective induced exposure of animals to 100 mM sodium azide (NaN_3) (Adler et al., 2014). Unlike the autotomy after RNAi, the chemically induced pharynx ejection needs to be dislodged with forceps or by vigorous pipetting. The chemical amputation together with the induced autotomy observed in this study suggest a natural mechanism of pharynx ejection at the wound level. The azide functional group of sodium azide (NaN_3) can be converted to an amine (i.e., amino acids) in the Staudinger reaction. If this reaction can take place inside living organisms like flatworms and if the new amine, product of this reaction, is responsible for the pharynx autotomy, this amine could mimic the effect of other amines abundant in RNAi animals.

The *Smed-white-sf2*, *Smed-ver* and S*med-tpr1* RNAi planarians might accumulate guanine, tryptophan and tyrosine. The loss of the enzyme Tyrosine hydroxylase by *Smed-tpr1* RNAi could produce the accumulation of tyrosine; an amino acid that might induce a similar effect of that of NaN_3. Furthermore, NaN_3 has a bacteriostatic action by inhibiting cytochrome oxidase irreversibly in gram-negative bacteria. In humans, sodium azide causes hypotension or death if it lasts more than 1 hour, and metabolic acidosis (Chang et al., 2003). Interestingly, the three enzymes that caused the pharynx autotomy are steps in pigment synthesis, melanin or ommochrome, where amino acids are key components. The analogous evisceration autotomy observed in *Thyone briareus* is caused by nervous stimulation, as demostrated the anaesthetics tested: Mg^{++} ion, chlorobutanol and propylene phenoxytol. It has been suggested that there may be a factor, a small molecule, a small peptide, potentially a neuropeptide (~150 MW), of unknown character that induces autotomy at the junction of tile pharyngeal retractor muscle in the sea cucumber and which probably plays other roles in muscle and connective tissue physiology (Smith et al., 1973; Byrne, 2001).

When melanin is absent, a range of retinal abnormalities are present in the mature mammalian retina (Jeffery, 1998). Albinos that lack a functional tyrosinase gene suffer from a systematic re-routing of chiasmatic fibres in favour of the crossed projection, underdevelopment of the central retina and a deficit in rods (Dräger et al., 1980). Although DOPA is an inhibitor of cell growth, the albino retina is excessively mitotic and lacking in DOPA (Kinear et al., 1985). Furthermore, the tyrosinase gene is expressed uniformly across the RPE in the early development of mice (Beerman et al., 1992). Furthermore, ectopic expression of tyrosine hydroxylase in mouse albino RPE cells reverses the retinal and visual function abnormalities common in albinos in the absence of melanin. This suggest that L-DOPA or one of its metabolic derivatives plays an important role in normal retinal development (Lavado et al., 2006).

3.7.2 *Smed-kinase* (rhodopsin kinase)

Smed-kinase has a high degree of homology with the serine/threonine-protein kinase, which has a rhodopsin binding domain that is probably involved in rhodopsin phosphorylation. Table 3.4 summarizes its full name, putative function, expression pattern, phenotype and phenotype penetrance. RNAi and in situ experiments were performed to analyze the functionality of the gene. *Smed-kinase* RNAi was lethal (Fig. 3.7.3); no animal survived this treatment. Nevertheless, *Smed-kinase* is expressed in the eyes (Fig. 3.7.4) and in the parenchymal tissue. It has to be taken into account that some of the signal in (Fig. 3.7.4) might be background.

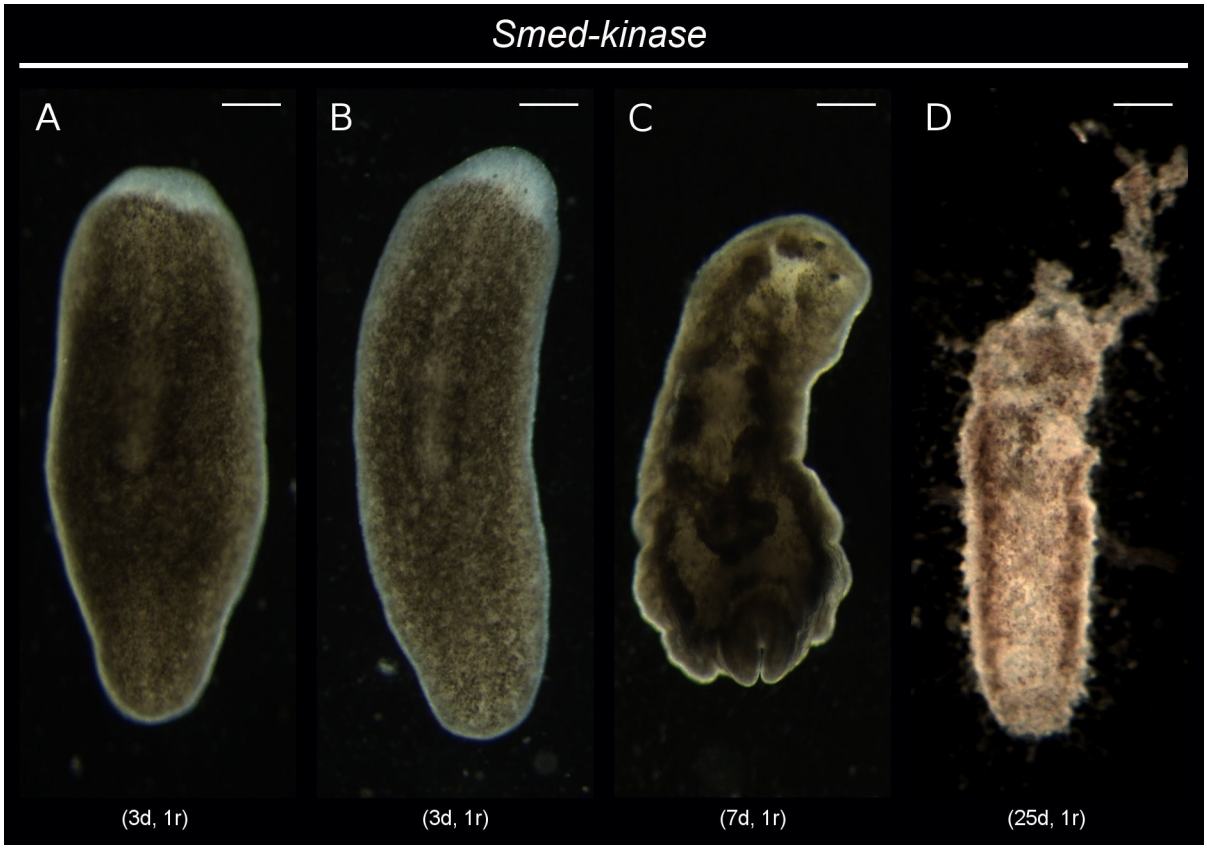

Figure 3.7.3 ***Smed-kinase*** **RNA interference is lethal.** On the seventh day, morphology defects were visible. No animal survived this treatment. **(A)** Regenerated body without eyes. **(B)** Eyes developed as the control. **(C)** Rounded eye cups, skin pigment defects, body morphology changed and motionless body. **(D)** Tissue destruction. Penetrance in: (A) n=13/21; (B) n=8/21; (C) n=21/21; (D) n= 21/21. Controls in Figure 3.3.2. Scale bars: (A, B) 500 µm; (C) 200 µm; (D) 100 µm.

Figure 3.7.4 In situ hybridization of *Smed-kinase* DIG-labelled antisense mRNA probe in an intact animal (NBT/BCIP developed). (B) *Smed-kinase* is expressed in the eyes; possibly in the photoreceptor cells. The background seems to intensify the eye labelling but at the same time it might hide other information. **(A)** Close-up view of eyes in B. Controls in Figure 3.3.5. Scale bar: 200 µm.

Smed-kinase has a kinase domain and a P21 rhodopsin binding domain. The structure of the catalytic core of kinases is built of a glycine-rich residue in the N-terminal extremity and an ATP-binding lysine residue (Hanks et al., 1995). This enzyme transfers phosphate groups from high-energy donor molecules, such as ATP, to specific substrates; a process referred to as phosphorylation (Manning et al., 2002). Light transiently converts rhodopsin into a substrate for phosphorylation. Rhodopsin kinase transfers and binds the terminal phosphate groups of ATP and GTP to serine and threonine residues in the protein moiety of rhodopsin (Kühn, 1978). Furthermore, phosphorylation of rhodopsin critically controls the visual transduction cascade by uncoupling it from the G-protein, transducin. Phosphorylation is abolished in rhodopsin kinase−/− mice, revealing an absolute requirement for rhodopsin kinase to phosphorylate rhodopsin (Adams et al., 2003). Nevertheless, the kinase activity present in the rod outer segment (ROS) also catalyzes the phosphorylation of other substrate proteins, besides rhodopsin; such as protamines and histones (Kühn, H et al., 1973). Phosphocreatine (PCr) can also be a kinase substrate. Creatine kinase (CK) is localized in the mitochondria of chicken photoreceptor cells. It accepts phosphocreatine (PCr) and uses it to regenerate ATP. This process seems to be especially pronounced in tissues and cells that consume ATP rapidly, such as skeletal muscle, brain and photoreceptor cells. The regeneration of the hydrolysed cGMP from ATP and GTP, mediated by enzymes present in the outer segment, is one of the most energy-consuming processes to occur in photoreceptor cell outer segments during phototransduction (Hemmer et al., 1993). The properties of the CK/PCr system seem well suited to overcoming the diffusional limitations in these polar cells by utilizing PCr and Cr as mediators between mitochondria and sites of energy utilization (Wallimann et al., 1994). Retinitis pigmentosa is a progressive degenerative retinal condition with characteristic features including nyctalopia (night blindness), ring scotoma (partially diminished visual acuity) and mottling of the RPE with black bone-spicule pigmentation in humans and mice.

These inherited diseases can be caused by the mutation of peptides corresponding to the C-terminal region of rhodopsin that can therefore not be phosphorylated by rhodopsin kinase (Ohguro, 1997).

The lethality of *Smed-kinase* RNAi (Fig. 3.7.3) could well be explained by the fundamental processes by which the kinase enzyme plays key roles, such as production, transport, conversion and utilization of energy. Furthermore, there is also evidence that creatinine kinase interacts with Na^+ /K^+-ATPase (Wallimann et al., 1994). In contrast, the expression pattern of *Smed-kinase* in the eyes of *S. mediterranea* (Fig. 3.7.4) correlates with its putative functionality in the rod outer segment and in the mitochondria of photoreceptor cells. Furthermore, the parenchymal expression could be due to the phosphorylation of other substrate proteins besides rhodopsin; for instance in muscle tissue (Wallimann et al., 1992).
During muscle contraction, the ADP increases while the ATP decreases; here the creatine kinase could transfer a phosphate radical to ADP, thereby restoring the ATP concentration (Walliman et al., 1992).

3.7.3 *Smed-VATP synthase* (vacuolar ATP synthase subunit C)

In order to explore the planarian energy source for phototransduction, *Smed-VATP synthase* was studied here. The *Smed-VATP synthase* DNA sequence has a high degree of homology with the vacuolar ATP-synthase subunit, with two ATP C domains. Vacuolar ATP-synthases are non-functional in retinitis pigmentosa patients. Table 3.4 summarizes the full name, putative function, expression pattern, phenotype and phenotype penetrance of *Smed-VATP synthase.* The mRNA of *Smed-VATP synthase* showed expression in the parenchymal tissue but restricted to cells involving the gut branches and eyes, which might indicate a broadly extended house-keeping functionality (Fig. 3.7.6). In addition, the relevance of this enzyme was supported by the severe and often fatal phenotypes. These were characterized predominantly by a less-developed blastema, skin lesions (Fig. 3.7.5, A, B; Appendix 3: Fig. 7.3.6 A, B, C, F, I), head fission (Fig. 3.7.5 C), the suppression of development in anterior structures (Fig. 3.7.5, E, F, I), inhibition of eye regeneration (Fig. 3.7.5, H, J) and complete general tissue destruction (Fig. 3.7.5 D, G, K; Appendix 3; Fig. 7.3.6 E, D, G, H). A decrease in the amount of the *Smed-VATP synthase* dsRNA probe injected, increased the survival rate by about 30%, which included flatworms with eyes and skin defects (Fig. 3.7.5 H, I, J). Furthermore, injection not followed by decapitation also provoked devastating effects (Appendix 3 Fig. 7.3.6 I), indicating the magnitude of the effects of *Smed-VATP synthase* also during morphogenesis.

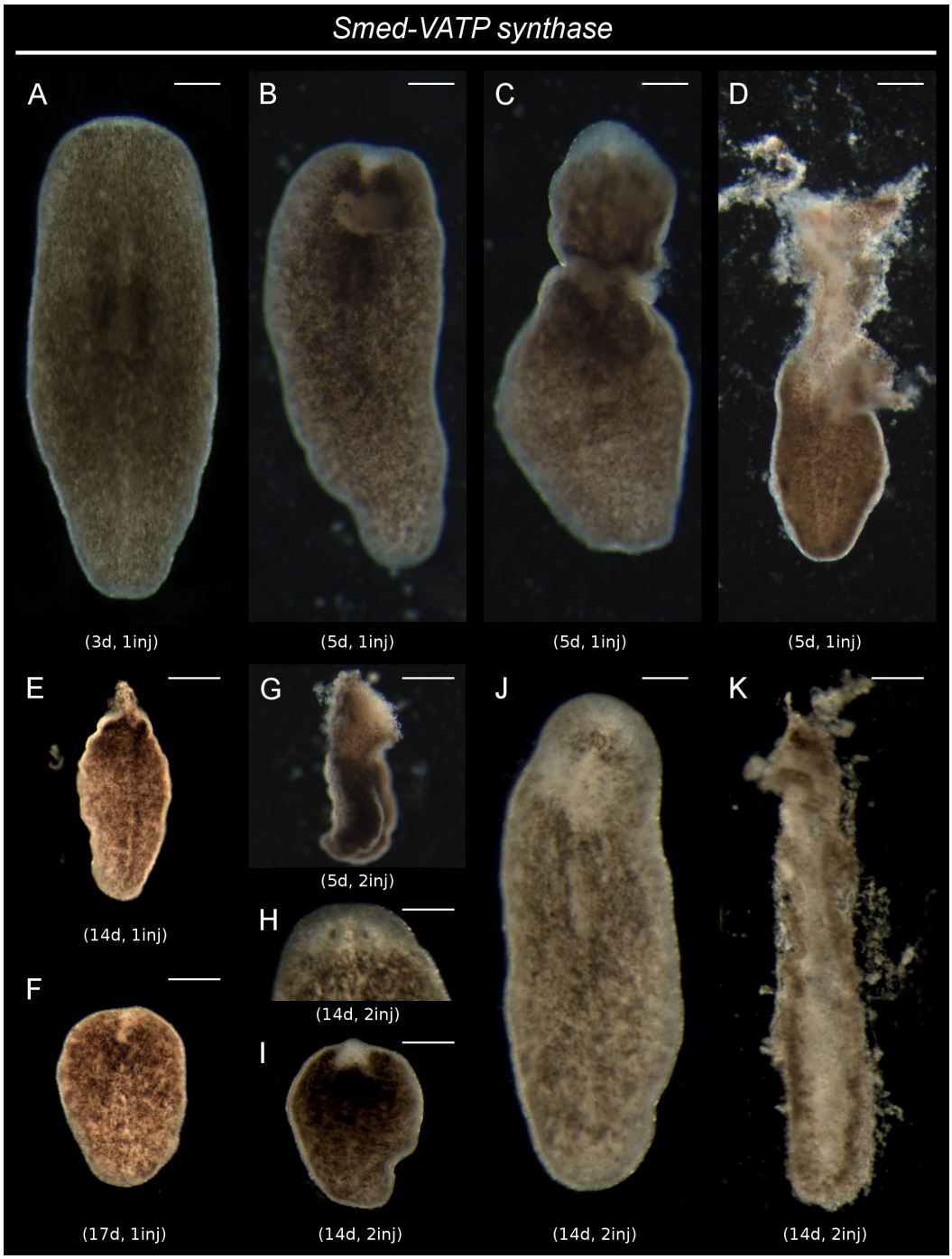

Figure 3.7.5 One and two injections of Smed-VATP synthase RNAi are enough to be lethal. (A) Less developed blastema. After five days, 3 different phenotypes appeared: **(B)** wound at the tip end, **(C)** head fission and **(D)** complete tissue destruction. After 14 and 17 days, the following phenotypes remained in the surviving flatworms: **(E)** tissue destruction; **(F)** suppression of anterior structures development complete immobilization. Two single injections had similar effects: **(G)** tissue destruction; **(H)** hypopigmented eye cups; **(I)** underdeveloped blastema; **(J)** head without eyes and hypopigmented skin; **(K)** destruction of all tissues. Penetrance in: (A) n=8/10; (B) n=5/10; (C) n=1/10; (D) n=2/10; (E) n=1/10; (F) n=1/10; (G) n=2/16; (H) n=1/16; (I) n=6/16; (J) n=1/16; (K) n=8/16. The controls are in Figure 3.3.4. If not specified, the photographs are decapitated bodies after the indicated number of days of regeneration. Scale bars: (A-C, G) 200 µm; (E, F, H-K) 100 µm.

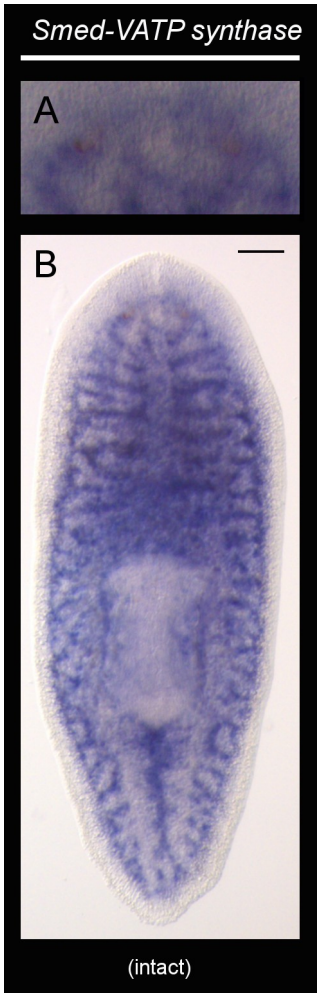

Figure 3.7.6 In situ hybridizations of *Smed-VATP synthase* DIG-labeled antisense mRNA probes of an intact animal (NBT/BCIP developed). (B) *Smed-VATP synthase* mRNA labelled cells surrounded the eyes and delimiting the border of the gut branches. **(A)** Close-up eye view of B. Controls in Figure 3.3.5. Scale bar: 200 µm.

The rod outer segment (OS) is a specialized compartment of the mammalian retinal photoreceptor, devoid of mitochondria (Calzia et al., 2013). Chemical energy supply for visual transduction remains controversial because phototransduction is an highly energy-demanding process and glycolysis does not seem to be a sufficient energy supply (Pepe, 2001; Hsu et al., 1994). Therefore, It has been proposed that phosphocreatine (PCr) may be transported from the rod inner segment (IS) to the rod outer segment for conversion to ATP (Linton et al., 2010). Oxidative phosphorylation (OXPHOS) would also produce a consistent amount of ATP, thanks to a transmembrane electrochemical gradient of H^+, generated by the electron transport chain (ETC) across disk membranes (Panfoli et al.,2009). In addition, extra-mitochondrial ATPase activity has been reported in myelin vesicles. It has been suggested the presence of ectopic ATP synthase, with both ATP synthetic and ATP hydrolytic activity depending on cell type, and that ATPase and ATP synthase activities of bovine rod outer segments represent the same protein (Calzia et al., 2013). Furthermore, the finding of electron transport chain proteins and ATP synthase in the outer segments confirmed the hypothesis that oxidative phosphorylation proteins (OXPHOS) are transferred from inner mitochondrial membranes to the outer segment (Calzia et al., 2013).

There are different types of ATPases, which can differ in function (ATP synthesis or hydrolysis), structure (F-, V-, and A-ATPases containing rotary motors) and in the type of ions they transport (Martin et al., 1980). A functional Vacuolar v-ATPase is made up of 13 subunits forming a complex with a V1 domain, responsible for ATP hydrolysis, and a Vo domain, responsible for proton translocation. The C terminal subunit is part of the V1 domain. It is located at the interface between the V1 and the Vo complexes, and acts as a flexible stator that holds both sectors of the enzyme together (Drory et al., 2004).

V-ATPases are found within the membranes of many organelles, such as endosomes, lysosomes and secretory vesicles, with the retinal outer segment phagosome as a candidate for a V-ATPases location. V-ATPase generates a proton gradient at the expense of ATP, generating pH values as low as 1. As a consequence, in synaptic transmission of neuronal cells, V-ATPase acidifies synaptic vesicles (Wienisch et al., 2006). Many retinopathies have oxidative stress or energy impairment as a common denominator (Sgarbi et al., 2006). Increased oxigen and an energy need (ATP) was hypothesized in rod–cone dystrophies, such as retinitis pigmentosa, due to the gradual rod degeneration (Shintani et al., 2009; Schon et al., 2001). Oxidative stress also contributes to the pathogenesis of AMD (Krishnadev et al., 2010).

3.8 Gene expression analysis and functional study of putative signalling and transport proteins

Three transport genes *Smed-dye, Smed-centrin, Smed-bbs* and one coding for a signal protein *Smed-ras* were found to have high homology with *dead eye, centrin, bardet-biedl syndrome* and *ras sarcoma*, responsible for channel, cilium transport in mitochondria and transport in the outer segments of the photoreceptor cells. Table 3.5 summarizes their full names, putative functions, expression patterns, phenotypes and phenotype penetrances.

The transport proteins *Smed-dye* and *Smed-centrin* appeared to be essential for eye regeneration, eye morphogenesis and the viability of the whole body of *S. mediterranea.* Nevertheless, the intraflagellar transport in the cilia conducted by *Smed-bbs* and the signalling pathway switched by *Smed-ras* seemed not to be essential for eye regeneration (in Appendix 3). Regarding the mRNA expression patterns, none of the four proteins were found specifically in the eyes, but neither were the eyes and close tissues free of labelling cells. This suggests the possibility of minimal expression to maintain functionality.

3.8.1 *Smed-dye* (dead eye)

Smed-dye shows a high degree of homology with the Nic96 nucleoporin domain of dead eye, a transport protein. Table 3.5 summarizes its full name, putative function, expression pattern, phenotype and phenotype penetrance. Flatworms injected with *Smed-dye* RNA did not regenerate eyes prior to death (Fig. 3.8.1). The in situ experiment showed *Smed-dye* ubiquitously expressed throughout the parenchyma (Fig. 3.8.2, A). The regenerated blastemas showed the same pattern as in the intact flatworms. No down- or up-regulation of *Smed-dye* was observed by the time course in situ hybridization over 6 hours, 1 day, 2 days and 3 days (Fig. 3.8.2, B-E).

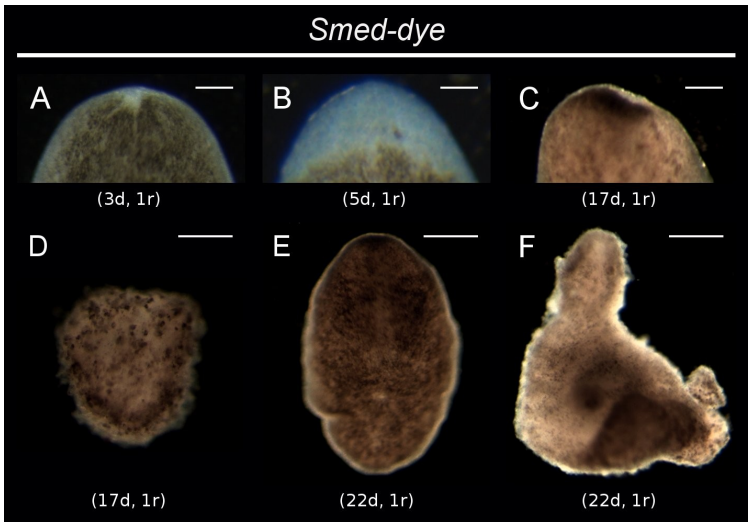

Figure 3.8.1 Interference with *Smed-dye* mRNA inhibited eye regeneration prior to death. (A) Small blastema and no eyes. **(B)** Regeneration of only one eye. **(C)** No blastema formation. **(D)** Tissue destruction without regeneration. **(E)** Regeneration failed before tissue destruction. **(F)** No regeneration and no morphogenesis persisted after 22 days. No animal regenerated its eyes and survived after *Smed-dye* treatment. Penetrance in: A n=2/18; B n= 4/18; C n=2/18; D n=16/18; E n=2/18; F n=16/18. Controls are in Figure 3.3.2. d: days of regeneration; r: round of injection. Scale bars: A, B and C: 200 µm; D, E and F, 100 µm.

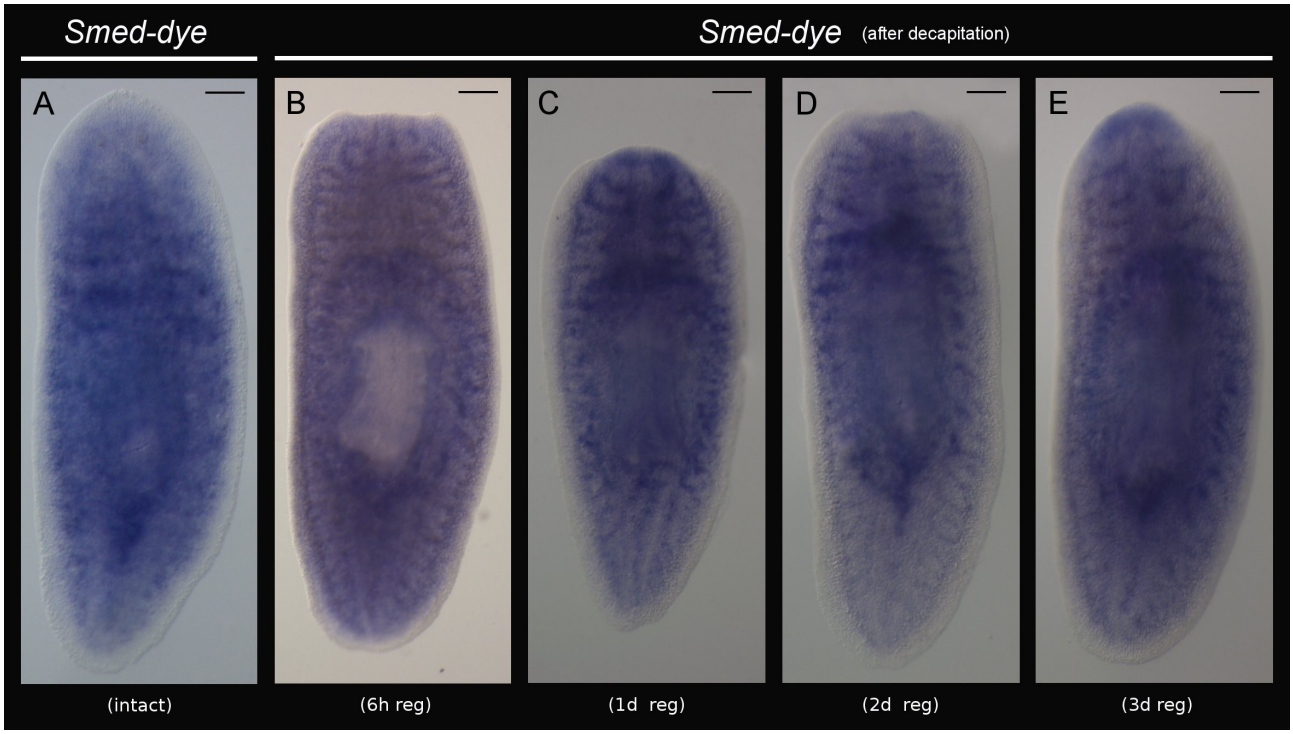

Figure 3.8.2 In situ hybridization of *Smed-dye* (DIG-labelled antisense mRNA probes, NBT/BCIP developed). (A) *Smed-dye* mRNA labels the parenchyma of intact animals. **(E-H)** Regenerating animals hybridized with *Smed-dye* mRNA show the same expression pattern as the intact animals with no difference in the blastema areas. After 6 hours, the pharynx is not hybridized. h: hours, d: days. Controls in Figure 3.3.5. Scale bars: A-E 500 µm; F-H 200 µm.

Smed-dye has an Nup93/Nic96 conserved domain. Nup93/Nic96 that belongs to NPC proteins and has mostly an alpha helical structure, is required for correct assembly of the NPC (Grandi et al., 1997; Gao et al., 2003). The *dead eye (dye*) gene encodes a protein of 820 amino acids that is homologous to genes of unknown function in human, mouse and, *Xenopus*, and to the yeast nucleoporin-interacting component (Nic96) genes (Allende et al.,1996). *Dye* mutants can be recognized on day 2 of embryogenesis by the presence of necrotic cells in the tectum (midbrain) and eyes (Allende et al.,1996). Nucleoporins form the nuclear transport channels that mediate all nuclear/ cytoplasmic transport in mammalian cells. Nups belong to a group of proteins with exceptional lifespans that has recently been linked to age-dependent defects, such as functional decline of neurons (Toyama et al., 2013). The Nup358 molecule contains numerous phenylalanine-glycine (FG) repeats that have been shown to form binding sites for transport receptors (Delphin et al., 1997). Moreover, nucleoporins have been found to be associated biochemically with centrin 2, a protein that could be part of the photoreceptor sensory cilium (Resendes et al., 2008). Centrin is one of the components of the enriched complex networks of phototransduction proteins in the connecting cilium (Gönczy, 2012; Yildiz et al., 2012). Furthermore, Drosophila Nup358 associates with kinesin (KIF5B) in mitochondria transport, enhancing the ATPase activity (Cho et al., 2007). Nup358 is also an important regulator of kinetochore assembly and the mitotic spindle in eukaryotes (Salina et al., 2003).

Nevertheless, in *Drosophila* retinal neurons, Nup358 acts as a chaperone for red/green opsin, to which it binds via its Ran-binding domain 4 (RBD4) and cyclophilin-like domain (Ferreira et al., 1996). Similarly, Nup358 interacts with red/green opsin in human and bovine cells but not with closely related blue-cone or rod opsin (Ferreira et al., 1997). In mice, Nup358 acts as a chaperone for the mitochondrial metallo-chaperone Cox11 (Aslanukov et al., 2006). Both proteins-copurify from retinal extracts and co-localize to mitochondria in several classes of neurons, including photosensory neurons and neurons of the CNS (Chatel et al., 2012). The nucleoporin Nup358 has a determinant role in glucose, energy and lipid homeostasis in CNS neurons and therefore in neurodegenerative diseases (Aslanukov et al., 2006; Cho et al., 2007). The lethality, on day 5 of development, observed in zebrafish *dye* mutants (Allende et al.,1996), was also found in all flatworms injected with *Smed-dye* mRNA. They also died, here after 22 days of regeneration (Fig 3.8.1). While Nup358 is highly expressed in mouse retinal neurons (Mavlyutov et al., 2002), *Smed-dye* was ubiquitously expressed throughout the body (Fig. 3.8.2, A). This expression could be explained either due to its dual function as part of the NPC and as the cilliary barrier in photoreceptor cells (Chatel et al., 2012), or due to the existence of dermal photoreceptors that would also justify its extended presence.

3.8.2 *Smed-centrin*

Smed-centrin has high homology with the EF-hand domain of centrin, a transport protein component of ciliated cells such as photoreceptors. Table 3.5 summarizes its full name, putative function, expression pattern, phenotype and phenotype penetrance. Interference with *Smed-centrin* mRNA provoked devastating effects (Fig. 3.8.3). Heads and eyes did not regenerate or they did it in an improper way, preceding tissue destruction. Furthermore, loss-of-function of *Smed-centrin* affected animal mobility and eye morphogenesis in a regenerating head (Fig. 3.8.3, G). Nevertheless, *Smed-centrin* expression is weak in the central parenchmal tissue and pharynx (Fig. 3.8.3, O).

The weak expression pattern of *Smed-centrin* (Fig. 3.8.3, O) correlates with the ubiquitously expressed human Centrin2; whereas Centrin1 expression is restricted to ciliated cells, such as retinal photoreceptors (Laoukili et al., 2000; Wolfrum et al., 1998). Similarly, locomotion processes such as the *Smed-centrin* RNAi previously appeared in *Smed-cen2* and *Smed-cen3 t*ested on planarians. While *Smed-cen2* RNAi planarians exhibit inching worming locomotion, *Smed-cen3* RNAi flatworms moved slowly; but both knockouts regenerated normally (Azimzadeh et al., 2012). *S. mediterranea* centrioles are present in multiciliated cells but not in proliferating cells, and the mechanism of centriole occurs through the acentriolar pathway. Nevertheless, the proteins required for centrosome duplication in proliferating cells in vertebrates and the centriole assembly through the acentriolar pathway in multiciliated cells of *S. mediterranea*, are largely conserved (Azimzadeh et al., 2012). Curiously, *S. mediterranea* electron microscopy carried out in this study showed the presence of cilia not only in the epidermis but also in internal tissues (Appendix 7.3, Fig. 7.3.10). Whether *Smed-centrin* plays *a* key role in the ciliogenesis of internal tissues and whether ciliogenesis is relevant for the maintenance of body structure are questions for further research.

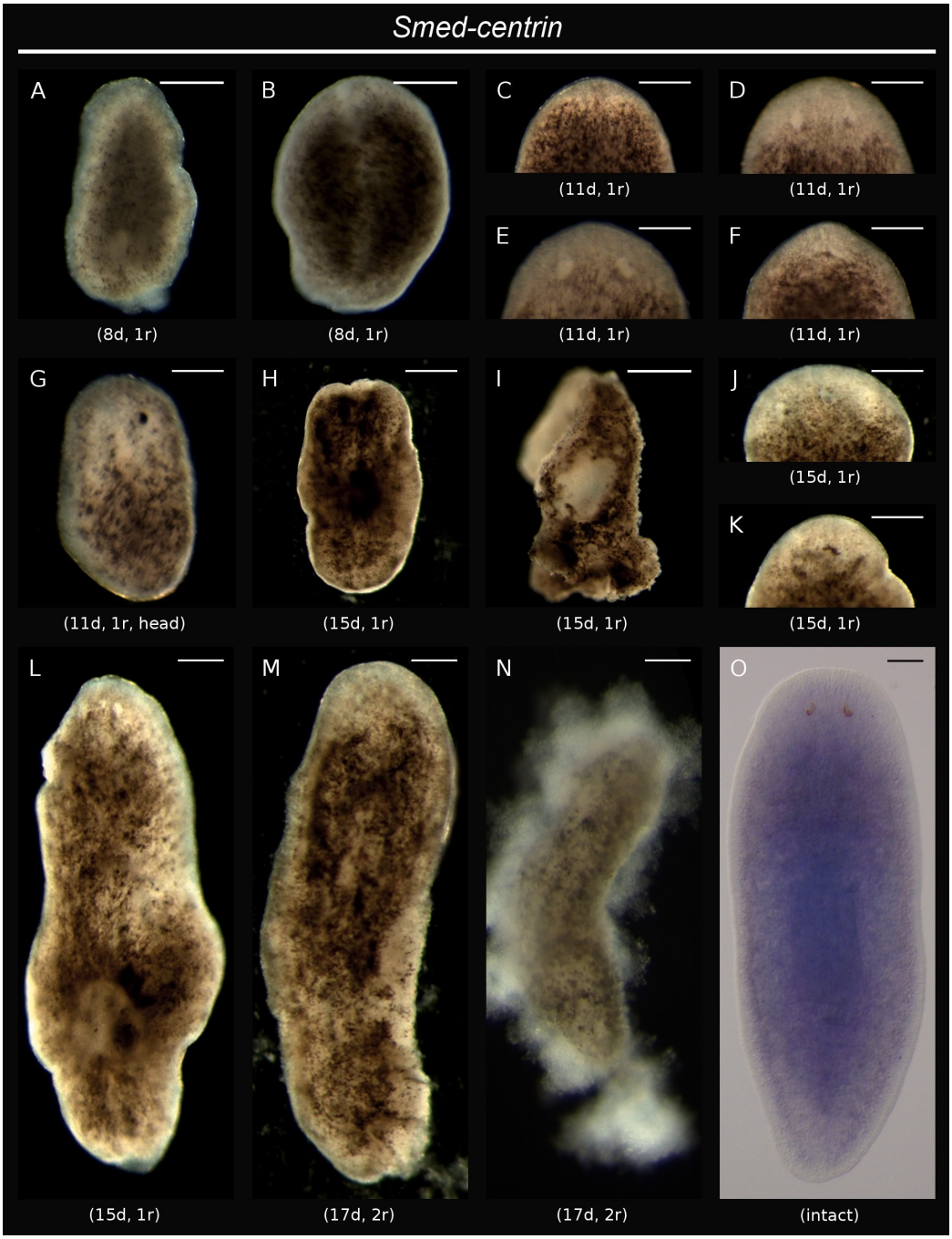

Figure 3.8.3 Lethal *Smed-centrin* RNAi and in situ hybridization with *Smed-centrin* (DIG-labelled antisense mRNA probe, NBT/ BCIP developed). (A) No regeneration and loss of pigmentation. **(B)** Inhibition of regeneration and immobilization. After 11 days: **(C)** eyes did not develop; **(D)** hypopigmented cups; **(E)** no eye cups; **(F)** fused eyes; **(G)** skin and left eye hypopigmented, and right eye cup too large. After 15 days: (**H)** regeneration failure, skin pigmentation defect and immobilization of the body; **(I)** tissue destruction; **(J)** eye regeneration failure, hypopigmented and asymmetric cups; **(K)** fused pigment cups; **(L)** pigmentation defects, beginning of body destruction. After 17days: **(M)** eyes and skin pigmentation defects, tissue destruction; **(N)** complete tissue destruction. **(O)** Weak expression pattern of *Smed-centrin* mRNA in centered parechymal tissue. Penetrance in: A n=4/14; B n=3/14; C n= 1/14; D n=2/14; E n=2/14; F n=2/14; G n=1/14; H n=3/14; I n=4/14; J n= 1/14; K n=1/14; L n=2/14; M n=1/14; N n=13/14. Controls are in Figures 3.3.2, 3.3.3 and 3.3.5. Scale bars: (A-G) 200 µm; (H-N) 100 µm; (N) 70 µm; (O) 500 µm.

Centrins, also known as caltractins, are members of a highly conserved subgroup of the EF-hand superfamily of Ca2-binding proteins (Salisbury, et al., 1995, Schiebel et al., 1995). An EF-hand domain consists of two alpha helices positioned roughly perpendicular to one another and linked by a short loop region (usually about 12 amino acids) that usually to binds calcium ions. EF hands also appear in each structural domain of the signalling protein calmodulin and in the muscle protein troponin-C (Durussel et al., 2000). The outer segment (OS) of photoreceptors is a modified sensory cilium (Yildiz et al., 2012). Light-induced exchanges of the visual G-protein transducin between the outer and inner segment of mammal rod photoreceptors; occurs through the narrow connecting cilium; the only cellular bridge between the two segments (Brann et al., 1987). The primary cilium is a microtubule-based membranous extension that grows from a basal body (or mother centriole) in nearly all cell types during the interphase (Kobayashi et al., 2011). Cilia are made of superfine filaments, composed of several heterogeneous components, including centrins (Salisbury et al.,1995). Ca^{2+}-activated centrin1 binds with high affinity and specificity to transducin, functioning as a Ca^{2+}-modulated cytoskeletal protein and its expression is restricted to ciliated cells, such as retinal photoreceptor cells in the mammalian retina (Wolfrum et al., 1998; Pulvermuller et al., 2002). It is estimated that approximately 10% of the OS disks are shed each day, and that to renew the related membrane components, nearly 2000 opsin molecules are transported per second in a normal human photoreceptor (Besharse et al., 1985). Therefore, any perturbations in the protein content of the outer segment results in photoreceptor dysfunction, degeneration and, eventually, blindness (Yildiz et al., 2012). Defects in cilia formation or function are associated with a large number of severe illnesses, collectively called ciliopathies (Anand et al., 2012). These include Bardet–Biedl syndrome (BBS) (mental retardation, retinitis pigmentosa), Joubert syndrome (JBTS) (retinitis pigmentosa) and Senior–Löken syndrome (SLSN) (a progressive eye disease that includes deficit of visual acuity, poor night vision and involuntary movement of the eyes, also called nystagmus) and photoreceptor degeneration (Anand et al., 2012; Pazour et al., 2002).

3.9 Gene expression analysis and functional study of sequences extracted from the Smed-Microarray gene selection

Many strategies to separate eye tissues from the rest of the body of *S. mediterranea* have failed over the years. As a consequence, no pure eye extract has been obtained. The use of the promising microarray approach in 2007 was an attempt to avoid this problem (doctoral thesis Eckelt, 2011, University of Barcelona). Afterwards, in 2012, a collagenase dissociation protocol to isolate intact planarian eyes was developed. For the first time, isolated *S. mediterranea* eye tissue was used in gene expression analysis (Lapan et al., 2012).

3.9.1 Smed-Microarray summary (doctoral thesis Eckelt, 2011).

A summary of the Smed-Microarray (doctoral thesis Eckelt, 2011) results should provide an overview of the array efficiency at finding genes responsible for eye regeneration and morphogenesis.

The strategy used to design the microchip consisted of comparing the genes of *S. mediterranea* that were expressed in regenerating tissues (head and tail-blastemas) at 1, 3 and 7 days of regeneration, against regenerating eyeless control *Smed-six* RNAi animals. As a result, the differential expression between heads vs. heads-controls and between heads vs. tails were used to separate the most expressed sequences, that are specific to the eye regeneration, from the house keeping genes. The results of this microarray analysis produced contig fragments and ESTs. Several Blast experiments confirmed the potential functions of these sequences in the organization of the cytoskeleton, transcriptional regulation, metabolism, post-translational modification, protein chaperoning, energy production and stress response. From the 54 genes validated in the array of Eckelt, 2011, three of them, *Smed-cat*, *Smed-mrp1* (here called *Smed-mrp2)* and *Smed-spectrin* had enriched expression in the eyes. Five sequences labelled the brain and possibly the eyes too: *Smed-Slc4a11*, *Smed-Ankrd17*, *Smed-kiaa0913*, *Smed-znfx1* and *Smed-tfIIf-alpha*. The cephalic ganglia, tissue connected to the eye cells, were labelled with mRNA of a further 31 sequences. In addition, interference with mRNA of 10 other genes caused problems with eye regeneration. Nevertheless, *Smed-mrp1* (called here *Smed-mrp2*), as reported in this study, was the only one of the 54 tested genes in the microarray selection that showed eye expression and at the same time presented eye defects. This represents approximately 2% of the genes tested in the microarray.

Furthermore, eye cells might be sensitive to cellular stress, as implied by the expression of the stress response related gene *Smed-cat.* This gene was specifically expressed in the pigmented cells and in the gut branches, while its substrate, H_2O_2 labelled only the digestive system. The high catalase concentration in the pigment cells might therefore maintain a permanent low level of the toxic H_2O_2 .

3.9.2 Smed-Microarray selection for this study

Table 3.6 summarizes the full names, putative functions, expression patterns, phenotypes and phenotype penetrances of eleven sequences studied here that were extracted from the Smed-Microarray. The selection of the genes wased based on expression intensity. One gene in the microarray group, *Smed-mrp,* from which two regions were analysed, *Smed-mrp1* and S*med-mrp2*, might be part of the genetic pathway involved in eye regeneration in *S. mediterranea*. The rest of the genes regenerated the eyes as in the control. Nevertheless, a low expression covered the eye areas and surroundings in six cases, *Smed-snap*, *Smed-titin*, *Smed-fib, Smed-myb, Smed-duk6 and Smed-duk10*. In addition, four genes, *Smed-duk3, Smed-duk5, Smed-duk6 and Smed-duk10,* containing domains of unknown function, had no eye regeneration defects but presented expression patterns in the dorsal and ventral lateral bands, in the pharynx, in the cerebral ganglion with no eye exclusion and in the parenchyma, respectively.

Smed-fgfl and Smed-titin are fragments of the same gene, *Smed-NDK3* (nou darake 3) which was published after the gene selection conducted for this study (Rink et al., 2009).

3.9.3 *Smed-mrp* (multidrug resistance protein)

Smed-mrp1 and *Smed-mrp2* are fragments of the same protein. Both have high homology with the multidrug resistance protein, an ABC transporter present in photoreceptor disk membranes. Table 3.6 summarizes its full names, putative functions, expression patterns, phenotypes and phenotype penetrances. Several elements of the secondary structure in human MRP1, such as the ABC transporter membrane region, the p-Loop NTPase and the Walker A/B-Loop, were also conserved in the *Smed-mrp1* and *Smed-mrp2* fragments (Fig. 3.9.1).

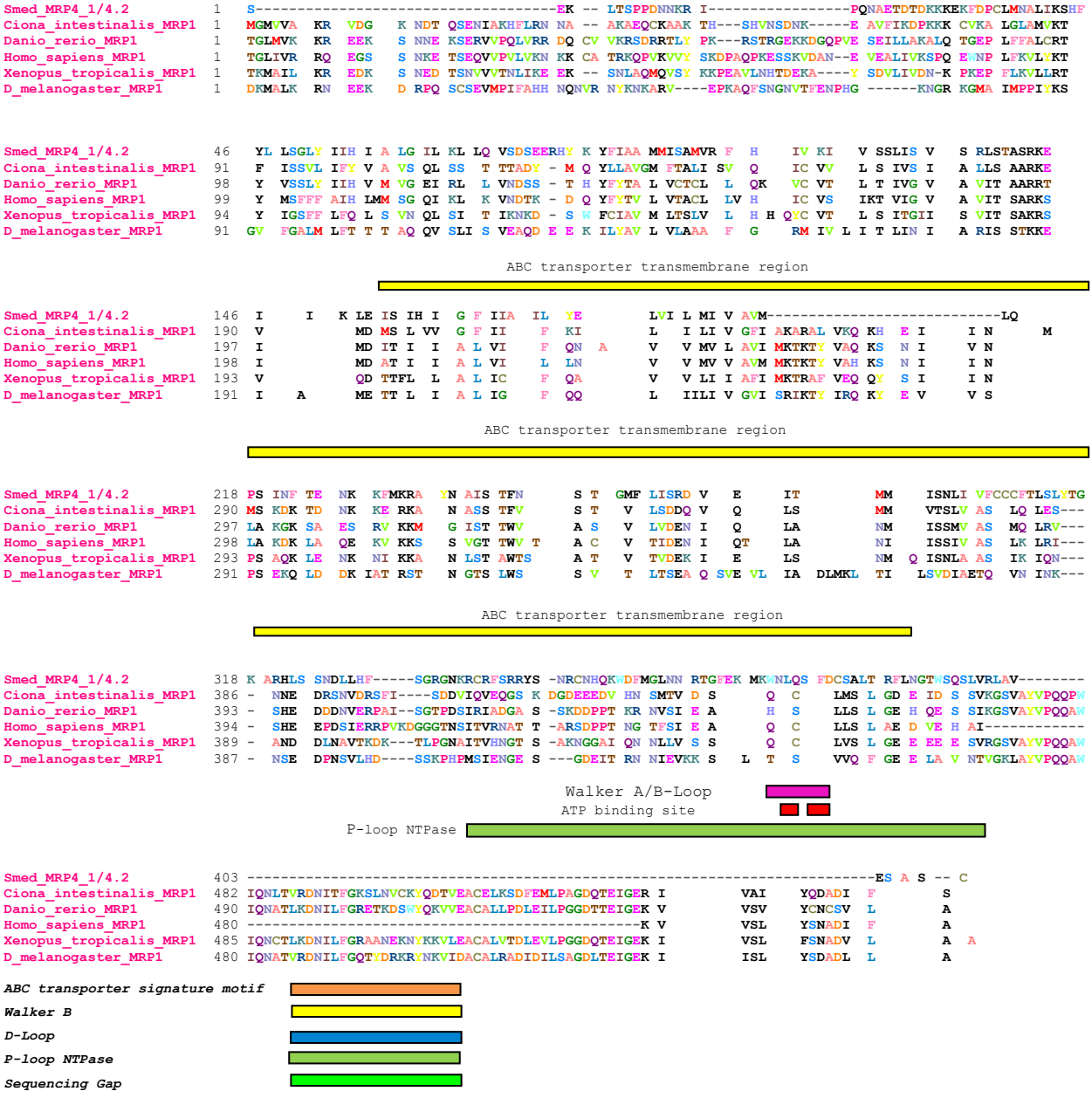

Figure 3.9.1 Partial alignment of the *Smed-mrp1* and *Smed-mrp2* sequence fragments and orthologues made with Clustal (v6.710b) software. *Smed-mrp1* and *Smed-mrp2* are fragments of the same gene and were aligned together. Light green labelling is the sequencing gap. Grey are similar and black background identical sequences. The human homologue protein MRP1 contains 17 transmembrane regions grouped into three transmembrane and two ABC intracellular domains. The secondary structural elements of human MRP1 are labelled in the alignment.

RNAi and in situ experiments were performed to elucidate its functionality. In situ hybridization of *Smed-mrp1* and *Smed-mrp2* showed expression in both the eyes and in the cephalic ganglia (Fig. 3.9.2, B, E, C, I). Although the cephalic ganglia were less labelled in *Smed-mrp1* than in *Smed-mrp2*, the expression pattern in regenerating heads and bodies was the same as for *Smed-mrp1* and *Smed-mrp2* RNAi of intact animals (Fig. 3.9.2, F, G, H, J, K, L).

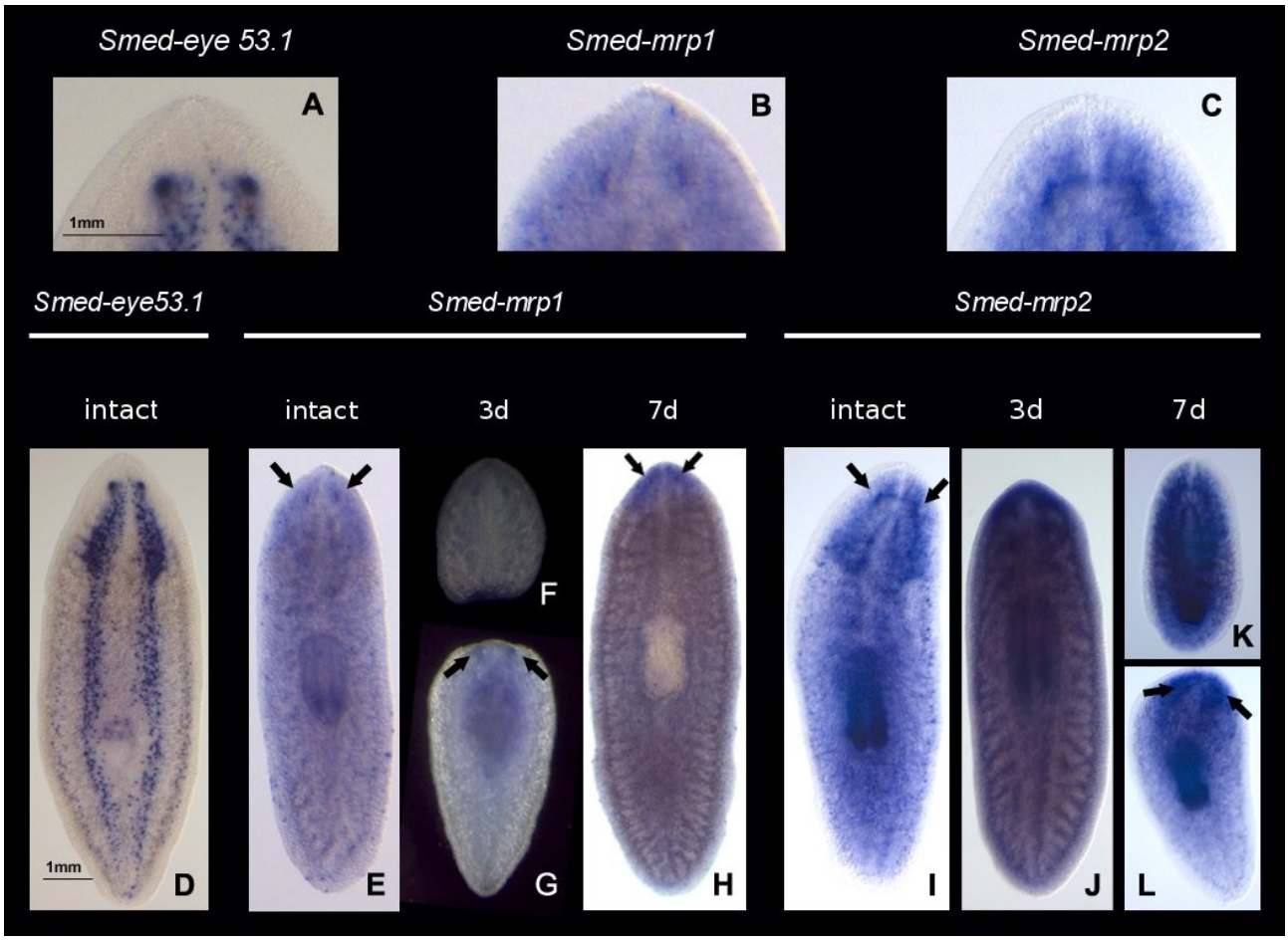

Figure 3.9.2: Eye expression patterns of *Smed-mrp1*, *Smed-mrp2* and *Smed-eye53.1* (DIG-labelled antisense mRNA probes, NBT/BCIP developed). (E, I) Arrows indicate expression in the eyes in intact, **(H, L)** regenerating bodies, and **(G)** in the cephalic ganglia in animals after 3 days regenerating. **(F)** Head after 3 and **(K)** 7 days of regeneration. **(J)** Decapitated body after 3 days of regeneration **(B)** and **(C)** are close-up of eyes in **(E)** and **(I)**, respectively. *Smed-mrp2* seemed to have more expression in the brain lobes and in the pharynx than *Smed-mrp1*. **(D)** The control *Smed-eye53.1* is expressed in the eyes, cephalic ganglia and nerve cords. **(A)** Close-up of the eyes in D. Scale bars: 1mm; B and C as in A; E-L as in D.

A reduction in size, together with changes in the symmetry and in the form of the pigment cups of the eyes were observed by *Smed-mrp2 RNAi* (Fig. 3.9.3, C). By *Smed-mrp1* RNAi, the pigment cups were too big and too close to the head tip; the periglobular area was also too small (Fig. 3.9.3, D).

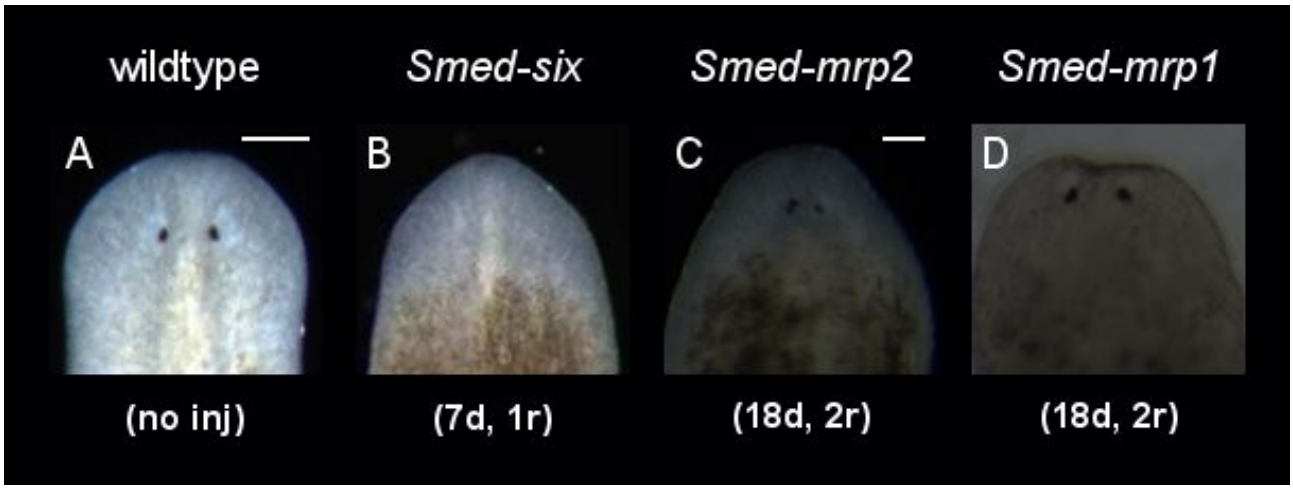

Figure 3.9.3: Interference with *Smed-mrp1* and *Smed-mrp2* dsRNA. (A) Intact eyes of *Schmidtea mediterranea*. **(B)** *Smed-six* RNAi without eyes 7 days after one round of injections. **(C)** *Smed-mrp2* RNAi with asymmetric pigment cups, abnormal periglobular area and skin hypopigmentation. **(D)** *Smed-mrp1* RNAi presents large pigment cups in small periglobular areas that are too close to the tip of the head. Penetrance in: B n= 5/5; C n=8/8; D n=8/8. Scale bars: 500 µm, B as in A and D as in C.

The sequences homologous to the multidrug resistance-associated member 1, belong to the ATP-binding cassette family (MRP) (Toyoda et al., 2008). MRP belongs, together with 6 other proteins (ABC1, MDR/TAP, ALD, OABP, GCN20, White), to the ABC (ATP-binding cassette) gene family. These proteins transport a variety of substrates throughout the membranes of prokariotes and eukaryotes. Interestingly, MRP was found in cancer cells that were able to pump drugs out of the cells; they were therefore multidrug resistance. These proteins also export endogenous and exogenous glutathions, glucuronate and sulphate conjugates (Jedlitschky et al., 1996).

Smed-mrp1-2 might transport toxic compounds generated in photoreceptor cells, such us glutathions. Glutathione S-transferases (GSTs) are structural components of the cephalopod cristalin SL11 in *Ommastrephes pacificus* and Lops 4 in *Loligo opalescenns* (Tomarev et al., 1995). GSTs are detoxificantion enzymes generally present in the cytosol, but they can also be peroxidases and isomerases that protect the cell against oxidants such as H_2O_2, which in turn can be a cell death inductor (Sheehan et al., 2001). Nevertheless, in human, the enzymes hGST Alpha P1-1-type isomerize 13-*cis* RA to all-*trans* RA, essential components for phototransduction (Chen et al., 1998). In addition, ATP-binding cassette proteins transport toxins such as 11-*cis*-retinal l, all-*trans*-retinal (RA) and bisretinoid compounds A2PE and its hydrolytic product A2E, from the photoreceptor disk membranes to the visual cycle in RPE cells (Sparrow et al., 2012). Moreover, RA signalling in mouse eye development, requires the transport of this vitamin A, from the RPE to the retina and from the retina to the RPE (Duester, 2008). Furthermore, mutations in the ATP-binding cassette ABCA4 cause Stargardt macular degeneration in mice (Quazi et al., 2014). It should be noted that retinoids and RAs in particular are known to be active morphogens regulating the growth and development of vertebrates (Meiden, 1995). In addition, in *S. mediterranea* and in *Girardia tigrina,* RA specifically inhibits eye regeneration and it might be involved in circadian rhythms (Romero et al., 2001; Ermakova et al., 2009).

3.9.4 *Smed-fgfl* (fibroblast growth factor receptor-like 1) *Smed-titin* (titin a)

Smed-fgfl and *Smed-titin* are part of the Smed-Microarray selection from 2008 (doctoral thesis Eckelt, 2011). These are fragments from the same gene, *Smed-NDK3* (nou darake 3), recently identified but not further characterized (Rink et al., 2009). Whereas *Smed-fgfl* has a fibroblast growth factor receptor-like structure, *Smed-titin* contains the CD47 immunoglobulin-like domain, also found in fibroblast growth factor receptors (FGFRs). Table 3.6 summarizes its full names, putative functions, expression patterns, phenotypes and phenotype penetrances. *Smed-fgfl* and *Smed-titin* RNAi treated animals regenerated as the controls (data not shown, control Figure 3.3.2). In addition, *Smed-fgfl* and *Smed-titin* were expressed in the parenchymal cells of intact animals as in regenerating heads and tails and in the pharynx (Fig 3.9.4, D-F, J-K).

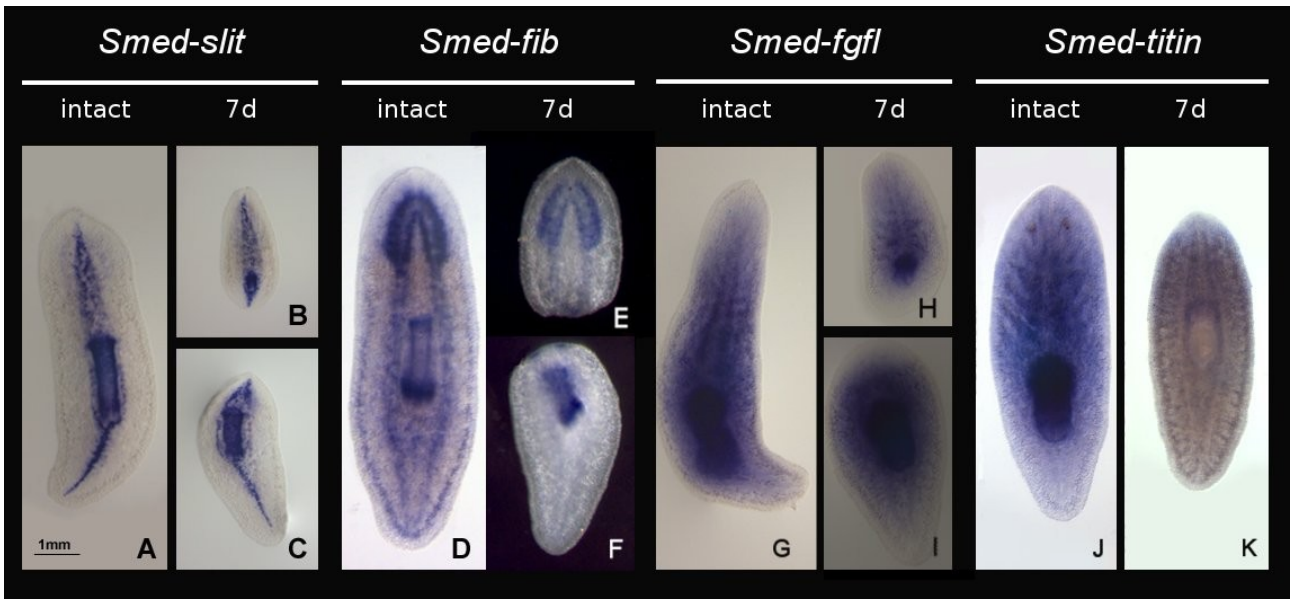

Figure 3.9.4: In situ hybridizations of DIG-labelled antisense mRNA (NBT/BCIP development). Parenchymal and pharynx expression pattern of *Smed-fib* **(D-F)**, *Smed-fgfl* **(G-I)** and *Smed-titin* **(J,K)** in intact animals and after 7 days of regeneration. **(K)** There is no expression of *Smed-titin* in the pharynx after 7 days of regeneration. **(D-F)** *Smed-fib* mRNA is expressed in the brain lobes, the nerve cords and the pharynx. **(F)** The pharynx and a primordium of the nerve cords are labelled, but the nerve cords of the decapitated body disappear after 7 days of regeneration. **(A-C)** *Smed-slit* is the control of this in situ hybridization. Scale bar: 1 mm B-K as in A.

Fibroblast growth factor receptors consist of a cellular ligand domain composed in turn of three immunoglobulin-like domains, a single transmembrane helix domain and an intracellular domain with tyrosine kinase activity. These receptors bind to fibroblast growth factors (FGF). They are members of the largest family of growth factor ligands, comprising 22 members (Ornitz et al., 2001; Belov et al., 2013). The fibroblast growth factor was first found in a cow brain extract and tested in a bioassay that caused fibroblast proliferation (Gospodarowicz, 1974). Thus, the functions of FGF in developmental processes include mesoderm induction, antero-posterior patterning in *Xenopus* (Koga et al., 1999), limb development, neural induction, neural development in vertebrates (Bottcher et al., 2005); and in mature tissues/systems angiogenesis, keratinocyte organization, and wound healing processes. Fibroblast growth factor (FGF) is critical during normal development of both vertebrates and invertebrates. Any irregularities in their function leads to a range of developmental defects (Amaya et al., 1991; Borland et al., 2001; Coumoul et al., 2003; Sutherland et al., 1996).

In *D. japonica,* a fibroblast growth factor receptor-like nou-darake (ndk) was exclusively expressed in the head region and RNAi resulted in the induction of ectopic brain tissues throughout the body (Cebria et al., 2002a).

3.9.5 *Smed-fib* (fibropellin/jagged)

Smed-fib has a high degree of homology with the four EGF-calcium binding domains. Table 3.6 summarizes its full name, putative function, expression pattern, phenotype and phenotype penetrance. The *Smed-fib* expression detected in the brain, nerve cords and pharynx (Fig 3.9.4 G-I) suggests a neuronal function that could not be observed. *Smed-fib* RNAi developed as the controls did (data not show, control Fig. 3.3.2).

The EGF-like domain is an evolutionary conserved protein domain, which derives its name from the epidermal growth factor where it was first reported. The main structure of EGF-calcium-binding domains are typically composed of 45 amino acids, arranged as two antiparallel beta sheets (Wouters et al., 2005; Stenflo et al., 2000). EGF stimulates cell growth, proliferation, and differentiation by binding to its receptor EGFR. EGF is a low-molecular-weight polypeptide that was first purified from the mouse submandibular gland, but since then has been found in many human tissues including submandibular gland, parotid gland, platelets, macrophages, urine, saliva, milk, and plasma (Kumar et al., 2005). Furthermore, EGF was detected in the CNS of the developing and adult albino rat in forebrain and midbrain. Thus EGF might have potential neurotransmitter-neuromodulator functions in structures of the extrapyramidal motor systems of the brain (Fallon et al., 1984).

3.9.6 *Smed-duk3, Smed-duk5, Smed-duk6 and Smed-duk10* (domains of unknown function)

Four sequences from the Smed-Microarray were found to have no homology with any known sequence. None of them presented regeneration defects in the eyes or in the head. In addition, their expression patterns were diverse. *Smed-duk6* and *Smed-duk10* showed expression in the cerebral ganglion. Nevertheless, the eye cells were not specifically labeled, but not specifically excluded (Fig. 3.9.5 J-P). *Smed-duk3* and *Smed-duk5,* in contrast, had specifically no expression in the eyes or surroundings. *Smed-duk3* mRNA was specifically and exclusively expressed in the dorsal and ventral lateral bands in regenerating and intact animals (Fig. 3.9.5, A-E). However, *Smed-duk5* mRNA expression was low in the parechymal tissue and more concentrated around and in the pharynx (Fig. 3.9.5, F-I).

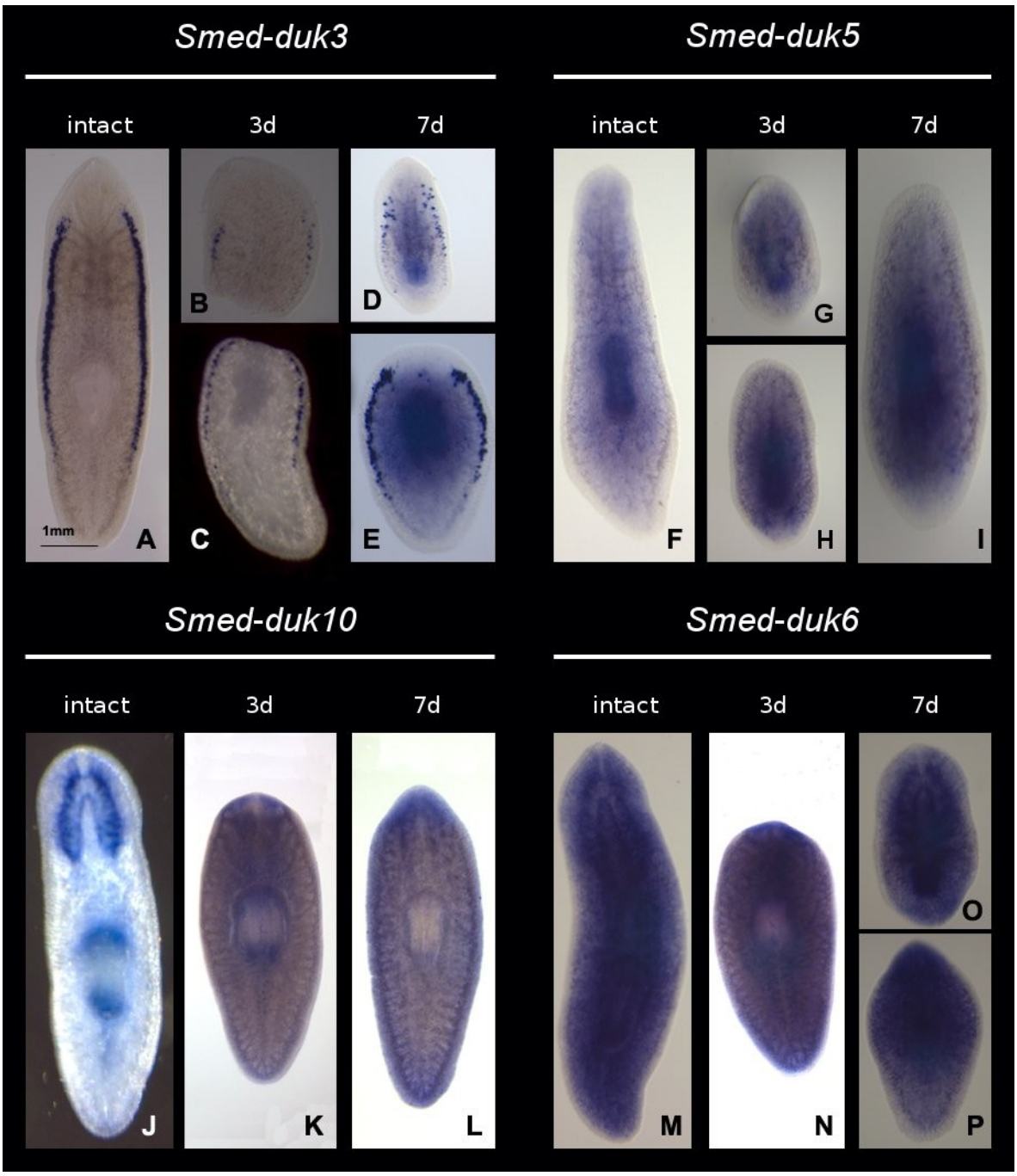

Figure 3.9.5: In situ hybridizations of DIG-labelled antisense mRNA from *Smed-duk3*, *Smed-duk5*, *Smed-duk6* and *Smed-duk10* (NBT/BCIP development). (A) *Smed-duk3* is strongly expressed in lateral bands in the middle of the body. **(J, K)** Expression in the brain lobes. **(B, G, D, O)** Regenerating heads, **(C, H, K, N)** and **(E, I, L, P)** decapitated bodies after 3 and 7 days of regeneration respectively. Control (*Smed-slit*, Figure 3.9.4) . Scale bar: 1 mm, B-P as in A.

4. CONCLUSIONS

1. Silencing of five opsins *Smed-rhodopsin1*, *Smed-rhodopsin2*, *Smed-rhodopsin10*, *Smed-melanopsin2*, *Smed-melanopsin3;* the transcription factor *Smed-exd* (*-pbx*); and the ABC transporter *Smed-white*, inhibits normal eye regeneration in *S. mediterranea*.
2. Thirteen out of fourteen opsin or light sensor genes studied showed ubiquitous mRNA expression throughout the body, which might be explained by the presence of a dermal light sense observed in other flatworms. These proteins might serve as photoentrainment regulators or as photolyases responsible for the repair of photodamaged DNA.
3. *Smed-peropsin1*, *Smed-yy1*, *Smed-hmt*, *Smed-tpr1*, *Smed-tpr2*, *Smed-kinase*, *Smed-mrp1-2* and *Smed-hox1* are expressed in the eyes.
4. *Smed-hox2*, *Smed-hox1, Smed-mitf2*, *Smed-mitf3* and *Smed-mrp1-2* silencing inhibits the regeneration of anterior structures, including the eyes.
5. Silencing of *Smed-VATP synthase*, *Smed-kinase*, *Smed-dye* and *Smed-centrin* inhibits regeneration and induces the death of the animals.
6. *Smed-tpr1* mRNA injection induced a rapid pharynx autotomy, also observed by *Smed-ver* and *Smed-white-sf2*. All three are melanin biosynthesis-related genes.
7. For the first time, the rhabdomeres of the *Schmidtea mediterranea* eye organ have been photographed with the electron microscopy. These structures are very similar to their homologues in other flatworms.

5. Material and methods

5.1. Planarian maintenance

A clonal line (BCN-10) of the diploid, asexual strain of *S. mediterranea* was cultured, using 1:1 (v/v) mixture of tap and filtered water. To prevent fungal infections the water was treated with 10mg/mL of gentamicin sulfate (Fargon Iberica, SAU, 664U.I./mg). To neutralize and stabilize heavy metals like chlorine and iron ions, AguaSafe was added (~100µL/L of AguaSafe, Tetra GmbH, D-49304 Melle, Germany). AquaSafe is made of seaweed extracts (natural biopolymers) that cover and protect the mucus and the gill of the organism and support the development of beneficial bacteria.

The flatworms were maintained in a temperature of 20ºC and in a light controlled closed room. Daily light cycles were eight hours of darkness and sixteen hours of light that came from a fluorescent lamp. The container lid was half ajar at all times to allow for a gas exchange and the normal oxygenation of the medium. The planarians were fed organic veal liver once or twice a week, and were starved for at least 7 days prior to analysis, amputation or fixation. Flatworms similar in length ~5mm were used for all experiments.

The *E. coli* DH5α strain was used to clone genes with the TA method (see section 5.5.1).

5.2. Databases for sequence selection.

The Smed-Microarray was the only database used in this study that was conceived to find eye genes. The sequence selection on this array was based on differential expression levels found between blastema tissue of the heads versus the tails of regenerating flatworms. The rest of the sequences cloned in this study were selected by gene ontology, Blast2GO. The databases used for the sequence selection were not eye specific transcriptomes. The resources for the sequences cloned in this study are described below. For BlastX, tBlastN and tBlastX, the NCBI RefSeq 2011 were used.

5.2.1. 454 pyrosequencing EST database (GS FLX Technology, Roche) (Abril et al., 2010).

By the 454 pyrosequencing of the transcriptome (ESTs) of *Schmidtea mediterranea* (Abril et al., 2010), more than 3 million novel transcribed nucleotides sequences were found. The assembly and mapping onto the genome scaffolds provided short read lengths but highly throughput sequences. To obtain the most representative set of planarian genes, expressed under different physiological conditions, both the head and tail were amputated and flatworms were irradiated. Total RNA was isolated from non-irradiated intact and non-irradiated head or tail regenerating planarians (1, 3, 5 and 7-days of regeneration), as well as irradiated intact and irradiated head or tail regenerating planarians (1, 3, 5 and 7-days of regeneration) were used. 454 sequencing reads were assembled. The annotation of the Smed454 dataset using gene ontology Blast2GO (B2G) was one of the databases used in this study as a source of gene sequences. Although this approach was not specifically constructed to find eye genes, many sequences related to this organ were found. The B2G is a tool that extracts relevant functional features of the sequences based on the use of the predicted annotation. B2G uses BLAST to find homologs in fasta formatted input sequences. The five steps for this application are as follows: (1) Blasting: a group of selected sequences is blasted against either the NCBI or custom databases, (2) Mapping: gene ontology (GO) terms are mapped on the blast results using annotation files provided by the GO Consortium that are downloaded on a monthly basis on the Blast2GO server, (3) Annotation: sequences are annotated using an annotation rule that takes parameters provided by the user, (4) Statistical analysis: optionally, analysis of GO term distribution differences between groups of sequences can be performed and (5) Visualization: annotation and statistics results can be visualized on the GO directed acyclic graph DAG (Conesa et al., 2005).

5.2.2. 454 EST and Illumina GAIIX database (Adamidi et al., 2011).

The assembly of this transcriptome contains an improvement of the older *S. mediterranea* genome resources. This group used two strategies to amplify the length of the assembled transcripts and to include missing transcripts. They first sequenced a full-length cDNA library with the 454 GS FLX platform (Methods) that provides few long reads and also sequenced with the Illumina paired-end sequencing technology, Illumina GAIIX, for many short reads. Second, cDNA libraries were normalized prior to sequencing to eliminate abundant transcripts.

5.2.3. Illumina ESTs, head regeneration transcriptome (Sandmann et al., 2011).

An Illumina paired-end sequencing of short expressed sequence reads (ESTs) allowed for the simultaneous de novo assembly and differential expression analysis of transcripts. This approach permitted the identification of genes that are functionally relevant during planarian head regeneration. The head of regenerating flatworms during 16 different periods of time were used for the preparation of the Illumina libraries.

5.2.4. Sm454EST flx titanium and ABI SOLiD 3 sequencing (Blythe et al., 2010)

The RNA of intact and mixed stages of the first 7-day regenerating planarians were sequenced, mapped and assembled using a dual platform approach formed by the SOLiD 3+ and 454 transcriptome sequencing. The reads from the 454 library have a mean of 278 bp but more transcripts identified are 400bp long. The ultra-deep sequencing that uses the short read technology SOLiD 3+ (50 bp reads) defined more transcribed regions. The two long and short datasets were combined, and the Blast2GO pipeline allowed transcript classification.

5.2.5. The Smed-Microarray (doctoral thesis Eckelt, 2011, Universitat de Barcelona).

This *S. mediterranea* microarray was designed in the E. Saló lab in colaboration with the NimbleGen company, to select specifically eye-related and regeneration gens. The synthetic sequences provided by this microarray were EST from the databases of *S. mediterranea* (Zayas et al., 2005), *D. japonica* (Mineta et al., 2003) and *Macrostomum lignano* (Morris et al., 2006) and eye-specific protein sequences from the NCBI RefSeq 2007. All of them were processed for oligo design by the NimbleGen Company and attached to the microarray. The array surface was hybridized with cDNA amplified from the RNA. It was extracted from the blastemas of the heads and tails of 3 and 7-day regenerating flatworms. As controls, blastemas from the sine oculis (*six1*) and the eye absent (*eya*) RNAi *S. mediterranea* mutants were used.

5.2.6. PFAM analysis

Selected sequences were translated into all 6 amino acid frames(http://ww.expasy.ch/tools/dna.html) and scanned for homology to pfam-a protein families (http://pfam.sanger.ac.uk/search), using the HMMSCAN algorithm applied to the hidden markov model dataset (pfam-a.hmm v.24) (Finn et al., 2009). An E-value cut-off at 1.0 was set to determine the family homology of each transcript.

5.3. Total RNA extraction

RNA extraction was performed with intact and 1, 3, 4, 5, 6 and 7-day regenerating *S. mediterranea*. This extraction was made with TRIZOL® Reagent (Life Technologies Invitrogen), a monophasic solution of phenol and guanidine isothiocyanate and other components. Guanidinium thiocyanate is used to lyse cells and virus particles in RNA and DNA extractions, where its function, in addition to its lytic action, is to prevent any of RNase and DNase enzyme activity. Phenol is used in this solution to separate the RNA/DNA from the proteins. Single steps are explained in appendix protocol 1.

5.4. cDNA REVERSE TRANSCRIPTION

Reverse transcriptase, which naturally occurs in retroviruses, operates on a single strand of mRNA, generating its complementary DNA, based on the pairing of RNA base pairs (A, U, G and C) to their DNA complements (T, A, C and G, respectively). The Super script III Invitrogen manufacture script is a 4 PCR step process. The first step degrades the genomic DNA with the DNAse, the second inactivates the DNAse by a 75ºC heat shock, the third polymerizes DNA with the retrotranscriptase enzyme, the fourth degrades RNA and the fifth inactivates the retrotranscriptase enzyme. For single steps see appendix protocol 2.

5.5. Sequence cloning

The cloning of genes in this study was done using two different approaches: the TA- and the T7-cloning methods explained below. Every DNA sequence cloned for this study is listed in the appendix**.**

5.5.1. The TA-cloning method

This technique consists in the ligation of Taq polymerase-amplified PCR products into copies of a plasmid vector, in this case pCRII-TOPO (fig. 5.1). This vector also contains genes that make cells resistant to particular antibiotics. The plasmids with the construct are introduced into competent bacteria (*E. coli* DH5α) by a process called transformation. Then, the bacteria are exposed to the particular antibiotic. Only bacteria that take up copies of the plasmid survive, since the plasmid makes them resistant. The protective genes are expressed and break down the antibiotics. In this way, the antibiotics act as a filter to select only the modified bacteria. Two types of modified bacteria will grow, the ones that contain plasmid with the insert that will be white and the ones that contain plasmids without insert that will be blue. The lacZ gene is responsible for the detection of the insert. If its reading frame is disrupted, white colonies will be produced. The white bacteria can then be grown in large amounts, harvested, and breaking down using the alkaline cell lysis method to isolate the plasmid of interest.

An efficient TOPO® Cloning reaction should produce several hundred colonies. The ligation efficiency of this construct is due to the plasmid vector (pCRII-TOPO) which is supplied in linear form (activated by the topoisomerase I) and with the single 3'-thymidine (T) overhangs for TA-cloning with the sticky end of PCR products. PCR inserts ligate efficiently with the vector because the Taq polymerase has a non-template-dependent terminal transferase activity that adds a single deoxyadenosine (A) to the 3' ends of PCR products. pCRII-TOPO plasmid includes the primers M13 F and M13 R (table 5.5) to linearize the insert and to confirm the right orientation of insert by sequencing them. The T7 and Sp6 are promoters for the Sp6- and T7-polymerases, respectively.

The J*ellyfish-gfp* dsRNA, injected as a control probe for RNA interference (fig. 3.2), is the GFP (green fluorescent protein) gen from the Jellyfish *Aequorea victoria*. It was cloned with the TA technique and is composed of 238 amino acid residues (26.9 kDa). It has no orthologs in the *Schmidtea mediterranea* genome and this flatworm is therefore free from any GFP hybridization.

Next, single steps of the TA-cloning procedure are described.

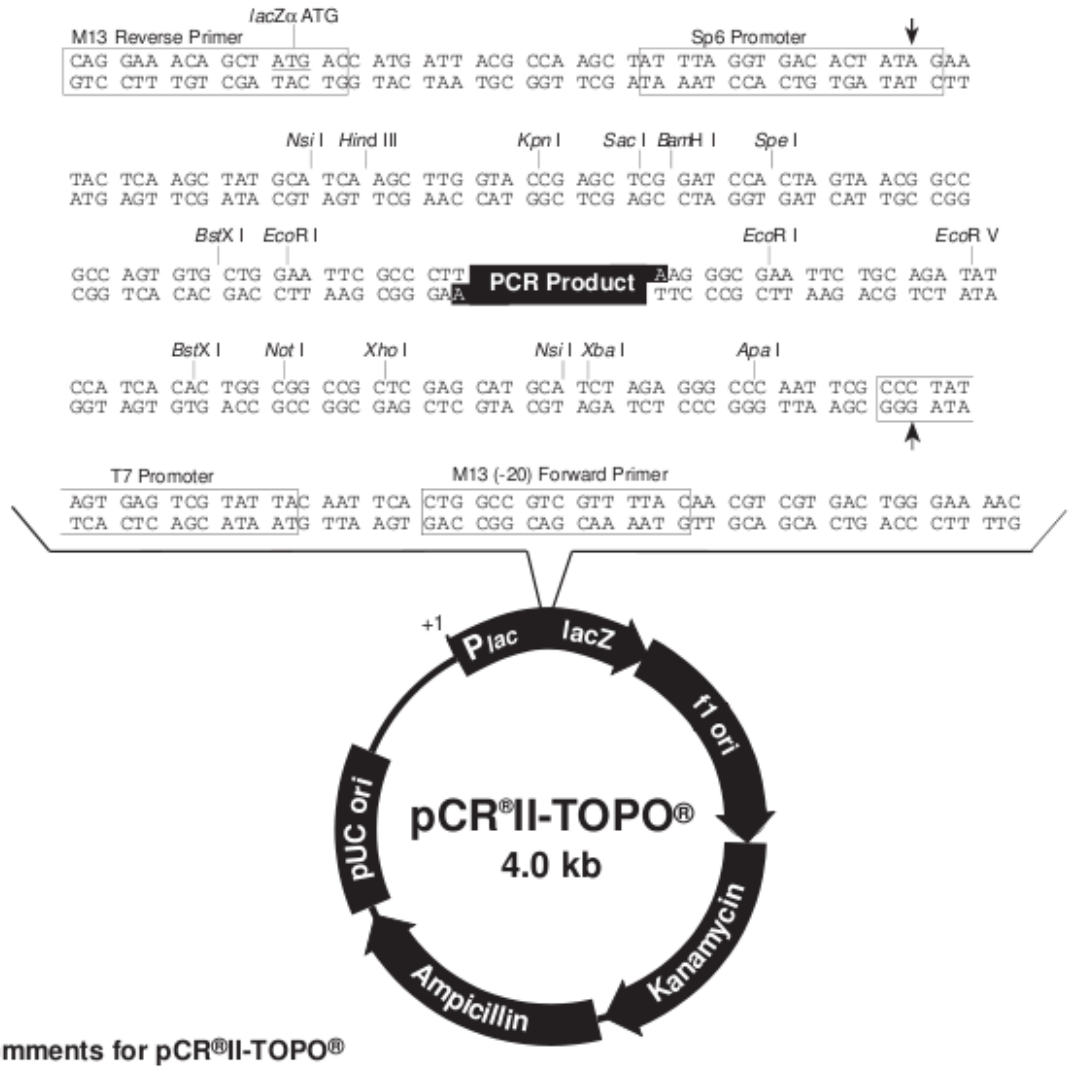

Comments for pCR®II-TOPO®
3973 nucleotides

*Lac*Zα gene: bases 1-589
M13 Reverse priming site: bases 205-221
Sp6 promoter: bases 239-256
Multiple Cloning Site: bases 269-383
T7 promoter: bases 406-425
M13 (-20) Forward priming site: bases 433-448
f1 origin: bases 590-1027
Kanamycin resistance ORF: bases 1361-2155
Ampicillin resistance ORF: bases 2173-3033
pUC origin: bases 3178-3851

Figure 5.1 Vector pCRII-TOPO. Represented is the multiple cloning site sequence with the lacZ gene for the white-blue screening. The promoter sites T7 and Sp6 for RNA transcription and M13 Forward and Reverse priming site for extraction of the cloned sequence. The place where the first PCR product ligates is black. The antibiotic resistance genes ampicillin and kanamycin are also labeled in black.

5.5.1.1. Primer design to amplify an open reading frame of the selected sequence.

The pFam program (1) was used to find the open reading frame of the selected sequences. The 20-30 bp long primers and a melting temperature (Tm) between 58 and 65ºC were calculated with the on line program (2). The GC content between 40% and 60%, no hairpins and no self annealing were calculated with the on line program (3). For the reverse and complement of sequences with the program (4), the primer oligos were provided by Sigma-Proligo (5). The computer program Primer_finder.pl designed from Gustavo Rodríguez-Esteban and Josep F. Abril was the most efficient of all the approaches tested to design primers.

Free on line addresses:

1. (http://pfam.sanger.ac.uk/search)
2. (www.appliedbiosystems.com/support/techtools/tm_calculator.cfm)
3. (www.basic.northwestern.edu/biotools/oligocalc.html)
4. (www.bioinformatics.org/sms/rev_comp.html)
5. (http://www.proligo.com/)

5.5.1.2. The first PCR were made using cDNA as the template and the design oligos as primers (appendix protocol 3.1). As a positive and quantitative test an agarose gel electrophoresis was made as explained below.

5.5.1.3. Agarose gels.

To test the amounts of DNA, ssRNA and dsRNA, probes were run in a 1% agarose gel electrophoresis. 40mL of 1% agarose gel contained 40mL of TBE, 0.4g of agarose and 0.5µL of Gel Red. The DNA or RNA probes were labelled with 1µl of Dye. The Dye was made by mixing 1mL of Loading Dye 6X with 0.1µL of Gel Red. The DNA probes were run in general at 100 volts during 30 min and 10 min for RNA. Usually the run was checked and photographed under UV light after 15 min. The control marker 1kb DNA ladder (Fermentas) was used as the quantitative standard. The gel bands were loaded with 6µL of solution made of 1µL of probe, 1µL of Loading Dye 6x-GelRed and 4µL of ddH_20 miliQ.

5.5.1.4. Purification of the PCR product. The Quiagen PCR purification kit was used to separate the PCR product from the other PCR components.

5.5.1.5. The ligation. The Vector PCRII-TOPO, the purified product from the first PCR and the ligase enzyme were mixed in a reaction at 14ºC over night, to insert the selected sequence into the plasmid (appendix protocol 3.2).

5.5.1.6. Transformation. The competent *E. coli* strain DH5α was transformed by heat shock with the ligation reaction in a process that took 2 hours (appendix protocol 3.3).

5.5.1.7. Bacteria culture in petri dish. The transformations were grown about 15 hours in Petri plates with ampicillin as an antibiotic selection and X-Gal as the inductor. Cells transformed with non-recombined plasmids, for example only the vector, grown into blue colonies. Only cells transformed with vectors containing recombinant DNA that produce white colonies were picked up and put into a liquid culture.

5.5.1.8. LB culture. White colonies were cultured over night in 3mL glass LB tubes with ampicillin.

5.5.1.9. MINI-Prep. The plasmid DNA was purified with the (NucleoSpin® Plasmid QuickPure, Isolation of high-copy plasmid DNA) MACHEREY-NAGEL.

5.5.1.10. Sequencing is necessary to verify the insertion direction of the sequence cloned into the plasmid. The M13F and M13R primers were used (appendix protocol 3.4; fig. 5.2 and fig. 5.3).

5.5.1.11. The second PCR is necessary to work with a linearized DNA sequence and at the same time increase the amount of the DNA template. The sequence amplified with the M13 F/ M13 R primers included the promoter sequences Sp6 and T7, necessary to amplify the ssRNA and dsRNA (appendix protocol 3.5; fig. 5.2 and fig. 5.3). As a positive and quantitative test, an agarose gel electrophoresis was made.

5.5.1.12. Purification of PCR. *QuiAquick PCR Purification Ki*t (Quiagen) was used to purify the DNA of the second PCR that thus was used as template for the ssRNA and the dsRNA transcription.

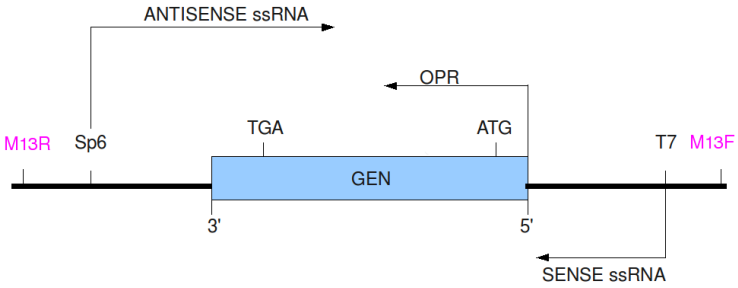

Figure 5.2 Graphic representation of the type 1 insertion of a DNA sequence into the pCRII-TOPO plasmid by the TA-cloning method. In this case the start point of the open reading frame is the T7-promoter side. For in situ hybridization, the Sp6-RNA polymerase is used to amplify the antisense RNA strand and the T7-RNA polymerase for the sense RNA strand.

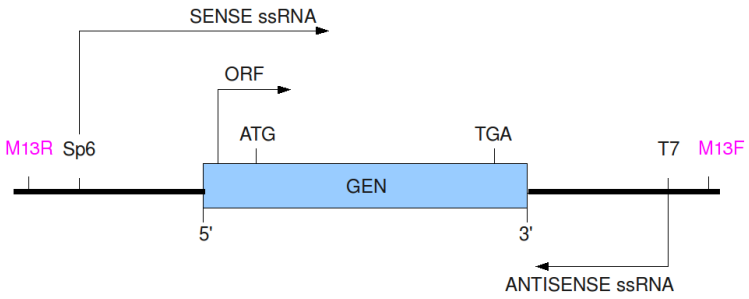

Figure 5.3 Graphic representation of the type 2 insertion of a DNA sequence into the pCRII-TOPO plasmid by the TA-cloning method. In this case the start point of the open reading frame is the Sp6-promoter side. The T7-RNA polymerase is used to amplify the antisense RNA strand and the Sp6-RNA polymerase for the sense RNA strand. Sense and antisense RNA strands are used to hybridize in situ samples.

5.5.2. The T7- cloning method

By this method the promoter sequence, where RNA polymerase can initiate the mRNA transcription, is added with the primer linkers and with the T7-Universal primers.

T7-cloning method steps are described below:

5.5.2.1. Sequence selection: identification of the start codon (ATG) is necessary to work with the sense strand in the 3'---> 5' direction

5.5.2.2. Primer design. The parameters and the programs used were the same as those used the TA-cloning. In contrast, with the T7-cloning method the linkers that are sort sequences of 8 nucleotides compose of the nucleobases guanine and cytosine (tables 5.1, 5.2, 5.3, 5.4, 5.5) were added to the 5' ends of the primers sequences. The forward primer F1 is the complement of the sense strand and the reverse primer R1 is the reverse and complement of the antisense strand in the 3' ---->5' direction.

5.5.2.3. First PCR T7-cloning. The sequence obtained by the first PCR contained the linkers at every end that provided a binding side for the T7-Universal Primers (fig. 5.3). Nested primers can be used in a second PCR, but it is not necessary. For PCR details see appendix protocol 4.1.

5.5.2.4. Agarose gel. As a template for the second PCR a gel electrophoresis followed by gel extraction of DNA were made in some cases. By the cloning of other genes, the PCR product from the first PCR was used as template for the second PCR.

5.5.2.5. Second PCR T7-Cloning. By the second PCR there are three possibilities. The first possibility is to use the forward and the reverse T7-Universal primers and therefore their linkers appear in the PCR product. This will be the template for the dsRNA transcription (fig. 5.4). The second possibility is to use the reverse T7-3'Universal primer and the forward specific primer F1 with linker. This PCR product will incorporate the end of the T7-3'primer sequence which is the binding and start side for the T7 RNA polymerase. The T7 RNA polymerase will transcribe the antisense RNA (fig. 5.5). The third possibility is to use the forward T7-5'Universal primer and the reverse specific primer R1 with linker. This PCR product will include the end of the T7-5'Universal primer that will provide the binding side for the T7RNA polymerase. Here the PCR product is the sense strand that can be used as a control for in situ hybridizations (fig. 5.6). Protocol details are described in appendix protocol 4.2.

5.5.2.6. Purification. To use the second PCR as template for RNA transcription the PCR product was purified (QUIAquick PCR Purification Kit)

5.5.2.7. Nanodrop. The PCR product was always quantified with the nanodrop or with a gel electrophoresis (NanoDrop® ND-1000Spectrophotometer, NanoDrop Technologies, Inc).

5.5.2.8. Sequencing was followed by a multialignment using the next on line program: (http://bioinfo.genotoul.fr/multalin/multalin.html)

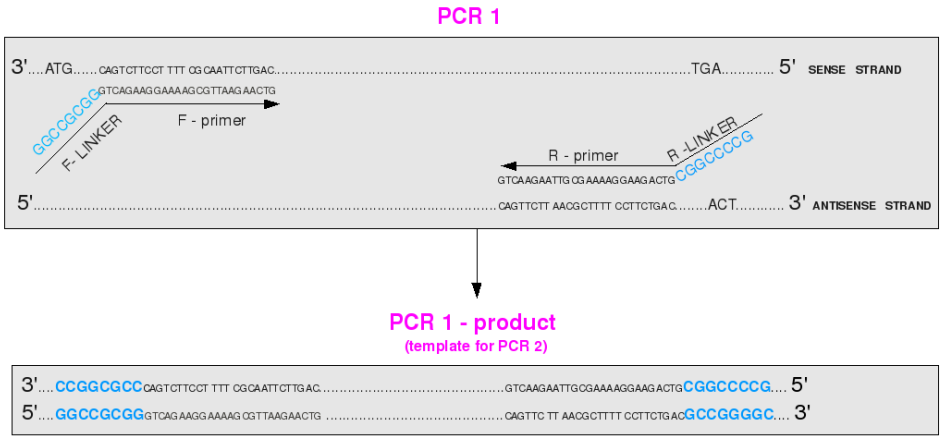

Figure 5.3 Graphic representation of the first PCR and its product by the T7-cloning method. The forward (F) and reverse (R) primer linkers, here blue labelled, introduced a new binding side necessary for the hybridization with theT7-Universal primers.

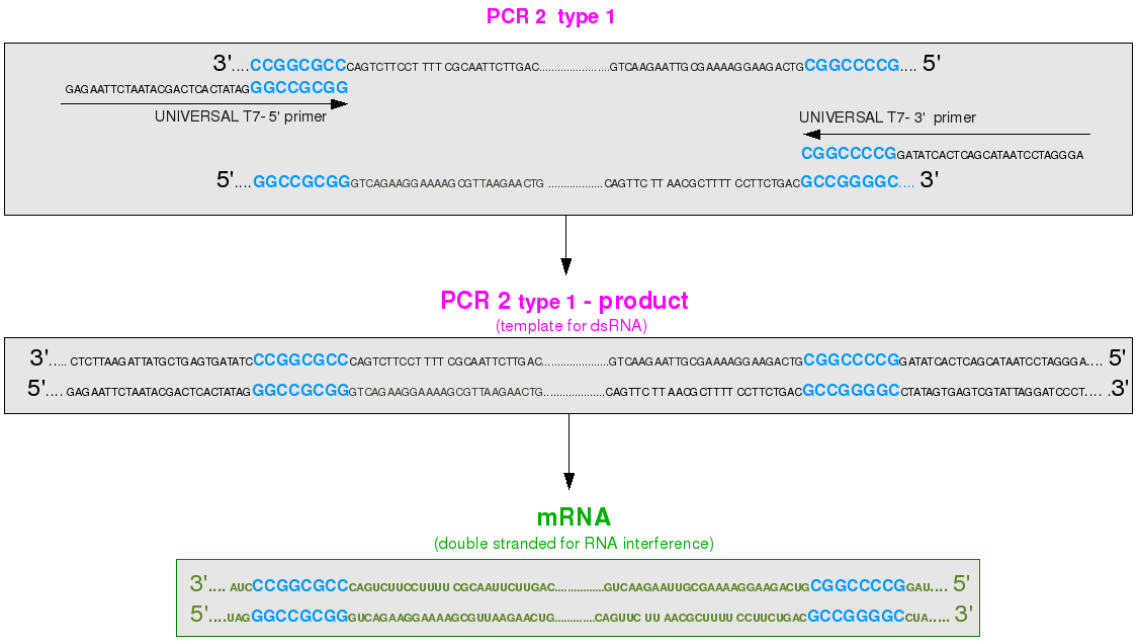

Figure 5.4 Graphic representation of the second PCR type 1 and its product by the T7-cloning method. The T7-Universal primers hybridize to the linker DNA fragment of the specific Forward and Rreverse primers and contain the promoter (an additional DNA fragment) necessary for the T7-RNA polymerase attachment. The product of this PCR (PCR2 type 1-product) provides the template for the double stranded messenger RNA transcription used for the RNAi experiments.

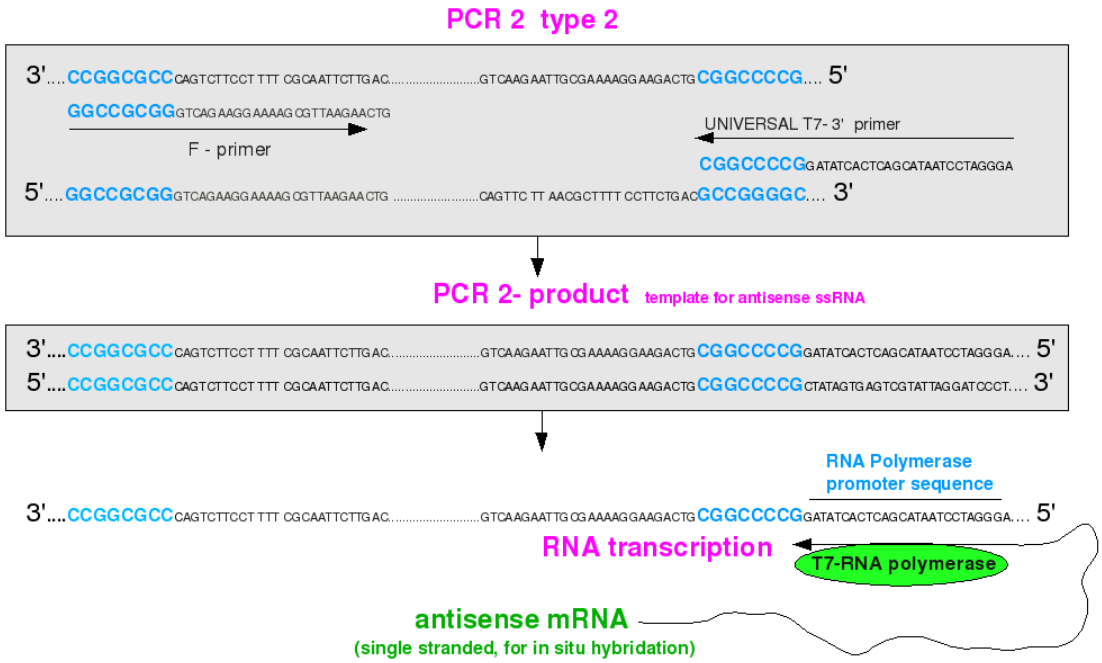

Figure 5.5: Graphic representation of the second PCR type 2 and its product by the T7-cloning method. Two primers are necessary for this PCR, the T7-3'Universal primer and the forward sequence specific. The T7-3'Universal primer contains the promoter DNA fragment at the 5'-end of the sequence, necessary for the T7-RNA polymerase attachment. The product of this PCR (PCR 2 product) provides the template for the antisense single stranded messenger RNA production, used in in situ hybridization experiments.

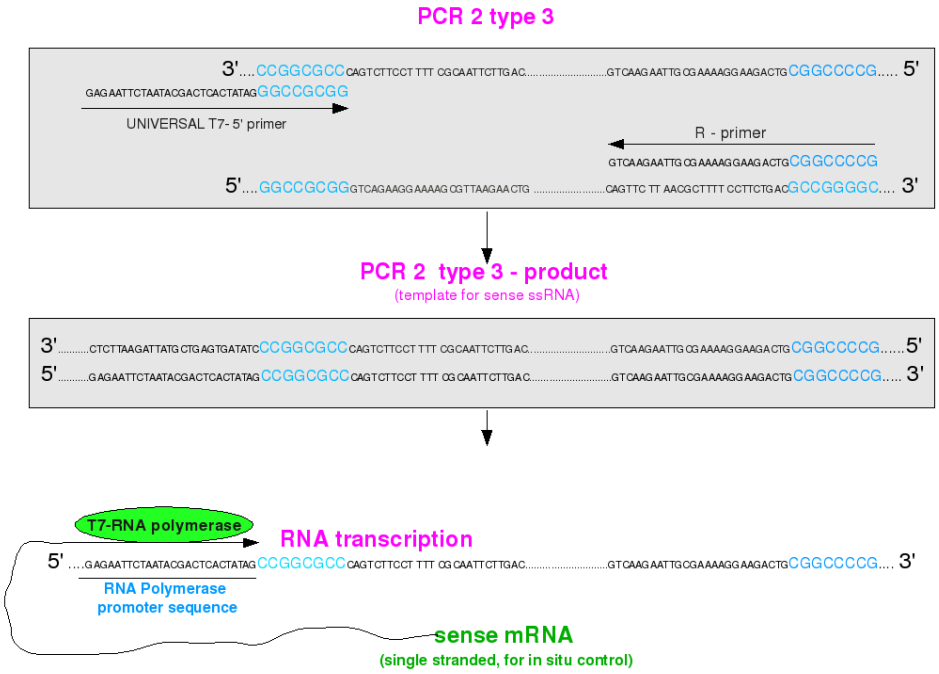

Figure 5.6 Graphic representation of the second PCR type3, by the T7-Cloning method. The T7-5'Universal primer and the Reverse sequence specific primer are necessary for this PCR. The T7-5'Universal primer contains the promoter DNA fragment at the 3'-end, necessary for the T7-RNA polymerase attachment. The product of this PCR (PCR 2 type 3-product) provides the template for the single stranded sense messenger RNA production, used in in situ experiments as the control.

5.5.3 Primer sequences

Table 5.1 Primers designed for cloning with the TA-method.

Gene	Forward Primer	Sequence	Reverse Primer	Sequence
Smed-Myb	160_1_MB_DN310639_F	ATGGATCAAATTGATAATGCAAAGTG	161_1_MB_DN310639_R	CAGCCAATATGACCAATAAAATATTGC
Smed-snap	178_9_SNAP-190_DN309134_F	GACACTCGAGATAATTTACTTAGCCAAG	179_9_SNAP-190_DN309134_R	CACTTTTTGAAGCACCGAAACG
Smed-mrp1	170_4.1_MRP_C1002.3_F1	CAGAAAAAGAGAAGCTTACTAGTCCACC	171_4.1_MRP_C1002.3_R1	CAATGACGGCATTTACCGGTATC
Smed-mrp2	172_4.2_MRP_C1002.3_F2	CCTCCAGGTTCTGAAATTATACGC	173_4.2_MRP_C1002.3_R2	CATATCCTTCCAGTTTATCTATTTCCC
Smed-fibropellin jagged	162_2_FiJ_Contig5890.3_F	GATTACAAATGTAACTGCAGCACC	163_2_FiJ_Contig5890.3_R	CAATGCTTGCCTTCAAATCC
Smed-titin	176_8_Titin_EE666519_F	CAGCTGGCAACTATTTCTGTGAGG	177_8_Titin_EE666519_R	GGTCGGCGGTTTATTGTCAAATAG
Smed-fgfl	174_7_FGFL_DN293522_F	GTTATTCGAAATGAAAGCGATTGG	175_7_FGFL_DN293522_R	GTAGCTTCCTTTTGTTCGCGTAC
Smed-duk6	168_6_Uk_EE281751_F	CAATTATGGTCGTTTATGAATTAGCC	169_6_Uk_EE281751_R	CAGGTATCACTTTATATTGGCAGACG
Smed-duk3	164_3_Uk_DN300643_F	GAGTGCAATCGGGATAATTTGC	165_3_Uk_DN300643_R	CGAACACCTGGTGAGCTGCC
Smed-duk10	180_10_unknown_AY067583_F	CGATGTTTAGAATTCCCTTTAGTTTTTC	181_10_unknown_AY067583_R	CCAACTCTCAGTCGCGAGAATAC
Smed-duk5	166_5_Uk_Contig6828.2_F	CTAAATCATTTTGCATTACTCGATTCTTC	167_5-Uk_Contig6828.2_R	CTCTTTTAATACTTTCTTGCTTCACATGC

Table 5.2 Primers designed for cloning with the TA-method with nested primer. The F2 and R2 are the nested primers.

Gene	Forward Primer	Sequence	Reverse Primer	Sequence
Smed-six	1_So_F6ZL_F1	CTGCTGCTCGATCTCGTTGG	1_So_F6ZL_R1	GTGGCACATCGACAGATTAGC
Smed-six	1_So_F6ZL_F2	CCAATTAGACACCTGAGTTGTTGTC	1_So_F6ZL_R2	CGAATGAAAGCGTCCTAACAGC
Smed-exd (pbx)	3_ED_F1	CGTCTTCTCTCATGCCACTGG	3_ED_R1	CAAATCCTTATCCTTCCGAAGAAGC
Smed-exd (pbx)	3_ED_F2	ACTGGCCTGCATCCAGTCG	3_ED_R2	GAAGAAGCAAAAGATGAATTGGCA
Smed-NCL	2_CN_F1	GTTGTTGGGTCTTTCTGTAAGTCC	2_CN_R1	GAACCTTCACCATTGGCTCG
Smed-NCL	2_CN_F2	GTCCAATAAGGAGTCATAAGGAAGGTC	2_CN_R2	GTGACCGCCGTTGTAGTTGG
Smed-mitf1	11_mitf1_F1	CGACGATCACACAGTCACAATGG	11_mitf1_R1	GATTAATCTGCTCTACTAATTTCATTGATG
Smed-mitf1	11_mitf1_F2	GGTGCTGAATTATCAAACAACAAAGT	11_mitf1_R2	CACAGTTAAGAAAGAACTCCGTTGG
Smed-mitf2	12_mitf2_F1	GTACAGCAGTGATTACGTGATTGACAG	12_mitf2_R1	CAATCGGGTCACATATTCCACTG
Smed-mitf2	12_mitf2_F2	GTACAGCAGTGATTACGTGATTGACAG	12_mitf2_R2	GGATTCATTGTCGGAATTCATTTC
Smed-mitf3	13_mitf3_F1	TGTAAATTATTTAGTCGAAAGAAAGCG	13_mitf3_R1	GTTTACCTGAATATGCTTGTAAAACACT
Smed-mitf3	13_mitf3_F2	CAGATCCAAGAACTTGGTCAATTATTACC	13_mitf3_R2	CACTGTAATTAGATTTTCTGATATTTGTGC

Table 5.3 Primers designed for cloning with the T7-method. The linkers are labelled in blue.

Gene	Forward Primer	Sequence	Reverse Primer	Sequence
Smed-melanopsin1	17_Op4_7F1	GGCCGCGGCAATTGGATTCCCGTTTCTTATGC	17_Op4_7R1	GCCCCGGCCTCATTTCCTTTATCTGATCCCGG
Smed-melanopsin2	8_PM_7F1	GGCCGCGGAGGACCCCAAGACAATACAAATGC	8_PM_7F1	GCCCCGGCCTGATATCGTGGACTTTTGCTATTTTTG
Smed-melanopsin3	18_Op4A_7F1	GGCCGCGGCTAAGAGCATGTGGACCCCATC	18_Op4A_7R1	GCCCCGGCCACGATATCAGAACAAGAAGAAATGACC
Smed-white-sf1	7_Wt_7F1	GGCCGCGGGGATCACCGAAGGGAGCTGT	7_Wt_7R1	GCCCCGGCGTCAGAAGGAAAAGCGTTAAGAACTG
Smed-leukemia homeobox	16_TCH1_7F1	GGCCGCGGCGCTTCTCTCGATTTATTATGAATTCC	16_TCH1_7R1	GCCCCGGCGTCGCCTCCATTTTGTTCTCC
Smed-kinase	20_PK1_7F1	GGCCGCGGATCCAGAAACCAGTGACTTTGTTGG	20_PK1_7R1	GCCCCGGCCAGTTAAAGCACCACCATCGAGG
Smed-vATP-syntase	15_Hv2_7F1	GGCCGCGGCTCCTTTCTTTGGTGTCATGGG	15_Hv2_7R1	GCCCCGGCCTAACTACCATAATCAACATCAGCGAGG
Smed-dead eye	6_DE_7F1	GGCCGCGGGATTTTGAACATCTCGATAGCAGATC	6_DE_7R1	GCCCCGGCCATCAGGACGATCCGAATGG
Smed-centrin	14_EH2_7F1	GGCCGCGGCTATGCCGTTAGACGGTCTTATCG	14_EH2_7R1	GCCCCGGCCCATCATTATCTCTATCAGCTTCATCAATC

Table 5.4 Primers designed for cloning with the T7-method and with nested primers. The linkers are labeled in blue. The F2 and R2 are the nested primers.

Gene	Forward Primer	Sequence	Reverse Primer	Sequence
Smed-Peropsin1	55_Rh2_Co_3556_F2	GGCCGCGGCAACGCATAGC	55_Rh2_Co_3556_R2	GCCCCGGCTCAACTTTACGG
Smed-Peropsin1	55_Rh2_Co_3556_F1	GCAAGACGTTTGATGGAGTTC	55_Rh2_Co_3556_R1	CATTCATCTTCGTTTAATTTACG
Smed-blue-opsin	56_LWO_Sg_F6AJIXP02JKU4O_F1	GTCATTTGCTGTTGGACGC	56_LWO_Sg_F6AJIXP02JKU4O_R1	GACTTTGTTTCTTTTGACAGGG
Smed-blue-opsin	56_LWO_Sg_F6AJIXP02JKU4O_F2	GGCCGCGGATTATCTCCATTCC	56_LWO_Sg_F6AJIXP02JKU4O_R2	GCCCCGGCTTTATCTGATCCC
Smed-rhodopsin10	58_Rga_Co_20395_F1	CTTGCTATGGCCGATGTACTCG	58_Rga_Co_R1	GGACACGAAGAGGAAACAATAGC
Smed-rhodopsin10	58_Rga_Co_20395_F2	GGCCGCGGGTTTGTTATGC	58_Rga_Co_20395_R2	GCCCCGGCGCATAGATATGG
Smed-rhodopsin1	59_Rgr5_Co_17768 _F1	GGATATATTTTCCCATTTGTTGGC	59_RGr5_Co_R1	CCAGATCAGTAAGTTGGTAGAACG
Smed-rhodopsin1	59_Rgr5_Co_17768_F2	GGCCGCGGTTGGCTTTATCG	59_Rgr5_Co_17768_R2	GCCCCGGCTAATTGTTGAACG
Smed-rhodopsin2	61_Rgr7_Co_9069_F1	GATGAACTGATTTTACTCTGTGG	61_Rgr7_Co_R1	GGGTTCTGACAATAGAGGTTCC
Smed-rhodopsin2	61_Rgr7_Co_9069_F2	GGCCGCGGCAAGTCATTGG	61_Rgr7_Co_9069_R2	GCCCCGGCGAGGTTCCAAGG
Smed-rhodopsin4	37_Rh4_Co_18503_F2	CTACTTCTGTTCACTCTCGTAAGC	37_Rh4_Co_18503_F2	GAATGCATCTCATCCAACTTCC
Smed-rhodopsin4	37_Rh4_Co_18503_F2	GGCCGCGGCATTTGTATGTCC	37_Rh4_Co_18503_F2	GCCCCGGCATGTTCAAGCTGC
Smed-rhodopsin7	57_Rh1_Co_4663_F1	CTAGTAATGCCAACAGCAGCAACTTGG	57_Rh1_Co_4663_R1	CTAGATAGCCATACTGGAATACTTTCC
Smed-rhodopsin7	57_Rd1_Co_4663_F2	GGCCGCGGTCGTTGACTACG	57_Rd1_Co_4663_R2	GCCCCGGCTTTATGCAAATCTGG
Smed-Rhodopsin8	60_Rgr6_Co_26968_F1	CTTCCCAAATCATAGCTAAATGC	60_Rgr6_Co_26968_R1	GTAAATCCAACAACCGATGAGC
Smed-Rhodopsin8	60_Rgr6_Co_26968 _F2	GGCCGCGGAATAATTGCCATC	60_Rgr6_Co_26968 _R2	GCCCCGGCATTAAGATAGATTTTCG
Smed-Rhodopsin9	62_Rgr8_Co_11411 _F1	GATTTCTCCTCGGCCTGTTG	62_Rgr8_Co_11411_R1	CATATCAAACGCCTCGACAGG
Smed-Rhodopsin9	62_Rgr8_Co_11411_F2	GGCCGCGGTTACGACATTTCG	62_Rgr8_Co_11411_R2	GCCCCGGCTCCATCATCTCTACG
Smed-rhodopsin5	54_F1	GCAAAACAACCAGATCAACG	54_R1	GATCAGGTTCAGAGGTCTG
Smed-rhodopsin5	54_F2	GGCCGCGGCGACATTTCATCTATTCCAGC	54_R2	GCCCCGGCAGGAAAACAATATCGCCCAG
Smed-cryptochrom	121_F1	GTATCACTTCATCGACATCAAC	121_R1	GAGTAACATTTCTCCTTGGCTG
Smed-cryptochrom	121_F2	GGCCGCGGCACGTCGAATTTCCGTTGAC	121_R2	GCCCCGGCGAAGCTCATTCCCAGAAATC
Smed-homeobox1	89_F1	GTTGCAATACTTGACAGTCTC	89_R1	CAAAGCAGCCAGTGGAAAC
Smed-homeobox1	89_F2	GGCCGCGGGGACTTCCAAGATCATTAAGAG	89_R2	GCCCCGGCGAAGTGAATGGAGTTGCACATG
Smed-homeobox2	90_F1	CAACCAGCTCTCCAAACTC	90_R1	CCCACATCCATTGAAAACAAAG
Smed-homeobox2	90_F2	GGCCGCGGCTGATTGATCATAGCTCGATG	90_R2	GCCCCGGCGAAATAACGGTCTCGGAGAC
Smed-tpr1	118_5420_R1	GTCGCCAGGATCAGCTTCTC	118_5420_F2	GGCCGCGGGATGCTGTCCAAGTTTCTGTC
Smed-tpr1	118_5420_F2	GGCCGCGGGATGCTGTCCAAGTTTCTGTC	118_5420_R2	GCCCCGGCGCACTTCGAGCTAACTGAC
Smed-tpr2	117_2066_F1	CATGACCGAAATTGCTGTTTC	117_2066_R1	CATAAATCAAGCATGCGAGC
Smed-tpr2	117_2066_F2	GGCCGCGGGACGTAGAACTTTGTGTAGAAG	117_2066_R2	GCCCCGGCCACTCTATTTCTTTGGTTGGTC
Smed-bbs	119_26456_F1	CGAAATGCGCTGGCATATTG	119_26456_R1	CAATTGGCTGAATCAGGTTTTG
Smed-bbs	119_26456_F2	GGCCGCGGCAGTGTGTAAATGCACAAGTC	119_26456_R2	GCCCCGGCCATCGGCAATTGAAGTATACC
Smed-ras	110_F1	GCAAACCAATTCGGACGATATC	110_R1	GAGGACAGTTATAGAAAGCAAG
Smed-ras	110_F2	GGCCGCGGCCAAGATGGCAAAAAATC	110_R2	GCCCCGGCGATACTGCTGGAACGGAAC
Smed-yyl	108_F1	CTGTAAGCAAAGCATTCAGG	108_R1	CATAGAAACGGTACTAGCGATC
Smed-yyl	108_F2	GGCCGCGGGTGGCAAACGATTCTCTCTG	108_R2	GCCCCGGCCCAATAGCAACAGTGTAACG
Smed-hmt	107_F1	CCTGCCGACACAATATTCTTG	107_R1	CTATCGAGTAGTTCAGAGAG
Smed-hmt	107_F2	GGCCGCGGCATAGGCATGGAACTCGAC	107_R2	GCCCCGGCGCACCAAAAATAGAGGCTGG
Smed-fox	109_F1	GCAATGGAGGTCTGAGGTGG	109_R1	CATGTCAGCCTCGTGTTAC
Smed-fox	109_F2	GGCCGCGGGACTGAGGATATTCGTTCTGG	109_R2	GCCCCGGCCAACCAGACCATCGAATAAC
Smed-white-sf2	113_24562_F3	GATTATTGTGGAGGCATTGG	113_24562_R3	CTTTACCTTCACTGAAGCATG
Smed-white-sf2	113_24562_F4	GGCCGCGGGAGCCCATTTTCTCCAA	113_24562_R4	GCCCCGGCATAAACACATGTTACGTTG
Smed-vermillion	102_13876_F1	GGATGAAAGAAATATGCGAGTG	102_13876_R1	GTCGACAAGTTGCATAGGTC
Smed-vermillion	102_13876_F2	GGCCGCGGCATTTACAAGCTGCCTCAGG	102_13876_R2	GCCCCGGCGTTCCAAGCTTACTACCAATC

Table 5.5 Universal primers used for TA- and T7-cloning. The linkers are labelled in blue.

Gene	Forward Primer	Sequence	Reverse Primer	Sequence
M13	M13 F	GTAAAACGACGGCCAG	M13 R	CAGGAAACAGCTATGAC
Universal T7	Universal T7 5'	GAGAATTCTAATACGACTCACTATAGGGCCGCGG	Universal T7 3'	AGGGATCCTAATACGACTCACTATAGGCCCCGGC

5.6. RNA INTERFERENCE (RNAi)

The introduction of double-stranded mRNA into the planarian body was found to inhibit specifically the expression of the gene from which that RNA was derived (Alvarado et al., 1999). To observe developmental processes, regeneration has to be induced by cutting the body. Antibodies or labeled RNA sequences have been used to identify regenerated tissues. Every gene transcript was amplified from first strand cDNA (appendix protocol 2) and synthesized from total RNA extracted from asexual *S. mediterranea* (appendix protocol 1). Selected genes were cloned by TA- or T7-methods (appendix protocol 3, protocol 4). Double strand RNA was synthesized in vitro, using the procedure described in protocol 5 for the TA- and protocol 6 for the T7 method. The amounts measured with the NanoDrop® ND-1000 Spectrophotometer (NanoDrop Technologies, Inc), ranged from 50 ng/uL to 4000 ng/uL. The double-stranded RNA solution was sucked up into the 3.5" glass capillaries (Drummond Scientific) of the nanoinjector (Nanoject II Drumond Scientific Company 500 parkway Broownall PA 19008). 96.6nL (3 x 32.2nL) were injected into the gut branch of each planarian from the ventral side anterior to the pharynx. Needles were pulled using a Flaming/Brown Micropipette Puller (Patterson Scientific) with the following settings: heat 295, time 150, pull 200, and velocity 120. In order to increase the effect of the RNA injections different kind of injections were tested.

5.6.1. Injection type 1. First, starvation of 7 days; second, three injections every day for three days in a row (3x 96.6nL) and thirth, a cut on the fourth day.

5.6.2. Injection type 2. First, starvation of 7 days; second, cut on the first day and after ~3h three injections of 96.6nL each for three days in a row.

5.6.3. Injection type 3. First, starvation of 7 days; second, three injections of 96.6nL each for 3 days in a row and without any cut.

5.6.4. Injection type 4. First, starvation of 7 days; second, one injection of 32.2nL and third, a cut on the next day.

5.6.5. Injection type 5. First, starvation of 7 days; second, two injections of 32.2nL each and third, cut the next day.

5.6.6. Injection type 6. First, starvation of 7 days; second, three injections of 32.2nL each and third, cut the next day.

5.6.7. Injection type 7. First, starvation of 7 days; second, three injections of 32.2nL each without any cuts.

5.6.8. Control injections. The negative control samples were injected with double stranded RNA of the *Jellyfish* gene, GFP. The injection of *Smed-six* dsRNA produced the complete loss of the eyes. This strong effect was used as a control to test the phenotype duration and the correct injection of the new genes. Flatworms were observed and photographed until they were fixed for in situ hybridization or electron microscopy analysis.

5.7. In situ Hybridization

In situ hybridization and immunostaining are techniques for determining gene expression patterns. A chromogene labeled mRNA or a fluorescent labeled protein were visualized. In situ hybridization was performed following standard protocols (appendix protocol 8). Intact and regenerating planarians were treated with hydrochloric acid to remove the mucous and carnoy as the alcohol-based fixation. Intact and regenerating planarians were killed in 2% HCl/Holtfreter and fixed with carnoy. Treatment with proteinase K for permeabilization was followed by hybridization with digoxigenin DIG-labeled single stranded RNA. DIG-labeled antisense RNA was prepared as described in appendix protocol 7. A sense RNA strand was used as a control for the in situ because of its theoretical non-sense activity. Samples were washed and then treated with Boheringer blocking reagent and incubated with anti-DIG antibody. In situ signals were detected by using the NBT/BCIP substrate (Sigma Chemicals Co. St. Louis, USA). All samples were observed through a Leica MZ16F stereomicroscope and images were captured with a ProgRes®C3 camera (Jenoptik). The software used was “IM50 (Leica).

5.8. Immunostaining

The flatworms were fixed using in situ hybridization with 2% of HCL and Carnoy. The samples were dehydrated through a graded series of methanol/PBS and Ethanol/PBS washes and then blocked in PBS/TritonX100 and BSA. The first monoclonal antibody was VC-1, specific for photosensitive cells. The secondary antibody anti-mouse antibody conjugated to Alexa 488 was added after washing with PBSTX. The DAPI antibody was added after incubation with PBSTX. Samples were then washed extensively with PBSTX between and after the antibody incubations, mounted in SlowFade® Gold antifade (Invitrogen) and imaged by confocal laser microscopy using a Leica SP2 microscope (appendix protocol 9). Images were processed and analyzed by the ImageJ program.

5.9. Transmission electron microscopy

7 and 10-days regenerating flatworms, injected with the gen *Smed-white,* were fixed for visualization of ultrastructural alterations. Flatworms injected with GFP were used as a control. 3% of glutaraldehyde was followed by a post fixation in 1% of osmium. All washing steps were done with 0.1 M of cacodilat buffer and further dehydration in a graded ethanol series followed by a mixture of resin spurr normal and ethanol. The material was embedded in the resin spurr normal. Thin sections were made on a Reichert Jung ultramicrotome. Serial sections (60 nm) of the embedded blocks were mounted on mesh grids, post-stained with toluidine blue, uranyl acetate and lead citrate. Electron micrographs were taken on the JEOL 1010 and the TECNAI G2 SPIRIT transmission electron microscopes (appendix protocol 10).

5.10. Phototaxis assay

Inoue et al., 2004 suggested that decapitated planarians temporarily suppressed the light avoidance behaviour and that it was recovered 5 days after decapitation. They also suggested that the recovery of the phototactic response was significantly suppressed in RNAi flatworms that produced morphological defects in either the brain or the visual neurons. Therefore RNAi flatworms that were not able to re-establish their light avoidance after 5 days of regeneration could be considered as eye defective individuals.

Flatworms were submerged into a 60 x 30 x 10 mm container filled with 10mL of autoclaved tap water. The container was exposed to a white light gradient coming from a 500 lux white led lamp. Planarian behaviour was recorded for 90 seconds using an overhead digital video camera (Canon–EOS 550D filter Sigma 150mm 12.8 DGMACRO Japan). The time the flatworms spent in a target quadrant, located in the dark end of the container opposite to the clear side, was measured.

5.11. Microscopy imaging and other instruments

Microscope 1: Stemi SV6 (45105 S1.6X) Zeiss Germany, fit together with the Camera Infinity χ-32 Deltap (TV2/3" C 0,63X, 1069-414) Canada. Used for filming moving flatworms.

Microscope 2: Binocular Stemi 2000-C (0,65-5,0X) Zeiss Germany. Used to visualize living flatworms.

Microscope 3: Leica MZ 16F- (0,11-11,5X) Germany connect with the Camera ProgRes C3 Jenoptic Germany. The software used was progRes Capture Pro 2.8.8, Jenoptic 10 optical Systems. Used for in situ imaging.

Microscope 4: Leica SP2 DMRI2, Leica confocal software ICS SP2, for confocal imaging.

Microscope 5: Electron microscope JEOL 1010.

Microscope 6: Electron microscope TECNAI G^2 SPIRIT.

Ultramicrotome: Ultracut (Reichert-Jung GmbH, Heidelberg, Germany).

Spectrophotometer: NanoDrop® ND-1000 Spectrophotometer, NanoDrop Technologies, Inc. Used for DNA and RNA measurements.

6. BIBLIOGRAPHY

Abd-El-Barr, M. M., Sykoudis, K., Andrabi, S., Eichers, E. R., Pennesi, M. E., Tan, P. L., ... & Wu, S. M. (2007). Impaired photoreceptor protein transport and synaptic transmission in a mouse model of Bardet–Biedl syndrome. Vision research, 47(27), 3394-3407.

Abril, J. F., Cebrià, F., Rodríguez-Esteban, G., Horn, T., Fraguas, S., Calvo, B., ... & Saló, E. (2010). Smed454 dataset: unravelling the transcriptome of *Schmidtea mediterranea*. BMC genomics, 11(1), 731.

Adamidi, C., Wang, Y., Gruen, D., Mastrobuoni, G., You, X., Tolle, D., ... & Chen, W. (2011). De novo assembly and validation of planaria transcriptome by massive parallel sequencing and shotgun proteomics. Genome research, 21(7), 1193-1200.

Adams, R., Liu, X., Williams, D., & Newton, A. (2003). Differential spatial and temporal phosphorylation of the visual receptor, rhodopsin, at two primary phosphorylation sites in mice exposed to light. Biochem. J, 374, 537-543.

Adler, C. E., Seidel, C. W., McKinney, S. A., & Alvarado, A. S. (2014). Selective amputation of the pharynx identifies a *FoxA*-dependent regeneration program in planaria. eLife, 3.

Agata, K., Soejima, Y., Kato, K., Kobayashi, C., Umesono, Y., & Watanabe, K. (1998). Structure of the planarian central nervous system (CNS) revealed by neuronal cell markers. Zoological science, 15(3), 433-440.

Allende, M. L., Amsterdam, A., Becker, T., Kawakami, K., Gaiano, N., & Hopkins, N. (1996). Insertional mutagenesis in zebrafish identifies two novel genes, *pescadillo* and *dead eye*, essential for embryonic development. Genes & development, 10(24), 3141-3155.

Allikmets, R., Shroyer, N. F., Singh, N., Seddon, J. M., Lewis, R. A., Bernstein, P. S., ... & Leppert, M. (1997). Mutation of the Stargardt disease gene (ABCR) in age-related macular degeneration. Science, 277(5333), 1805-1807.

Alvarado, A. S. (2012). Q&A: What is regeneration, and why look to planarians for answers?. BMC biology, 10(1), 88.

Alvarado, A. S., & Newmark, P. A. (1999). Double-stranded RNA specifically disrupts gene expression during planarian regeneration. Proceedings of the National Academy of Sciences, 96(9), 5049-5054.

Amaya, E., Musci, T. J., & Kirschner, M. W. (1991). Expression of a dominant negative mutant of the FGF receptor disrupts mesoderm formation in *Xenopus* embryos. Cell, 66(2), 257-270.

Ammann, F. (1970). Investigations cliniques et génétiques sur le syndrome de Bardet-Biedl en Suisse. Editions Médecine et hygiène. J. Genet. Hum. 18(suppl), 1−310

Anand, M., & Khanna, H. (2012). Ciliary transition zone (TZ) proteins RPGR and CEP290: role in photoreceptor cilia and degenerative diseases. Expert opinion on therapeutic targets, 16(6), 541-551.

Ansley, S. J., Badano, J. L., Blacque, O. E., Hill, J., Hoskins, B. E., Leitch, C. C., ... & Katsanis, N. (2003). Basal body dysfunction is a likely cause of pleiotropic Bardet–Biedl syndrome. Nature, 425(6958), 628-633.

Arendt, D. (2003). Evolution of eyes and photoreceptor cell types. International Journal of Developmental Biology, 47(7/8), 563-572.

Asada, A., Orii, H., Watanabe, K., & Tsubaki, M. (2005). Planarian peptidylglycine-hydroxylating monooxygenase, a neuropeptide processing enzyme, colocalizes with cytochrome b561 along the central nervous system. FEBS Journal, 272(4), 942-955.

Asano, Y., Nakamura, S., Ishida, S., Azuma, K., Shinozawa, T., (1998). Rhodopsin-like proteins in planarian eye and auricle: detection and functional analysis. The journal od experimental biology 201, 1263-1271.

Aslanukov, A., Bhowmick, R., Guruju, M., Oswald, J., Raz, D., Bush, R. A., ... & Ferreira, P. A. (2006). RanBP2 modulates Cox11 and hexokinase I activities and haploinsufficiency of RanBP2 causes deficits in glucose metabolism. PLoS genetics, 2(10), e177.

Atamna-Ismaeel, N., Finkel, O. M., Glaser, F., Sharon, I., Schneider, R., Post, A. F., ... & Belkin, S. (2012). Microbial rhodopsins on leaf surfaces of terrestrial plants. Environmental microbiology, 14(1), 140-146.

Azimzadeh, J., Wong, M. L., Downhour, D. M., Alvarado, A. S., & Marshall, W. F. (2012). Centrosome loss in the evolution of planarians. Science, 335(6067), 461-463.

Azuma, K., Iwasaki, N., & Ohtsu, K. (1999). Absorption spectra of planarian visual pigments and two states of the metarhodopsin intermediates. Photochemistry and photobiology, 69(1), 99-104.

Bailes, H. J., & Lucas, R. J. (2010). Melanopsin and inner retinal photoreception. Cellular and molecular life sciences, 67(1), 99-111.

Bailey, M. J., & Cassone, V. M. (2004). Opsin photoisomerases in the chick retina and pineal gland: characterization, localization, and circadian regulation. Investigative ophthalmology & visual science, 45(3), 769-775.

Beadle, G. W., & Ephrussi, B. (1936). Development of eye colors in *Drosophila*: transplantation experiments with suppressor of *vermilion*. Proceedings of the National Academy of Sciences of the United States of America, 22(9), 536.

Beall, E. L., Manak, J. R., Zhou, S., Bell, M., Lipsick, J. S., & Botchan, M. R. (2002). Role for a *Drosophila* Myb-containing protein complex in site-specific DNA replication. Nature, 420(6917), 833-837.

Beermann, F., Schmid, E., & Schütz, G. (1992). Expression of the mouse tyrosinase gene during embryonic development: recapitulation of the temporal regulation in transgenic mice. Proceedings of the National Academy of Sciences, 89(7), 2809-2813.

Bellingham, J., Chaurasia, S. S., Melyan, Z., Liu, C., Cameron, M. A., Tarttelin, E. E., ... & Lucas, R. J. (2006). Evolution of melanopsin photoreceptors: discovery and characterization of a new melanopsin in nonmammalian vertebrates. PLoS biology, 4(8), e254.

Belov, A. A., & Mohammadi, M. (2013). Molecular mechanisms of fibroblast growth factor signaling in physiology and pathology. Cold Spring Harbor perspectives in biology, 5(6).

Besharse, J. C., Forestner, D. M., & Defoe, D. M. (1985). Membrane assembly in retinal photoreceptors. III. Distinct membrane domains of the connecting cilium of developing rods. The Journal of neuroscience, 5(4), 1035-1048.

Biesemeier, A., Kreppel, F., Kochanek, S., & Schraermeyer, U. (2010). The classical pathway of melanogenesis is not essential for melanin synthesis in the adult retinal pigment epithelium. Cell and tissue research, 339(3), 551-560.

Bingham, S., Chaudhari, S., Vanderlaan, G., Itoh, M., Chitnis, A., & Chandrasekhar, A. (2003). Neurogenic phenotype of mind bomb mutants leads to severe patterning defects in the zebrafish hindbrain. Developmental dynamics, 228(3), 451-463.

Byrne, Maria (2001). The morphology of autotomy structures in the sea cucumber *Eupentacta quinquesemita* before and during evisceration.The Journal of Experimental Biology 204, 849–863

Blacque, O. E., Reardon, M. J., Li, C., McCarthy, J., Mahjoub, M. R., Ansley, S. J., ... & Leroux, M. R. (2004). Loss of *C. elegans* BBS-7 and BBS-8 protein function results in cilia defects and compromised intraflagellar transport. Genes & development, 18(13), 1630-1642.

Blassberg, R. A., Felix, D. A., Tejada-Romero, B., & Aboobaker, A. A. (2013). PBX/extradenticle is required to re-establish axial structures and polarity during planarian regeneration. Development, 140(4), 730-739.

Blatch, G. L., & Lässle, M. (1999). The tetratricopeptide repeat: a structural motif mediating protein-protein interactions. Bioessays, 21(11), 932-939.

Bluhm, A. P. C., Obeid, N. N., Castrucci, A. M. L., & Visconti, M. A. (2012). The expression of melanopsin and clock genes in *Xenopus laevis* melanophores and their modulation by melatonin. Brazilian Journal of Medical and Biological Research, 45(8), 730-736.

Blythe, M. J., Kao, D., Malla, S., Rowsell, J., Wilson, R., Evans, D., ... & Aboobaker, A. A. (2010). A dual platform approach to transcript discovery for the planarian *Schmidtea mediterranea* to establish RNAseq for stem cell and regeneration biology. PLoS One, 5(12), e15617.

Borland, C. Z., Schutzman, J. L., & Stern, M. J. (2001). Fibroblast growth factor signaling in *Caenorhabditis elegans*. Bioessays, 23(12), 1120-1130.

Bottcher, R. T., & Niehrs, C. (2005). Fibroblast growth factor signaling during early vertebrate development. Endocrine reviews, 26(1), 63-77.

Boye, S. E., Alexander, J. J., Boye, S. L., Witherspoon, C. D., Sandefer, K. J., Conlon, T. J., ... & Gamlin, P. D. (2012). The human rhodopsin kinase promoter in an AAV5 vector confers rod-and cone-specific expression in the primate retina. Human gene therapy, 23(10), 1101-1115.

Brann, M. R., & Cohen, L. V. (1987). Diurnal expression of transducin mRNA and translocation of transducin in rods of rat retina. Science, 235(4788), 585-587.

Breslow, D. K., Koslover, E. F., Seydel, F., Spakowitz, A. J., & Nachury, M. V. (2013). An in vitro assay for entry into cilia reveals unique properties of the soluble diffusion barrier. The Journal of cell biology, 203(1), 129-147.

Brown, H. M., & Ogden, T. E. (1968a). The electrical response of the planarian ocellus. The Journal of general physiology, 51(2), 237-253.

Brown, H. M., Ito, H., & Ogden, T. E. (1968b). Spectral sensitivity of the planarian ocellus. The Journal of general physiology, 51(2), 255-260.

Bryant, D. A., & Frigaard, N. U. (2006). Prokaryotic photosynthesis and phototrophy illuminated. Trends in microbiology, 14(11), 488-496.

Burke, J. M., & Hjelmeland, L. M. (2005). Mosaicism of the retinal pigment epithelium: seeing the small picture. Molecular interventions, 5(4), 241.

Callaerts, P., Munoz-Marmol, A. M., Glardon, S., Castillo, E., Sun, H., Li, W. H., ... & Saló, E. (1999). Isolation and expression of a Pax-6 gene in the regenerating and intact planarian *Dugesia* (G) *tigrina*. Proceedings of the National Academy of Sciences, 96(2), 558-563.

Calzia, D., Candiani, S., Garbarino, G., Caicci, F., Ravera, S., Bruschi, M., ... & Panfoli, I. (2013). Are rod outer segment ATP-ase and ATP-synthase activity expression of the same protein?. Cellular and molecular neurobiology, 33(5), 637-649.

Campo, R. V., & Aaberg, T. M. (1982). Ocular and systemic manifestations of the Bardet-Biedl syndrome. American journal of ophthalmology, 94(6), 750-756.

Cebrià, F., Kobayashi, C., Umesono, Y., Nakazawa, M., Mineta, K., Ikeo, K., ... & Agata, K. (2002). FGFR-related gene nou-darake restricts brain tissues to the head region of planarians. Nature, 419(6907), 620-624.

Cebrià, F., & Newmark, P. A. (2005). Planarian homologs of *netrin* and netrin receptor are required for proper regeneration of the central nervous system and the maintenance of nervous system architecture. Development, 132(16), 3691-3703.

Cebrià, F. (2007). Regenerating the central nervous system: how easy for planarians!. Development genes and evolution, 217(11-12), 733-748.

Cebrià, F., & Newmark, P. A. (2007a). Morphogenesis defects are associated with abnormal nervous system regeneration following *roboA* RNAi in planarians. Development, 134(5), 833-837.

Cebrià, F., Guo, T., Jopek, J., & Newmark, P. A. (2007b). Regeneration and maintenance of the planarian midline is regulated by a *slit* orthologue. Developmental biology, 307(2), 394-406.

Cepko, C. L., Austin, C. P., Yang, X., Alexiades, M., & Ezzeddine, D. (1996). Cell fate determination in the vertebrate retina. Proceedings of the National Academy of Sciences, 93(2), 589-595.

Challoner, C. M., & Gooding, R. H. (1997). A white eye color mutant in the tsetse fly *Glossina morsitans submotsitans* Newstead (Diptera: Glossinidae). Genome, 40(1), 165-169.

Chamling, X., Seo, S., Bugge, K., Searby, C., Guo, D. F., Drack, A. V., ... & Sheffield, V. C. (2013). Ectopic expression of human BBS4 can rescue Bardet-Biedl syndrome phenotypes in Bbs4 null mice. PloS one, 8(3), e59101.

Chang, L., & Goldman, R. D. (2004). Intermediate filaments mediate cytoskeletal crosstalk. Nature Reviews Molecular Cell Biology, 5(8), 601-613.

Chang S. Lamm S.H. (2003). Human health effects of sodium azide exposure: a literature review and analysis. Int. J. Toxico. 22(3): 175-86.

Chatel, G., & Fahrenkrog, B. (2012). Dynamics and diverse functions of nuclear pore complex proteins. Nucleus, 3(2), 162-171.

Chaudhary, J., & Skinner, M. K. (1999). Basic helix-loop-helix proteins can act at the E-box within the serum response element of the *c-fos* promoter to influence hormone-induced promoter activation in Sertoli cells. Molecular Endocrinology, 13(5), 774-786.

Chaves, I., Pokorny, R., Byrdin, M., Hoang, N., Ritz, T., Brettel, K., ... & Ahmad, M. (2011). The cryptochromes: blue light photoreceptors in plants and animals. Annual review of plant biology, 62, 335-364.

Chen, H., & JUCHAU, M. (1998). Recombinant human glutathione S-transferases catalyse enzymic isomerization of 13-cis-retinoic acid to all-trans-retinoic acid in vitro. Biochem. J, 336, 223-226.

Chen, C. C. G., Wang, I. E., & Reddien, P. W. (2013). *pbx* is required for pole and eye regeneration in planarians. Development, 140(4), 719-729.

Cho, K. I., Cai, Y., Yi, H., Yeh, A., Aslanukov, A., & Ferreira, P. A. (2007). Association of the kinesin-binding domain of RanBP2 to KIF5B and KIF5C determines mitochondria localization and function. Traffic, 8(12), 1722-1735.

Collins III, J. J., Hou, X., Romanova, E. V., Lambrus, B. G., Miller, C. M., Saberi, A., ... & Newmark, P. A. (2010). Genome-wide analyses reveal a role for peptide hormones in planarian germline development. PLoS biology, 8(10), e1000509.

Cross, R. L., & Müller, V. (2004). The evolution of A-, F-, and V-type ATP synthases and ATPases: reversals in function and changes in the H sup/sup/ATP coupling ratio. FEBS letters, 576(1), 1-4.

Conesa, A., Götz, S., García-Gómez, J. M., Terol, J., Talón, M., & Robles, M. (2005). Blast2GO: a universal tool for annotation, visualization and analysis in functional genomics research. Bioinformatics, 21(18), 3674-3676.

Coste, B., Houge, G., Murray, M. F., Stitziel, N., Bandell, M., Giovanni, M. A., ... & Patapoutian, A. (2013). Gain-of-function mutations in the mechanically activated ion channel PIEZO2 cause a subtype of Distal Arthrogryposis. Proceedings of the National Academy of Sciences, 110(12), 4667-4672.

Coumoul, X., & Deng, C. X. (2003). Roles of FGF receptors in mammalian development and congenital diseases. Birth Defects Research Part C: Embryo Today: Reviews, 69(4), 286-304.

Cowles, M. W., Brown, D. D., Nisperos, S. V., Stanley, B. N., Pearson, B. J., & Zayas, R. M. (2013). Genome-wide analysis of the bHLH gene family in planarians identifies factors required for adult neurogenesis and neuronal regeneration. Development, 140(23), 4691-4702.

Cunningham, T. J., & Duester, G. (2015). Mechanisms of retinoic acid signalling and its roles in organ and limb development. *Nature Reviews Molecular Cell Biology*, *16*(2), 110-123.

Daiker, V., Häder, D. P., Richter, P. R., & Lebert, M. (2011). The involvement of a protein kinase in phototaxis and gravitaxis of *Euglena gracilis*. Planta, 233(5), 1055-1062.

Das, A. K., Cohen, P. T., & Barford, D. (1998). The structure of the tetratricopeptide repeats of protein phosphatase 5: implications for TPR-mediated protein–protein interactions. The EMBO journal, 17(5), 1192-1199.

Davis, L. K., Meyer, K. J., Rudd, D. S., Librant, A. L., Epping, E. A., Sheffield, V. C., & Wassink, T. H. (2008). Pax6 3′ deletion results in aniridia, autism and mental retardation. Human genetics, 123(4), 371-378.

de Castro, F., López-Mascaraque, L., & De Carlos, J. A. (2007). Cajal: Lessons on brain development. Brain research reviews, 55(2), 481-489.

Delphin, C., Guan, T., Melchior, F., & Gerace, L. (1997). RanGTP targets p97 to RanBP2, a filamentous protein localized at the cytoplasmic periphery of the nuclear pore complex. Molecular biology of the cell, 8(12), 2379-2390.

Dickson, B. J. (1998). Photoreceptor development: breaking down the barriers. Current biology, 8(3), R90-R92.

Draeger, U. C., & Olsen, J. F. (1980). Origins of crossed and uncrossed retinal projections in pigmented and albino mice. Journal of Comparative Neurology, 191(3), 383-412.

Drory, O., Frolow, F., & Nelson, N. (2004). Crystal structure of yeast V-ATPase subunit C reveals its stator function. EMBO reports, 5(12), 1148-1152.

Dryja, T. P., McGee, T. L., Hahn, L. B., Cowley, G. S., Olsson, J. E., Reichel, E., ... & Berson, E. L. (1990). Mutations within the rhodopsin gene in patients with autosomal dominant retinitis pigmentosa. New England Journal of Medicine, 323(19), 1302-1307.

Dryja, T. P., Briggs, C. E., Berson, E. L., Rosenfeld, P. J., & Abitbol, M. (1998). ABCR gene and age-related macular degeneration. Science, 279(5354), 1107-1107.

Dryja, T. (2001). Retinitis pigmentosa and stationary night blindness. The Online Metabolic and Molecular Bases of Inherited Diseases, Scriver C, Beaudet A, Sly W, Valle D (eds), 5903-5933.

Dubois, F. (1949). Contribution á l'ètude de la migration des cellules de règènèration chez les Planaires dulcicoles. (Doctoral dissertation), Bulletin Biologique de la France et de le Belgique 83, 213-283..

Duester, G. (2008). Retinoic acid synthesis and signaling during early organogenesis. Cell, 134(6), 921-931.

Durussel, I., Blouquit, Y., Middendorp, S., Craescu, C. T., & Cox, J. A. (2000). Cation-and peptide-binding properties of human *centrin 2.* FEBS letters, 472(2), 208-212.

Eckelt, K. (2011). Multi-approach Analysis for Identification and Functional Characterization of Eye Regeneration Related Genes of *Schmidtea mediterranea* (Doctoral dissertation). Genetic Department Biology Faculty. Universitat de Barcelona.

Eiraku, M., Takara, N., Ishibashi, H., Kawada, M., sakakura, E., Okuda, S., & sasai, Y. (2011). Self-organizing optic-cup morphogenesis in three-dimensional culture. Nature, 472(7341), 51-56.

El-Amraoui, A., & Petit, C. (2005). Usher I syndrome: unravelling the mechanisms that underlie the cohesion of the growing hair bundle in inner ear sensory cells. Journal of cell science, 118(20), 4593-4603.

Ermakova, O. N., Ermakov, A. M., Tiras, K. P., & Lednev, V. V. (2009). Retinoic acid as a regulator of planarian morphogenesis. Russian journal of developmental biology, 40(6), 367-372.

Ermakova, O. N., Ermakov, A. M., Tiras, K. P., & Lednev, V. V. (2009). Melatonin effect on the regeneration of the flatworm *Girardia tigrina*. Russian journal of developmental biology, 40(6), 382-385.

Fallon, J. H., Seroogy, K. B., Loughlin, S. E., Morrison, R. S., Bradshaw, R. A., Knaver, D. J., & Cunningham, D. D. (1984). Epidermal growth factor immunoreactive material in the central nervous system: location and development. Science, 224(4653), 1107-1109.

Fernald, R. D. (2006). Casting a genetic light on the evolution of eyes. Science, 313(5795), 1914-1918.

Ferreira, P. A., Nakayama, T. A., Pak, W. L., & Travis, G. H. (1996). Cyclophilin-related protein RanBP2 acts as chaperone for red/green opsin. Nature; 383:637-40.

Ferreira, P. A., Nakayama, T. A., & Travis, G. H. (1997). Interconversion of red opsin isoforms by the cyclophilin-related chaperone protein Ran-binding protein 2. Proceedings of the National Academy of Sciences, 94(4), 1556-1561.

Finn, R. D., Mistry, J., Tate, J., Coggill, P., Heger, A., Pollington, J. E., ... & Bateman, A. (2009). Pfam protein families database. Nucleic Acids Research,1-12.

Flygare, S., Campbell, M., Ross, R. M., Moore, B., & Yandell, M. (2013). ImagePlane: An Automated Image Analysis Pipeline for High-Throughput Screens Using the Planarian *Schmidtea mediterranea*. Journal of Computational Biology, 20(8), 583-592.

Fogle, K. J., Parson, K. G., Dahm, N. A., & Holmes, T. C. (2011). Cryptochrome is a blue-light sensor that regulates neuronal firing rate. Science, 331(6023), 1409-1413.

Foley, L. E., Gegear, R. J., & Reppert, S. M. (2011). Human cryptochrome exhibits light-dependent magnetosensitivity. Nature communications, 2, 356.

Foster, R. G., & Helfrich-Forster, C. (2001). The regulation of circadian clocks by light in fruit flies and mice. Philosophical Transactions of the Royal Society-Ser B-Biological Sciences, 356(1415), 1779-1790.

Fraguas, S., Barberán, S., & Cebrià, F. (2011). EGFR signaling regulates cell proliferation, differentiation and morphogenesis during planarian regeneration and homeostasis. Developmental biology, 354(1), 87-101.

Fu, Y., & Yau, K. W. (2007). Phototransduction in mouse rods and cones. Pflügers Archiv-European Journal of Physiology, 454(5), 805-819.

Furukawa, T., Kozak, C. A., & Cepko, C. L. (1997). Rax, a novel paired-type homeobox gene, shows expression in the anterior neural fold and developing retina. Proceedings of the National Academy of Sciences, 94(7), 3088-3093.

Gao, H., Sumanaweera, N., Bailer, S. M., & Stochaj, U. (2003). Nuclear accumulation of the small GTPase Gsp1p depends on nucleoporins Nup133p, Rat2p/Nup120p, Nup85p, Nic96p, and the acetyl-CoA carboxylase Acc1p. Journal of Biological Chemistry, 278(28), 25331-25340.

Garmory, H. S., & Titball, r. W. (2004). ATP-binding cassette transportes are targets for the development of antibacterial vaccines and therapies. Infection and immunity, 72(12), 6757-6763.

Gehring, W. J., & Ikeo, K. (1999). *Pax6* mastering eye morphogenesis and eye evolution. Trends in genetics, 15(9), 371-377.

Gehring, W. J. (2001). The genetic control of eye development and its implications for the evolution of the various eye-types. Zoology, 104(3), 171-183.

Gehring, W. J. (2012). The evolution of vision. Wiley Interdisciplinary Reviews: Developmental Biology, 3(1), 1-40.

Giménez, E., Lavado, A., Giraldo, P., & Montoliu, L. (2003). Tyrosinase gene expression is not detected in mouse brain outside the retinal pigment epithelium cells. European Journal of Neuroscience, 18(9), 2673-2676.

Gomez-Marin, A., Partoune, N., Stephens, G. J., & Louis, M. (2012). Automated tracking of animal posture and movement during exploration and sensory orientation behaviors. PloS one, 7(8), e41642.

González-Sastre, A., Dolores Molina, M., & Saló, E. (2012). Inhibitory *Smads* and bone morphogenetic protein (BMP) modulate anterior photoreceptor cell number during planarian eye regeneration. International Journal of Developmental Biology, 56(1), 155.

Gospodarowicz, D. (1974). Localisation of a fibroblast growth factor and its effect alone and with hydrocortisone on 3T3 cell growth. Nature, 249, 123-127.

Gouge, A., Holt, J., Hardy, A. P., Sowden, J. C., & Smith, H. K. (2001). *Foxn4* a new member of the forkhead gene family is expressed in the retina. Mechanisms of development, 107(1), 203-206.

Gonczy, P. (2012). Towards a molecular architecture of centriole assembly. Nature Reviews Molecular Cell Biology, 13(7), 425-435.

Graham, D., Kolb, H., Fernandez, E., & Nelson, R. (2014). Melanopsin ganglion cells: A bit of fly in the mammalian eye. Webvision: The Organization of the Retina and Visual System.

Grandi, P., Dang, T., Pané, N., Shevchenko, A., Mann, M., Forbes, D., & Hurt, E. (1997). *Nup93*, a vertebrate homologue of yeast *Nic96p*, forms a complex with a novel 205-kDa protein and is required for correct nuclear pore assembly. Molecular biology of the cell, 8(10), 2017-2038.

Gunther, K. L., Neitz, J., & Neitz, M. (2006). A novel mutation in the short-wavelength-sensitive cone pigment gene associated with a tritan color vision defect. Visual neuroscience, 23(3-4), 403-409.

Guido, M. E., Carpentieri, A. R., & Garbarino-Pico, E. (2002). Circadian phototransduction and the regulation of biological rhythms. Neurochemical research, 27(11), 1473-1489.

Guo, T., Peters, A. H., & Newmark, P. A. (2006). A bruno-like gene is required for stem cell maintenance in planarians. Developmental cell, 11(2), 159-169.

Ha, A., Perez-Iratxeta, C., Liu, H., Mears, A. J., & Wallace, V. A. (2012). Identification of *Wnt/β-catenin* modulated genes in the developing retina. Molecular vision, 18, 645-656.

Haltia, M. (2006). The neuronal ceroid-lipofuscinoses: from past to present. Biochimica et Biophysica Acta (BBA)-Molecular Basis of Disease, 1762(10), 850-856.

Hanks, S. K., & Hunter, T. (1995). Protein kinases 6. The eukaryotic protein kinase superfamily: kinase (catalytic) domain structure and classification. The FASEB journal, 9(8), 576-596.

Hao, W., & Fong, H. K. (1996). Blue and ultraviolet light-absorbing opsin from the retinal pigment epithelium. Biochemistry, 35(20), 6251-6256.

Hao, W., & Fong, H. K. (1999). The endogenous chromophore of retinal G protein-coupled receptor opsin from the pigment epithelium. Journal of Biological Chemistry, 274(10), 6085-6090.

Hara, T., & Hara, R. (1972). Cephalopod retinochrome. In Photochemistry of Vision (pp. 720-746). Springer Berlin Heidelberg.

Hardie, R. C., & Raghu, P. (2001). Visual transduction in *Drosophila*. Nature, 413(6852), 186-193.

Hardie, R. C. (2001). Phototransduction in *Drosophila* melanogaster. Journal of Experimental Biology, 204(20), 3403-3409.

Harvey, J. J. (1964). An unidentified virus which causes the rapid production of tumours in mice. Nature 204, 1104–5.

Hase, S., Wakamatsu, K., Fujimoto, K., Inaba, A., Kobayashi, K., Matsumoto, M., ... & Negishi, S. (2006). Characterization of the pigment produced by the planarian, *Dugesia ryukyuensis*. Pigment cell research, 19(3), 248-249.

Hatini, V., Tao, W., & Lai, E. (1994). Expression of winged helix genes, BF-1 and BF-2, define adjacent domains within the developing forebrain and retina. Journal of neurobiology, 25(10), 1293-1309.

Hattar, S., Liao, H. W., Takao, M., Berson, D. M., & Yau, K. W. (2002). Melanopsin-containing retinal ganglion cells: architecture, projections, and intrinsic photosensitivity. Science, 295(5557), 1065-1070.

Hattar, S., Lucas, R. J., Mrosovsky, N., Thompson, S., Douglas, R. H., Hankins, M. W., ... & Yau, K. W. (2003). Melanopsin and rod–cone photoreceptive systems account for all major accessory visual functions in mice. Nature, 424(6944), 75-81.

Haupts, U., Tittor, J., & Oesterhelt, D. (1999). Closing in on bacteriorhodopsin: progress in understanding the molecule. Annual review of biophysics and biomolecular structure, 28(1), 367-399.

Houseley, J., & Tollervey, D. (2009). The many pathways of RNA degradation. Cell, 136(4), 763-776.

Hemmer, W., Riesinger, I., Wallimann, T., Eppenberger, H. M., & Quest, A. F. (1993). Brain-type creatine kinase in photoreceptor cell outer segments: role of a phosphocreatine circuit in outer segment energy metabolism and phototransduction. Journal of cell science, 106(2), 671-683.

Herrera, E., Marcus, R., Li, S., Williams, S. E., Erskine, L., Lai, E., & Mason, C. (2004). *Foxd1* is required for proper formation of the optic chiasm. Development, 131(22), 5727-5739.

Herrera, E., & Garcia-Frigola, C. (2008). Genetics and development of the optic chiasm. Frontiers in Bioscience, 13(5), 1646-1653.

Hershey, C. L., & Fisher, D. E. (2004). *Mitf* and *Tfe3*: members of a b-HLH-ZIP transcription factor family essential for osteoclast development and function. Bone, 34(4), 689-696.

Hingorani, M., Hanson, I., & van Heyningen, V. (2012). Aniridia. European Journal of Human Genetics, 20(10), 1011-1017.

Hirami, Y., Osakada, F., Takahashi, K., Okita, K., Yamanaka, S., Ikeda, H., ... & Takahashi, M. (2009). Generation of retinal cells from mouse and human induced pluripotent stem cells. Neuroscience letters, 458(3), 126-131.

Holme, R. H., Thomson, S. J., & Davidson, D. R. (2000). Ectopic expression of *Msx2* in chick retinal pigmented epithelium cultures suggests a role in patterning the optic vesicle. Mechanisms of development, 91(1), 175-187.

Hsu, S. C., & Molday, R. S. (1994). Glucose metabolism in photoreceptor outer segments. Its role in phototransduction and in NADPH-requiring reactions. Journal of Biological Chemistry, 269(27), 17954-17959.

Huh, S., Hatini, V., Marcus, R. C., Li, S. C., & Lai, E. (1999). Dorsal–ventral patterning defects in the eye of BF-1-deficient mice associated with a restricted loss of *shh* expression. Developmental biology, 211(1), 53-63.

Iglesias, M., Gomez-Skarmeta, J. L., Saló, E., & Adell, T. (2008). Silencing of *Smed-βcatenin1* generates radial-like hypercephalized planarians. Development, 135(7), 1215-1221.

Inoue, T., Hayashi, T., Takechi, K., & Agata, K. (2007). Clathrin-mediated endocytic signals are required for the regeneration of, as well as homeostasis in, the planarian CNS. Development, 134(9), 1679-1689.

Inoue, T., Kumamoto, H., Okamoto, K., Umesono, Y., Sakai, M., Alvarado, A. S., & Agata, K. (2004). Morphological and functional recovery of the planarian photosensing system during head regeneration. Zoological science, 21(3), 275-283.

Isoldi, M. C., Rollag, M. D., de Lauro Castrucci, A. M., & Provencio, I. (2005). Rhabdomeric phototransduction initiated by the vertebrate photopigment melanopsin. Proceedings of the National Academy of Sciences of the United States of America, 102(4), 1217-1221.

Itoh, M. T., Shinozawa, T., & Sumi, Y. (1999). Circadian rhythms of melatonin-synthesizing enzyme activities and melatonin levels in planarians. Brain research, 830(1), 165-173.

Jedlitschky, G., Leier, I., Buchholz, U., Barnouin, K., Kurz, G., & Keppler, D. (1996). Transport of glutathione, glucuronate, and sulfate conjugates by the MRP gene-encoded conjugate export pump. Cancer Research, 56(5), 988-994.

Jeffery, G. (1998). The retinal pigment epithelium as a developmental regulator of the neural retina. Eye, 12, 499-503.

Jeong, H. W., Kim, J. H., Kim, J. Y., Ha, S. J., & Kong, Y. Y. (2012). *Mind bomb-1* in dendritic cells is specifically required for Notch-mediated T helper type 2 differentiation. PloS one, 7(4), e36359.

Katagiri, N., Terakita, A., Shichida, Y., & Katagiri, Y. (2001). Demonstration of a rhodopsin-retinochrome system in the stalk eye of a marine gastropod, Onchidium, by immunohistochemistry. Journal of Comparative Neurology, 433(3), 380-389.

Kato, T., Sawada, H., Yamamoto, T., Mase, K., & Nakagoshi, M. (2006). Pigment pattern formation in the quail mutant of the silkworm, *Bombyx mori*: parallel increase of pteridine biosynthesis and pigmentation of melanin and ommochromes. Pigment cell research, 19(4), 337-345.

Katsanis, N., Lupski, J. R., & Beales, P. L. (2001). Exploring the molecular basis of Bardet–Biedl syndrome. Human molecular genetics, 10(20), 2293-2299.

Kaufmann, E., & Knöchel, W. (1996). Five years on the wings of fork head. Mechanisms of development, 57(1), 3-20.

Khan, A., Chieng, K. S., Baheerathan, A., Hussain, N., & Gosalakkal, J. (2013). Novel CLN1 mutation with atypical juvenile neuronal ceroid lipofuscinosis. Journal of pediatric neurosciences, 8(1), 49.

Kim, J. C., Badano, J. L., Sibold, S., Esmail, M. A., Hill, J., Hoskins, B. E., ... & Beales, P. L. (2004). The Bardet-Biedl protein BBS4 targets cargo to the pericentriolar region and is required for microtubule anchoring and cell cycle progression. Nature genetics, 36(5), 462-470.

Kim, S. J., Zhang, Z., Lee, Y. C., & Mukherjee, A. B. (2006). Palmitoyl-protein thioesterase-1 deficiency leads to the activation of caspase-9 and contributes to rapid neurodegeneration in INCL. Human molecular genetics, 15(10), 1580-1586.

Kinnear, P. E., Jay, B., & Witkop Jr, C. J. (1985). Albinism. Survey of ophthalmology, 30(2), 75-101.

Kirsten, W. H., Schauf, V., & McCoy, J. (1970). Properties of a murine sarcoma virus. Bibliotheca haematologica, (36), 246.

Kishida, Y. (1967). Electron microscopic studies on the planarian eye. II. Fine structures of the regenerating eye. The science reports of the Kanazawa University= 金沢大学理科報告, 12(1), 111-142.

Kleinlogel, S., & White, A. G. (2008). The secret world of shrimps: polarisation vision at its best. PloS one, 3(5), e2190.

Kobayashi, C., Saito, Y., Ogawa, K., & Agata, K. (2007). Wnt signaling is required for antero-posterior patterning of the planarian brain. Developmental biology, 306(2), 714-724.

Kobayashi, T., & Dynlacht, B. D. (2011). Regulating the transition from centriole to basal body. The Journal of cell biology, 193(3), 435-444.

Koga, C., Adati, N., Nakata, K., Mikoshiba, K., Furuhata, Y., Sato, S., ... & Yokoyama, K. K. (1999). Characterization of a Novel Member of the FGF Family, XFGF-20, in *Xenopus laevis*. Biochemical and biophysical research communications, 261(3), 756-765.

Koinuma, S., Umesono, Y., Watanabe, K., & Agata, K. (2000). Planaria FoxA (HNF3) homologue is specifically expressed in the pharynx-forming cells. Gene, 259(1), 171-176.

Koinuma, S., Umesono, Y., Watanabe, K., & Agata, K. (2003). The expression of planarian brain factor homologs, DjFoxG and DjFoxD. Gene expression patterns, 3(1), 21-27.

Kolbe, M., Besir, H., Essen, L. O., & Oesterhelt, D. (2000). Structure of the light-driven chloride pump halorhodopsin at 1.8 Å resolution. Science, 288(5470), 1390-1396.

Kopan, R., & Ilagan, M. X. G. (2009). The canonical Notch signaling pathway: unfolding the activation mechanism. Cell, 137(2), 216-233.

Koyanagi, M., Kubokawa, K., Tsukamoto, H., Shichida, Y., & Terakita, A. (2005). Cephalochordate melanopsin: evolutionary linkage between invertebrate visual cells and vertebrate photosensitive retinal ganglion cells. Current biology, 15(11), 1065-1069.

Krishnadev, N., Meleth, A. D., & Chew, E. Y. (2010). Nutritional supplements for age-related macular degeneration. Current opinion in ophthalmology, 21(3), 184.

Kuehn, H. (1978). Light-regulated binding of rhodopsin kinase and other proteins to cattle photoreceptor membranes. Biochemistry, 17(21), 4389-4395.

Kumar, V., Abbas, A. K., & Fausto, N. (2005) Robbins and Cotran pathologic basis of disease. Saunders Elsevier Publication, Philadelphia, Indian Reprint, 571-87

Laoukili, J., Perret, E., Middendorp, S., Houcine, O., Guennou, C., Marano, F., ... & Tournier, F. (2000). Differential expression and cellular distribution of centrin isoforms during human ciliated cell differentiation in vitro. Journal of Cell Science, 113(8), 1355-1364.

Lapan, S. W., & Reddien, P. W. (2011). *dlx* and *sp6-9* control optic cup regeneration in a prototypic eye. PLoS genetics, 7(8), e1002226.

Lapan, S. W., & Reddien, P. W. (2012). Transcriptome analysis of the planarian eye identifies *ovo* as a specific regulator of eye regeneration. Cell reports, 2(2), 294-307.

Lavado, A., & Montoliu, L. (2005). New animal models to study the role of tyrosinase in normal retinal development. Frontiers in bioscience: a journal and virtual library, 11, 743-752.

Lavado, A., Jeffery, G., Tovar, V., Villa, P., & Montoliu, L. (2006). Ectopic expression of tyrosine hydroxylase in the pigmented epithelium rescues the retinal abnormalities and visual function common in albinos in the absence of melanin. Journal of neurochemistry, 96(4), 1201-1211.

Law, M. H., MacGregor, S., & Hayward, N. K. (2012). Melanoma genetics: recent findings take us beyond well-traveled pathways. Journal of Investigative Dermatology, 132(7), 1763-1774.

Levy, C., Khaled, M., & Fisher, D. E. (2006). MITF: master regulator of melanocyte development and melanoma oncogene. Trends in molecular medicine, 12(9), 406-414.

Li, B. X., Satoh, A. K., & Ready, D. F. (2007). Myosin V, Rab11, and dRip11 direct apical secretion and cellular morphogenesis in developing *Drosophila* photoreceptors. The Journal of cell biology, 177(4), 659-669.

Li, S., Mo, Z., Yang, X., Price, S. M., Shen, M. M., & Xiang, M. (2004). Foxn4 Controls the Genesis of Amacrine and Horizontal Cells by Retinal Progenitors. Neuron, 43(6), 795-807.

Linton, J. D., Holzhausen, L. C., Babai, N., Song, H., Miyagishima, K. J., Stearns, G. W., ... & Hurley, J. B. (2010). Flow of energy in the outer retina in darkness and in light. Proceedings of the National Academy of Sciences, 107(19), 8599-8604.

Lipsick, J. S. (1996). One billion years of Myb. Oncogene, 13(2), 223-235.

Lodish H, Berk A, Zipursky SL, Matsudaira P, Baltimore D, Darnell J (2000). "Chapter 25, Cancer". Molecular cell biology (4th ed.). San Francisco: W.H. Freeman.

Lorente, M., Pérez, C., Sánchez, C., Donohoe, M., Shi, Y., & Vidal, M. (2006). Homeotic transformations of the axial skeleton of YY1 mutant mice and genetic interaction with the Polycomb group gene Ring1/Ring1A. Mechanisms of development, 123(4), 312-320.

Lukáts, A., Szabó, A., Röhlich, P., Vigh, B., & Szel, A. (2005). Photopigment coexpression in mammals: comparative and developmental aspects. Histology and histopathology; 20:551–574.

Lupi, D., Oster, H., Thompson, S., & Foster, R. G. (2008). The acute light-induction of sleep is mediated by OPN4-based photoreception. Nature neuroscience, 11(9), 1068-1073.

Mackenzie, S. M., Brooker, M. R., Gill, T. R., Cox, G. B., Howells, A. J., & Ewart, G. D. (1999). Mutations in the white gene of *Drosophila melanogaster* affecting ABC transporters that determine eye colouration. Biochimica et Biophysica Acta (BBA)-Biomembranes, 1419(2), 173-185.

Maeda, T., Imanishi, Y., & Palczewski, K. (2003). Rhodopsin phosphorylation: 30 years later. Progress in retinal and eye research, 22(4), 417-434.

Manak, J. R., Mitiku, N., & Lipsick, J. S. (2002). Mutation of the Drosophila homologue of the Myb protooncogene causes genomic instability. Proceedings of the National Academy of Sciences, 99(11), 7438-7443.

Mangelsdorf, D. J., & Evans, R. M. (1995). The RXR heterodimers and orphan receptors. Cell, 83(6), 841-850.

Manning, G., Whyte, D. B., Martinez, R., Hunter, T., & Sudarsanam, S. (2002). The protein kinase complement of the human genome. Science, 298(5600), 1912-1934.

Mannini, L., Rossi, L., Deri, P., Gremigni, V., Salvetti, A., Saló, E., & Batistoni, R. (2004). *Djeyes* absent (*Djeya*) controls prototypic planarian eye regeneration by cooperating with the transcription factor *Djsix-1*. Developmental biology, 269(2), 346-359.

Marszalek, J. R., Liu, X., Roberts, E. A., Chui, D., Marth, J. D., Williams, D. S., & Goldstein, L. S. (2000). Genetic evidence for selective transport of opsin and arrestin by kinesin-II in mammalian photoreceptors. Cell, 102(2), 175-187.

Martin, S. S., & Senior, A. E. (1980). Membrane adenosine triphosphatase activities in rat pancreas. Biochimica et Biophysica Acta (BBA)-Biomembranes, 602(2), 401-418.

Martín-Durán, J. M., Monjo, F., & Romero, R. (2012). Morphological and molecular development of the eyes during embryogenesis of the freshwater planarian *Schmidtea polychroa*. Development genes and evolution, 222(1), 45-54.

Marshall, H., Morrison, A., Studer, M., Pöpperl, H., & Krumlauf, R. (1996). Retinoids and Hox genes. *The FASEB Journal*, *10*(9), 969-978.

Matsushita, A., Yoshikawa, T., Okano, T., Kasahara, T., & Fukada, Y. (2000). Colocalization of pinopsin with two types of G-protein α-subunits in the chicken pineal gland. Cell and tissue research, 299(2), 245-251.

Mavlyutov, T. A., Cai, Y., & Ferreira, P. A. (2002). Identification of RanBP2-and Kinesin-Mediated Transport Pathways with Restricted Neuronal and Subcellular Localization. Traffic, 3(9), 630-640.

Medeiros, N. A., Burnette, D. T., & Forscher, P. (2006). Myosin II functions in actin-bundle turnover in neuronal growth cones. Nature cell biology, 8(3), 216-226.

Meiden, M., (1995). Involvement of retinoic acid in embryonic and postembryonic development. Ontogenez, vol.26,no.6, pp. 419-929.

Menzel, R. (1979). Spectral sensitivity and color vision in invertebrates. In Comparative physiology and evolution of vision in invertebrates (pp. 503-580). Springer Berlin Heidelberg.

Mineta, K., Nakazawa, M., Cebrià, F., Ikeo, K., Agata, K., & Gojobori, T. (2003). Origin and evolutionary process of the CNS elucidated by comparative genomics analysis of planarian ESTs. Proceedings of the National Academy of Sciences, 100(13), 7666-7671.

Miranda-Astudillo, H. V. (2012). Estructura y función de la ATP sintasa de las arqueas aeróbicas. TIP. Revista especializada en ciencias químico-biológicas, 15(2), 104-115.

Miyashita, Y., Moriya, T., Yamada, K., Kubota, T., Shirakawa, S., Fujii, N., & Asami, K. (2001). The photoreceptor molecules in *Xenopus* tadpole tail fin, in which melanophores exist. Zoological Science, 18(5), 671-674.

Molina, M. D., Saló, E., & Cebrià, F. (2007). The BMP pathway is essential for re-specification and maintenance of the dorsoventral axis in regenerating and intact planarians. Developmental biology, 311(1), 79-94.

Moore, K. J. (1995). Insight into the microphthalmia gene. Trends in Genetics, 11(11), 442-448.

Moose, H. E., Kelly, L. E., Nekkalapudi, S., & El-Hodiri, H. M. (2009). Ocular forkhead transcription factors: seeing eye to eye. International Journal of Developmental Biology, 53(1), 29.

Morgan, M. J., Woltering, J. M., der Rieden, P. M. I., Durston, A. J., & Thiery, J. P. (2004). YY1 regulates the neural crest-associated slug gene in *Xenopus laevis*. Journal of Biological Chemistry, 279(45), 46826-46834.

Morgan, T. H., (1910). Sex limited inheritance in *Drosophila*. Science 32, (812),120–122.

Morita, M., Hall, F. L., & Best, J. B. (1988). An optic neurosecretory cell in the planarian. Fortschr Zool, 36, 207-210.

Morita, M., & Best, J. B. (1993). The occurrence and physiological functions of melatonin in the most primitive eumetazoans, the planarians. Experientia, 49(8), 623-626.

Morita, M., Hall, F., Best, J. B., & Gern, W. (1987). Photoperiodic modulation of cephalic melatonin in planarians. Journal of Experimental Zoology, 241(3), 383-388.

Morris, J., Ladurner, P., Rieger, R., Pfister, D., De Miguel-Bonet, M. D. M., Jacobs, D., & Hartenstein, V. (2006). The Macrostomum lignano EST database as a molecular resource for studying platyhelminth development and phylogeny. Development genes and evolution, 216(11), 695-707.

Moutsaki, P., Whitmore, D., Bellingham, J., Sakamoto, K., David-Gray, Z. K., & Foster, R. G. (2003). Teleost multiple tissue (tmt) opsin: a candidate photopigment regulating the peripheral clocks of zebrafish?. Molecular brain research, 112(1), 135-145.

Murphy, T. C., Saleem, R. A., Footz, T., Ritch, R., McGillivray, B., & Walter, M. A. (2004). The wing 2 region of the FOXC1 forkhead domain is necessary for normal DNA-binding and transactivation functions. Investigative ophthalmology & visual science, 45(8), 2531-2538.

Musio, C. (1997). Extraocular photosensitivity in invertebrates. Biophysics of Photoreception, 245-262.

Nagao, T., Endo, K., Kawauchi, H., Walldorf, U., & Furukubo-Tokunaga, K. (2000). Patterning defects in the primary axonal scaffolds caused by the mutations of the extradenticle and homothorax genes in the embryonic *Drosophila* brain. Development genes and evolution, 210(6), 289-299.

Nagashima, K., Matsue, K., Konishi, M., Iidaka, C., Miyazaki, K., Ishida, N., & Kanosue, K. (2005). The involvement of Cry1 and Cry2 genes in the regulation of the circadian body temperature rhythm in mice. American Journal of Physiology-Regulatory, Integrative and Comparative Physiology, 288(1), R329-R335.

Nagata, T., Koyanagi, M., Tsukamoto, H., & Terakita, A. (2010). Identification and characterization of a protostome homologue of peropsin from a jumping spider. Journal of Comparative Physiology A, 196(1), 51-59.

Nakada, C., Satoh, S., Tabata, Y., Arai, K. I., & Watanabe, S. (2006). Transcriptional repressor foxl1 regulates central nervous system development by suppressing shh expression in zebra fish. Molecular and cellular biology, 26(19), 7246-7257.

Nakayama, A., Nguyen, M. T. T., Chen, C. C., Opdecamp, K., Hodgkinson, C. A., & Arnheiter, H. (1998). Mutations in microphthalmia, the mouse homolog of the human deafness gene MITF, affect neuroepithelial and neural crest-derived melanocytes differently. Mechanisms of development, 70(1), 155-166.

Nakazawa, M., Cebrià, F., Mineta, K., Ikeo, K., Agata, K., & Gojobori, T. (2003). Search for the evolutionary origin of a brain: planarian brain characterized by microarray. Molecular biology and evolution, 20(5), 784-791.

Nathans, J., Thomas, D., & Hogness, D. S. (1986). Molecular genetics of human color vision: the genes encoding blue, green, and red pigments. Science, 232(4747), 193-202.

Neveu, M. M., & Jeffery, G. (2007). Chiasm formation in man is fundamentally different from that in the mouse. *Eye*, *21*(10), 1264-1270.

Nishimura, K., Kitamura, Y., Inoue, T., Umesono, Y., Yoshimoto, K., Takeuchi, K., ... & Agata, K. (2007). Identification and distribution of tryptophan hydroxylase (TPH)-positive neurons in the planarian *Dugesia japonica*. Neuroscience research, 59(1), 101-106.

Nikonov, S. S., Daniele, L. L., Zhu, X., Craft, C. M., Swaroop, A., & Pugh, E. N. (2005). Photoreceptors of Nrl−/− mice coexpress functional S-and M-cone opsins having distinct inactivation mechanisms. The Journal of general physiology, 125(3), 287-304.

Nogi, T., & Levin, M. (2005). Characterization of *innexin* gene expression and functional roles of gap-junctional communication in planarian regeneration. Developmental biology, 287(2), 314-335.

Obado, S. O., & Rout, M. P. (2012). Ciliary and nuclear transport: different places, similar routes?. Developmental cell, 22(4), 693-694.

Obojes, K., Andres, O., Kim, K. S., Däubener, W., & Schneider-Schaulies, J. (2005). Indoleamine 2, 3-dioxygenase mediates cell type-specific anti-measles virus activity of gamma interferon. Journal of virology, 79(12), 7768-7776.

Oesterhelt, D. (1998). The structure and mechanism of the family of retinal proteins from halophilic archaea. Current opinion in structural biology, 8(4), 489-500.

Oetting, W. S., Fryer, J. P., Shriram, S., & King, R. A. (2003). Oculocutaneous albinism type 1: the last 100 years. Pigment cell research, 16(3), 307-311.

Ohguro, H. (1997). High levels of rhodopsin phosphorylation in missense mutations of C-terminal region of rhodopsin. FEBS letters, 413(3), 433-435.

Okamoto, K., Takeuchi, K., & Agata, K. (2005). Neural projections in planarian brain revealed by fluorescent dye tracing. Zoological science, 22(5), 535-546.

Oliver, G., Mailhos, A., Wehr, R., Copeland, N. G., Jenkins, N. A., & Gruss, P. (1995). *Six3*, a murine homologue of the *sine oculis* gene, demarcates the most anterior border of the developing neural plate and is expressed during eye development. Development, 121(12), 4045-4055.

Orii, H., & Watanabe, K. (2007). Bone morphogenetic protein is required for dorso-ventral patterning in the planarian *Dugesia japonica*. Development, growth & differentiation, 49(4), 345-349.

Orii, H., Katayama, T., Sakurai, T., Agata, K., & Watanabe, K. (1998). Immunohistochemical detection of opsins in turbellarians. Hydrobiologia, 383(1-3), 183-187.

Ornitz, D. M., & Itoh, N. (2001). Fibroblast growth factors. Genome Biol, 2(3), 1-12.

Oxenkrug, G. F. (2010). The extended life span of *Drosophila melanogaster* eye-color (white and vermilion) mutants with impaired formation of kynurenine. Journal of neural transmission, 117(1), 23-26.

Pai, C. Y., Kuo, T. S., Jaw, T. J., Kurant, E., Chen, C. T., Bessarab, D. A., ... & Sun, Y. H. (1998). The Homothorax homeoprotein activates the nuclear localization of another homeoprotein, extradenticle, and suppresses eye development in *Drosophila*. Genes & development, 12(3), 435-446.

Palczewski, K. (2006). G protein–coupled receptor rhodopsin. Annual review of biochemistry, 75, 743.

Palmer, D. N., Fearnley, I. M., Walker, J. E., Hall, N. A., Lake, B. D., Wolfe, L. S., ... & Jolly, R. D. (1992). Mitochondrial ATP synthase subunit c storage in the ceroid-lipofuscinoses (Batten disease). American journal of medical genetics, 42(4), 561-567.

Panda, S., Provencio, I., Tu, D. C., Pires, S. S., Rollag, M. D., Castrucci, A. M., ... & Hogenesch, J. B. (2003). Melanopsin is required for non-image-forming photic responses in blind mice. Science, 301(5632), 525-527.

Panfoli, I., Calzia, D., Bianchini, P., Ravera, S., Diaspro, A., Candiano, G., ... & Pepe, I. M. (2009). Evidence for aerobic metabolism in retinal rod outer segment disks. The international journal of biochemistry & cell biology, 41(12), 2555-2565.

Parker, G. H., & Burnett, F. L. (1900). The reactions of planarians with and without eyes to light. Am. Jour. Physiol, 4, 373-385.

Pazour, G. J., Baker, S. A., Deane, J. A., Cole, D. G., Dickert, B. L., Rosenbaum, J. L., ... & Besharse, J. C. (2002). The intraflagellar transport protein, IFT88, is essential for vertebrate photoreceptor assembly and maintenance. The Journal of cell biology, 157(1), 103-114.

Peifer, M., & Wieschaus, E. (1990). Mutations in the *Drosophila* gene extradenticle affect the way specific homeo domain proteins regulate segmental identity. Genes & Development, 4(7), 1209-1223.

Peirson, S. N., Bovee-Geurts, P. H., Lupi, D., Jeffery, G., DeGrip, W. J., & Foster, R. G. (2004). Expression of the candidate circadian photopigment melanopsin (Opn4) in the mouse retinal pigment epithelium. Molecular brain research, 123(1), 132-135.

Pennisi, E. (2013). Opsins: Not Just for Eyes. Science, 339(6121), 754-755.

Pepe, I. M. (2001). Recent advances in our understanding of rhodopsin and phototransduction. Progress in retinal and eye research, 20(6), 733-759.

Pineda, D., Gonzalez, J., Callaerts, P., Ikeo, K., Gehring, W. J., & Saló, E. (2000). Searching for the prototypic eye genetic network: *sine oculis* is essential for eye regeneration in planarians. Proceedings of the National Academy of Sciences, 97(9), 4525-4529.

Pineda, D., Gonzalez, J., Marsal, M., & Saló, E. (2001). Evolutionary conservation of the initial eye genetic pathway in planarians. Belg J Zool, 131(Supplement 1), 77-82.

Pineda, D., Rossi, L., Batistoni, R., Salvetti, A., Marsal, M., Gremigni, V., ... & Saló, E. (2002). The genetic network of prototypic planarian eye regeneration is Pax6 independent. Development, 129(6), 1423-1434.

Plachetzki, D. C., Degnan, B. M., & Oakley, T. H. (2007). The origins of novel protein interactions during animal opsin evolution. PloS one, 2(10), e1054.

Plachetzki, D. C., Fong, C. R., & Oakley, T. H. (2010). The evolution of phototransduction from an ancestral cyclic nucleotide gated pathway. Proceedings of the Royal Society B: Biological Sciences, 277(1690), 1963-1969.

Plachetzki, D. C., Fong, C. R., & Oakley, T. H. (2012). Cnidocyte discharge is regulated by light and opsin-mediated phototransduction. BMC biology, 10(1), 17-26.

Pratt, T., Tian, N. M. L., Simpson, T. I., Mason, J. O., & Price, D. J. (2004). The winged helix transcription factor Foxg1 facilitates retinal ganglion cell axon crossing of the ventral midline in the mouse. Development, 131(15), 3773-3784.

Press, N. (1959). Electron microscope study of the distal portion of a planarian retinular cell. The Biological Bulletin, 117(3), 511-517.

Provencio, I., Jiang, G., Willem, J., Hayes, W. P., & Rollag, M. D. (1998). Melanopsin: An opsin in melanophores, brain, and eye. Proceedings of the National Academy of Sciences, 95(1), 340-345.

Pulvermüller, A., Gießl, A., Heck, M., Wottrich, R., Schmitt, A., Ernst, O. P., ... & Wolfrum, U. (2002). Calcium-dependent assembly of centrin-G-protein complex in photoreceptor cells. Molecular and cellular biology, 22(7), 2194-2203.

Quazi, F., & Molday, R. S. (2014). ATP-binding cassette transporter ABCA4 and chemical isomerization protect photoreceptor cells from the toxic accumulation of excess 11-cis-retinal. Proceedings of the National Academy of Sciences, 111(13), 5024-5029.

Ramirez D., M., Speiser, D. I., Sabrina Pankey, M., & Oakley, T. H. (2011a). Understanding the dermal light sense in the context of integrative photoreceptor cell biology. Visual neuroscience, 28(04), 265-279.

Ramirez, D., & Oakley, T. (2011b). Dermal expression of three phototransduction cascade genes in the cephalopod, *Octopus bimaculoides*. In Integrative and Comparative Biology 51, pp. E241-E241).

Ramon y Cajal, Santiago (1898). Estructura del quiasma óptico y teoría general de los entrecruzamientos nerviosos. Revista trimestral micrográfica, núm. 1 tomo 3.

Rauskolb, C., Peifer, M., & Wieschaus, E. (1993). extradenticle, a regulator of homeotic gene activity, is a homolog of the homeobox-containing human proto-oncogene pbx1. Cell, 74(6), 1101-1112.

Rauskolb, C., Smith, K. M., Peifer, M., & Wieschaus, E. (1995). extradenticle determines segmental identities throughout *Drosophila* development. Development, 121(11), 3663-3673.

Reddien, P. W. (2013). Specialized progenitors and regeneration. Development, 140(5), 951-957.

Reddien, P. W., Bermange, A. L., Kicza, A. M., & Alvarado, A. S. (2007). BMP signaling regulates the dorsal planarian midline and is needed for asymmetric regeneration. Development, 134(22), 4043-4051.

Reed, R. D., & Nagy, L. M. (2005). Evolutionary redeployment of a biosynthetic module: expression of eye pigment genes vermilion, cinnabar, and white in butterfly wing development. Evolution & development, 7(4), 301-311.

Resendes, K. K., Rasala, B. A., & Forbes, D. J. (2008). Centrin 2 localizes to the vertebrate nuclear pore and plays a role in mRNA and protein export. Molecular and cellular biology, 28(5), 1755-1769.

Rink, J. C., Gurley, K. A., Elliott, S. A., & Alvarado, A. S. (2009). Planarian Hh signaling regulates regeneration polarity and links Hh pathway evolution to cilia. Science, 326(5958), 1406-1410.

Rivera, A. S., Ozturk, N., Fahey, B., Plachetzki, D. C., Degnan, B. M., Sancar, A., & Oakley, T. H. (2012). Blue-light-receptive cryptochrome is expressed in a sponge eye lacking neurons and opsin. The Journal of experimental biology, 215(8), 1278-1286.

Rocks, O., Peyker, A., & Bastiaens, P. I. (2006). Spatio-temporal segregation of Ras signals: one ship, three anchors, many harbors. Current opinion in cell biology, 18(4), 351-357.

Romero, Rafael and Bueno, David, (2001). Disto-proximal regional determination and intercalary regeneration in planarians, revealed by retinoic acid induced disruption of regeneration. International Journal of Developmental Biology, 45(4), 669-674.

Rossi, L., Batistoni, R., Salvetti, A., Deri, P., Bernini, F., Andreoli, I., ... & Gremigni, V. (2001). Molecular aspects of cell proliferation and neurogenesis in planrians. Belg J Zool, 131(Suppl 1), 83-87.

Ruth, T. Y., Chiang, M. Y., Tanabe, T., Kobayashi, M., Yasuda, K., Evans, R. M., & Umesono, K. (2000). The orphan nuclear receptor Tlx regulates Pax2 and is essential for vision. Proceedings of the National Academy of Sciences, 97(6), 2621-2625.

Sakai, F., Agata, K., Orii, H., & Watanabe, K. (2000). Organization and regeneration ability of spontaneous supernumerary eyes in planarians-eye regeneration field and pathway selection by optic nerves. Zoological science, 17(3), 375-381.

Salina, D., Enarson, P., Rattner, J. B., & Burke, B. (2003). Nup358 integrates nuclear envelope breakdown with kinetochore assembly. The Journal of cell biology, 162(6), 991-1001.

Satisbury, J. L. (1995). Centrin, centrosomes, and mitotic spindle poles. Current opinion in cell biology, 7(1), 39-45.

Salisbury, J. L., Suino, K. M., Busby, R., & Springett, M. (2002). Centrin-2 is required for centriole duplication in mammalian cells. Current Biology, 12(15), 1287-1292.

Saló, E., Abril, J. F., Adell, T., Cebricá, F., Eckelt, K., Fernández-Taboada, E., ... & Rodríguez-Esteban, G. (2009). Planarian regeneration: achievements and future directions after 20 years of research. International Journal of Developmental Biology, 53(8), 1317.

Saló, E. (2006). The power of regeneration and the stem-cell kingdom: freshwater planarians (Platyhelminthes). Bioessays, 28(5), 546-559.

Saló, E., Pineda, D., Marsal, M., Gonzalez, J., Gremigni, V., & Batistoni, R. (2002). Genetic network of the eye in Platyhelminthes: expression and functional analysis of some players during planarian regeneration. Gene, 287(1), 67-74.

Samardzija, M., Wenzel, A., Thiersch, M., Frigg, R., Remé, C., & Grimm, C. (2006). Caspase-1 ablation protects photoreceptors in a model of autosomal dominant retinitis pigmentosa. Investigative ophthalmology & visual science, 47(12), 5181-5190.

Sancar, A. (2000). Cryptochrome: the second photoactive pigment in the eye and its role in circadian photoreception. Annual review of biochemistry, 69(1), 31-67.

Sánchez-Arrones, L., Nieto-Lopez, F., Sánchez-Camacho, C., Carreres, M. I., Herrera, E., Okada, A., & Bovolenta, P. (2013). Shh/Boc Signaling Is Required for Sustained Generation of Ipsilateral Projecting Ganglion Cells in the Mouse Retina. The Journal of Neuroscience, 33(20), 8596-8607.

Sandmann, T., Vogg, M. C., Owlarn, S., Boutros, M., & Bartscherer, K. (2011). The head-regeneration transcriptome of the planarian *Schmidtea mediterranea*. Genome Biol, 12(8), R76.

Sanges, D., Romo, N., Simonte, G., Di Vicino, U., Tahoces, A. D., Fernández, E., & Cosma, M. P. (2013). Wnt/β-Catenin Signaling Triggers Neuron Reprogramming and Regeneration in the Mouse Retina. Cell reports, 4(2), 271-286.

Schiebel, E., & Bornens, M. (1995). In search of a function for centrins. Trends in cell biology, 5(5), 197-201.

Schnitzler, C. E., Pang, K., Powers, M. L., Reitzel, A. M., Ryan, J. F., Simmons, D., ... & Baxevanis, A. D. (2012). Genomic organization, evolution, and expression of photoprotein and opsin genes in *Mnemiopsis leidyi*: a new view of ctenophore photocytes. BMC biology, 10(1), 107.

Schon, E. A., Santra, S., Pallotti, F., & Girvin, M. E. (2001). Pathogenesis of primary defects in mitochondrial ATP synthesis. In Seminars in cell & developmental biology (Vol. 12, No. 6, pp. 441-448). Academic Press.

Schuff, M., Rössner, A., Wacker, S. A., Donow, C., Gessert, S., & Knöchel, W. (2007). FoxN3 is required for craniofacial and eye development of *Xenopus laevis*. Developmental Dynamics, 236(1), 226-239.

Scimone, M. L., Lapan, S. W., & Reddien, P. W. (2014). A forkhead transcription factor is wound-induced at the planarian midline and required for anterior pole regeneration. PLoS genetics, 10(1), e1003999.

Searles, L. L., Ruth, R. S., Pret, A. M., Fridell, R. A., & Ali, A. J. (1990). Structure and transcription of the *Drosophila melanogaster* vermilion gene and several mutant alleles. Molecular and cellular biology, 10(4), 1423-1431.

Sedmak, T., & Wolfrum, U. (2010). Intraflagellar transport molecules in ciliary and nonciliary cells of the retina. The Journal of cell biology, 189(1), 171-186.

Sekaran, S., Lupi, D., Jones, S. L., Sheely, C. J., Hattar, S., Yau, K. W., ... & Hankins, M. W. (2005). Melanopsin-dependent photoreception provides earliest light detection in the mammalian retina. Current biology, 15(12), 1099-1107.

Senthilan, P. R., Piepenbrock, D., Ovezmyradov, G., Nadrowski, B., Bechstedt, S., Pauls, S., ... & Göpfert, M. C. (2012). *Drosophila* Auditory Organ Genes and Genetic Hearing Defects. Cell, 150(5), 1042-1054.

Sgarbi, G., Baracca, A., Lenaz, G., Valentino, L., Carelli, V., & Solaini, G. (2006). Inefficient coupling between proton transport and ATP synthesis may be the pathogenic mechanism for NARP and Leigh syndrome resulting from the T8993G mutation in mtDNA. Biochem. J, 395, 493-500.

Shapard, P. B. (1960). A physiological study of the vermilion eye color mutants of *Drosophila melanogaster*. Genetics, 45(4), 359.

Sheehan, D., Meade, G., Foley, V., & Dowd, C. (2001). Structure, function and evolution of glutathione transferases: implications for classification of non-mammalian members of an ancient enzyme superfamily. Biochem. J, 360, 1-16.

Shen, W. L., Kwon, Y., Adegbola, A. A., Luo, J., Chess, A., & Montell, C. (2011). Function of rhodopsin in temperature discrimination in *Drosophila*. Science, 331(6022), 1333-1336.

Shibata, M., Yamashita, H., Uchihashi, T., Kandori, H., & Ando, T. (2010). High-speed atomic force microscopy shows dynamic molecular processes in photoactivated bacteriorhodopsin. Nature nanotechnology, 5(3), 208-212.

Shintani, K., Shechtman, D. L., & Gurwood, A. S. (2009). Review and update: current treatment trends for patients with retinitis pigmentosa. Optometry-Journal of the American Optometric Association, 80(7), 384-401.

Silverman, R. H. (2007). A scientific journey through the 2-5A/RNase L system. Cytokine & growth factor reviews, 18(5), 381-388.

Simeone, A., Acampora, D., Mallamaci, A., Stornaiuolo, A., D'Apice, M. R., Nigro, V., & Boncinelli, E. (1993). A vertebrate gene related to orthodenticle contains a homeodomain of the bicoid class and demarcates anterior neuroectoderm in the gastrulating mouse embryo. The EMBO Journal, 12(7), 2735.

Simon, M. A., Bowtell, D. D., Dodson, G. S., Laverty, T. R., & Rubin, G. M. (1991). Ras1 and a putative guanine nucleotide exchange factor perform crucial steps in signaling by the sevenless protein tyrosine kinase. Cell, 67(4), 701-716.

Simmons, J. L., Pierce, C. J., & Boyle, G. M. (2013). Evidence for an Alternatively Spliced MITF Exon 2 Variant. Journal of Investigative Dermatology.

Smith, T. S., Spitzbarth, B., Li, J., Dugger, D. R., Stern-Schneider, G., Sehn, E., ... & Smith, W. C. (2013). Light-dependent phosphorylation of Bardet–Biedl syndrome 5 in photoreceptor cells modulates its interaction with arrestin1. Cellular and Molecular Life Sciences, 70(23), 4603-4616.

Smith G. N. JR, and Greenberg M.J. (1973). Chemical control of the evisceration process in *Thyone briareus*. Biol. Bull., 144: 421-436.

Sopott-Ehlers, B. (1991). Comparative morphology of photoreceptors in free-living plathelminths—a survey. Hydrobiologia, 227(1), 231-239.

Sparrow, J. R., Gregory-Roberts, E., Yamamoto, K., Blonska, A., Ghosh, S. K., Ueda, K., & Zhou, J. (2012). The bisretinoids of retinal pigment epithelium. Progress in retinal and eye research, 31(2), 121-135.

Spudich, J. L. (2006). The multitalented microbial sensory rhodopsins. Trends in microbiology, 14(11), 480-487.

Stabell, M., Eskeland, R., Bjørkmo, M., Larsson, J., Aalen, R. B., Imhof, A., & Lambertsson, A. (2006). The *Drosophila G9a* gene encodes a multi-catalytic histone methyltransferase required for normal development. Nucleic acids research, 34(16), 4609-4621.

Staniszewska, M. M., & Nagaraj, R. H. (2005). 3-Hydroxykynurenine-mediated modification of human lens proteins structure determination of a major modification using a monoclonal antibody. Journal of Biological Chemistry, 280(23), 22154-22164.

Stenflo, J., Stenberg, Y., & Muranyi, A. (2000). Calcium-binding EGF-like modules in coagulation proteinases: function of the calcium ion in module interactions. Biochimica et Biophysica Acta (BBA)-Protein Structure and Molecular Enzymology, 1477(1), 51-63.

Stevenson, C. G., & Beane, W. S. (2010). A low percent ethanol method for immobilizing planarians. PloS one, 5(12), e15310.

Strauss, O. (2005). The retinal pigment epithelium in visual function. Physiological reviews, 85(3), 845-881.

Sullivan, D. T., & Sullivan, M. C. (1975). Transport defects as the physiological basis for eye color mutants of *Drosophila melanogaster*. Biochemical genetics, 13(9-10), 603-613.

Sullivan, D. T., Bell, L. A., Paton, D. R., & Sullivan, M. C. (1980). Genetic and functional analysis of tryptophan transport in Malpighian tubules of *Drosophila*. Biochemical genetics, 18(11-12), 1109-1130.

Summers, K. M., Howells, A. J., & Pyliotis, N. A. (1982). Biology of eye pigmentation in insects. Advances in insect physiology, 16, 119-166.

Sun, H., Gilbert, D. J., Copeland, N. G., Jenkins, N. A., & Nathans, J. (1997). Peropsin, a novel visual pigment-like protein located in the apical microvilli of the retinal pigment epithelium. Proceedings of the National Academy of Sciences, 94(18), 9893-9898.

Sun, H., & Nathans, J. (2000). ABCR: rod photoreceptor-specific ABC transporter responsible for Stargardt disease. Methods in enzymology, 315, 879.

Sutherland, D., Samakovlis, C., & Krasnow, M. A. (1996). Branchless encodes a *Drosophila* FGF homolog that controls tracheal cell migration and the pattern of branching. Cell, 87(6), 1091-1101.

Swoboda, P., Adler, H. T., & Thomas, J. H. (2000). The RFX-type transcription factor DAF-19 regulates sensory neuron cilium formation in *C. elegans*. Molecular cell, 5(3), 411-421.

Takahashi, K., & Yamanaka, S. (2006). Induction of pluripotent stem cells from mouse embryonic and adult fibroblast cultures by defined factors. cell, 126(4), 663-676.

Takai, Y., Sasaki, T., & Matozaki, T. (2001). Small GTP-binding proteins. Physiological reviews, 81(1), 153-208.

Tamamaki, N. (1990). Evidence for the phagocytotic removal of photoreceptive membrane by pigment cells in the eye of the planarian, *Dugesia japonica*. Zoological science, 7(3), 385-393.

Tan, D. P., Nonaka, K., Nuckolls, G. H., Liu, Y. H., Maxson, R. E., Slavkin, H. C., & Shum, L. (2002). YY1 activates Msx2 gene independent of bone morphogenetic protein signaling. Nucleic acids research, 30(5), 1213-1223.

Tarttelin, E. E., Bellingham, J., Bibb, L. C., Foster, R. G., Hankins, M. W., Gregory-Evans, K., ... & Lucas, R. J. (2003). Expression of opsin genes early in ocular development of humans and mice. Experimental eye research, 76(3), 393-396.

Tearle, R. (1991). Tissue specific effects of ommochrome pathway mutations in *Drosophila melanogaster*. Genetical research, 57(03), 257-266.

Teixeira, A. M., & Borges, G. F. (2012). Creatine Kinase: Structure and Function. Brazilian Journal of Biomotricity, 6(2), 53-65.

Terakita, A., Kawano-Yamashita, E., & Koyanagi, M. (2012). Evolution and diversity of opsins. Wiley Interdisciplinary Reviews: Membrane Transport and Signaling, 1(1), 104-111.

Tomarev, S. I., Chung, S., & Piatigorsky, J. (1995). Glutathione S-transferase and S-crystallins of cephalopods: evolution from active enzyme to lens-refractive proteins. Journal of molecular evolution, 41(6), 1048-1056.

Torii, M., Kojima, D., Okano, T., Nakamura, A., Terakita, A., Shichida, Y., ... & Fukada, Y. (2007). Two isoforms of chicken melanopsins show blue light sensitivity. FEBS letters, 581(27), 5327-5331.

Toyama, B. H., Savas, J. N., Park, S. K., Harris, M. S., Ingolia, N. T., Yates III, J. R., & Hetzer, M. W. (2013). Identification of long-lived proteins reveals exceptional stability of essential cellular structures. Cell, 154(5), 971-982.

Toyoda, Y., Hagiya, Y., Adachi, T., Hoshijima, K., Kuo, M. T., & Ishikawa, T. (2008). MRP class of human ATP binding cassette (ABC) transporters: historical background and new research directions. Xenobiotica, 38(7-8), 833-862.

Tsukamoto, H., & Terakita, A. (2010). Diversity and functional properties of bistable pigments. Photochemical & Photobiological Sciences, 9(11), 1435-1443.

Ullrich-Lüter, E. M., Dupont, S., Arboleda, E., Hausen, H., & Arnone, M. I. (2011). Unique system of photoreceptors in sea urchin tube feet. Proceedings of the National Academy of Sciences, 108(20), 8367-8372.

Umesono, Y., Watanabe, K., & Agata, K. (1999). Distinct structural domains in the planarian brain defined by the expression of evolutionarily conserved homeobox genes. Development genes and evolution, 209(1), 31-39.

van Wolfswinkel, J. C., Wagner, D. E., & Reddien, P. W. (2014). Single-Cell analysis reveals functionally distinct classes within the planarian stem cell compartment. Cell stem cell, 15(3), 326-339.

Vella, P., Barozzi, I., Cuomo, A., Bonaldi, T., & Pasini, D. (2012). Yin Yang 1 extends the Myc-related transcription factors network in embryonic stem cells. Nucleic acids research, 40(8), 3403-3418.

Viaud, G. (1948). VIII.-Recherches expérimentales sur le phototropisme des planaires. Le signe primaire positif et la polarité tropistique. L'année psychologique, 49(1), 175-221.

Vogg, M. C., Owlarn, S., Rico, Y. A. P., Xie, J., Suzuki, Y., Gentile, L., ... & Bartscherer, K. (2014). Stem cell-dependent formation of a functional anterior regeneration pole in planarians requires Zic and Forkhead transcription factors. Developmental biology, 390(2), 136-148.

Waardenburg, P. J. (1951). A new syndrome combining developmental anomalies of the eyelids, eyebrows and noseroot with pigmentary anomalies of the iris and head hair and with congenital deafness; Dystopia canthi medialis et punctorum lacrimalium lateroversa, hyperplasia supercilii medialis et radicis nasi, heterochromia iridum totaliis sive partialis, albinismus circumscriptus (leucismus, polioss) et surditas congenita (surdimutitas). American journal of human genetics, 3(3), 195.

Wald, G. (1968). The molecular basis of visual excitation. Nature, 219, 800-807.

Wallimann, T., Wyss, M., Brdiczka, D., Nicolay, K., & Eppenberger, H. M. (1992). Intracellular compartmentation, structure and function of creatine kinase isoenzymes in tissues with high and fluctuating energy demands: the'phosphocreatine circuit'for cellular energy homeostasis. Biochemical Journal, 281(Pt 1), 21-40.

Wallimann, T., & Hemmer, W. (1994). Creatine kinase in non-muscle tissues and cells. In Cellular Bioenergetics: Role of Coupled Creatine Kinases (pp. 193-220). Springer US.

Wallimann, T., Tokarska-Schlattner, M., & Schlattner, U. (2011). The creatine kinase system and pleiotropic effects of creatine. Amino acids, 40(5), 1271-1296.

Walther, C., & Gruss, P. (1991). Pax-6, a murine paired box gene, is expressed in the developing CNS. Development, 113(4), 1435-1449.

Weese-Mayer, D. E., Berry-Kravis, E. M., Zhou, L., Maher, B. S., Curran, M. E., Silvestri, J. M., & Marazita, M. L. (2004). Sudden infant death syndrome: case-control frequency differences at genes pertinent to early autonomic nervous system embryologic development. Pediatric research, 56(3), 391-395.

Wienisch, M., & Klingauf, J. (2006). Vesicular proteins exocytosed and subsequently retrieved by compensatory endocytosis are nonidentical. Nature neuroscience, 9(8), 1019-1027.

Wicks, N. L., Chan, J. W., Najera, J. A., Ciriello, J. M., & Oancea, E. (2011). UVA phototransduction drives early melanin synthesis in human melanocytes. Current Biology, 21(22), 1906-1911.

Winter, E., & Ponting, C. P. (2002). TRAM, LAG1 and CLN8: members of a novel family of lipid-sensing domains?. Trends in biochemical sciences, 27(8), 381-383.

Wirleitner, B., Neurauter, G., Schrocksnadel, K., Frick, B., & Fuchs, D. (2003). Interferon-γ-induced conversion of tryptophan: immunologic and neuropsychiatric aspects. Current medicinal chemistry, 10(16), 1581-1591.

Whitmore, D., Foulkes, N. S., & Sassone-Corsi, P. (2000). Light acts directly on organs and cells in culture to set the vertebrate circadian clock. Nature, 404(6773), 87-91.

Wolfrum, U., & Salisbury, J. L. (1998). Expression of centrin isoforms in the mammalian retina. Experimental cell research, 242(1), 10-17.

Wolfrum, U., & Schmitt, A. (2000). Rhodopsin transport in the membrane of the connecting cilium of mammalian photoreceptor cells. Cell motility and the cytoskeleton, 46(2), 95-107.

Wolken, J. J. (1988). Photobehavior of marine invertebrates: extraocular photoreception. Comparative Biochemistry and Physiology Part C: Comparative Pharmacology, 91(1), 145-149.

Wouters, M. A., Rigoutsos, I., Chu, C. K., Feng, L. L., Sparrow, D. B., & Dunwoodie, S. L. (2005). Evolution of distinct EGF domains with specific functions. Protein science, 14(4), 1091-1103.

Xuan, S., Baptista, C. A., Balas, G., Tao, W., Soares, V. C., & Lai, E. (1995). Winged helix transcription factor BF-1 is essential for the development of the cerebral hemispheres. Neuron, 14(6), 1141-1152.

Yang, L., & Baker, N. E. (2001). Role of the EGFR/Ras/Raf pathway in specification of photoreceptor cells in the *Drosophila* retina. Development, 128(7), 1183-1191.

Yang, T., Li, X., Huang, Q., Li, L., Chai, Y., Sun, L., ... & Wu, H. (2013). Double heterozygous mutations of MITF and PAX3 result in Waardenburg syndrome with increased penetrance in pigmentary defects. Clinical genetics, 83(1), 78-82.

Yildiz, O., & Khanna, H. (2012). Ciliary signaling cascades in photoreceptors. Vision research, 75, 112-116.

Yokoyama, S., Zhang, H., Radlwimmer, F. B., & Blow, N. S. (1999). Adaptive evolution of color vision of the Comoran coelacanth (*Latimeria chalumnae*). Proceedings of the National Academy of Sciences, 96(11), 6279-6284.

Yoshida, M., & Ohtsuki, H. (1966). Compound ocellus of a starfish: its function. *Science*, *153*(3732), 197-198.

Yoshimura, T., & Ebihara, S. (1996). Spectral sensitivity of photoreceptors mediating phase-shifts of circadian rhythms in retinally degenerate CBA/J (rd/rd) and normal CBA/N (+/+) mice. Journal of Comparative Physiology A, 178(6), 797-802.

Young, R. W. (1984). Cell death during differentiation of the retina in the mouse. Journal of Comparative Neurology, 229(3), 362-373.

Zamanian, M., Kimber, M. J., McVeigh, P., Carlson, S. A., Maule, A. G., & Day, T. A. (2011). The repertoire of G protein-coupled receptors in the human parasite *Schistosoma mansoni* and the model organism *Schmidtea mediterranea*. BMC genomics, 12(1), 596.

Zayas, R. M., Hernández, A., Habermann, B., Wang, Y., Stary, J. M., & Newmark, P. A. (2005). The planarian *Schmidtea mediterranea* as a model for epigenetic germ cell specification: analysis of ESTs from the hermaphroditic strain. Proceedings of the National Academy of Sciences, 102(51), 18491-18496.

Zhang, C. L., Zou, Y., Ruth, T. Y., Gage, F. H., & Evans, R. M. (2006). Nuclear receptor TLX prevents retinal dystrophy and recruits the corepressor atrophin1. Genes & development, 20(10), 1308-1320.

Zoltowski, B. D., Vaidya, A. T., Top, D., Widom, J., Young, M. W., & Crane, B. R. (2011). Structure of full-length *Drosophila* cryptochrome. Nature, 480(7377), 396-399.

7. APPENDIX

7.1 DNA SEQUENCES

Smed-rhodopsin1

>Contig_Planarian_90_17768
TGATCCCAAAACTGAAAATATCAATATAAATTGTGCAATTAGTGAAATCCTCGGATTTCATCGGGATATATTTTCCCATTTGTTGGCTTTATCGGTG
TTGTAAGCAATATTTATATTTGTTATATCTTTCTTTTCAGATACCCAAAACGAACAAGACAGACGATTTTGTTGTCATACTTGGCGTTAGCGGACCT
TTTTGAACATTCTAGCATTCGGTTGGTTGTGGATATTTCCTGCTAAAGGATTACCATATATGACTAATGGGAATATTTACTTTTTTATTATAAATCA
ATCAAGCGTTTWCTGTACAGTTTTTCGAACTTTGTACTTTTTTACCTCAACTGTCACATTTGCTATTTTTCTTTTAGTTTGCCTTGACAGATGTTTT
GCCATTTATTTCCCATTTAGATCGTTGAGAATCACAAACAAAATGACATTCTTAACCTGCTCGATAGTATTTCTTTTTTGTCTTCCTCTAACGGTTT
TGTACACGGGTTTTATTCGAACAATTTACCAACATCCGTATTTTTTCTGTACAATCGGAAACAA

Smed-rhodopsin2

>Contig_Planarian_90_9069
ATTTGGGGAAGTTTTTTTNTTCGGGCAGTGGTTCTGTGTAGAAAATCAATGTCTCATATATCGTCATATATCTATTTGGCGACTTTAGCTATTTTTG
ATGAACTGATTTTACTCTGTGGTCTTTTCAGAAAATGGATCGAGCATGTGACAGACTGGTCATTGGAGAATCACTCGATCAGTTTCTGTAAATTATT
CCAAGTCATTGGTGTTTCGAGTAGTTTTATTTCCGTGTGGCTAATCGTAACTCTAACTGTCGAACGAGTGTTGATCATTAAAAGACCATTTGAAGCT
TCAAAATATGCAAAAGCTAGCAGAGCCAAATATATAATAGTATCCTTGATAATTATCAGCTTTACAACCAGCTGTCATTTCTTTGAAACTGTAACAT
TACAAAATTTAAATCATAAAAACGTCAATACAAACTTTTCCTCAGACAAAGGATCGAATTCAATCAAAAAATGTCAATTCAAAACGGAATATACAAA
ATTTACGAATAGCTTGGTTTTTCATAGATGGAGCATTCTACAGTTGGATACCATTATTTTGTTAATTATTAATAATCTAATCATACTTTCCGAAATT
TACAAAGTCCCGACAATATCCACAATTCAATGATCAACACAAATCACGATGAAAATAAAACCCTTGGAACCTCTATTGTCAGAACCCAATTACCAAG
AAGAATGAAAAGAATCTT

Smed-rhodopsin4

>Contig_Planarian_90_18503
TCWACTACTTCTGTTCACTCTCGTAAGCTTCATTTGTATGTCCACTTGTGGTTTGATTCTTGGTGGTTTCTACGACTTGTTTATCGTCTTCAGGATC
CAGTTGAGACATTGAACTTTCTCTTTCACTCTGATATTTACTCGGTTTCGTTGCYGATGCTGCACTTGTAGTGTCCCTTTCTTTTGGTTTTGGTGGA
CAGCAACAAATCAAACATGGAAATTTCTTTTCCAGCTGAATTCGAAATTTTGGATGATTTATTGCGTATATAAATGGGTTGTACATAGCTGAGGTCT
TAGCAAAGAGTACCGGCAATTCTGCAGTGTAATGGATTCAGATGATCTCTACGCCCTGTGAGAGCCATAAGGGCAATTATTGCATATGGTGTCCATG
ATAACATATATAAAAGACAATTATGACAGAAATCTTTAGCAGCTTGAACATCAGCCTTTTTTGCTACCCGTTTTCATGGAAGTTGGATGAGATGCAT
TCATCTTTTGACG

Smed-rhodopsin5

>Contig_Planarian_90_1193
TTTCGGKGCCGTTAGACGGTCTTATCGAAATCTATATAAATCTTATATGGATCAACTTTACGGAATTCTATTAGGAATTTCAGGAATTTTGGGTGCA
AAACTCTACTATGATTTACGTAATACCTTGCAAAACAACCAGATCAACGAAGATTGCCGGAAAATTCACCGACATTTCATCTATTCCAGCTTAGGAG
TTGTCCTCGGTGCAATCCTTGCTGCCCCTTCTCGATTCGTTGGAAGATGGCTTTTCGGAGATTTCTTGTGCCAATTTTATGCCTTTGAAGGCTTTGT
TTTTGGTATTTCTAATATTAATATTATCGTTGTTATTGCCATGGAACGATACTATTCTACAAGAAAGATTCAATTACCTTGGAATGTTAATCAGATT
CTTTATGTTTGCTGGATAGTGGGACTTTTTTGGTCATTACTGCCATTATTTGGATTTGGCAGCTATGCGTTGGAACTCCATCAAACGTCTTGCACGA
TAAAGATATTTGACTTGTCACATAATCATCAATTGTATATGGGAGGTCTCATTATTGTCGGATTTTTATTGCCGGTTTCTATTGGTATAATGTTTCA
TTTGTTTACACTGAGTCTAGAGACTAGAAAAACGGAGAAAATTAATTCGTTTGAAAAAATAATGAATAACGTTTCACGTAAACTTTTTTTGATGGAT
CTATTTTCATGGTGTGGATATTTGGTGTTGTGTTTGATTGGATTGGTTTCCAATCAAGATTCTCCCTGGGCGATATTGTTTTCCTCCGTGTCACCTT
TACTTACAAAATTTGGAATCGCACTTTTACCAATGTTATATTGGTCTGTGAAATAATGAAAATTCGTTGAATTTTCAATTTGCGCACAAATTTATGA
TTACTGCATCTTATTGAATTAATTAATAATATAATTCAGTATTTAATTTAGATTTTTTCGTAATGTTTTTCATTGGTCATGGAGATGGTTAAATATA
TCTGGAATTTACCAGACCTCTGAACCTGATCGTGGTTCACTAATTTTATATGTGAATAGTGTTTAATTCATCGAATTTAAATTTTACAATATCATTT
AATTTTAATCGTCAGTATGATGTTTATTACAATCTTCGACTTTGCATGTTATTTATTCCATTTAGTTTTCTTTGATTATACAACAAATATTATTTGG
TCTCTAATCTCCGTTAACTATTTTTTTAAAATTTCATCTCAGTTTTTATCTTTTCAACACAAATAAATAATATAAAATTTAGAATTTACGAGAGATG
TACTTTTGTATTTATTACGGTTATACAAAAACATGTAAAAATCAATATTTTTTCTGAGGAAAAGCAGAGTCATGTAATAAATCGAAAGATAACGAAC
AGTGTGTACAA

Smed-rhodopsin7

>Contig_Planarian_90_4663
GAATTAGCGTAAAACTGGGAGAAATCATTTACAAATGAATTCTAGTAATGCCAACAGCAGCAACTTGGTCGTTGACTACGGTTTGGTAACCTTCATT
AGAAATTGCAGCTCCTGTTTGGAAAAGAAAAACGGTATGCCAATCACCTATACTTATATTACATTCGTCTTGGTCGTTACTAATATTCTCGGAAACA
TGTTCGCTGTGATCATTCTCTCCGATAGTGTTTGGAACAAGTCCGTCCTAACTACAATTCTTAAAGCAATTTCATACTTTGAAATCCTTTTCAATTT
GTTGAATTTCATCAATAACATATGCCAACTAACAGAGCCGTTGAAACCTTTTCAGTATTTTGGATTAAAAGCGTTAGCAACTGTTGAGATTCTTCTT
TTGATTTGTGATTCCTTGATGATTGGATTCCAAATGGCACGAAACTGGTCCGTGACGATTCTTGCACTATTCCGGTACGATATGGTTTGTAGGTCGA
AAACCGTGAGACGACTAAATAACCAATCGAATTTCTTCTCCAACGAAAATTTACCGAAAATATTCACTTTTCTCATGATTTTCTGTATTGGTTTAGC
TTTGCCACGAATGTTTGAAGTTACTCCCCAGATTTGCATAAACACAGCAGTCATATGTCATTATGCCGATTTCCTGAGTGTAAGGAAAGTATTCCAG
TATGGCTATCTAGGAGTTGTAATGTTTATTTTTCAATCTGGTGGCCCGATTATTATTACAAGCTGTGTTAGTTTAATGCTTATTAGAAAGATTCAAT
ATCGTCATGCGATACGTAAAAGACAAACGAACGCAACCTCAAACCGATTCCAGAGATCACAAAGAAACCCAGGAACACTTGTAATGGCTGTTTGTAT
AACCTTTATGGTTCTTGAATTTCCATCATTCTTTAGCAAACTAGCGTTCTATGCATTTGACAATAACAATATTCACATTGGTATTATTCCGAATCTT
CTCATTTATCTCGACTCTTGCTTGAATTTATTCATTTATTTGGCGTCAAATAAAACCTTCCGGAAAACAAGTCTTAATAGGATTCGTTGTGCCAAGT
CTTTCGAATCTTGGGAAATTCAAACAACAATGACAGTAAGAGTCAACAATAGCGAGAAAAACGATAAAAATGAGGAATTTTAACCATAACATTTTGT
ATTATTGATTTTTAGAAATCTTCGGAAATTTTGGTGCTTTTCCTTGWWTTTTCTTGGAAAAATACTTATTGCATGCATTTTGATATTAAATCAAACT
GTCTGCCAGTGGAGGATGRAATGTTCAACACTGTTGGATCCGTRGATGACTG

Smed-rhodopsin8

>Contig_Planarian_90_26968
GGAAATTGATTTTCAGAATGTAAAGAATGAACACTAAAGAAAATGTTGWCTTTTTTTGAACCATTTAATGCTTCAATTTCATCAAATAAACTCGGCA
TTTCTTCCCAAATCATAGCTAAATGCATYAAAACCTTGCTTTTGTCTACAATAATTGCCATCGCAATATTTGGAAATGGTCTCGTAATAGTCAGTGT
ACTTCGGTTTCATAAATTACGACGAATTATTACCAATCGGTTCGTTGTGTCGCTTGCGCTGGCTGACTTATTGGTTTCTTGTTGCGTAATGACTTTC
AGCGCAAGCATGGTTGCGTCGGATGGACTGTGGCTGTTCGGACCGTTTCTCTGTGATCTATTTAACGCCAATGATGTTTTATTTTCCACCGCCTCAA
TTGCTCATTTGGCCAGCATAAGTATGGATAGGTACATTTCCATTAAAATGCCATTTCAATACAATCAAATTATGACAAGTCGAAAATCTATCTTAAT
GCTCATCGGTTGTTGGATTTACGCTCTTGTCGT

Smed-rhodopsin9

>Contig_Planarian_90_11411
TAAGTAAAAACCAAACTTCATAAACATTTAAACAAAAATAAATACTTTCATTCTGATGAATATTAATTTACAAATTAAAACACTAATAAATTAATTT
ATACTGTTCAAATTGGTTTTTATTACCCTTTTTTCTAAAATTATGCAGATTTCTCCTCGGCCTGTTGATAAAATAGAGATTTGTCGAAAAATGAGTT
TTCTTACGACATTTCGGGTTGAATTTTTGATATATACTTTTTTAAATCACAGACCAACTTTTCTTTGTAGAACGAATCACAAATTAATATAACAATC
GGATTAAAACAACAATAACTAATGGCTAACCAATGCAACAAATTCGGCAGCCCCGGGTACAGTTTTAAATATGTATACGCCACTGGGAAAATGTCAA
TGACATTCCAAATATGAATCGGGAGCCAGCACAAAATGAAGTTTAACATTAAAACAATAGCAAACTGCAYGACTTTGGTTGATTTTTTCGTTAAGCC
CGTCAGAAGATTTTCCGTTGACGTTGAAGGGATTTCCGTTTTGGCCAAATTCCTCGTATTTACTTTTCAACAAATAGCAAATGTGGCTGTATGAAAA
ACAAATAATTCCGAACGGTATAGTAAAGTGCACCATGTTGACATARATTTGATAGGCTATTCTCCAGTTGACCGTGAAAATATCTGGTTTAATCAAC
CAAGGCTCACCGCAATATTTCTTTCTGTAGTAATCCTCGAATATCAAATTGACGAATGCGGCCGGAATCGTAGAGATGATGGAGATTAGCCATGAAA
TCCCGATGTAGAGCCTGTCGAGGCGTTTGATATGGTTGAAGAAGCTATTATATCGCGTTACTTGCCACCGACAAATACTCAGCGCCGCAGTTATATG
GATGTTACTACTTATC

Smed-rhodopsin10

>Contig_Planarian_90_20395
TAGTCTTGCTATGGCCGATGTACTCGTGGCCTTGTTTGTTATGCCTTTCAATCTTACTCAAATWGTAACCAACGGATTTTGGCCGTTTGGTTCTCTT
ATGTGCGAAATCTACAATTCYAATGATGTATTTCTGAGTACTGCAAGCATAATTCATCTATGCTGTATCAGTATGGACCGTCATTTTGCCATCATTC
ATCCTCTCACATACGACAGCATTATGACGAAAACTCGAGTGGGTTTGATGCTTCTCGGTTGTTGGACCTCTTCGATTCTTATATCATACATTCCAAT
TTATTCTGGTCTGTATACGACAAATGAAAATTTAAATTTGTTAACGATTCTGTAGCGAAATCTGCAACTTCAAAGTCAACCATATCTATGCTATTGT
TTCCTCTTCGTG TCCTTCT

Smed-melanopsin1

>Contig_Planarian_90_11401
TTTCGATTTGGTTTGTTCAGATTTTTTAATATGTACAATTGGATTCCCGTTTCTTATGCTGAGTTCATTTTATCAGAGCTGGATTTTTGATATTTCG
GGTTGTTACGTTTATGNTTTTTCCATGTCTATTACTGGAATGCACTCCATCTTCATCCTTTTTGTAATTGCCGTTGAGCGGTTCAATGCTGTATTCT
ATCCCTTACAAACTGTCAAAACTGTCACAGTTAAAAGATCTATTTATTTTGTCATTTGCTGTTGGACGCTTGGAGTGATTATCTCCATTCCTCCTCT
AGTTGGTTGGAATCGATATGTTTTGGAAGGTCTACAGATATCTTGCAGTTTTGATATGTTTGACACTTCATGGCAAAGCAAAAGCTACACCATGTTG
CTTATCGGAACGTTTCTCCTGATTTTGACAGCAATTATCATCTGCTACGTAAAAATATTTTTCAAAGTCCGGGATCAGATAAAGGAAATGAGAATTG
TCTATACAAAATCATTCAATAATTTGCAAAGAATTAAAGAGAGCAAAGTAGAAAGAAAATTAATATACATGGGATTCAATGTGACATTATTCTTTGT
TTTATCATGGGGACCATATGCAATGGTCACAATTTTGGCTCTTTGTAATGTGCTGACCGAGAAAGGCTCTGTGCTAATTGTAGCCATCCCGGCTTAT
TTCGCAAAATCATTCACCATTTGTAATCCCGTCATTTACATTTTAAACTATCCGCAATTCAAAAGAGAACTTTATAAGTTATTATGTGTTTTGAAGC
AGATACCCTGTCAAAAAGAAACAAAGTCAAA

Smed-melanopsin2

>F6AJIXP02JW3BU
TACGAGAGCATAAGGACCCCAAGACAATACAAATGCTAATGTAATGTTACATCCCATCCATATCAATTTATTCTCTCTTTGTCTTTCTCGTTCTGCT
AATAAATCTCTCGAGTCTTTGATCATAACACGCATTGAGGTAGCTTGTCTTTGAACTTTTAAGAATAAAGCAAGATAACAAAAGATAATAATTAAAA
GAACGACAAGGAATATTCCAATTAGGAATACGATATAGCTTTTACTTCTCCAGGATCCATCAAACATGTCATAGCTACACGAGATATGTAAACCTTC
TAAAACATAACGATTCCAACCAAGGAGCGGAGGGATGGACACAAAAATAGCAAAAGTCCACGATATCAGAA

Smed-melanopsin3

>F6AJIXP02IZI79
CTTTCTTCAGATCTAAGAGCATGTGGACCCCATCAAATGTGTTTATATTCGATCTTGCTCTTTCTGATCTCCTCATCTGTATTCTTGGATTTCCATT
TTTAACAATCAGCGGTTTCTGTAAGGAATGGATATTCTCAGAAGCAGGTTGCTCGGCTTATGCGTTTTCCATGTCGGTCACAGGAATGCATTCGATA
TTCATTCTCACGATTCTAGCTGTTGAGCGTCTGAAAGTAATTAGCCGACCATTGAAGATGGTAAAAATTGTATCTAAGAAAAGGTCATTTCTTCTTG
TTCTGATATCGTGGACTTTTG

Smed-cry

>Contig_Planarian_90_7259
AAACTAGAACTATTTATTCACTAATACATGTATCACTTCATCGACATCAACTATTGGAGTGTATTTTGATTGCCTATAAGTCGACTCAAAYAATTTC
ACGTCGAATTTCCGTTGACAGCCCTTGTAGTTCATGTAGCGTATTTTACCGAATACCGCTCGCTCAGCCCAGCCCTGGTCATGGACACCGCAAATAG
ACCACATGATCCCCGTGTACCCATTTGGATCCCGCCCATCTATACTATATCGATCGTTCAACCAGATCGCTCTCTTCAAAGCTTCACCCGGCCCTTC
TTCAGTCCATTCAAGGATCTTTTTCGCCCAATACATGCGTAAAAACCCGTGCATTTTGCCCTCCCTAACCATCTGCAATTGGGCCGCATTCCATAAA
TGGTCATGTGTCTTTCCTGAGTCCAGCTGTTCAATAGTGTACTTGTATGGTCTCTCGTCGTGCCTGTGGATCTCAAGCGTCTCACGAGCCCAATTAG
CCCCTCCCGATAAACTATCATAATGCGGGTTATAGTAACAGAAATTATCAGCTAGTTCTCTGCGGACTAGAGATTCCTCAATGAAAATATCAACTCC
CTCTTTAGCCGTGGATTTCTGGGAATGAGCTTCTAAAATACACCTCTGAGCTGAGATTTGGCCAAAATGCAGCCAAGGAGAAATGTTACTCAAGCAA
CTTTTGTGG

Smed-peropsin1

>Contig_Planarian_90_3556

TTTGATTGGAAACCAATCCAATCAAACACAACACCAAATATCCACACCATGAAAATAGATCCATCAAAAAAAGTTTACGTGAAACGTTATTCATTAT
TTTTTCAAACGAATTAATTTTCTCCGTTTTTCTAGTCTCTAGACTCAGTGTAAACAAATGAAACATTATACCAATAGAAACCGGCAATAAAAATCCG
ACAATAATGAGACCTCCCATATACAATTGATGATTATGTGACAAGTCAAATATCTTTATCGTGCAAGACGTTTGATGGAGTTCCAACGCATAGCTGC
CAAATCCAAATAATGGCAGTAATGACCAAAAAAGTCCCACTATCCAGCAAACATAAAGAATGTGATTAACATTCCAAGGTAATTGAATCCTTCTTGT
AGAATAGTATCGTTCCATGGCAATAACAACGATAATATTAATATTAGAAATACCAAAAACAAAGCCTTCAAAGGCATAAAATTGGCACAAGAAATCT
CCGAAAAGCCATCTTCCAACGAATCGAGAAGGAGCAGCAAGGATTGCACCGAGGACAACTCCTAAGCTGGAATAGATGAAATGTCGGTGAATTTTCC
GGCAATCTTCGTTGATCTGGTTGTTTTGCAAGGTATTACGTAAATCATAGTAGAGTTTTGCACCCAAAATTCCTGAAATTCCTAATAGAATTCCGTA
AAGTTGATCCTTCTTATTAGCAAAGCAATTACAAATTACAACTACTGAAGTATTGAAGTAATTACTAAATTAAATCACACACGGTTCAATTAACAGA
AACATTTCAAGATGTGATTAAGCACAAATTCAACAATTACTTCAAAGTTATCACAGTTTGATGATTCTAATAAAGTTGTTATTCTCGTGAATTAATT
TTGAATACTTAATAACGTAAATTAAACGAAGATGAATGCAAAAGAAACAATGGAATTCGAGAATAATAAGATAATTAATGACAAAATAAACCAATTG
TTAGTAGAAAACAAAGTTTTAAAATCGAA

Smed-blue-opsin

>F6AJIXP02JKU4O

TCACAGTTAAAAGATCTATTTATTTTGTCATTTGCTGTTGGACGCTTGGAGTGATTATCTCCATTCCTCCTCTAGTTGGTTGGAATCGATATGTTTT
GGAAGGTCTACAGATATCTTGCAGTTTTGATATGTTTGACACTTCATGGCAAAGCAAAAGCTACACCATGTTGCTTATCGGAACGTTTCTCCTGATT
TTGACAGCAATTATCATCTGCTACGTAAAAATATTTTTCAAAGTCCGGGATCAGATAAAGGAAATGAGATTGTCTATACAAAATCATTCAAGTAATT
TGCAAAGAATTAAAGAGTAACTTTAATAAGTTATTATGTGTTTTAGAGTCAGATACCCTGTCAAAAGAAACAAAGTCAAAACAACT

Smed-white-sf1

>Contig_Planarian_90_5500

TAGTACAGTTTACATGGGATCACCGAAGGGAGCTGTAAATTTTTTCAAATCGTGTGGCATGCCTTGTCCAATAAATTATAATCCTGCTGATCATTAT
GTACATTGCATAGGTACAAGAGATGACGCTGTCGTCAATTGTTCAGTACAAGAATTGGCAACAAGGTACCTAAAGACCGAAGAACATGCAAAAGTTC
AAAAGTCCATAACTGAAGCTAACTGTACAATGGATAATTCTCTTTTAGAACAAACGTATGAAATAATTTCCAATTCAAAATATAAAGTCAGATGGTG
CAATCAGCTGCGGGGATTATTGTGGAGGCATTGGATTAACATTGTGAGAGATAAAAATCTTTTCCTAGTCCGAGTTGGTCAAACAGTTTTCCTTTCA
ATCATGATTTCCTTGATATTTTTCCAACAAAATTACAACGATCCAAGGAGTCAATTTAATTTGAACGGAGCCCATTTTCTCCAAACCACTTTAATGA
CTTATAATATATTTTATACAGTTCTTAACGCTTTTCCTTCTGACTTGCCAATATTTTTTAGGGAACACAGTGCCGGCATGTACAGAGTTGATGCATA
TTTTATTAGCAGGAATATAACAGATTTGTTAATTTTTGTTGTAATGCCAGTAATTCTTTCATGTTTTGTTTTTGGCTTGGTAATGACAGATCATTCG
ATAGAGAAATTTATTATTCTTATTCTTACGGATATCGCTGTCTGTAAATGTTCGGTTTCGTTGGCATATTTATTATCTACGGCAACTGTAGACATCG
ACTTTTCATTGGCTATTACTCCGCCAATTCTCTATTTGTTTATGTTGTGTTCGGGTTATTTGATTAATTTGGAAAGTATCCTTGTTCCGTTCAAATA
CATTCAGTACTTTTCATGGTTGAGATATGGATTTGAAAATTTAGTAATAAATCAGTGGATTGACGTCCACAACGTAACATGTGTTTATCCGAATTTA
ACAACAAAATCGCCATGCTTCAGTGAAGGTAAAGACATGATTAAGTTCCTCCAATTTGAACCGTCAAAAACAAGATATTACTTCAATTTTATTATGC
TTCTCATAATTATCATTGTCTTTA

Smed-white-sf2

>ISOTIG24526

AAAATGACGGATAATATGAAATTTATGATGAAGAATTACGATGATGATTTTGATTTGAAAGACAATATCAATTTGATTTCAGAGGAAAGTGGAGAAT
CGGAAACGTTTCTCTATGACAGCGTGATTGAACAGGGAAATGTTGAGGTGACCCCAAGAGCTCTGTTGTTTACTGGGGCAAAAAACGTATATAAAAA
CTCAGCTGTACCAAATTATCATAAAAAGAAAGGTCATCAACGATCTTTAAGTTTTGCCGAAACAGTTGAACCCCTGACAATAACATGGAATGATATA
AACGTCTTTGCAGAATTAAGAGGAACTGGATTATGTGGAAGATCTTATAAAACCGGGGAGACTAGACAACTTATTACTAGTCTTTCAGGAATAGCAT
ATCCAGGAAGGATTCTTGCAATATTAGGTCCGTCTGGATGTGGCAAAACTACTTTATTAAATGTCTTAAACGACAGAAATCTTGGTGAGCTTTTGGT
TGAAGGAGAGGTAAAAACAAATGGTCAAGCCTTAGGGTCAGGCATTAAAACTGTATCAGCATATGTGCAAGAATCGGATGTTTTCATTGGTAACTTA
AAGGTTAAAGAACACATTTGGTTTTACGCTCTAATGAAGATGGATAATCATTTCTCAATAGATGATCGAGAGGCGAGAATAGAAGAATTGCTGCTAG
AACTGGGGTTGAAAAAGTGTGCTAATACATACATTGGAATTCCGGGAACAGTGAAAGGAATTTCCGGTGGTGAAATGAAACGCTTAAGTTTTGCTAG
TGAACTTTTGATAAATCCCCCAATAATGTTCCTTGATGAGCCAACTTCTGGATTGGATTCATACATGGCAGAAAATATTTTACATATTTTGAAAAAA
ATGGCAAGAAAAAATAAAACAATAATATGCACAATTCATCAACCGAATTCGGAAGTATATACAATGTTTGATGATATTTTGTTAATGGGAGAAGGGA
GTACAGTTTACATGGGATCACCGAAGGGAGCTGTAAATTTTTTCAAATCGTGTGGCATGCCTTGTCCAATAAATTATAATCCTGCTGATCATTATGT
ACATTGCATAGGTACAAGAGATGACGCTGTCGTCAATTGTTCAGTACAAGAATTGGCAACAAGGTACCTAAAGACCGAAGAACATGCAAAAGTTCAA
AAGTCCATAACTGAAGCTAACTGTACAATGGATAATTCTCTTTTAGAACAAACGTATGAAATAATTTCCAATTCAAAATATAAAGTCAGATGGTGCA
ATCAGCTGCGGGGATTATTGTGGAGGCATTGGATTAACATTGTGAGAGATAAAAATCTTTTCCTAGTCCGAGTTGGTCAAACAGTTTTCCTTTCAAT
CATGATTTCCTTGATATTTTTCCAACAAAATTACAACGATCCAAGGAGTCAATTTAATTTGAACGGAGCCCATTTTCTCCAAACCACTTTAATGACT
TATAATATATTTTATACAGTTCTTAACGCTTTTCCTTCTGACTTGCCAATATTTTTTAGGGAACACAGTGCCGGCATGTACAGAGTTGATGCATATT
TTATTAGCAGGAATATAACAGATTTGTTAATTTTTGTTGTAATGCCAGTAATTCTTTCATGTTTTGTCTTTGGCTTGGTAATGACAGATCATTCGAT
AGAGAAATTTATTATTCTTATTCTTACGGATATCGCTGTCTGTAAATGTTCGGTTTCGTTGGCATATTTATTATCTACGGCAACTGTAGACATCGAC
TTTTCATTGGCTATTACTCCGCCAATTCTCTATTTGTTTATGTTGTGTTCGGGTTATTTGATTAATTTGGAAAGTATCCTTGTTCCGTTCAAATACA
TTCAGTACTTTTCATGGTTGAGATATGGATTTGAAAATTTAGTAATAAATCAGTGGATTGACGTCCACAACGTAACATGTGTTTATCCGAATTTAAC
AACAAAATCGCCATGCTTCAGTGAAGGTAAAGACATGATTAAGTTCCTCCAATTTGAACCGTCAAAAACAAGATATTACTTCAATTTTATTATGCTT
CTCATAATTATCATTGTCTTTCGATTTGGTGCGTTTATTTGTTTGCTTATTCGATGCAGAGAAATAAAAAGAAAGCCAAAAAAATGATTTGCTCGAT
TTATTTTATTTTTGATAATTTGATTAAATAGAAAATTTTTAAAAGAA

Smed-ver

>AAA.454ESTABI.13876

ATTATAATGGAAAATATTGAAATAGAAAAAAGTGAAAGCAGTGGTTGCACTTTTAATAGACAATCAAGTAAATTTTCACTACACTCGATTAATGAAAAGCA
AAGTCTTACATACTCTTCGTATTTAAATGTATTTTTGTTTTATTTTTAATTTAAGTATATTAATGAATTTTAGTTAGATAAATTGTTGTCCTGCCAAACGC
TAATAGAATGCGGTAAATATACTCATGATCAACTGCTTTTTCAGATAACTCATCAAGTCTATGAGCTTTGGTTCAAGCAAATAATTTTTGAAATTGATTCA
ATAAAAGAAATGTTTCAGCAAATTGTTATGGATGAAAGAAATATGCGAGTGATTATTAATCGACTTAATAGAGTTGTTTTAATACTCAAAACATTGGTAGA
TCAGATCAGTATACTAGAAACAATGACGGCGATAGATTTTATGGACTTTAGAGGACATTTACAAGCTGCCTCAGGATTTCAGAGCCTCCAATTTCGTTTAT
TGGAAAATAAACTTGGAGTTTCGGAAGCGTCACGAGTTAGATACAACAAGCAAAACTATAAATCAGTATTTGAAAAGGACCCAATAGCTAAAGAAAGAGTG
GAAAATTCTCTTGATGAAGAATCTTTGCAAGTACTATTAGAGAGGTGGCTCGAAAGAACGCCTGGTTGCAATGATGCCGATTCGAATTTTTGGGAAAGTTA
TTGTCTAGCAGTGAGAAAATATCTGAAAGATTGTTATGAGGATCAAATTGCAAAATTGCAAGAAGGTCCTGAAAAGAAATTATTAACAGCTGATTATGAAA
AAGAAAAAAAATCTTATGAGACAATAACAGATGAAAATCATTACAACGAACTTATAAAGAGAGGTGAAAAACGATTCTCTTACAACGCTTTCAAAGGTGCC
TTGATGATTTCTCTGTACAGGGATGAGACTCGGTTTTCACAGCCGTATCAAATGTTGAGTCTTATTTTAGATATAGATGCATTTCTAACTAAATGGAGATA
TAATCACGTCATAATGGTGCAGCGTATGATTGGTAGTAAGCTTGGAACCGGTGGATCATCTGGATATCAATATTTAAGGTCCACTGTAAGCGATCGGTACA
TGCCATTCTGTGACCTATGCAACTTGTCGACATACTTGATTCCAAGAGAATACATTCCAAAGCTCAGTTCGGAAATGCTTCGACGACTGAGCCAAATGGAT
TTTAGTTATAATAGTTAAATTTAAGTTAGAAACTTCGGTGGAAAGTTTATTGGAATTTATTTTAAATAAATAAATAGTCTT

Smed-nc1

>Contig_Planarian_90_4163

TTTTTTGGTAAAAACAATATATTCTCTCTATGTGAAATAAACATCAGTTATAAAGGCTAAAACGAAWGAACATTTATATATGTTAGGATTCATTTAT
TTTCTTTTTACATCTCCATTTGCTATTGGATTCTGAAAATTGAAATCAAATGGCATGATAAGTTGTTGGGTCTTTCTGTAAGTCCAATAAGGAGTCA
TAAGGAAGGTCACTAAAAACAAACCACCGTAGATGAGCATAAGAAAGTAAAAAGGAACTTGAGTGATTATTGAATTATAATTTTTGTAAGTGACATA
CCAGAAATATACTTCAATGACCGATCTCACGTGAAACAAATGAACAAGGATAAACTGATTAGTTTTCCAGAGTTTTGTATCACTCATTCGACATTTG
AGCAAAGTCCAACAGATCGCTGAAAATGGAGTAGTCATTTCTAAAACCAGGCCACTGCAACCGAAAAAATGCATTTTCCCAACTACAACGGCGGTCA
CATAGTTCATCAGCGCGAGCCAATGGTGAAGGTTCAACAAAACCTGGAAACCACCGTAATAAAAATCTGATAATGTCACCACTAAAGATTCAAACAT
GAAAAACGCAATCGTTATCGATATGGTGCAATGACTGAACCACGTTTCTCCATTCACGACATCATTGTTGAGGTCTTCTGAATATCCGATAGCCCAG
ACTCCAACGCAAGCCCCAAAGACACCAAATAAAGCTCTCACGATTGTCATGTGCCAGAATATTTTCTCTTTCGCTTTCAAGCATCTGTAGGTTTTCA
CTAGCTGACTGAAAAGACATGAAAATATGAAGACTCCAATAATTGATATGAGTGAAGCGAATATCACAATTAAGTTTTCAGTAAAGGAGAACATTTA
CTAAATTTCAATAAATTATATATTGTCATCTCATCACTTTTATTACTAATTTC

Smed-hox1

>Contig_Planarian_90_8368

TAATACGAATACAACATTAGCAATATTATTTGCATTAAGGTTTTAATAATCTATCTTCCATGAGCATTCTTCATATGTTCTGCAAATTCTTTTCGAC
ACTGGAAAGCTTGATCACGGACACAAGTTTCTGTATAGGCCAACTTGTATAGGACAATAAATATTAGAAAATGTAATAATAAACTATATAAAAAAGC
GAATAATCGCGCCGTTCGATTACTCATTACAAATTTACCCAAACTTAGAACGATTTTCTCATAAGGCGGAAGAGCTTGATATTGTCTTTGTTTTCCT
GACGGTTGAATGTTTCGAAAGGATTAATATTTGCTTCGTATTCATTCGAGTAGCGCGACATTGTAGTATCATCTAATGTGCCCTTGGAATTTCTAGA
ATAACTTTGAAGAAATCGAATCTTTTCGTATAATTTGACATTGTCAGCTCGGATCTGATCATTCTCAGAGTGCATATTTTGGATCGAATGTTGCAAT
ACTTGACAGTCTCTTTCCAATTCCTGTGAACGATTTTTAAAGCGATCCCGTTGACTTTGAACAATTGCCAAAAGGGAACTTTGACCTATTTCACGCG
GGCATTCACTGGTTTTATCTAGAACATCAGCCAAAATATTGGCCTCGTTAATTTTATTATTTGGACTTCCAAGATCATTAAGAGAAATAGAACTGAA
CTCCTCGGTTACGTCCCCGGGATTTGTTACAGATGACTGAAACGATCTAACATTTCGCAAATCATCTTCTAACTGATTTATCAATTGAAACTGAGCT
TTCATCTTTAATCGGTTCTCAAAATCTTCCTCTTTTATCTTTTCTAGCTCCATTTGTATCTGAGTAAAWGATGCTTTGACTTGAAGTAATTCATTTT
GCAAATGCCGGTTTTTTCTCATTCAGAAGCTGCTCGATAGACTTATTATGGACAGATGGAATTTCATCGCTATTCTGAGAGAAGGAGCCGTTTGGAG
AACGATGTAACTCAAAATCCTGAAATTCTATAGATTTAATGATTTGGAGTTCCTTTTTTGATTTCTTCATAATCGCTTTGAGATTGCAATTCAGCTT
CTAGCCTAGATATGGTCTGTTTCTTTTCAAAAATTTCATTTTCCAGTTGTTCAGTAAGAGATTTCATTTGTTTGTCACTCTGCACCAAGTGCATATT
GATATTCCTCAACTCATCACTGAGTTTGGCTATCTCGCTGTCCTTCACAGCCAGTTCCATGTGCAACTCCATTCACTTCATTGGTTTCCCGCTCGTT
TCCACTGGCTGCTTTGACCGAGTGCTTCAAAAGCACCAAATTATTTGCTGTGCCCGACTCAGAATTGGCAAGTTGGCTTTTCAGCTGACTCCAGGCG
TTCATTGGTTCGCTCGA

Smed-hox2

>Contig_Planarian_90_8762

GACTGATTAACGAAATTCAAACAATCAAAACAACCCGAAATGGAATCAGCTGTTTTGCAATTTCTGTTCCCAAATTATTCTAGATAAATTCTATTTT
GAGGTAGACGGGGCTCCTATGGCACAGCAGTTGTCTACGATGTAACGCTTGTCAAGTCAGTCTAAGCAACATGAGGTCATGTTTTACTAAAAATAAA
AAGTTTTGGTGTCGACAAGATTACGACAGGCAATTTAAATGCCAGAAATGCTGCGAACCATTAAAATCTTCAGATTTGATTATGAGATCTGGAAGTT
CCGGTTTACCGTACCATGTCGGTTGTTTCAGATGTGATCTTTGCAACGTTTTACTATTAGCAGGAGATTTCTACGGTTGCTCGAACAGCCAATTGTT
TTGCAAAAATGATTTTCTCGTTACTCAGAGAGATGTGAATAATCGTTCGGAAAATTGGCGATATTCTACCGAGACTGGATCACTCAATACGACTGAT
GTGAATGGGAATTCGTCCACAGTCACCGATAATCCGTTATCTGCTCTTTGCCAACTAAATGTTGACGAATATCTCAGAAATAAAACCTCAACATCTG
TAGTAGTTCCGCTAATTGATAAAATCAACCAAATCAAACTCGAAAACAACCAGCTCTCCAAACTCAAATTATGAACCGGATGAAAAAAATATCGACG
AAACCGTTGAGTCGAATGAAATGTCTTCGGAAACAGACATGGGAAAAGAGCTGATTGATCATAGCTCGATGCATGAAGCATCAACTCTCGGAACAGA
AGACGACGACGGAAGTGGCGGATCTTGCTGTGAAAGTGAAGACAAAATTGTTATTTCTACCAAACAAGGAATCTCAAAAAAAGGATCAAATAGTTTG
AGACAAAAAAGAGTTCGAACATCATTTAAGCATCAACAGTTAAGAACGATGAAAGCTTACTTTTCCATGAATCATAATCCAGATTCAAAAGATCTAC
GGCAACTTTCGCAAAAAACTGGATTATCGAAAAGAGTTCTACAAGTTTGGTTTCAGAATGCGCGCGCAAAATTCCGCCGAAGTCTTTGTCGGCAAAC
TGGAGTAATGTGCGGCCCATCTGCCAACCAAATACAAATGCCAAACGTGTTCGATGACACTTCCCTAATCAGCATTGACAAAAATGGCAATTACTCA
ACTAAAACCACAATGACAACTTTCAGTGACATATCCTCGTCGATTTTGAATCATTCCGTACAAAACAATCACCTACTCTGTTCAATGAACGATATCA
ACTATCAGAATCCAGCAAATAACGGATTGCTACAACAATCGACGATGTCAAGTCTCCGAGACCGTTATTTCCCAAATGGTAAACAATCCTTCATTCC
TGTAACCTCATATTACAGTAGCACCATTAATCCCGCCTCCCAAAGTTCTCCGTCTTTGTTTTCAATGGATGTGGGAAATCTAGCCGTTAATTTAGGA
TTGGCTGAATTTCCCCGTGATACTGGAGATTCGTTTCATTTAACAGAAATTGGAATA

Smed-exd (pbx)

>Contig_Planarian_90_2925

TAAAATAACAATATTTTAAATTTATTGTATAATACGTGTAAAATATTAAATCAAAATACAAACTATAAAACTGTAGATTTTGAAAAGAAATGATTGT
CAATGCTATCAAGGAATCAAACACTATAATACACAAACTGTACACATTAAACAAGATTATTTAAAAGAATTTTCGTCAAAATGCATTTCAATCGCAA
CTAATCCGAATGAAATCTGCTTGTTAATGTTTCAGCTTCTTCATATCTGGTTCGTCTTCTCTCATGCCACTGGCCTGCATCCAGTCGTTTTCTGACA
TCAGCTGATTGGAAAATTCATAATTATTGCCAGAATGACCGCCATAACTCATAGATGTGGAAACTGTCGGACAGGAACCTGAAATTTGACCAGATGA
TGCTACTGTAACAGAAGCCGCGGCGGCGGCTGCTGCTGTGGCAGCGGCATAAAGATTAGCTTCTTCCTGTGCTTTAACTATATTTTTCTTATACCTT
ATGCGCTTATTGCCAAACCAATTTGAAACTTGAGACACTGTTATGCCACATTTTTTTGCCAATTCATCTTTTGCTTCTTCGGAAGGATAAGGATTTG
CCAAATGAGAATAAAAATATTCATTTAAAATCTCAGTAGCCTCTTTACTGAAATTTCTTCGTTTCCTCCTAGCATCAAGAAATCTGCTCCTTAATAT
CATGACTGCTTCACAGGTACTTTGTTTAAGTTGTGTTTCAATTGCGCGGAATTTCTTCTTTATTATACCAACCATTAATTCAATTTCAGCTGGACTA
ATAGGCCGACTGCGGCTTTGTTCTCTTAGCAAATTAATTACGTGTCCGGTAAATTCATTACAGGCATTTTTGTATTTTTCGAGCTCGGAATGATAAA
TTTGTCTAATTTGAGCCAATTTAGCCCTATAATCTGCATGTTCTATTTGATTACTTTCAGACTGATTACCACCGTATTCACTATCAATATCTCCAAT
ATTATTCGTATTATTTCCAGTTACACCTTCAGCAATAAGCATTTTATCCAATCTTAGAAGTTGTGGGTCTGGAGAATTAGAATCATCTTCCGAATTT
ATTTGAGCGGTGTTTCTCAAGCTTAAAGACGTCTTTTCTTTTATTTCACAAAACACACTGTACAACGCAGGCTTCAATCGATGATTATTTAATGAAT
GTTTTCTCTCTTGAGCTTCATCTAAACTTTGATGAGCCACACTTAAAATATTTTGTAGCTCTCTTCCAGTACACTGGAWTTTTTTGATCTAGCACCA
AATTAGGATCAGCATGATTCATATCATACGAATAATTATTTCGTGTATTTTGAGTCATATAATGTGAATTTGGGGGTTGTAGGGGTGCGAATRCCAA
CTACTCGGAGGCTGGTGTAAATTCTCACTCATTTTAAACTAGTTTTGTTCTTTAAAAATCTTTAATTTGGTATTTAAGCTTTGATTCTATCTAAAGC
TTAAATGCAAATTCTTTATTATATAAAATATTATCTCAAAATGTATACATCACAAAATGGTATAGAAAATACCTYTATTTC

Smed-yy1

>Contig_Planarian_90_13309

TACGTCGATGCGTGCTGTACCCTGTCCACNCAAAGGCTGTAAGCAAAGCATTCAGGGATAATTCATCGATGCGCAAGCACTTGCATACTCATGGTCC
TCGTGTTCACGAGTRSAGTRMGYGTGGGRAAGCATTTGTCGAAAGCAGTAAATTGAAGCGTCACAGATTGGTCCACACAGGAGAAAAGCCGTTTCAG
TGCTCATTTGAAGGCTGTGGCAAACGATTCTCTCTGGATTTCAATTTGCGCACTCATATCCGTATTCACACCGGCGACAGGCCGTACACATGTCCTT
ATGCCGGTTGCGGCAAGGGATTCGCCCAATCGACAAACCTCAAGTCACACATCCAAACCCACAACAAGAACAAATACAAGACTCTCAAAACATTTTG
CGCTCCTAACAAAATTTCTAGTCAATCCAATGCCAGTTGTCGCAATTCTAATTTAATCGATGAACAACAGCTCACTGCACCGATTAGTGGCCAATTA
CGCCGTCTGAATTCATCTCAGGGCTCCTCGTCGAGTTCTTCGTCTCGGGAATTGCGCGTCCAGAAACGAAGTGCCGTGCAGCAAGTCGACATGAATT
GCCTCGATTCCAGCGGCATGATGCTGCATCAAAACAATGGTGCCTCCGGCACAACAGGAACAAAGGGAGAAAGTCTTCCATTGGATGAAGCTGAAGA
TAATTCGTCATTTGAATTCTGATTTCTATGATCTGATCTGAATCACCATCATAATCATTTTTCATACTCGTTGTCGTTGTCGCCATCTTCGTCGTGT
TTTAATCAATTACTTTATCTCGTTACACTGTTGCTATTGGCGATGATCGCTAGTACCGTTTCTATGGATTCCATTAGCATTTTCAATTTGTAAATAG
ACATTTGGACTTCGTGTCCGCTATAATATGCAGCTGTTACCTGTGGAGATTTACCCATGTACATATTTCTCGATATCTGTTAACGTTCCCTCGTACC
CCAGGTTCTCAATCCGACAACTATCGATTGATTA

Smed-tlx

>Contig_Planarian_90_12057

GGATTTGATTTGATCGCTTCTCTCGATTTATTATGAATTCCTTTTCTGGAATTCTTACACAATCCCAGCAAATATGTCAGCATCGTTTTCCATTGAT
GGAATATTGTCGACGAAAAAAGAGCTTTCCGAATCCATTATTACCTCGAAATCAGAAGAATCAACGAAGACTCATTCGAATTCTTTGAAACATTTAT
TATCCACAATTTTCCCTCCTTCTCTTCCAAGGCATTGGAGTAGAAATATTGCGACAGGATCGTTATCCCCGACGAGTTGGTCATCCATATCAGAATA
GAACCCCTCCAAAAGAAAAAAAGACCTCGAACATCCTTTAATCGGCAACAGATCATGGAACTTGAGAGACGGTTTCATCGTCAGAAGTATCTCGCAT
CATCAGAACGATGCGATCTAGCGAAAGATCTCGATATGACAGACTCTCAAGTGAAGACTTGGTTTCAAAACCGGAGAACAAAATGGAGGCGACAAAC
CAGCGAAGAAAGAGAAGCAGAAAGACAAGCAGCCAGTCGGTATTTATTGACACTTCAAAACGAAATCAACCAATCTAACAATCCTTCTTTTAATTAT
ACCAGCTCTACTCTTTCCGCCATATCCAACCTCCAACCTTGGGCAATACCACAACTCATATCCGAAATGTCTTCTGAAACGTCTTCTCCAGGGGGTC
ATATTGACGATWCTCATTCGGAGAAAA

Smed-hmt

>Contig_Planarian_90_6564

TATCCACCTGCCGACACAATATTCTTGCTCACACATTTCAGATGTATCATAATATATTATTGACAAATAACTTGTCCAATAATAATAGGGAAAAAAT
GAAAATTTACATTACAAAAATAATTTCAATAGCAATATTTCGTTTCAAATCATGCGTAAGTAATCTTATTTTTTGACTCGATCTGGAAAATCGATAT
TCAGAATATATAATAGTGAAAATACGTTTTATTAATATAAGAATTTTCGGCATTTTTCCGATTTGCATAGGCATGGAACTCGACCTGTGATCTGTAA
AGAACTTGTGCTTTCAGAACCAGCCTCGTATTTTGTGTTAACATTTATCGAAGATGTTGAAGTACTAACCACTGAGCCTTCATTTTCCTTGTTATCC
GATATAGCTCCTGTCATCATATAATCAAATGTCAATTCTTCGCCTGCTTTAATATCCCGAGCGGCGAAAAATGCAATTCTGGGCATTCTAATGTCAA
GGTTATTTATAAAAACGCAACGACTCGTCATATTGGGATTGCAAGAGTGATTAATAAAATGAGACATGTTGCCTTTTTTGTATGCATCGACTGTGAA
TTCCGGATCACCGGCGAAATCCAGATCAAAAAGATATGTCAAATTTTGTTGATCATACAACTTTCCTCTTTCTTCTGCTTCGTCAACTGCAACAATC
TCTCCAAGATATTCCATTATAAAATTCCCTCTGATAATTTTGGTGAGAGTTTTCAAGCCCCAGCCTCTATTTTTGGTGCGGAAAATTTTCAACTGTA
ACTTGACCCCTCTCTGAACTACTCGATAGGGACAATTTAAATCACATGAACAGGCGGAATTGCACTCATATATCGGTACACCGAATTTCGGGATTAC
TTTTCCCGTGACTGTGTAAGGGGGGTCACCGCCGTGGATTGATGAGCAATCCTTTTTATTGTCAATACACGAGGTAGTGCAATAACAGGCAATAGGA
GGGTCTGAATGGATTTCTATGCTAA

Smed-mitf1

>S_mediterranea_3.1_Cont566.3

AGATGAATACAAAATCTGGTAATGATAAAATAAAAATTCTTAAACTTGAATCGTTTTCTAATCCTCAATTAAAACGACGACGATCACACAGTCACAA
TGGTGCTGAATTATCAAACAACAAAGTTTTCAACTCAAATGGAAGTGGTTGTCAGTTATTTTTGTCTGCACACAAAGAATCTTCCCCTATAGATAAT
TCTCAACTAAAACCAATTATAAATAATTGCCACTCACCTTTTGTAAACAATCAATTAATCAAAGATAAACACAAGAAAGAAACTCACAATCGTGTTG
AAAGGAAAAGACGGGATTTTATTAATTGCCAAATTCAAAAATTAGCTGAGCTTTTGCCAACGGAGTTCTTTCTTAACTGTGATCTTAAAATGAATAA
AGGAGTGATTTTAAAAAATTCAGTGGAATATATAACATCAATGAAATTAGTAGAGCAGATTAATCATCAATTAATTCATGAAAATGAATTAGGAGCA
AAATTAATTCGCTCTTTAATTAGTTCAAATTACACTGACGTAAGTGT

Smed-mitf2

>Contig_Planarian_90e_7577

GATAATACTTATCTTCCGAGTTTAAGTTACCCAATTAACAATATTAATCCAAATTATGATTACTGTGAATCCTATACAAACAATCCAACTAATGTTC
ACTTTAATCAAGATATGGCAAATAATTGCTTTGATGTGGATGACTTTATCGCACTCGAAAGCAATTATCACAGGAGAAACGACTCACCTTATATAGT
TTCCCCAGCATGCCAATATGATAAATACAATATTTTACAGTACAGCAGTGATTACGTGATTGACAGTAAACAAGATTTACCTATGCAATACCGAGAT
AATACCAGCAAAAGCCTTCTTCAACCTTATGAAGTACTTAATAATAAAAACGATATTTCCCTTTCATGTCCTGTAACCGGTGAACGGTCAGAGGTCA
GTATGAATCATGCAATGAGTAGTTGTAATTTCCCACCAACTCCATCGTCGTCAGTACAGGGTCAATATCAAAATGACAACCTCAAAAATCAAAAAGA
CCGTAACAAAAAAGAAAGCCATAATAGAATCGAAAGAAAGCGACGTGATTATATTAATCATCAAATAACCGAATTGGGTAAATTGATTCCCTCAGAA
ATGAATTCCGACAATGAATCCAAGAAAAACAAAGGAAATAATCCTAAAAAAAATTACAGTGGAATATGTGACCCGATTGAAAATGAATTTAATAATA
TTTCCAATTATGTTAAAGAAACAGAAATGMCATTTATGTTACTGGAGACTTATCGAAAAAGAAATCAGGAACTGGAAAATCAAATAAAAACCTATTA
CTCTAATACCACAAACTCTATTGACAGTCAAAATCTGGCGACGAATTATCATAACTACCTGTTATTACACGAGCAAAATCAGAAAATTTATCAGTCC
AACGGAAAACAAATGTACTTAAAGAATACTAAACCAATTATTACAGACATAAATCGTCGGTTAGGTCCGATGAAAGATAAACAGCTTTCTCCTTTGG
AAAATCAAATTGCATTTAAAATTGAGCCGAGTTCTGCACATTCTTCCGGTGGAAATAATTCGCTTTCAACTACCTATCGGATTGAAGAAGAAGTTGA
TCTTCAATTCAATCTATCCCATGAAATGATTAATATACAAAATGCTTATCAGATCACAAATAATAATCATCCGTCCTTGCCGTCCATGCACAATGAC
TCGTATTTCAGTTCCAACACTCACTTTCGGTGCATGGACAATCAAAAATATGAA

Smed-mitf3

>S_mediterranea_3.1_Cont1634.1

AGAATTTATTTGTAAATTATTTAGTCGAAAGAAAGCGAAGAGATTATATAAATAATCAGATCCAAGAACTTGGTCAATTATTACCAGAGAAATTATT
TTTAAGCACGTAATTTTATATAATTTCTGTTTGACTAATGAAATCCATTGTTATTTATTCGTTTTCAAGAGAATCCAAACGTAACAAAGGTGGAATA
TTGAAAAACTCTGTGATTTATATTCAACAGTTACAAGAATCAATTTCTTGTATTCAGCATTTGCAAAAGGAAGCACAAATATCAGAAAATCTAATTA
CAGTGTTTTACAAGCATATTCAGGTAAACATATTATTGT

Smed-fox

>Contig_Planarian_90_4830

TGCAAATAAAAACTTATATTCATTAAATGCACTGAAAATTTAACAAAAATTGCAGAATTTCATGGTTTATTAGAAAACCATCACCACCACCACGATT
TAAACAGATTAATTTCTAAAAATTGGTCAGGAAATTTCTTGAGGATGAGATAAATAGTTGCTCAATAAATATGGATTCGGTTTCTGCATAAAATTCA
TGCTGTAAGGCAATGGAGGTCTGAGGTGGTTATTTGACTGAGGATATTCGTTCTGGGGGCTAATATTTGAAAAATAAGGAAATTGGTTGTATAACCC
ATTAGGATTGAAATCAAAAGCTTGTTTGTTCGTAAATTCTCTATTTCTTTTATAACATTCGGCTTAATAGTTGATGAATTTTGAWWATGATTCTTTC
GACTGACAGTCAWAAAGTTCTTGACATTCATCGCCAAAAGTACTATTTTTCTTCAATGAAAAATTCAAACCTTTGAAGTCATTTGTTATAGAATGAG
GATTTTCAACTTTGGATGTATGAACCTTTTCAAGATCATCAGAATTTGAAATTATTATATCTGAGTTTGTAGCAGTTGCTTCAGCTGATATCGTATC
GTCCTTATACTTAAAACGGCGTCTTCTACGAAGAAAAGATCCATTTTCAAACATATTATATGCATTCGGGTGCAAAGTCCAATAACTGCCTTTTCCA
GATCTTTGGTCACCTCTAGATACCTTAATGAAACACTCATTGAGCGATAAATTATGCCTAATAGAATTCTGCCAGCCTTGCTTATTCTCACGATAAT
AAGGAAATCTTTCTGAAATAAACTGATAGATGCCATTCAAAGTTATTCGATGGTCTGGTTGAGATGTTATTGCCATTGTTATCAGTGCTATATATGA
ATATGGGGGCTTAACTAAAGATCTGTTATCGTTTTTATTCTCCATTTTAATATTATTCTGATTATCGATAGGGGAATTAGGATATTTTGAATCGGTA
TTAATGATTGGGAATTGGTTTTGATAATTATTGTAACACGAGGCTGACATGGAATAAAAATCTGAATGAATTGATTTGTGAAAAAGCAAATCTTGTT
GAACATCTTGAGAATTCAACGATGGATAGTAAGAATTTAGATGATGGGGATCTGAATTTAAGTAGGCAGCTTTCCAGGAATCCGAATTAGAATTGTA
TGAAGAATTTGGCCACAAGAAGCTCGAAGATTCACATCCGGGAAATTGATAAGCTGATGAATAATACAACAACGACGCATGATCGGAAATTGGATGG
CGCGGAATTTGTGGCGCTGAATTTGCCGCAGTTAATACCGAGATGTGATCAACATTCATTTTCGRCTTTATGGATAACTTGAATAAACAAATTTGTT
TTTCTAATTGACAGAATTGGTTTTGGGAAGAGTTTTTTTCCTCCTATATCTAAGATAAATAATAAAAACAATATTGTGAAACTTGTCCTATTGGCAC
TTGTTGAAATATCTTATTATTTGTGA

Smed-tpr1

>Contig_Planarian_90_5420

CACATAATTTTGTATTTAGAATAATTGTAATTGATATAGAAAATTTATTTGATATCGTTTTGTTAATAAAATTGATGCCATAATTTTATTTTWTTTA
AAATTKAKCGTTTGTTTAAATCAATTATAAAATGGAAACTGATAGCGGTAAAATTTCTTGGATTGATGCTGTCCAAGTTTCTGTCAGGGAAGAATTG
GTGCATATTGCAAAATTGGCTGAGCAAGCTGAAAGATACGATGATATGGCAGTCGCAATGAAACGGGTTACTGAAAAAGGAAATGAATTGAGCAATG
AAGAACGTAATTTGTTGTCTGTTGCATATAAGAACGTTGTTGGATCACGTCGATCATCTTGGAGAGTTATATCAAGTATTGAACAGAAAACCGATGG
AAATGAGAAAAAAGTTAAGTTTAGTGGTGAATATAGACTTAAAATTGAGAAAGAATTGCATGATATTTGTCGTGATGTTTTGAAACTGCTGCGCGAA
TATTTAATACCAAAAGCAACAATATCTGAAAGCGTTGTATTCTTTTTGAAAATGGAAGGCGACTATTATCGCTACTTAGCTGAAGTAGCTTCTGGTG
ATGTTAAAGATGAAGCTGTTCAGAAATCAATGGATGCCTATCAAAATGCTACCGTACACGCTGACAAGGAATTAGAAACGACTCATCCAATAAGGTT
AGGATTAGCTCTTAATTATTCGGTTTTTTTCTATGAAATTAAAAACGAACCTGAACGAGCTTGTCAGTTAGCTCGAAGTGCTTTTGATAGTGCAATT
GCAAATATAGATGATCTTCAGGAAGAATCTTATAAAGATAGCACTTTAATAATGCAACTTTTGAGGGACAATTTAACGTTGTGGACTTCAGAACAAG
ATGCTGAGCCTGGAGAAGCTGATCCTGGCGACAACTGAAATTTTTCCATTGCTA

Smed-tpr2

>Contig_Planarian_90_2066

AATAATAAACAATTAATTAATACGTATTTTTTTAAATTCTACACGATGTATTCTAAAGATGATAATCTTTACATGGCAAAATTGTCTGAACAAGYAG
AACGATATGAAGAAATGACAAAATACATGACCGAAATTGCTGTTTCAGACGTAGAACTTTGTGTAGAAGAACGAAATTTACTTTCCGTTGCTTTCAA
AAACCTTATCGGCTCAAAGCGTGTTTCTTGGAGAGTTTTACATAGTATTGAATTAAAGGAGAAAACTCGCCAATCCCAAGAGAAGCTTGCTATCGTT
TTAGAATATAAAGCTAAAATTGAAACTGAAATGAAAAATATTTGTCAAAATATTTTCCGATTACTTGAGGATTATTTAATTAAAAATGCCACATCTG
GAGAATCAAAAGTATTTTTTCATAAAATGAAAGGCGATTATTATCGCTATATGGCTGAATTTTCAAAGGACAGAAAAGAAGCTGCTGATAATAGTTT
AACTGCTTATAAATTTGCAACTGACATTGCAACTACAGAGCTGGCTCCGACTCATCCGATACGTTTAGGACTAGCTCTTAATTTTTCCGTTTTCTAT
TTTGAGATTACAAATGACTCTGTCAAGGCTTGCCAATTGGCCAAGCAGGCTTTTGATGATGCAATAACGGAGTTAGATTCATTACCAGAAGATGTTT
ATAAAGATTCTACTTTAATTTTACAATTATTGAGAGATAATTTGACTCTATGGAGAACTGATGTTCCCCCTGCTGAAGATGAAATTTCAAAAGACCA
ACCAAAGAAATAGAGTGATCTGATTGGTTTAACCATGACAGATGTTTATTTAGCTGTTTTTACAAGCTTCGATAGCTTTAAATCTGTAGAATGCTCG
CATGCTTGATTTATGAATATTTTTCATTATTTTGGTCTCATTTTGCAGATGTAATTTTACAATAGAAATATAGAAATCTTTTGTCAAAAAAA

Smed-kinase

>Contig_Planarian_90_1343

AGTTTATTAAATTACTTTGGAAGTTATTTTTTCATGTTAAAGTTCTTTAAAAATTTAAAAAGTGGGGCTAACAAGAAGGAAGAGCCATTTGAAATAT
CTAATCCCAACTAACGTAACAAAAGAAAGTCCATGTCACATTTGATCCAGAAACCAGTGACTTTGTTGGATTACCAGATTACTGGAAAAAACTGTTA
GATCAAGCGGATTTTAGCAAAGAAGAAAAAACTAAACATCCTAATGAAATTTACAATGCTGTAATTTTTATGAAAGATTATGAADAAAAACACGAAA
AATTTTTGGGAAACAAAGAAAATTATGAAGATAAAGATGAAACTGGCGAACCCCGTGATAATGGCTTAAAACCAGTTGTAGAAGAGAAAACTCCACC
AGAAATCGTTGAAACAGAAAATCAAAAAAAACTTGAAACAAATACAAGCACACCAGTTAAGCGAAAGAAAAATAAAATGTCAGACAACGAATTTTAT
GCAGCTCTAGATGAAATTGTCACAAAGGAAAATCCACTCGACAAATACGAATTAAACGAAAGATTAGGCGCTGGTGCATCAGGTACAGTTAGATTGG
CCACTGCCAAAGAAACTGGTAACAAAGTCGCGATTAAAATCATGAATCTACTGAAACAACCAAATCGAGATTTGATTCTAACTGAAATCAAGGTGAT
GAAACAAACTCAACATCCGAATATTGTGAATTATATTGAGTCGTTTCTAATTATGGAAGACAAAGAATTATGGGTTGTCATTGAATACCTCGATGGT
GGTGCTTTAACTGATGTCGTCACCGAAACAATCATGGACAATGGATTAATTGCCTCCGTCGTTAAGGAGTGTCTGAATGCCTTGGAATTCCTCCATG
AGAATAACATTATTCACCGTGATATTAAATCAGACAATGTATTGCTTGGTAAGAGTGGCCAGGTAAAAGTGACTGATTTTGGGTTTTGTGCCCAACT
TGGATCTCGAACAAGTCGTAGACAAACTATGGTTGGCACCCCATACTGGATGGCACCGGAAGTTGTTAATAGAACTGTGCAGTATGATGAGAAAATC
GATATTTGGTCTCTGGGAATAATGATAATTGAGATGCTTGACGGTGAGCCTCCATATATGGATGAAACGCCACTCAAAGCAATATACAACATCCAGA
CGAAAGGCAGGCCGTCTCCAAAAGCCAAAGTGGATGGTGATTTGGAAAGCTTTCTCCATGATTGCTTGGAAATTGACCCAAATTTGAGAAAAAGTGC
AGAAAGTCTTTTAAAGCATGACTTTTTGAAACAATGTAAATCTTTGAAAACTATCGCAGCCTCTATTGACGCGGCCAAGAAAAATCTGAATAAGAAG
CATTGAAATTATTTTTTACAAGACATAATCATTATGATAATTTGTACTATAACGTTTCTATTCTTTCAAATAATGTCCAAATATATTTATAAATTTT
TTAAAGGTTGACAATAAATAAATGATAGCTTGTTTWTGT

Smed-VATP-synthase

>Contig_Planarian_90_1263

TTATTTAAATAATTACGTTTTTGGAAGTAATAATTACTATTTTAATAATATTGCAAATGTCAGAACCTATTTATACTCCTTTCTTTGGTGTCATGGG
GGTAACCTCGGCTATGGTATTTTGCGCCCTAGGTGCCGCTTATGGAACTGCTAAGTCAGGAACTGGAATTGCATCTATGGCCGTGATGAGACCAGAA
TTAATCATGAAGTCCATTATTCCAGTTGTTATGGCGGGTATTATAGCTATTTATGGACTAGTTGTTGCTGTTCTTATTGCGCAAAAATTGGACTCCA
GTCTTAAAATGGAAAATTCTCTGAAATATCTTGGAGCCGGATTAAGTGTTGGTCTCAGTGGTTTGGCAGCTGGCTTTGCAATCGGTATAGTTGGTGA
TGCAGGTGTTCGAGGTACTGCACAACAACCTCGTCTATTCGTCGGAATGATTCTTATTCTAATTTTTGCTGAAGTCCTTGGATTATATGGCCTAATT
GTTGCTTTAATATTGTCCACAAAGTAAATGCAAACAACTGAAATGTGATTAACTTAAGCATAATTCGTTAAAAGTATCGCCATTATTTGTAAAATGT
TAGAATATATTTTGACAATTTTATGTAATTTGTTATACGTATTTGCAATATCTTAGTTCTGTCAAATAATTTGATGTTTGTTAATATTGACCTCGCT
GATGTTGATTATGGTAGTTAGTGGACTGTTATTAAAGCAATGTATTTATTTATATTGTAATTGGATTAATTATAATATTGACAAGAAATTATTTTTT
AATGCATGGTTTCTCAGTGATAGTTTTTAGGAAATAGGTTATTTTTTCTGAAATCTATAAGTCCATTAAAAA

Smed-dye

>Contig_Planarian_90_10138

TTACCGGGAGATTTTGAACATCTCGATAGCAGATCGAATCGATCCAGAATCTGAGCTAACCGGTAGCAATTGTGTGCGATCTAACGCTGCCAGTGCA
GCTTCAATATCCCCTTCCATACTGGAGAATATGAAACGACCAATAGTAAGAATACAKGACAACAATGACCCTTCGGCAGACTCAGGCATCCGACTGA
GCACGAATTCCGCCTTCGATTGCAGCCTGGACACATCCGGATGACTACTCGGTAGAGATATCGAATTGGCGATCAATTCAGCAAGATCAGCCGCAGC
CTCTTGATATTTCCCAGCCAATTGCAGCGCGTCACAAGCGGATTCAGTACGGCCGGTCTGTCGGAACCGCTTGGAAACCGCCTCCAGCACATCGTCA
GCGACATGGCCGTATCTCGACAGTAAGCCCTGATGAGTTCGACCGTCTTCCTCCATCACGCGAGAGAACAGCAACTCCAATGAGACGCTCTCAACGG
CGAGACTGCTGGCGCATGTAACGAATCCATTCGGATCGTCCTGATGTCCCGGCAAACTCGATAGGACATAGAATAAATCCAGCGCCTCTTTCGGATG
GCTGGACTCGAATTTCCGAGTGTATAACGTGACGAGACGCATCAAATTGATTCTTGATAAGCCTTGA

Smed-centrin

>Contig_Planarian_90_4066

TTATTAATATTTATATTATTAATCATAATTAAAATTTGATTTTATATCACAAAATAATCTATGCCGTTAGACGGTCTTATCGAAATCTATATAAATC
TTATATGACTAGTCTAAAAAAAGGATCAGCAGGTGGAATCAACCAAAAGAAAAAAGGTGGTTCAGGTGATCGCCCAGAATTAACTGAAGAACAGAAA
CAAGAAGTTCGAGAGGCTTTTGATTTATTTGATGCTGATGGCTCAGGAACAATAGATATAAAAGAACTAAAAGTTGCCATGAGGGCTTTAGGATTTG
AACCCAAAAAAGAAGAAGTTCGGAAATTAATAGCTGATTATGATATCGAAGGGAAAGGCATCATTGAATTTAGTGATTTTCTTAGTATGATGACGCA
AAAAATGGCAGAAAAAGATACGAAAGAAGAAATATTAAAAGCATTTAAATTGTTCGATGATGATGAAACGGGAAAAATTTCTTTTAAAAATTTAAAA
AGAGTTGCAAAAGAATTAGGCGAAAATTTAACAGACGAAGAACTTCAAGAAATGATTGATGAAGCTGATAGAGATAATGATGGAGAAATTAACGAGC
AAGAATTCTTAAGAATAATGAAGAAAACAAATTTATATTAGTGTTTTGTGTAATTATAAAATGAGCTTTGTAATATAATTGAAATWTTCC

Smed-bbs

>isotig26456

TAGAAAATCCATTTTATATTTGGGAAGCCAAACAAAAGTGCAATAAAACGTGAATTTACTTTCTATAAGATGAGTGCAAATTTCAAAAAAAATCTTC
TAAGTTCTCTTTCTTGGATTTGGTAGCATTGTGATCATTTTCGGATGGGGGGTGGTCGACCGGCCCATCAAATTCAATTGATCCAACATTCATGGTT
GCCTCAAGCGTCCTGCTTGCGTTAAGAATCTCTTGGATTTGATTATTTTCCTGTTTTGAATCCGCCTTTTCCAACAGAATGACAATAGTTTTATTTA
ATTTTAACGATTCTTTATATTTTTTCTGTTTATAAAGAAATACTGCATAATTATACAGCAATAAAGGATCTGATTCGTTGATTTTCACAGCTTCTTG
ATATGCTTTTTCAGCATTTTCAGGATCTTCCAGATGAGACAGAGATATTGCGAGCATCATGTAAAGCTTGCTGTTAGCATTTGATTTGACTAGTTGA
ATAGCTGAACTCAAAAAGCGAAATGCGCTGGCATATTGTTCAGTGTGTAAATGCACAAGTCCAAGATTGGAAGCAATTTTCCACTCGAATGGTGCCA
AATAATAGGCTCTATTAAGACAACTGATTGCAGCAACATATTTCTTTTTAGCGAAAAATGCCATTCCAATATTGCTCCAAATCGGACCGTTTTCTGG
TGCCTTTTGTGCGGCAATCCGATATTTATTCAAGGCAACATCATAATCACCATGCTGTTGTATTATACTACTTGCAGCTATTATGGAATTTACATGA
GTTGGATCATTAGATAGAGCGTTTCCAAATTGTTCGAAAGCCTTATTTGTTTGACCTAGATCCATGTACAGTAAACCCAGCGTCATGAGAATATCAG
AATTCTCAGGAGCAATTTCTGTTGCAATTTTATAATTGGCAATAGCATTTTCAAAATCCTTTTCAATGACAAATATTTTCCCCAACATTAAATATGA
GGATTCAGATTTTCTGCAATTTATGGCATTTCTGAAAAATACCTTGGCCAATTCAAATTCATTGCACTGCATGTGACACAGTCCTAAATTGTGATTA
ATTTCCCAATCTTCGCCAGCTAATTTCAAGGCATCTTGGTATACTTCAATTGCCGATGAAATACGGCCCAAAATAAATAAAGTCTTTGCAACTTGTT
TGAAATTATTTACATTAGAGCTATTTAGCAATGCACATTGTTGGAAATAACTTAGAGATTCAGAAATATTTCCTTTTTGTCGACATATTAGTCCATA
TGTATATAATGCATATTCACAAGCAAAACCTGATTCAGCCAATTGTTCTTTTATTAATAATTCGCAAGCTTCATAATTTTTCTGAATGAAGTACATG
TGAATTAACCAGTTTCTACGTTCAACCGGGGGAATATCAATAGTTCTTGACGGCTGAATAATTTTAGGTTTTGGTTGTGTTAATTCATTTTTCGGAT
GGTCATTAATATCTGAAAACTCTTTATTTGCAGACATATTT

Smed-ras

>Contig_Planarian_90_234

ASWAAATAAAAAGCTTTGTATTTCAGTATGACAAAGATAAATCAAAATTAACTTTAGAAAACTGATATCATAGATTTCCGTAATTTACACAAACACA
CGAATTATTATTCAGACTGTTAACGTGAGAAAATCCAAATTGTCTATATTATGCAACACACTGCAAACCAATTCGGACGATATCTTTGATACTTCCA
ACACAAAATGAAAACATAAATATTCAAATAATAAATCAAACATCTTGCCAATTACAAAATTTCATCTTCAATTGTTTTAATTTAGCTATTATTAAAA
ATTCGAAATAACTTCTTCCTAAATATTATAAAAATGATTATAAAGAAATCAACAAATTCAAAAGAAAATATTAAAGCAGCCAAGATGGCAAAAAATC
GTTTTTCTAACAAGTCAAATGTGCTTCAAATATCATATTGTAATCACCATTCATTCAAATCGAATTGTAAATACGCCATTCATAAACAATGACTCAG
AACTGCTTTAAAAGTAATTTATTTTGTAATTATAGCAAATTGCATGTTTTCTTTCTTTTCTTTACATCTTTACTAGTCGGTGCTTGTTTGTTAATTT
GCCGAACTAAGTCATAAAATATTTCGTTAACATTAATTTTATTCTTAGCACTGGTTTCCATAAATGAACAGTTAAATTTTCTTGCTAAAACTTGACC
TTGCTCTTTTCCCACACTTCTATCGTCTTCTAAATCACATTTGTTACCCACTAAAACCATAGGTACATTGTCAGTATCTTTAACACGCAAAATTTGT
TCGCGTAAATCCTCCAATTCATTAAAAGATGATTGCGCAGTAATAGAATATACTAATACAAATCCTTGTCCATTTTTCATATATAAATCTCTCATAG
CGGTGAATTGTTCCGTTCCAGCAGTATCGAGAATTTCTAACATACACTGGCTACCATCAACCTCGACTTGCTTTCTATAACTGTCCTCTATAGTTGG
GTCATATTTTTCAACAAATATTCCTTGAACAAATTGAACAGTAAGAGCACTCTTACCAACACCTCCAGTACCCAAAACTACAAGTTTATATTCTTTC
ATTTATCATATTAAGATTTATATAGATTTCGATAAGACCGTCTAACGGCATGAATCATTATAAAAAAAAATCATACATCCAATTTTTAGATGTATAAT
GGCTAATATTATTAAATGTAAAATTAATAAATTC

Smed-snap

>DN309134_ PL06003X1F10

GAACTACAATGAACAGCTTAACAAATTACTTTTAGAAATGAATTCAATTATTGAAAGAAGAATTGAATCTATAAATGACACTCGAGATAATTTACTT
AGCCAAGTTAAGAAAGAAGACCAAAATAAAGGCAGTTATATTATACAGATTTTGAATGGGAGAAATTCTAGTATTATTCGAAAACCGTTTTTTATAA
CACCAATTGGATTGACTCCTCCAACAATTCAAACAGTCCTCAATAAAAATAGTAGTGGAAGCTATGATTTTTACGATTTAAAACAACAGTTAGCAGT
AATCGGCTCAAGTAAAGAATTAAATATTTTAAAAGAAGCAATTGGTACAAACGTTTTTGATATCAAAAAGCAACTTTTAATAACTTCCTCGGAGAAA
GTAATTGCTCGAGAATTGAATGCTTTGAACACACAGTCATTTGCACAACTGACAAGTAAATGTGACAGCTATATGATAGATAGAATCGACTGGCTGG
GAATTTCTACTCAAAACTTGAAAGGCAGAATTTCAGCTGAAAATTGTCGTAAAATCTGTTCGCAATTATTTAATCCTGATTTTGCGGTGCCGAAATG
GACAGATTATGAGTGCCAGGAACTACTTCGTTTAGTGTCAGAAATAGGTTCCCAAGGGCATTGGGTAGAAATTGCATCAAGAATGCCTATGAAAATT
CTACCGTTTCGGTGCTTCAAAAAGTGGCTTGACTTAACCAGTAAAATGGAATCTTGTCAAGAAT

Smed-myb

>DN310639_PL06008A1A03

ATTCAATTGGTCAACAAATTGTTCTTTATATACAACAAATTTTAACAAATCAATGGATCAAATTGATAATGCAAAGTGGATAGGATTAGAGAAAGTA
AACAACTTTCAAGACCATATTTGGAAATGGACTGCTGTATTAGTTGTTTGTGCCCTGTGGCATGTTGTAAAATATCATCAACGGCAATTTTATAAAT
GTCCAAACGCTACAAAACCCGAAACCGGAATCATTTTCCCTGAAACTACAGTGCAAAGCATCGATGATAGTTTAATAAATTTATTTAAATTCTGCAT
AAATTTTGCTTTTTACAAACTTGGACTTGAATTGAGTTTTATCGTCACGGTTATCGTTGCATGTTTACGAGTTGATGTTTATTCACTTGTTTATTTA
ATATTACTTCTCATTTTTCTCTGCACACAAAGGAAAATATGTTCGAAAATTTGGCTGCCATATATGCTGTTTTTAGGCGTTTTACTTCCGATTGAAT
ATGCTATTTGTGTTGGACTGCCACCTGGACTCTGTCAAAAATATCCATTAACAAGTCTTAAAGAAAATCTTCAAAGATGGCTCTTTTTACCAAGTTA
TGAATATCCTCCTTCTGCTAAAAAAATAATGGCGGACTTCTTTCAATTTGTATTTGTGGCTCTTCAGTACAGAGTGTTTATAATTGAAAATTCACTT
ACTGTTAACAATTACGGTGGTGGAAGGAACCGACCTATTCTCTGCAATGAATTGCCAAAGACTATCGATAAAGATTTTGTCAGCACTAAAGATTCCT
ACGTTGATTATTTGAAACATGCAATATTTTATTGGTCATATTGGCTGAG

Smed-mrp1

>Contig1002.3_18425_18580/20312_20596/ 27101_27364 4--MRP

TATTATTATTTTACTTATTATTTTAATTATTCTTTATTATTATTATTATTACAATTAATTATTTATTTTTATTTATTATTATTTCAGAAAGAATGTC
CAGAATATTATTCATCATTTCTCTCAAGAATAATATTTTTTTGGTTTACTCCGTTAGTT

AAAGAAATCGAAGAACCAGAAAAAGAGAAGCTTACTAGTCCACCTGATAACAACAAAAGGAGCATCCCTCAAAATGCAGAAACTGGTATATTATGAG
ACGTTTTGGTATGTGAATAAATATTTCTATCAGATACTGACAAGAAAAAAGAAAAATTCGATCCTTGCTTGATGAACGCCCTTATCAAATCTCATTT
TCCATATCTTTTACTCTCAGGGTTATATAAGATTATTCACGATATTCTTGCATTTCTAGGGCCTATTTTGCTCAAGTAATTCAATTTAATT

TCGTTACGGCTCAGTACTGCGTCTCGGAAAGAATCAACAGTTGGTGAAATTGTTAACCTAATGTCAATTGATGCTCAAAAGTTCCTTGAGCTAATCA
GTTATATCCACATGATCTGGAGTGGCCCATATCAGATTATAGCCGCTCTAATTCTATTATGGTACGAATTGGGGCCGTCAGTTTTGGCTGGTTTGGT
GATTATGTTACTAATGATACCGGTAAATGCCGTCATTGGCAATATCACTAGGAAAATTCAGGTTATCTCA

Smed-mrp2

>Contig1002.3_31578_32270

TTAACCACAATTTCATCATACCTCCAGGTTCTGAAATTATACGCATGGGAACCTTCGTTTATCAACTTCGTTACAGAAATAAGAAACAAGGAATTGA
AGTTCATGAAACGGGCAGCTTACTATAATGCCGCGATTTCATTTACTTTCAATTGTGCACCGTTCCTCGTCTCTTTGACGACTTTTGGAATGTTCGT
TCTGATATCGCGCGACAACGTCCTGGATGCTGAAAAGGCATTCGTATCGATAACCCTATTCAACATTCTCAGATTCCCCTTAATGATGTTACCAATG
GTCATATCAAATTTGATTCAAGTTTTTTGTTGTTGTTAATTTACTCTCTCGCTTTACACAGGTAAATTTGCCAGGCATCTGTCTCTCTCAAACGACT
TACTACATTTCTCAGGCGCGAGGAAATAAATAAAGATGCCGTTTCTCACGACGATACTCCTGGAATCGCTGCAACCATCAAAAATGGGATTTTTAAA
TGGGACTCAACAACCCCAGAACCGGTTTTGAAAAAGTATAAATGAAATGGAAATTACAGTGAAGTAAATTTGATTGTTCAGCATTAACATTACGTTT
CCTGAACGGCACTTGGTCGCAATCGTTGGTCCGGTTGGCTGTGGAAAGTCCAGCATCCTCAGTGCATTGTTAGGGGAAATAGATAAACTGGAAGGAT
ATGTAAATATGAAG

Smed-fib

>Contig5890.3_9873_10079/10136_10996

TGTTTCGCAAAACTTTTTATAAATATTTTGCAGGATTCAATAAACGATTACAAATGTAACTGCAGCACCAGTTTCAAAGGAAAGAATTGTGAGCTTA
ATATAGCTTGTCAGAACCAACCCTGCAAGAATGGCGGTGTTTGCCAGGAAGTTGACACCGGATACACTTGTAAATGTAAAACTGGATATACTGGCAC
AAACTGCGAGGTG

TGCAGTCCAAATCCTTGTTTAAATGGTGCTTACTGTTACACTATCAATCAGGACTTTTACTGTCACTGCAATAAGGAATTTTGGGGTAAACGCTGTG
AACATTCACGACCTTATTGTGGTAATGAATCATGTGAAAGCGCCTACGATGCGTGTTCTATGCCACAAATGTTAAATTCTAGTGGTATTAAGCATAA
CTATTGCGGCAAATACGGAACATGTTTGAGTCATGAAAAGGAAAAGTTCATATGCAGATGCATGCCAGGGTTTGAGGGTGACTCGTGTGAAATTGAT
ATTGATGATTGTAAAACGAATCCGTGCAAAAACGGAGGAATATGCATTGACAGCATCAATAATTTTGAATGTATTTGTGACAACGGATTCTTTGGGA
AAACTTGTGAAGAAAGTAATCATTTTCTACTTTCAAAATCAGAGTGTCATTAATTACTGATAACTTTAGGAACGGATTATTGCATCAAAAGTCCTTG
TATGAATTACGGTGTCTGCCTCCGGCATTCGGATGAATTATATAACGATTTCATCTGTGAATGCAAAAATAATTGGGGAGGCAGACTTTGCCATCTT
CCGAAGCATTCGATATGTGACAGTAATCCTTGTTTGAATGGAGGAAGTTGTTCTAGATTATCTACGTTAAATGGCTTTCAGTGCCATTGTAATCAAG
GCTGGATTGGGACCGTTTGTCAGTTTCTTCACATTGACTTTCAGCCTTGTAGAAGAAAAAATCTTTGTAAAAATGAAGGGGTTTGTATCAACGTTGG
CTATAATGATTTCACTTGTCACTGCAAACCGGGATTTGAAGGCAAGCATTGTGACATAAACACAAACGAATGCAATCCAAATCCT

Smed-titin

>EE666519_SAAH-aab61d12.g1

GCAAATAATCGCAAAACAATATTGACGATTAATAAATCTTCCACTCTTAAACTCGATGTCAATGACAAATCAGCTGGCAACTATTTCTGTGAGGTCA
GGACGAAGGCCGGCGCGAAACTTGAGCGAGTATTTGAATTATTAGTAATATCAGAAGAAAATACACATAATAACTTCGCAATTTCGATAGAAAACAC
TGAAACAATCAACATTACAATGAAAAATTTAAAAAAACAACAATTAAATTGTCGCACAAATGAACAAATTTTTGAAAAGATTCAAACGGTAAAATGG
GGCAAAAAGTTGGATTTAGCAATGAAAAACTTTGATAAATCTCAAACGATTCCATGGGAAGGAAATCTTTACAAACTGTTGCCAGACAATCAAATTG
TGACCCCAGTGGATCCAGAAAACCGAATAGTGAGCTCGTACTATTTCAAAGACGTCTCATTGGAAATGGCAGGAGAATACATGTGCGCAATTATCAC
CAACAGCGGCACGATCAAATATAAAACCTTCAATGTCTATGTTATAAATAACTCTGTCGAAGAAGAAATTCGACAAAGTTTATTCTTTTTATACATT
TTAATTCCTTCGTTAATAATTGCAATTTGCTCTTTCATTGGTATCTATTTGACAATAAACCGCCGACCGGCCCGAAAGCCATCGAATTT

Smed-fgfl

>DN293522_PL030014A20D08

AGTCTCTGAAATCAACTTAAGTAATTGAAATTTTATTAAAATTCTTATATTACTCTAAATGTTATTCGAAATGAAAGCGATTGGATTTCTAATATTA
TTGACAGTAGGAACCAAAGCCTCAATTAATAAATTGTTTTTCATTGGTTCAAATATGGAAATAATCTGTCCGCTTGATGCTACATTCTATCAATGGA
AAAAATATCATAATAATAAAGTAACGAATATTTTCCAAGATGATAAAAGAAAATTGAATGTTTCCCTAAAATTGGAAGAATCTCCCACAATTTATGA
GTGCGGTGCTACTAGTGGATTTGGTCAAAGAAGCGTTAATATTACTGTATTCATTATAGATCAAAACTCAAAATTGGCCCAAGAATTGTGCTACGTC
GTTCCTTTTGATCCGGCATCGCGAGTAAAACATCAGGTTCAATATCCTTGTTTTGTACGCGAACAAAAGGAAGCTACTTTCA

Smed-duk6

>EE281751

TGAACACCAATAACAATTATGGTCGTTTATGAATTAGCCATTTTTAAAATGGCTGGCAGGTAATTTTTTTAATAAAGTATATTTTAGGGCTTGAATT
GTGATCTCGTATGTTTATGAGATCATTGTTCAAGCTCTTAAATAATACTTTTAATCATCATTTATTATAAATTTTGTTTTAATTAGTTTTTTTAGGT
TTTTTAGGAATTTATGCCAATTTATGCAAATTAATGGAATTATTTTCTAATAAATTTTGCTGTTATCGGATTAGCGGATGCAGTCATATTTGCTGGT
AGACTGGTGGGCGGAGCTGTGGCTGGTGGTGTTATTGGATTTGGTGCAGCTTTGGGTGCTGTTAAAGCTCTGAAATTGCCTTTTCCTTTAGCATGGA
AAAAAAATCACTTGGCTATCAGAAGCATGTGGAATTCATTCGAGTCGGTATTGACCGACAGCTACAACAGATTCCGTGATAATATGACATCCAACAT
CACAGAAATTATTACAATAATTGAAGCAAAAGCAATGAAAATTCGAAACAATTTGAACAGTATAGCTAAAGATTTGAACAATTTCCCGAATAGGCCA
TAGGCCAAAGAAAATGTCCATCGTCTGCCAATATAAAGTGATACCTGGCAATACTTTTTAAATTTACTTCACAACTGTAATAATCTA

Smed-duk3

>DN300643

ATCAAAAATGAAACTTTTGTTATTAATAATTGTGTTGAGTGCAATCGGGATAATTTGCAAAGATTCGGAACAAGATTTGTGGCAAATCGTATCTGAA
GAATTGAAAGAAAAACGCGCAATTGGACTTCCGAAAGATCTTACTTTGACTGGCGCGGATTTTTACGAGGAAAATCTAAAATTCCAAACCAATCCGA
AATCAGTTTCAAGCTCTGCCGACAGCATTCAGAATGATGGAAAGTTCAATTCGGAAAATGGGATAATGTTCAAGCCGAGTGAAACACCAATTGTTCT
TGACGTGGTTTTACCACGAAATAAAAGTAATGTTTGTGGTTTATTAATTAGACCAGGAAAGAACGGAAAAGATGTTATTAAAACTATTGAAATAATA
TGGAAAGGTTCATCAAAAGGTCCCTGGAATCTTGTAGCAGTCCCAACAACAGGGGATCTAGGATTTAATCTCACTCTTTCTGCAAATAATGAAAATA
AAGTTTTAATCATTGATCCGGTGCCTGCTGAAGAATTGAAGCTTATCCTACATGCGGACAAAGAAAAAGGTTCAAGCATCCGGCTGTCAGTAATGCA
CAACTGCCAATATTCTCCAACAATGAAGATTAGCGATTGTCTCGAATCATTTGAAACGAATGAAAAATTGCAGAATTCCCAAACCGAAGGACCGGTA
AGTGTTTCTTGCCCGACGACCTGCAACTCATCTTCGGTTTGTGTCGGCTTCAAAGTTTATTCAACAGCGAGTCCAATTTGTTGGGCAGCTCACCAGG
TGTTCGGTAGCAACGGA

Smed-duk10

>AY067583

GTATATCCTCTTTAGCTCGTTTAATTAACTTTTGTTTATTAATTAGTTCCTCAAGATTGTTATTTTCGATGTTTAGAATTCCCTTTAGTTTTTCTAT
AATTTTTGTTGGTTCCATCTAAAATTATTAAATCTCTTTTAATTACCCATTAAATTTATTTAAATATTAACTAAATTGTGTGTTATTCATTCAACTC
TTAGTTTAATGTTTTGTTTTAATAAACTGCTACTTTAATTACTATAATTACTCGTTATTTATTTTATTATCGTTCTATTGCTTTTCCCCGTTTGTCG
TTATTCCCTTTACTTACCCCATTTCATTTTATCCCGCATTTTGCCCTTTTAATTATATGTTGTTTGCTTATGCGTCTTGTGAGTGTCGTTGGTATCT
TCAAGGGTGTTGTGTCATCAAGTATTAATGGATGTTGAATGCTTTGGCGTTGATATCTATTTCACTTAATTTCATATCAGTTTGTTTGCTTGGGTTT
NTGCAAAATAGTCATTGTTTATCTCTGTATGTATTCTCGCGACTGAGAGTTGGTTTCCATGGTTTCGATGATNAATTGGTCATTTTNATTTAAAATA
AATTATAAATTCATTG

Smed-duk5

>Contig6828.2

TCATATAATTAAATATTTATTTAGAATAAATATGAAAAATTTCACATTTATTCACTAAATCATTTTGCATTACTCGATTCTTCGACAACTTCCACAC
AACATTTTTCAAACACTTTGTTTACATCTTGGTCAGGGAAATGAGTTCGTCGTAATGCTTCTAATTCGTATCGTCTTCGTTCAAGTTTTCTTATTTG
ATAAACTAATCTGTTGATCTTTTCTCTGTCAATGCCTAAACCGTAAATTCCACTTGATATTTTTCCAATGTCTTCCAAATGTGCTTGTACATTTGCA
TAGATTGGACCCGATACACGGGCCCTGAGTCCAATTAGAAAATGATTGATTGCCGGGATCTCTAATACTGATCGATAATATCCGGCTCCCAAGTACA
GACCCAATCTTAATCCCAAGTCAGCCTTAATGAGGCCCGCCACATTCAATTTCAGTCCCGTCAAAAGTCTGAGATCCACAAAACCATTCACATACAT
GCATGTGAAGCAAGAAAGTATTAAAAGAGATAATTT

Smed-six

>F6AJIXP02FICZL

TTCTGCTGCTCGATCTCGTTGGCGTCGGTTTTTAAACCAATTAGACACCTGAGTTGTTGTCAAACTCGTCATTTCAGCGAGATCTTTCTTTTCTCTC
GGTGACGGGTAGGGATTATGCAAATACCATTGTCGAAGAACGGCTCTTGATTTTTCTTTGAAACAATAACTGGTTTCTTCACCGTCCCAAATCGTTC
TCGGCAATGGATATTTTCGTCGAATTCTGTACTTTGCCACAGCTCCCAGCGAGCGACCTTTGATTTTTTCTCTTCAATGTAATGTGCTTGCAACCAG
AGTGCCTGTAGTTTGTAATGGTTGTGCGGTGAAAAAGTGTACGATTCTAATATTCTATAGAGTTCTTTGAAATTTTGCCGATGAAAAGCAACTGCGG
CTTTTGCTGTTAGGACGCTTTCATTCGTTTGCAGCTGCTGGCAAGGTGGCAGAGACCAAATGAACAATGCTAATCTGTCGATGTGCCACCGTTTTCA
AGGACTTCGACAAACGCATGC

7.2 STEP-BY-STEP PROTOCOLS

This section provides a detailed guide for each protocol used in this study, which has been added to contribute to its easy reproducibility.

PROTOCOL 1: TOTAL RNA ISOLATION using the TRIZOL reagent (Life Technologies)

STEP	PREPARE BEFORE STARTING
1	Gloves: always wear gloves, include them during solutions and sterile RNAse-free materials preparation.
2	To have sterile equipment for RNAse-free experiments, autoclave for 2 times.
3	TRIZOL is toxic, mutagen, corrosive, light sensitive. Store it in the dark, avoid skin contact, do not breathe it and use eye protection.
4	DEPC-treated H_2O: dissolve diethylpirocarbonat 1% (1mL DEPC in 1L H_2O) in Mili-Q H_2O, shake vigorously with a magnet and incubate over night in a fume hood, then autoclave.
5	Cool the centrifuge to 4ºC, it takes 20 min.
6	Warm the metal block or water bath to 65ºC.
7	Maintain 70 % EtOH to -20 ºC.
8	Ice: transport the eppendorf tubes always on ice
9	Planarian: cut each planarian in 2 pieces and place them in a 1,5 mL eppendorf tube, then remove the water with a pipette.

	Procedure	Solution	Vol.	Temp.	Time	Remarks
10	Add to the 50-100 mg planarian	TRIZOL	500 µl	RT		TRIZOL: Use it in a chemical fume hood. Use eye protection. Avoid breathing vapour. Store in the dark. Keep below RT.
11	Homogenize tissue samples			RT	5 min	Homogenize tissue samples with a small blender (the blender should be clean with EtOH or autoclaved).
12	Incubation			RT	5 min	Necessary to dissociate nucleoprotein complexes.
13	Centrifuge 12000 x g*			4 ºC	10 min	Transfer the pink supernatant (containing ARN and ADN) to a new tube. The dark pellet contains all cell membranes.
14	Add to the pink supernatant and shake	chloroform	100 µl	RT	15 sec	Shake the tube by hand (200 µL chloroform /ml probe) to brake up the proteins.
15	Incubation			RT	3 min	There are three phases: in the clear upper aqueous phase is the ARN, the interphase and the lumpy lower layer contains the DNA and proteins respectively.
16	Centrifuge 12000 x g*			4 ºC	15 min	
17	Take the clear upper phase (RNA)					Transfer the clear upper phase with a 200 µL pipette to a fresh tube, do not touch the interphase.
18	To RNA precipitation add	2-propanol	250 µl			Mix by inverting the tube 3 times, to allow the ARN to precipitate (250 µL 2-propanol / mL TRIZOL).
19	Incubation			RT	10 min	
20	Centrifuge 12000 x g*			4ºC	10 min	The dark pellet contains the ARN.
21	Remove the colourless supernatant					At the bottom of the tube is a dark pellet.
22	Add	70% EtOH	500 µl			This wash step is used to remove the DNA and the chloroform impurities.
23	Vortex very gently					Be careful, do not take off the RNA pellet from the bottom.
24	Centrifuge 5000 x g*			4ºC	5 min	
25	Dry RNA			RT	7 min	Do not let completely dry.
26	Incubation (heat block)	DEPC H_2O	25µl	65ºC	10 min	To dissolve RNA: first incubate 2 min with the tube open, second 8 min with the tube close, third pipette the solution up and down several times.
27	Yields test: Nanodrop					1µL probe, as blanc 1µl DEPC-H_2O . Expected yields for RNA: ($A_{260/280}$ > 1.8) from 1-100 µg.
28	Yields test: 1% Gel					0,5µL probe + 4,5 µL H_2O Mili-Q +1µL Dye, 105 mV, Marker 1kb DNA.
29	Store	LiCl / EtOH	0,1/4(v/v)	-80ºC		LiCl 4M/EtOH 100%.

* rcf = g , 12000 g = 10600 rpm
Centrifuge: Eppendorf Centrifuge 5804R
Blender: Pellet Restle Motor, ON ISO-9001 Registered Firm Vineland, New Jersey 08360 Kontes Glass Company.

PROTOCOL 2: REVERSE TRANSCRIPTION OF RNA TO PRODUCE cDNA (SuperScript™ III Invitrogen)

STEP	HANDLING PRECAUTIONS
1	The mRNA used is treated with RNAse because it is not desired to amplified introns.
2	Gloves: wear always globes, also to prepare solutions and sterile RNAse free materials.
3	Sterile equipment: autoclaved 2 times for RNAse free.
4	Spin all the enzymes before use.
5	65ºC incubation: in a heat block.
6	Ice: transport always the tubes in ice.
7	Depc. H_2O: disolve diethylpirocarbonat 1% (1mL Depc in 1L H_2O) in Mili-Q H_2O, shake vigorously (with a magnet) and incubate over night in a fume hood, then autoclave.
8	The mRNA should appear as a smear between 500 bp and 8 kb. Most of the mRNA should be between 1.5 kb. and 2 kb.
9	Negative control: to verify that there have not been contamination, follow the same procedure but without RNA, check it out with the nanodrop.

	PROCESS	Solution	Vol.	Temp.	Time	Remarks
10	Mix and Incubate	RNA Buffer (of RT) 5X first strand DNAsa (RNAse free 10000 U/µL) H_2O Depc	1 µL = 3µg 2 µL 1 µL or 0.5µL 6 µL 10 µL	37ºC	20 min	Into the PCR machine (the DNAse degrade genomic DNA) 10X PCR Buffer [200 mM Tris-HCl (pH 8.4), 500 mM KCl]
11	Incubation			75ºC	5 min	Into the PCR machine (inactivate the DNAse)
12	Incubation			Ice	2 min	
13	Spin				briefly	
14	Mix and Incubate	Oligo dT dNTP Mix (RNAse free)	1 µL 1 µL 12 µL	65ºC	5 min	Into a PCR machine, here the DNA will be denatured 50 µM oligo$(dT)_{20}$: 900 ng/µL 10 mM dNTP Mix: 10 mM each dATP, dGTP, dCTP and dTTP, at neutral pH
15	Incubation			ice	1min	at least 1min on ice
16	Spin				briefly	
17	Mix and Incubate	Buffer first strand 5X DTT (0,1 M) RNAse OUT (40 units/µL) H_2O Depc RT SuperScript ™ III (200 U/µL)	2 µL 1 µL 1 µL 3 µL 1 µL 20 µL	50ºC	1h	Into a PCR machine Mix by pipetting gently up and down.
18	Incubation			70ºC	5 min	Inactivation of the RT (retrotranscriptase enzyme)
19	Store			-20ºC		
20	Controls					Nanodrop as a quality control, cDNA sould be tested in a PCR with primers from an already known gen .

PROTOCOL 3.1: CLONING WITH THE TA-METHOD

FIRST PCR: with the Taq DNA polymerase that has a nontemplate-dependent terminal transferase activity and adds a single deoxyadenosine (A) to the 3' ends of PCR products

STEP	PROCESS
1	Mix the components at RT, maintain in ice until PCR

[stock]	[final]	Components	1 x
		H_20 miliQ	18 µL
10 x	1 x	PCR Buffer (Invitrogen)	2.5 µL
50 mM	1.5 mM	$MgCl_2$ (Invitrogen)	0.75 µL
10 mM	0.2 mM	dNTP mix	0.5 µL
10 µM	0.5 µM	Primer 5' specific	1.25 µL
10 µM	0.5 µM	Primer 3' specific	1.25 µL
		Template DNA (cDNA superscript III)	0.5 µL
5 U/µL	0.1U/uL	Tag DNA polymerase (Invitrogen)	0.25 µL
		Total	25 µL

STEP	PROCESS
2	Set the following Touch Down PCR cycles

Process	Temperature	Time	Cycles
hold	94ºC	3'	1
Denaturation Annealing Extend	94ºC	30"	3
	65ºC	30"	
	72ºC	20"	
Denaturation Annealing Extend	94ºC	30"	3
	61ºC	30"	
	72ºC	20"	
Denaturation Annealing Extend	94ºC	30"	3
	59ºC	30"	
	72ºC	20"	
Denaturation Annealing Extend	94ºC	30"	26
	56ºC	30"	
	72ºC	20"	
hold	72ºC	7'	1
hold	4ºC	∞	

3	Test: Electrophoresis in a 1% Agarose gel: **Gel:** 40 mL 1% agarose gel contains 40 mL TBE, 0.4 g agarose and 0.5 µL Gel Red **Dye:** 0.1 µL Gel Red (Fermentas) + 1 mL LoadingDye 6x (Fermentas) **Control marker:** 6 µL : 1 µL 1kb DNA ladder (Fermentas) + 1 µLDye 6x-GelRed+ 4µL ddH_20 miliQ **Probe loaded in the gel bands**: 6 µL : 1 µL probe + 1 µL Dye + 4 µL H_20 Mili-Q **Volts :** 100 V **Time :** 15 min
4	Optional: it is possible to design nested primers and make a second PCR. This is used to increase the amount of PCR product.
5	Purification: *QuiAquick PCR Purification Kit* (Quiagen), purified elution in 30 µl dd H_2O mili-Q
6	Quantification: *Nano-Drop 1000* (Thermo Fischer Scientific inc)
	NEXT STEP: The PCR product is ligated into a vector, PCRII-TOP

PROTOCOL 3.2: CLONING WITH THE TA-METHOD (TA CLONING KIT)

LIGATION: using the vector PCRII-TOPO that contains several promoter sites.

This process takes at least 4 hours, optional ON.

STEP	PROCESS
1	Set the PCR machine to 14ºC
2	Mix the following components and maintain at 14ºC, 4 hours or ON in a PCR machine.

[stock]	[final]	TUBE	1X
100 ng/µL	5 ng/µL	Fresh PCR product	0.5 µL
10X	1X	Ligation Buffer	1 µL
4 U/µL	0.2U/µL	T4 Ligase	0.5 µL
25 ng/µL	2.5ng/µL	pCR®II	1 µL
---	---	H_2O	7 µL
		Total	10 µL

NEXT STEP: The bacteria *E. coli* will be transform by a heat shock with the ligation product and will be grown in LB medium to produce a big amount of plasmids, to clone it.

PROTOCOL 3.3: CLONING WITH THE TA-METHOD

TRANSFORMATION: using *E. coli* DH5α strain

STEP	PREPARE BEFORE STARTING
1	Ice is necessary to thaw and maintain *E.coli* before use
2	LB glass tubes without Ampicilin (*L-Broth, Miller, Luria-Bertani*, 25g/L)
3	LB plates with 100 µg/mL Ampicilin (*L-Broth, Miller, Luria-Bertani*, 25g/L)
4	Competent bacteria: *E. coli* DH5α strain
5	42 ºC heat block or water bath
6	37 ºC shaker

	PROCESS	Solution	Vol.	Temp.	Time	Remarks
7	Defrost	*E. coli* cells DH5α strain	50 µL	ice	10 min	Defrost *E.coli* by introducing the tube with the bacteria in ice no longer than 10 min.
8	Add	Ligation + *E.coli*	5 µL	ice	30 min	Add 5 µl ligation to the cells, after pipetting gently 3 times, place it in ice 30 min.
9	Prepare	LB plates, LB glass tubes	1 petri dish / gen 1 glass tube / gen	37 ºC RT	30 min	Let LB plates in 37 ºC room downwards, and LB tubes at RT at least 30 min before use.
10	Heat shock	(Ligation + *E.coli*) tube	55 µL	42º C	1 min	After placing the tube in a heat block at 42ºC just during 1 min, place it rapidly in ice.
11	Add	LB medium	250 µL	ice		Add 250 µL LB media to the transformation
12	Shaker	Transformation + LB	300 µL		1h	Cultivate the bacteria by shaking the tube at 37ºC during 1h.
13	Prepare	X-Gal [20 mg/µl]	60 µl	RT	~1h	Work steril: add 60 µL X-Gal [20 mg/µL] to the plate and let it at 37 ºC upwards.
14	Spread	culture	150 µl	RT	15 min	Work steril: spread 150 µL transformation to each plate upwards, let it 15 min at RT to dry.
15	Growth	culture			15-16 h	Place the plate at 37ºC downwards ON. The bacteria with the right transformant will grow withe colonies.
16	Pick up	white colonies	single colony	RT	~18h	Next day let grow single colonies in 3 mL LB glass tubes at 37ºC, ~18h or ON.
17	MINI-PREP	LB culture	3 mL	RT		Plasmid DNA Purification (NucleoSpin® Plasmid QuickPure: Isolation of high-copy plasmid DNA from E.coli) MACHEREY-NAGEL

NEXT STEP: Sequencing is necessary to see the insertion direction of the gene ligated into the plasmid.

PROTOCOL 3.4: CLONING WITH THE TA-METHOD

SEQUENCING: with M13F or M13 R primers

STEP	PROCESS
1	Prepare reaction mix on ice

[stock]	[final]	Components	1 x
3.2 µM	0.32 µM	Primer M13 R or M13F	1 µL
10X	1X	MIX: BYG DIE 3.1	1 µL
		Template DNA	1 µL
		H_20 miliQ	7 µL
		Total	10 µL

STEP	PROCESS
2	Set the following PCR cycles

Process	Temperature	Time	Cycles
hold	96ºC	1'	1
Denaturation	96ºC	10''	25
Annealing	50ºC	10''	
Extend	60ºC	4'	
hold	4 ºC	∞	

3	Adding 10 µl H_20 to every probe after PCR can be necessary depending on the current sequencing facilities used.
4	Alignment of the sequencing result is necessary to check the direction of the insert into the plasmid and consequently use the Sp6- or T7-promoter to amplified the sense or antisense ssRNA. The following multiple sequence alignment program can be used (http://bioinfo.genotoul.fr/multalin/multalin.html)
	NEXT STEP: a second PCR to amplified the insert with the M13F and the M13R

PROTOCOL 3.5: CLONING WITH THE TA-METHOD

PCR 2: to extract the insert out of the plasmid, with the M13 F and M13 R primers.

STEP	PROCESS
1	Prepare reaction mix on ice

[stock]	[final]	Components	1 x
		H_20 miliQ	74.6 µL
10 x	1x	PCR Buffer (Invitrogen)	10 µL
50 mM	1.5 mM	$MgCl_2$ (Invitrogen)	4 µL
10 mM	0.2 mM	dNTP mix	2 µL
10 µM	0.5 µM	M13 F	4 µL
10 µM	0.5 µM	M13 R	4 µL
		Template DNA (Mini-Prep dilutet 1:20)	1 µL
5 U/µl	2.5 U	Tag DNA polymerase (Invitrogen)	0.4 µL
		Total	100 µL

STEP	PROCESS
2	Set the following PCR cycles

Process	Temperature	Time	Cycles
hold	95ºC	5'	1
Denaturation	94ºC	30''	35
Annealing	55ºC	30''	
Extend	72ºC	1' 2"	
hold	72ºC	10'	1
hold	4ºC	∞	

3	Test: Electrophorese in a 1% Agarose gel: **Gel:** 40 mL 1% agarose gel contains 40 mL TBE, 0.4 g agarose and 0.5 µL Gel Red **Dye:** 0.1 µL Gel Red (Fermentas) + 1 mL LoadingDye 6x (Fermentas) **Control marker:** 1 µL 1kb DNA ladder (Fermentas) + 1 µLDye 6x-GelRed + 4 µL ddH_20 miliQ **Loaded** : 1 µL probe + 1 µL Dye + 4,5 µL H_20 Mili-Q **Volts :** 100 **Time :** 15 min
4	Purification: *QuiAquick PCR Purification Kit* (Quiagen), purificat elution in 30 µL dd H_2O mili-Q
	NEXT STEP: make dsRNA with T7- and Sp6-RNA-polymerase, or make antisense RNA with Sp6- or T7 -RNA polymerase depending on the promoter position. As a control for the in situ is possible to make a sense RNA. The polymerase used will also depend on the promoter position.

PROTOCOL 4.1: CLONING WITH THE T7-METHOD

FIRST PCR: specific primers with linkers

STEP	PROCESS
1	Prepare the reaction mix on ice

[stock]	[final]	Components	1 x
		MiliQ H_2O	36.5 µL
10 x	1 x	PCR Buffer (Invitrogen)	5 µL
50 mM	1.5 mM	$MgCl_2$ (Invitrogen)	1.5 µL
10 mM	0.2 mM	dNTP mix	1 µL
10 µM	0.5 µM	Primer 5' specific	2.5 µL
10 µM	0.5 µM	Primer 3' specific	2.5 µL
		Template DNA (cDNA superscript III)	0.5 µL
5 U/µL	2.5 U	Tag DNA polymerase (Invitrogen)	0.5 µL
		Total	50 µL

STEP	PROCESS
2	Set the following touch down PCR cycles

Process	Temperature	Time	Cycles
hold	94ºC	3'	1
Denaturation	94ºC	30''	3
Annealing	65ºC	30''	
Extend	72ºC	50''	
Denaturation	94ºC	30'	3
Annealing	61ºC	30'	
Extend	72ºC	50''	
Denaturation	94ºC	30'	3
Annealing	59ºC	30'	
Extend	72ºC	50''	
Denaturation	94ºC	30''	26
Annealing	56ºC	30''	
Extend	72ºC	50''	
hold	72ºC	7'	1
hold	4ºC	∞	

3	**Test:** Electrophorese in a 1% agarose gel: **Gel:** 40 mL 1% agarose gel contains: 40 mL TBE, 0.4 g agarose and 0.5µL Gel Red **Dye:** 0.1 µL Gel Red (Fermentas) + 1 mL LoadingDye 6x (Fermentas) **Control marker:** 1 µL 1kb DNA ladder (Fermentas) + 1 µL Dye 6x-GelRed + 4 µL miliQ ddH_20 **Loaded:** 1 µL probe + 1 µL Dye + 4,5 µL miliQ ddH_20 **Volts:** 100 **Time:** 15 min
4	**Purification of PCR:** Quiagen PCR purification kit.

PROTOCOL 4.2: CLONING WITH THE T7-METHOD

SECOND PCR: to make the template for ss- and ds-RNA, with specific Primers + Universal Primers T7

STEP	PROCESS
1	Prepare reaction mix on ice

[stock]	[final]	Components	Sense 1 x	Antisense 1 x	dsDNA 1 x
		H_20 miliQ	32 µL	32 µL	32 µL
10 x	1x	PCR Buffer (Invitrogen)	5 µL	5 µL	5 µL
50 mM	1.5 mM	$MgCl_2$ (Invitrogen)	1.5 µL	1.5 µL	1.5 µL
10 mM	0.2 mM	dNTP mix	1 µL	1 µL	1 µL
10 µM	0.5 µM	Primer 5' specific	------	2.5 µL	------
10 µM	0.5 µM	Primer 3' specific	2.5 µL	------	------
10 µM	0.5 µM	Universal T7 Primer 5'	2.5 µL	------	2.5 µL
10 µM	0.5 µM	Universal T7 Primer 3'	------	2.5 µL	2.5 µL
		Template DNA (first PCR product)	5 µL	5 µL	5 µL
5 U/µL	2.5 U	Tag DNA polymerase (Invitrogen)	0.5 µL	0.5 µL	0.5 µL
		Total	50 µL	50 µL	50 µL

STEP	PROCESS
2	Set the following PCR cycles

Process	Temp.	Time	Cycles
hold	94ºC	3'	1
Denaturation	94ºC	30"	35
Annealing	55ºC	30"	
Extend	72ºC	1'30"	
hold	72ºC	7'	1
hold	4ºC	∞	

3	**Test:** Electrophorese in a 1% Agarose gel: **Gel:** 40 mL 1% agarose gel contains 40 mL TBE, 0.4 g agarose and 0.5 µL Gel Red **Dye:** 0.1 µL Gel Red (Fermentas) + 1 mL LoadingDye 6x (Fermentas) **Control marker:** 1 µL 1kb DNA ladder (Fermentas) + 1 µL Dye 6x-GelRed + 4 µL miliQ ddH_20 **Loaded:** 1 µL probe + 1µL Dye + 4,5 µL miliQ ddH_20 **Volts:** 100 **Time:** 15 min
4	**Purification:** QUIAquick PCR Purification Kit, elution in 30 µL mili-Q dd H_2O
5	**Sequencing:** is recommended to be sure of the cloned sequence.
	The products of these PCR are the templates to make dsRNA for immuno and ssRNAs for in situ experiments.

PROTOCOL 5: dsRNA PROBE TRANSCRIPTION WITH THE TA-CLONING METHOD AND PRECIPITATION.

Template DNA amplified with M13F and M13R primers.

STEP	PROCESS
1	Preheating 2 water baths or heat 2 blocks at 68ºC and 37 ºC. Cool the centrifuge at 4ºC. Prepare the reaction mixtures on ice.
2	Mix PCR components for **TRANSCRIPTION with T7 polymerase**

[stock]	[final]	Components	1 x
		H_20 DEPC	2 µL
10 x	1x	T7 Transcription buffer Roche	2 µL
40 U/µL	40 U	RNase inhibitor Roche	1 µL
25 mM	3,75 mM	rNTP mix Roche	3 µL
20 U/µL	40 U	T7 RNA polymerase Roche	2 µL
(200 ng/µL)	2 µg	PCR Product	10 µL
		Total	20 µL

Mix PCR components for **TRANSCRIPTION with SP6 polymerase**

[stock]	[final]	Components	1 x
		H_20 DEPC	2 µL
10 x	1 x	Sp6 Transcription buffer Roche	2 µL
40 U/µL	40 U	RNase inhibitor Roche	1 µL
25 mM	3,75 mM	rNTP mix Roche	3 µL
20 U/µL	40 U	Sp6 RNA polymerase Roche	2 µL
(200 ng/µL)	2 µg	PCR Product	10 µL
		Total	20 µL

3	**TRANSCRIPTION:** Incubate into the heat block 4h at 37 ºC the Sp6 transcription and T7 transcription separately, to get the sense and the antisense mRNA strand.
4	Add: 1µL DNAse I recombinant 10 U/ µL (RNAse free) to each transcription -----> 30 min heat block warming at 37ºC ------> store ON at -20ºC or go ahead with precipitation after step 5.
5	Mix sense and antisense RNA into the same tube.
6	**PRECIPITATION**: Add to the mix : Glycogen 1 µL Stop solution 579 µL Phenol : Chloroform : Isoamyl alcohol (25: 24:19) 600 µL (very toxic, work under the hood ! ! !) (mix gently by hand during 10 sec.)
7	Spin: 5 min, 12000 g, 4ºC ----------> Take out the upper phase and add: Chloroform 600 µL (mix by hand turning over)
8	**DENATURATION**: Spin: 5 min 12000 g 4ºC ----------> Take out the upper phase ---------> and heat 20 min in the 68ºC water bath
9	**HYBRIDATION**: heat the same tube 45 min in the heat block at 37ºC
10	**PRECIPITATION:** Add: Glycogen Invitrogen ref Nº 10814 1 µL Ethanol 100% -20ºC (RNAse free) 800 mL 3h or ON at -20ºC
11	Spin : 20 min, 16000 g, 4ºC (if you do not see a pellet, add Glycogen and centrifuge) -------> remove the supernatant
12	Wash the pellet by adding 200 µL ethanol 70% , precool Ethanol 70% at -20ºC (Ethanol 70% diluted in H_20 DEPC)
13	Spin : 20 min, 16000 g, 4ºC ----------> Discard the supernatant ----------> dry at 37ºC ----------> Resuspend in 11,5 µL H_20 (dsRNA is very stable)
14	Test of concentration Nº1: measurement with the Nanodrop; Test of concentration Nº2: run the probes in a gel 1%, 120V, 15 min
15	Store at -20ºC until injection.
	SOLUTIONS : Stop solution: 1,8M NH_4OAc + 0,5M EDTA + 10% SDS in DEPC H_2O diluted in H_2O. 25mM rNTP mix: CTP + GTP + ATP + UTP (25mM each).

PROTOCOL 6: dsRNA PROBE TRANSCRIPTION WITH THE T7-CLONING METHOD AND PRECIPITATION.

Template DNA was amplified with T7 -5'- and T7- 3' Universal Primers.

STEP	PROCESS
1	Preheating 2 water baths or 2 heat blocks at 68ºC and 37 ºC and cool the centrifuge at 4º C. Prepare the reaction mixture on ice
2	Mix PCR components for **TRANSCRIPTION with T7 polymerase**

[stock]	[final]	Components	1 x
		H_20 DEPC	2 µL
10 x	1x	T7 Transcription buffer Roche	2 µL
40 U/µL	40 U	RNase inhibitor Roche (Cat Nº 03335402-001)	1 µL
25 mM	3,75 mM	rNTP mix Roche	3 µL
20 U/µL	40 U	T7 RNA polymerase Roche	2 µL
(200 ng/µL)	2 µg	PCR Product	10 µL
		Total	20 µL

3	**TRANSCRIPTION:** Incubate into the water bath 4h at 37 ºC the T7 transcription --------> after 2 h do a spin to recollect some evaporated water.
4	Add: 1µL DNAse I recombinant 10 U/ µL (RNAse free) to each transcription ----------> warm it into the heat block 30 min at 37ºC ----------> go ahead with precipitation or store ON at - 20ºC
5	Go ahead with the purification or store at -20ºC ON or longer if necessary until precipitation. Instead the precipitation described as follows, a quick column purification kit, the Mini Quick Spin RNA Columns (Roche) can be used. This column yields an 80 % of the amount obtained by the transcription.
6	**PRECIPITATION:** Add to the mix : Glycogen 1 µL Stop solution 579 µL Phenol : Chloroform : Isoamyl alcohol (25: 24:19) 600 µL (very toxic, work under the hood ! ! !) (mix gently by hand during 10 sec.)
7	Spin: 5 min, 12000 g, 4ºC ----------> Take out the upper phase and add: Chloroform 600 µL (mix by hand turning over).
8	**DENATURATION:** Spin: 5 min, 12000 g, 4ºC ----------> Take out the upper phase ---------> and heat 20 min in the 68ºC water bath.
9	**HYBRIDATION:** heat the same tube 45 min in the heat block at 37ºC.
10	**PRECIPITATION:** Add: Glycogen Invitrogen ref Nº 10814 1 µL Ethanol 100% -20ºC (RNAse free) 800 mL 3h or ON at -20ºC
11	Spin : 20 min, 16000 g, 4ºC (if a pellet is not to see, add Glycogen and centrifuge) -------> remove the supernatant
12	Wash the pellet by adding 200 µL ethanol 70% precool Ethanol 70% at -20ºC, (Ethanol 70% is diluted in DEPC H_20)
13	Spin : 20 min, 16000 g, 4ºC ---------> Discard the supernatant ----------> dry to 37ºC ----------> Resuspend in 11,5 µL H_20 (dsRNA is very stable)
14	Test of concentration Nº1: measurement with the nanodrop. Test of concentration Nº2: run the probes in a gel 1%, 120V, 15 min
15	Store at -20ºC until injection.
	SOLUTIONS: Stop solution : 1,8M NH_4OAc + 0,5M EDTA + 10% SDS in DEPC H_2O. 25mM rNTPmix: CTP + GTP + ATP + UTP (25mM each)

PROTOCOL 7: TRANSCRIPTION OF THE ANTISENSE SINGLE STRANDED RNA PROBE (ssRNA)

For in situ hybridization with DIG or FITC labeling, using T7-, SP6- or T3-RNA polymerase, for TA- and T7-method.

STEP	PROCESS
1	Preheating 2 water baths or 2 heat blocks at 37 ºC and 65ºC. Prepare the reaction mixture on ice
2	The template used for this transcription can be : the purified PCR 2 (antisense or sense) from the T7-method; or the purified PCR 2 (amplified with M13 primers) from the TA-method
3	Mix PCR components: FITC or DIG, both can be labeled in red or green colour. DIG: Digoxigenin . FITC: fluorescein isothiocyanate

[stock]	[final]	Components	1 x
		H_20 DEPC	3 µL
10 x	1x	T7 Transcription buffer Roche	2 µL
40 U/µL	40 U	RNase inhibitor Roche Cat Nº 03335402-001	1 µL
25 mM	3,75 mM	Nucleotide mix DIG or FITC labeled	2 µL
20 U/µL	50 U	T7 RNA polymerase (or T3, or Sp6) Roche	2 µL
	0,5 µg	PCR Product (purified DNA as template)	10 µL
		Total	20 µL

4	**TRANSCRIPTION:** Incubate all the PCR components 2h at 37ºC with T7, T3 or Sp6 polymerases from Roche ----------> Spin the components shortly before use.
5	Add: DNAse I recombinant 10 U/ µL (RNAse free) 1µL ----------> incubate 30 min at 37ºC
6	Incubate: 1h at -20ºC, and go ahead with precipitation.
7	**PRECIPITATION:** add the following components to the 21µL mix, and let precipitate 30 min at -20ºC ---------> Add: 30 µL H_20 DEPC 5 µL Amonium acetat 5M 150 µL EtOH 100% (-20 ºC precooled)
8	Spin: 20 min, 12000 g, 4ºC ---------> if you do not see a pellet, do not remove all the upper phase.
9	Add: 200 µL Ethanol 70% (-20ºC) (Ethanol 70% is diluted in H_20 DEPC)
10	Spin: 15 min, 12000 g, 4ºC ---------> remove the Ethanol
11	Dry the pellet at RT 5-10 min
12	Resuspend 2-3 min, 65ºC in 50 µL H_20 DEPC (H_20 DEPC is preheated at 65ºC)
13	Store at -20ºC or maintain on ice for the following procedures.
14	Test of concentration Nº1: run the probes in a Agarose gel 1%, 120V, 15 min. Test of concentration Nº2: measurement with the nanodrop.
15	The necessary amount for in situs depends on the probe, from 90 ng/ µL to 600 ng/ µL. Higher amounts are possible.

PROTOCOL 8.1: IN SITU HYBRIDIZATION

DAY 0: What to do before starting an in situ hybridization

STEP	TO PREPARE FIRST	SOLUTIONS	REMARKS
FIRST	Labeled probes		- Be sure the DiG or FITC labeled ssRNA probes are prepared.
SECOND	3 basic solutions	SSC 20X MAB 5X ----> pH calibration PBS 10X ----> pH calibration	- The 3 basic solutions have to be made at least 2 days before the beginning of the in situ. - The preparation needs one day long. - After pH calibration of two of them, autoclave all 3 solutions
THIRD	2 solutions	Prehybridization solution Hybridization solution	- Prepare the Hybridization solution with the Prehybridization solution. - Both solutions can be made a day before used - It takes about 5 hours to dissolve Dextransulfat in the Prehybridization solution with the shaker.
FOURTH	1 solution	4% PFA / Holtfreter	- Do this solution at least one day before the beginning of the in situ. It will be needed at the end of the second day.
FIFTH	Other solutions		- The rest of the solutions can be made at the beginning or during the day of use, as recommended.

PROTOCOL 8.2: IN SITU HYBRIDIZATION (The process is RNAse free)

DAY 1: Animal fixation with Carnoy

STEP	TO PREPARE FIRST	SOLUTIONS	VOL.	TEMP.	TIME	REMARKS
1		H_2O	~ 25 ml	on ice	1- 5 min	- Place 30-35 small animals, in a petridish with water, on ice until they stop moving. - Remove the water.
2	HCL stock is 32%	2% HCl/Holtfreter	~ 25 ml	on ice	3 - 5 min	- To kill the animals, add 2% HCl/Holtfreter solution into a 50 mL or 25mL falcon. - Critical !: Invert the tube gently for the first minute and every ~ 60 seconds to remove the mucus and to avoid shrivelled animals. - Regenerating animals should not be in the HCl solution more than 3 min.
3		Carnoy (fresh,4°C)	~ 40 ml	4°C	120 min	- Remove the HCL. - Shake the falcon when adding carnoy to prevent animals from sticking to each other.
4		MetOH (-20°C)	~ 25 ml	4°C	60 min	- Throw Carnoy away, add MetOH and let it shaking.
5	H_2O_2 Stock is 30%	6% H_2O_2 in MetOH	~ 25 ml	RT	ON (12-20h)	- Bleaching: H_2O_2 removes the pigmentation. - Leave animals in H_2O_2 /MetOH under a cold lamp. Avoid the solution to overheat !!! - After 20 h remove the animals if they are discoloured, otherwise, let them longer.
6		MetOH	3X~ 25ml	RT	30 min	- Wash 3 x10 min in MetOH. - Store in MeOH at -20 ºC for several weeks in 2mL tubes.
7	Prepare for the next day	- 4% PFA/Holtfreter - Prehybridization solution - Hybridization solution				

PROTOCOL 8.3: IN SITU HYBRIDIZATION (The process is RNAse free)

DAY 2: Probe Hybridization

STEP	TO PREPARE FIRST	SOLUTIONS	VOL.	TEMP.	TIME	REMARKS
8	4% PFA/Holtfreter: prepare the day before	70% EtOH/Holtfreter (4°C)	~50 mL	4°C	30 min	Shaking the solution with animals in baskets
9	Prepare for later: a 37°C bath	50% EtOH/Holtfreter (4°C)	~50 mL	4°C	30 min	Shaking the solution with animals in baskets
10		30% EtOH/Holtfreter (4°C)	~50 mL	4°C	30 min	Shaking the solution with animals in baskets
11	Preheat the solution with Proteinase K	TPBS 1X	~50 mL	4°C	30 min	Shaking the solution with animals in baskets
12	37°C Room	New TPBS with 20 µg/ml proteinase K (proteinase K stock is 20 mg/mL)	35 mL	37°C	6-8 min	- 6 min for regenerating, 8 min for non regenerating animals. - Do not shake animals, just move the solution every 2 min.
13		Holtfreter	~50 mL	4°C	1 min	Shaking the solution with animals in baskets
14	Very toxic	4% PFA/Holtfreter (fresh, 4°C)	~25 mL	4°C	60 min	Shaking the solution with animals in baskets. Fixative.
15	Preparing a 55°C oven	Holtfreter	~25 mL	4°C	1 min	Shaking the solution with animals in baskets
16		Holtfreter	~25 mL	4°C	60 min	Shaking the solution with animals in baskets
17		TEA (0.1M) (fresh) (pH: 7.6)	10 mL	RT	15 min	Shaking the solution with animals in baskets
18		TEA (0.1M) (fresh) (pH: 7.6)	10 mL	RT	15 min	Shaking the solution with animals in baskets
19		New TEA with 25 µL of Acetic Anhydride	50 mL	RT	15 min	Shaking the solution with animals in baskets. AA is very aggressive !!
20		New TEA with 50 µL of Acetic Anhydride	50 mL	RT	15 min	Shaking the solution with animals in baskets. AA is very aggressive !!
21	Preparing a 70°C bath	TPBS	40 mL	RT	10 min	Shaking he solution with animals in baskets
22		Prehybridization solution	500 µL	55°C	≥ 60 min	- 4 animals in every eppendorf. - Animals can be stored in Prehybridization solution at -20ºC.
23	Prepare days before: transcription of antisense RNA labeled with (DIG) or FITC, (see protocol 7)	Hybridization solution + probe (single stranded mRNA: 0. 2 - 2 ng/ µL)	500 µL	55°C	ON (≥ 15h)	- Before adding, preheat the probe 10 min at 70°C in Hybrid. Solution, and maintain at 55ºC until hybridization. - Calculate the necessary amount by every probe concentration.

PROTOCOL 8.4: IN SITU HYBRIDIZATION (The process is RNAse free)

DAY 3: Antibody Hybridization

STEP	TO PREPARE FIRST	SOLUTIONS	VOL.	TEMP.	TIME	REMARKS
24	Prepare a 55°C bath	100% Hybe solution	~50mL	55°C	1 min	Wash the animals in baskets
25		100% Hybe solution	~50mL	55°C	10 min	Wash the animals in baskets
26		75% Hybe solution	~50mL	55°C	10 min	Wash the animals in baskets
27		50% Hybe solution	~50mL	55°C	10 min	Wash the animals in baskets
28		25% Hybe solution	~50mL	55°C	10 min	Wash the animals in baskets
29	Prepare a 60°C bath	2X SSC + 0.1% Triton	~50mL	55°C	30 min	Wash the animals in baskets
30		2X SSC + 0.1% Triton	~50mL	55°C	30 min	Wash the animals in baskets
31		0.2X SSC + 0.1% Triton	~50mL	55°C	30 min	Wash the animals in baskets
32		0.2X SSC + 0.1% Triton	~50mL	55°C	30 min	Wash the animals in baskets
33		Buffer I	50 mL	RT	10 min	Wash the animals in baskets
34		Buffer I	50 mL	RT	10 min	Wash the animals in baskets
35	Dissolve the Blocking Solution in 60°C water bath	Buffer II eluate Blocking Sol.	500 µL	RT	30 min	Change the baskets for a 24 wells plate. Shake the plate.
36		1: 2000 anti-DIG AP/Buffer II	500µL	RT	≥ 3 h	24 wells plate. Shake. (3.25 µL anti-DIG AP in 6.5 mL Buffer II)
37		Buffer I 8 times	~50mL	RT	8X 10 min	Wash in baskets . Shake. Total number of washings ≥ 8.
38	Prepare PVA for the next day	Buffer I	5 mL	4°C	ON	Washing in baskets . Shake.

PROTOCOL 8.5: IN SITU HYBRIDIZATION (THE PROCESS IS RNASE FREE)

DAY 4: Development

STEP	TO PREPARE FIRST	SOLUTIONS	VOL.	TEMP.	TIME	REMARKS
39		TMN	1 mL	RT	10 min	24 wells plate. Shaking.
40	NBT/BCIP Stock (Roche)	20µL NBT/BCIP Stock Solution / 1 ml PVA	500 µL	RT	minutes to days !	- In 24 wells plate. In darkness. With developing solution. - Developing time depends on each probe: from minutes to days.
41	**STOPPING THE REACTION NBT/BCIP**			**---------->**	When it reaches the desired colour intensity.	
42	Wash 2 times	PBS 1X	20 mL	RT	5 min	
43	Fix	4 % PFA	10 mL	RT	1h	PFA must not be fresh.
44	Wash 2 times	PBS 1X	20 mL	RT	5 min	
45	Series of Ethanol washes	30% EtOH/PBS	10 mL	RT	5 min	
46		50% EtOH/PBS	10 mL	RT	5 min	
47		70% EtOH/PBS	10 mL	RT	5 min	
48		100% EtOH	10 mL	RT	5 min	
49		70% EtOH/PBS	10 mL	RT	5 min	
50		50% EtOH/PBS	10 mL	RT	5 min	
51		30% EtOH/PBS	10 mL	RT	5 min	
52	Wash 2 times	PBS 1X	20 mL	RT	5 min	
53	Prepare maintenance solution	70% glycerol/PBS		4°C	days	Use the necessary amount of solution to cover every probe
54	Mount the objects	With Slow Fade Medium	a drop	RT	seconds	On a glass slide with cover, for long term storage

LEGEND :

Vol.: Volume,
Temp.: Temperature,
RT: Room temperature,
ON: Over night,
PFA: Paraformaldehyde,
PVA: Polyvinyl alcohol
BCIP: 5-bromo-4- chloro-3-indolyl phosphate
NBT: NitroBlue Tetrazolium
anti-DIG: anti-digoxigenin antibody

- An (anti-DIG) conjugated to alkaline phosphatase, (BCIP) and (NBT) is used to detect the hybridized probe colorimetrically.
- 4% PFA/Holtfreter: Prepare it fresh. Dissolve the PFA in Holtfreter by vortex and warming the solution at 70°C. Cool the solution at 4°C before using.

PROTOCOL 8.6: IN SITU SOLUTIONS

Fixation solutions: (1-4). Basic solutions: (5, 6, 7) to prepare 3 days before. Probe hyb. Solutions: (8-19) 8 and 9 prepare at day 1.

	SOLUTION	[ ] in VOLUMEN	COMPOUNDS	REMARKS
1	Holtfreter (HF)	2 L	14.98 ml/2L (NaCl 5 M) 8.32 ml/2L (KCl 0.1 M) 4.54 ml/2L (CaCl 0.25 M) 11.9 ml/2L ($NaHCO_3$ 0.25 M)	- Mix the four components and add 2000 mL dd H_2O mili-Q. - Autoclave after the mix.
2	2% HCl / Holtfreter	2 % in 200 mL	12.5 ml HCl 32% 187.5 ml HF	- **FRESHLY PREPARE** - Prepare HCl under the hood. (HCl stock is at 32%)
3	Carnoy	200 mL	60 % EtOH (120 mL) 30 % Chloroform (60 mL) 10 % Acetic Acid (20 mL)	- **FRESHLY PREPARE** - Prepare the Chloroform solution under the fume hood and with glass mess cylinder. Chloroform destroys plastic pipettes.
4	6% H_2O_2 / MetOH	6% in 25 mL	Keep H_2O_2 stock at 30 %	
5	**20X SSC**	20 X in 1 L	3 M NaCl 0.3 M Tri-sodium citrate.	- 175.32 g NaCl (58.44 g/mol) - 88.23 g Tri-sodium citrate (294.1 g/mol) + H_2O ---> **AUTOCLAVE** the SSC solution
6	**5X MAB**	5 X in 1 L	500 mM maleic acid (116.07 g/mol) 750 mM NaCl (58.44 g/mol)	- Adjust the pH to 7.5 with white pills of NaOH. Add ~41.0 g NaOH ~ 197 pills, one by one until the solution turn colourless. Be careful, exothermic reaction. After adjust the pH **AUTOCLAVE** it. 58.3 g maleic acid, 43.83 g NaCl
7	**PBS**	10 X in 1 L	80 g NaCl 2 g KCl 14.4 g Na_2HPO_4 2.4 g KH_2PO_4	- Add the 4 components in 800 ml H_2O mili-Q, - Adjust the pH 7.4 with HCl (pH low), or NaOH (pH high) - **AUTOCLAVE** the PBS solution
8	Prehybridization solution	200 mL	50 % Formamide 5 X SSC 1 mg/ml Yeast total RNA 0.1 mg/ml Heparina 0.1 % Tween 20 (stock 10%) 10 mM DTT (Stock 1M)	100 mL Formamide 50 mL SSC 20X 200 mg Yeast 0.4 mL Heparina (is stored in eppendorfs at 50 mg/mL) 2 mL Tween 20 2 mL DTT (50 mL recipient)
9	Hybridization solution	50 mL	Prehybridization Solution 10 % Dextran Sulfat.	- In 50 mL falcon: 5 g Dextran Sulfat + 45 mL Prehybridization Solution. - Dissolve it in the shaker a day before use.
10	70% EtOH/ Holtfreter	50 mL	32.5 mL EtOH + 17.5 mL Holtfreter	
11	50% EtOH/ Holtfreter	50 mL	25 mL EtOH + 25 mL Holtfreter	
12	30% EtOH/ Holtfreter	50 mL	15 mL EtOH + 85 mL Holtfreter	
13	4% PFA /Holtfreter (4g / 100 ml)	4% in 50 mL	Paraformaldehyde	- **Very toxic, use the hood !!! FRESHLY PREPARED**. After dissolve 2g Paraformaldehyde + 45mL Holtfreter by vortex and warming the solution at 70 ºC, add Holtfreter until 50 mL. Keep the solution at 4ºC in the fridge.
14	TPBS	100 mL	0.1 % Triton 1x PBS	- Mix 10 mL PBS 10X + 1 mL Triton 10X + 89 mL H_2O - Filter the solution before use.
16	Proteinase K / TPBS	20 µg/mL in 35 mL	35 mL TPBS 27 µL Proteinase K	- Preheat TPBS at 37ºC. - **Add the proteinase K just before use** (Stock 25 mg/mL) .
17	TEA	0.1 M in 200 mL	Triethanolamine	- **FRESHLY PREPARE.** Viscous solution. Cut the 2ml tip to take 2.654 mL Triethanolamine in 200 mL H_2O - Adjust the pH to 7.6 with 1550 µL HCl 32%
18	TEA with Acetic Anhydride	2.5 µL / mL in 50 mL	125 µL Acetic Anhydride 50 mL TEA	- **FRESHLY PREPARE,** prepare it just before use (Acetic Anhydride is a liquid that needs special store conditions)
19	TEA with Acetic Anhydride	5 µL / mL in 50 mL	250 µL Acetic Anhydride 50 mL TEA	- **FRESHLY PREPARE**, prepare it just before use.

PROTOCOL 8.7: IN SITU SOLUTIONS : Prepare hybridization and antibody solutions: (20-28) at day 3, development solutions: (29-36) at day 4.				
	SOLUTION	**[ ] in VOL.**	**COMPOUNDS**	**REMARKS**
20	Buffer I	400 mL	1X MAB 0,1% Triton X-100/ H_2O	Add autoclaved mili-Q dd H_2O (do not autoclave the solution) 80 mL MAB 5X + 4 mL Triton X-100 (10X)
21	Buffer II	100 mL	Buffer I 1% Blocking Solution	100 mL Buffer 1 + 1g Blocking Solution. For nucleic acid hybridization and detection. To dilute Blocking Solution in Buffer II warm the solution to 60ºC bath.
22	100% Hybe solution	500 mL	50% Formamide 5X SSC	250 mL Formamide + 125 mL SSC 20X + 125 mL H_2O mili-Q autoclaved
23	2X SSC + 0.1% Triton	200 mL	2X SSC 0.1% Triton	20 mL SSC 20X + 2 mL Triton 10X + 178 mL H_2O
24	0,2X SSC + 0.1% Triton	100 mL	0,2X SSC 0.1% Triton	1 mL SSC 20X + 1 mL Triton 10X + 98 mL H_2O
25	75% Hybe solution	50 mL	75% (100% hybe solution) 25% (2X SSC, 0.1% Triton)	37,5 mL (100% hybe solution) + 12,5 mL (2X SSC, 0.1% Triton)
26	50% Hybe solution	50 mL	50% (100% hybe solution) 50% (2X SSC, 0.1% Triton)	25 mL (100% hybe solution) + 25 mL (2X SSC, 0.1% Triton)
27	25% Hybe solution	50 mL	25% (100% hybe solution) 75% (2X SSC, 0.1% Triton)	12,5 mL (100% hybe solution) + 37,5 mL (2X SSC, 0.1% Triton)
28	1:2000 anti-DIG / Buffer II	10 mL	0,25 µL anti-DIG 500 µL Buffer II	5 µL anti-DIG + ~10 mL Buffer II
29	TMN	100 mL	0.1 M TrisHCl pH 9.5 (stock 1M) 0.1 M NaCl (stock 1M) 0.05 M $MgCl_2$ (stock 1M)	10 mL M TrisHCl 1M + 10 mL NaCl 1M + 5 mL $MgCl_2$ 1M + 75 mL H_2O H_2O mili-Q autoclaved + (1% Twen ---> optional)
30	PVA	50 mL	10% Polyvinyl alcohol (98-99% hydrolyzed)	**Prepare it the day before.** After dissolve 5 g PVA in 40 mL TMN by warming the solution at 37ºC, add TMN until 50 mL and then let it shake **ON.**
31	20µL NBT/BCIP Stock Solution / 1mL PVA	20 µL/mL in 10mL	2 00 µL NBT/BCIP 9,8 mL PVA	
32	30% EtOH/PBS	100 mL	30 mL EtOH + 7 mL PBS 10X + 63 mL H_2O	
33	50% EtOH/PBS	100 mL	50 mL EtOH + 5 mL PBS 10X + 45 mL H_2O	
34	70% EtOH/PBS	100 mL	70 mL EtOH + 3 mL PBS 10X + 27 mL H_2O	
35	100% EtOH	100 mL	100 mL EtOH	
36	70% Glycerol / PBS	50 mL	46,6 mL Glycerol 75% + 0,34 mL PBS 10X + 3,06 mL H_2O	

PROTOCOL 9.1: IMMUNOSTAINING

DAY 1: Animal fixation with carnoy

STEP	TO PREPARE FIRST	SOLUTIONS	VOL.	TEMP.	TIME	REMARKS
1		H_2O	~ 25 mL	on ice	4 - 5 min	- Put 30-35 small animals in a petri dish with water on ice until they stop moving. - Remove the water.
2	HCL stock is 32%	2% HCl/ H_2O	~ 25 mL	on ice	3 - 5 min	- To kill the animals, add 2% HCl/H_2O solution into a 50 mL or 25mL falcon. - Critical point : Invert the tube gently for the first minute and every ~ 60 seconds to remove the mucus and to prevent animals from sticking to each other, after 3 min start to remove the HCl. - Regenerating animals should not be in the HCl solution more than 3 min.
3		Carnoy (fresh, 4°C)	~ 40 mL	4°C	120 min	- Remove the HCL. - Let the falcon shake to prevent animals from sticking to each other.
4		MetOH (-20°C)	~ 25 mL	4°C	60 min	- Throw Carnoy away, add MetOH and let it shaking.
5	H_2O_2 Stock is 30%	6% H_2O_2 in MetOH	~ 25 mL	RT	ON (16 - 20h)	- Bleaching: removes the pigmentation. - Leave animals in H_2O_2 /MetOH under a cold lamp. Avoid the solution overheat !!! - After 20 h remove the animals unless the colour persist, in this case, let the solution longer working.
6		MetOH	3X~ 25 mL	RT	30 min	- Wash 3 x 10 min in MetOH. - Store in MeOH at -20ºC for several weeks in 2 mL tubes.

PROTOCOL 9.2: IMMUNOSTAINING

DAY 2: Hybridization primary antibody

STEP	TO PREPARE FIRST	SOLUTIONS	VOL.	TEMP.	TIME	REMARKS
7	Wash	75% MetOH /PBSTX (0,3 % triton X-100)	~250 µL/ well	RT	10 min	Shaking the planarias in a 24 well plate. (Triton stock 10%)
8	Wash	50% EtOH/PBSTX	~250 µL/ well	RT	10 min	Shaking the planarias in a 24 well plate
9	Wash	25% EtOH/PBSTX	~250 µL/ well	RT	10 min	Shaking the planarias in a 24 well plate
10	Wash	PBSTX	~250 µL/ well	RT	10 min	Shaking the planarias in a 24 well plate
11	Wash	PBSTX	~250 µL/ well	RT	10 min	Shaking the planarias in a 24 well plate
12	Block	1% BSA/ PBSTX (store fresh 4ºC)	~250 µL/ well	RT	2h	Shaking (BSA: albumin bovine serum)
13	Incubation	**FIRST ANTIBODY**: **VC1** or **3C11** in 1% BSA/ PBSTX if added separate [VC1] = 1: 10000 [3C11] = 1: 50 if added together [VC1] = 1:15000 [3C11] = 1: 200	~250 µL/ well	4ºC	20 h	Shaking ------> the antibody used can be recycled for another time, store at 4ºC.

PROTOCOL 9.3: IMMUNOSTAINING

DAY 3: Hybridization secondary antibody

STEP	TO PREPARE FIRST	SOLUTIONS	VOL.	TEMP.	TIME	REMARKS
14	Wash	PBSTx	~250 µL/ well	RT	7-8h	Shaking -----> Change the solution every hour
15	Wash	1% BSA/ PBSTx	~250 µL/ well	RT	10 min	Shaking
16	Incubation	**SECONDARY ANTIBODY:** **Alexa fluor 488 goat-anti-maus (2 mg/mL)** **dissolved in 1% BSA/PBSTX**	~250 µL/ well	RT	14-16h	Shaking in the dark

PROTOCOL 9.4: INMUNOSTAINING

DAY 4: Hybridization secondary antibody

STEP	TO PREPARE FIRST	SOLUTIONS	VOL.	TEMP.	TIME	REMARKS
17	Washing	PBSTX	~250 µL/well	RT	3-4 h (changing every hour)	Shaking
18	Incubation	DAPI (5 µg/mL) /PBST	~250 µL/well	4ºC	At least 2h, otherwise ON	Shaking (DAPI stock 5mg/mL)

PROTOCOL 9.5: IMMUNOSTAINING

DAY 5: Wash, mount and document the probes.

STEP	TO PREPARE FIRST	SOLUTIONS	VOL.	TEMP.	TIME	REMARKS
19	Washing	PBSTX	~250 µL/well	RT	7-8h	
20	Mounting	Antifading (preserve the fluorescence)	one drop	RT	Probe dependent	Place the animals in ventral position on a glass slide with cover. Visualize DAPI staining under the UV light filter blue with a fluorescence microscope. VC1 an 3C11 staining under the GFP 3 filter. Do photographs under this two filters and with the confocal microscope too.

LEGEND :

Vol.: Volume

Temp.: Temperature

RT: Room temperature

ON: Over night

PROTOCOL 9.6: IMMUNOSTAINING SOLUTIONS.

Prepared them about 3 days before the start of the immuno, (1-3) fixation solutions; (4,5) basic solutions.

STEP	SOLUTION	VOLUMEN [ ]	COMPOUNDS	REMARKS
1	2% HCl / Holtfreter	200 mL at 2 %	12.5 mL HCl 32% 187.5 mL HF	**- FRESHLY PREPARE** - Prepare HCl under the hood. (HCl stock is at 32%)
2	Carnoy	200 mL	60 % EtOH 30 % Chloroform 10 % Acetic Acid	**- FRESHLY PREPARE** - Prepare chloroform under the clean bench and with glass mess cylinder, do not use plastic mess cylinder!!!, chloroform destroys plastics.
3	6% H_2O_2 / MetOH	25 mL at 6%	H_2O_2 stock at 30 %	
4	**PBS**	1 L at 10 X	80 g NaCl 2 g KCl 14.4 g Na_2HPO_4 2.4 g KH_2PO_4	- Add the 4 components in 800 ml H_2O mili-Q, - Adjust the pH 7.4 with HCl (pH low), or NaOH (pH high) **- AUTOCLAV**
5	**PBSTX**	500 mL	50 mL PBS 10X 15 mL tritonX-100 10X 435 mL ddH_2O	
6	75% MetOH / PBSTX (0,3 % triton X-100)			
7	50% EtOH / PBSTX			
8	25% EtOH / PBSTX			
9	1% BSA / PBSTX	20 mL	200 mg BSA 20 mL PBSTx	BSA = albumin bovine1: 10000 serum
10	**FIRST ANTIBODY**	Stock VC1= 1:50	0.5 µL VC1 1x 24.5 µL PBSTX 15 µL 3C11 735 µL PBST x	**VC1** or **3C11** in 1% BSA/ PBSTX if added separate [VC1] = 1: 10000 [3C11] = 1: 50 if added together [VC1] = 1:15000 [3C11] = 1: 200
11	**SECOND ANTIBODY**		2 µL DAPI (5mg/mL) 10mL PBSTx	Alexa fluor 488 goat-anti-maus (2mg/mL) in 1% BSA/PBSTX
12	**DAPI**		2 µL DAPI 5mg/mL in 10mL PBSTx	(4',6-diamidino-2-phenylindole)

PROTOCOL 10.1: ULTRAMICROTOMY TRANSMISSION ELECTRON MICROSCOP ULTRASTRUCTURE

DAY	STEP	PROCESS	SOLUTIONS	TIME	TEMP.	REMARKS
1	1	Fixtation	Glutaraldehyde 3%	2h	4ºC	The animals have first to be immobilized with beer or vichi water (carbonated mineral water). To get the animals flat, put them over an glass slide with slide cover. Incubate the probe with glutaraldehyde 3% over an ice block.
	2	Wash	Cacodilat buffer 0,1 M	1h	4ºC	Wash with cacodilat buffer 0,1 M. Change the solution 2 or 3 times every 15 min.
	3	Wash	Cacodilat buffer 0,1 M	ON	Fridge	Shaking.
2	4	Osmification	Osmic acid 1%	2h	4ºC	Shaking.
	5	Wash	Cacodilat buffer 0,1 M	10 min x 4	4ºC	Shaking.
3	6	Dehydration	Ethanol 50%	10 min x 1	4ºC	Shaking with ethanol to dehydrate the probe.
	7	Dehydration	Ethanol 70%	10 min x 2	4ºC	Shaking.
	8	Dehydration	Ethanol 90%	10 min x 3	4ºC	Shaking.
	9	Dehydration	Ethanol 96%	10 min x 3	4ºC	Shaking.
	10	Dehydration	Ethanol 100%	15 min x 3	4ºC	To maintain ethanol 100% anhydrous, store it in the fridge with Cl_2Ca or use a new recipient (being opened not longer than 15 days).
	11	Infiltration	1V SPURR + 3V ethanol	1h	RT	Incubate with the resin.
	12	Infiltration	2V SPURR + 2V ethanol	1h	RT	Incubate with the resin.
	13	Infiltration	3V SPURR + 1V ethanol	1h	RT	Incubate with the resin.
	14	Infiltration	1V SPURR	1h	RT	Incubate with the resin.
	15	Infiltration	1V SPURR	ON	RT	Incubate with the resin.
4	16	Infiltration	1V SPURR	2h	RT	Incubate with the resin.
	17	Infiltration	1V SPURR	2h	RT	For the next step: let the blocks within the labeled paper etiquettes in the oven at 60ºC during 15 min.
5	18	Elaboration of blocks	SPURR	variable	RT	Place the probe in the desire position into the tip of the block and give the resin very slowly.
	19	Polymerization	object + SPURR	48h	60ºC	Warm the blocks into an oven.
6	20	Thin cuts		variable		The block should be first cut with a glass blade in 0.5 µm thick pieces (ULTRACUT Reichert Jung) and place into a water drop over a glass slide. Dry in a 150ºC warm plate 1 min and stain with methylene blue 0,5 % during 15 sec. After that wash with distilled water. See under the microscope and make photographies to find the desired area. If you find the right place you can go on with the next step.
	21	Ultra-thin cutting				Cut the bloc in 50-60 nm thick pieces.
	22	Ultra-thin cuts staining	Uranyl acetate 2% Lead citrate (Reynols) Mili-Q water			For optical microscopy ultra-thin sections have to be stained: 1. 30 min with uranyl acetate 2%, 2. wash with abundant Mili-Q water, 3. 5 min in lead citrate (Reynolds), 4. and then wash with abundant Mili-Q water. 5. analyze the samples with the electron microscopes: JEOL 1010 at 80 Kv or TECNAI G^2 SPIRIT at 120Kv.

PROTOCOL 10.2: SOLUTIONS for the ultramicrotomy protocol

STEP	SOLUTION	[ ]	COMPOUNDS	REMARKS
				Always work under the hood. Globes are necessary during the process of dehydration
1	Glutaraldehyde 3%	3%	Glutaraldehyde 25 % 3 mL Cacodilat buffer 0,1 M 22 mL	Eluate glutaraldehyde 25 % in cacodilat buffer 0,1 M during 2 h
2	Cacodilat buffer 0,1 M (Dimetil arsinic acid)	0,1 M	Dimetil arsinic acid Phosphat buffer PB	Dilute in PB during 1h
3	Osmic acid 1%		4% Osmium tetroxide OsO_4 3,6% ferricianur potasic $K_3Fe(CN)$ Cacodilat buffer 0,1 M	Eluate 4% tetraoxid osmic OsO_4 with 3,6% ferricianur potasic $K_3Fe(CN)_6$ in cacodilat buffer 0,1 M during 2 h. If the 4% stock has a black colour, it has to be made new.
4	Ethanol 50%, -70%, -90%, -96%, -100%		Ethanol 100% H_2O	Eluate Ethanol in ddH_2O. To maintain ethanol 100% anhydra, store it in the fridge with Cl_2Ca or use a new recipient (opened before 15 days).
5	**RESIN SPURR NORMAL**	1V	ERL 10 g DER 6 g NSA 26 g DMEA 0.4 g DBP 0.8 g	Because of their viscosity, every liquid component have to be weigh. Mix with the magnet 1 h long. Store in the fridge. ERL = (Vinylcyclohexene dioxide, mixture of isomers $C_8H_{12}O_2$) DER = (d_4^{20} 1.14 a shorter chain aliphatic diepoxide than DER 732 gives slightly less flexibility) NSA = (2-Nonen-1yl; succinicanhydride $C_{13}H_2OO_3$) DMEA = (N,N-dimethylethanol-amine, + 99,5% $C_4H_{11}NO$) DBP = (Dibutyl Phthalate (1,2-Benzenedicarboxylic acid dibutyl-ether, $C_6H_4(COOC_4H_9)_2$)
6	Staining		Uranyl acetate 2% Lead citrate (Reynols) Mili-Q water	For optical microscopy ultra-thin sections staining
7	0,5% Methylen blue	0,5%	Tetraborat sodic (solid) 0.5 g Methylen blue 0.5 g	Mix 0.5 g methylen blue with 90 mL H_2O with the magnet, until its complete dissolution. Then add 0.5 g tetraborat sodic crystallized (Borax) and H_2O until 100mL. Continue mixing with the magnet. Filter with Watman paper and a second time with a 0.2 µm filter.

7.3 Low evidence genes

7.3.1 Blue-opsin

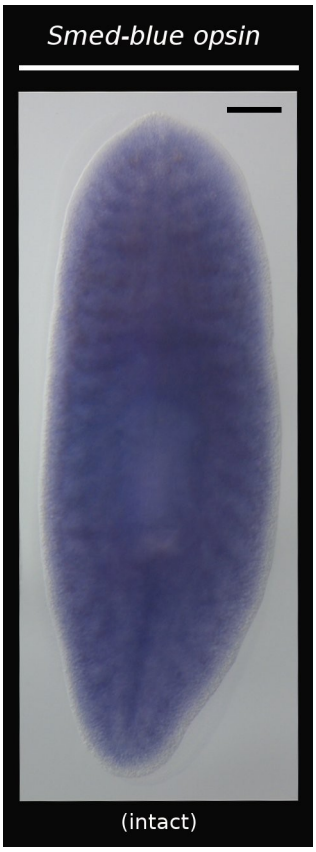

Figure 7.3.1 Whole-mount in situ hybridization showing the expression pattern of Smed-blue opsin in intact planarians (DIG-labelled antisense mRNA probes, NBT/BCIP developed). *Smed-blue opsin* with enriched expression in parenchymal tissue. Controls are in Figure 3.3.5. Scale bars: 200 µm.

Smed-blue shows high homology with the 7 -helix transmembrane domain found in proteins in the rhodopsin family. Table 3.1 summarizes its full name, putative function, expression pattern, phenotype and phenotype penetrance.

Smed-blue opsin loss-of-function flatworms did not show any difference compared to the controls (data not shown) (controls Fig. 3.3.2). The expression of *Smed-blue opsin* mRNA was found in the parenchyma and not specifically in the photoreceptor cells of *S. mediterranea,* as expected (Fig. 7.3.1).

The seven-helix transmembrane domain blue opsin is one of the animal opsins involved in vision. It belongs to the ciliary opsins that convert light signals into nerve impulses via cyclic nucleotide-gated ion channels, which work by increasing the charge differential across the cell membrane (i.e. hyperpolarization). As a cone opsin, it is employed in colour vision. It is thermally less-stable than rhodopsin and is located in the cone photoreceptor cells in vertebrates (Plachetzki et al., 2010). The short-wavelength S-cone opsin has absorption maxima at approximately 430 nm, in the blue region of the electromagnetic spectrum (Nathans et al., 1986). In the rat retina, S-cone opsins (blue), M-cone opsins (green) and rhodopsin are distributed homogeneously, but S-cone opsins are under-represented in number, 1:16:1983, respectively (Szel et al., 1992). In some mammals such as mice and humans, S- and M-cone opsins co-express in a common cell (Nikonov et al., 2005; Lukáts et al., 2005). Strangely enough, cones are among the first cell types to be generated from the retinal progenitor cells (Cepko et al., 1996). *Smed-blue* opsin expression (Fig. 7.3.1) could indicate that if this protein conserves the same function as its orthologues, it might be spread widely through the skin. Only blue light can reach substantial depth in water (Yokoyama et al., 1999) and eyeless and blind planarians such as *Castrada, Mesosloma lingua, Fonticola vitta* and *Planaria lugubris* have been shown to have dermal photosensitivity (Viaud, 1948). These proteins might therefore have evolved to be expressed in other tissues such as the skin. Nuances such as the tritan colour vision deficiency, observed in humans, caused by defects in the function of the short-wavelenght-sensitive (S) cones (Gunther et al., 2006), can not be measured in planarians yet.

7.3.2 Cryptochromes, the flavin-based blue-light photopigment

Smed-cry shows a high degree of homology with the FAD binding domain of DNA photolyases, which play an important role in photic entrainment. Table 3.1 summarizes its full name, putative function, expression pattern, phenotype and phenotype penetrance. *Smed-cry* RNAi flatworms presented skin and eye periglobular area pigmentation defects after 7 days of regeneration and 2 rounds of injections (Fig. 7.3.2 B, C). This mutation also affected regenerating heads (Fig. 7.3.2, D). Other possible defects, such as deviation of the standard photoentrainment, and circadian and magnetosensitivity defects, cannot be measured in planarians yet. Furthermore, the ubiquitous expression of *Smed-cry* in the parenchymal tissue that does not exclude the eyes (Fig. 7.3.2 A); might suggest widespread functionality across the body. Some of the signal in the in situ experiment in Fig.7.3.2 might be background.

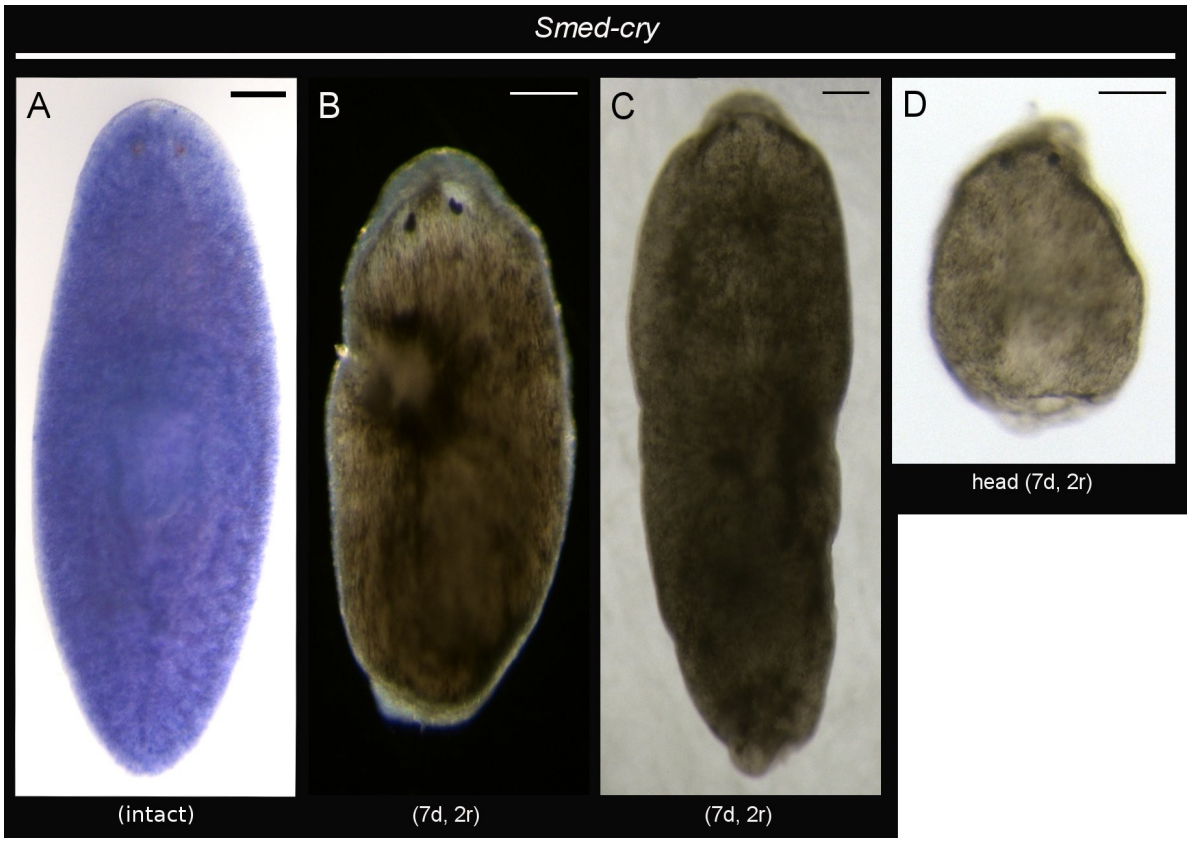

Figure 7.3.2 *Smed-cry* whole-mount in situ hybridization of intact planarians (DIG-labelled antisense mRNA probes, NBT/BCIP developed) and *Smed-cry* RNAi. (A) The *Smed-cry* mRNA had enriched expression in parenchymal cells. *Smed-cry* RNAi resulted in defects in skin pigmentation including the periglobular area of the eyes. **(B)** Periglobular area misplaced and abnormal skin pigmentation. **(C)** Folded head tip and eyes without periglobular area. **(D)** Shrunken and less developed head tip. Eyes without periglobular area. Penetrance in: (B) n=1/25; (C) n=2/25; (D) n=1/25. Controls are in Figures 3.3.2, 3.3.3 and 3.3.5. If not specified, the photographs are decapitated bodies after the specified number of days of regeneration. Scale bars: (A) 200 µm; (B-D) 150 µm.

Cryptochromes are structurally related to photolyases; evolutionarily ancient flavoproteins that catalyse light-dependent DNA repair. The structural fold of CRYs binds to two light-absorbing chromophores in the N-terminal, methenyltetrahydrofolate (MTHF) and flavin adenin dinucleotide (FAD). In contrast, the long C-terminal extension is not found in photolyases (Zoltowski et al., 2011). Cryptochromes have lost or reduced their DNA repair activity and gained a novel role in signalling. These proteins have been identified in most animals (Chaves et al., 2011). The spectral sensitivity of cry corresponds to ultraviolet and blue wavelengths and is expressed in the large lateral ventral neurons in the brain of *Drosophyla melanogaster* (Fogle et al., 2011). Cryptochromes function in the animal circadian clock and are proposed as magnetoreceptors in migratory birds and in Drosophila (Chaves et al., 2011; Foley et al., 2011).

It should be noted that the larval sponges *Amphimedon queenslandica* that lack nervous system and opsin genes but have pigment ring lens eyes (with unknown visual capacities) and phototactic swimming, have two cryptochrome genes, Aq-Cry1 and Aq-Cry2. The mRNA of one gene (Aq-Cry2) is expressed in the pigment ring eye (Rivera et al., 2012). In addition, the human cryptochrome hCRy2, expressed in the retina, has the molecular capability to function as a light-sensitive magnetosensor, or as part of a magnetosensing pathway. Using a behavioural assay, CRY-deficient *Drosophila* expressing the hCRY2 transgene, manifested magnetosensitivity under full-spectrum light (Foley et al., 2011).

7.3.3 Smed-cnl (ceroid neuronal lipofuscinosis)

Smed-cnl shows high homology with the TLC domain of neuronal ceroide lipofuscinoses (CNL) proteins in neuronal tissues. Table 3.2 summarizes its full name, putative function, expression pattern, phenotype and phenotype penetrance. The injection of *Smed-cnl* doubled-stranded RNA produced local hypopigmented skin (Fig. 7.3.3) just 5 days after one round of injections. This phenotype remained after 12 days of regeneration. The absence of pigment at the tail end might be the remains of wound of a fissioning process (Fig.7.3.3 A, B). Nevertheless, the eyes of all the flatworms injected regenerated as those of the controls did (data not shown) (controls Figure 3.3.2). In addition, no specific expression was found in the eyes by the in situ hybridization (Fig. 3.5.9, D). Nevertheless, the ubiquitous parenchymal expression suggests a widespread function across the body that affected the pharynx and the tail part.

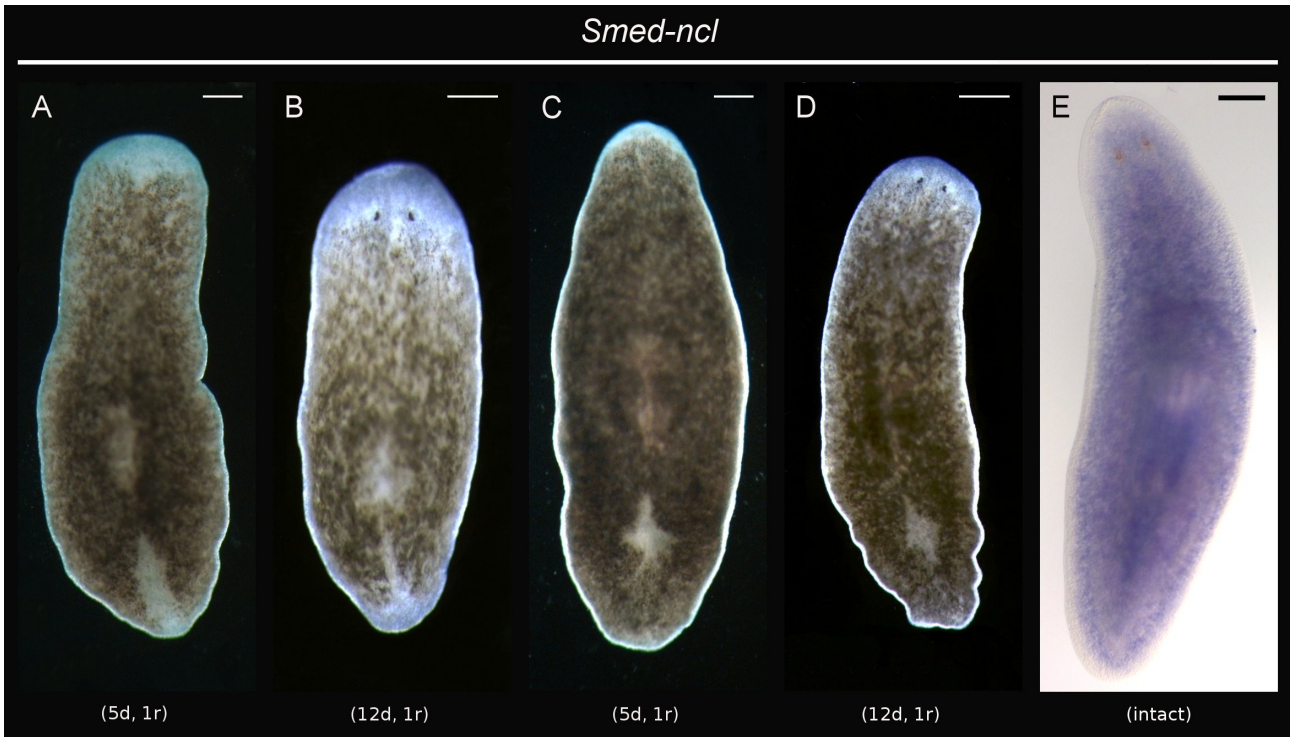

Figure 7.3.3 ***Smed-ncl*** **RNAi phenotypes and whole-mount in situ hybridization in an intact flatworm (DIG-labelled antisense mRNA probes, NBT/BCIP developed). (A)** Pharynx and tail hypopigmented skin after 5 days of regeneration. **(B)** The same specimen as in A after 12 days of regeneration. The hypopigmented areas remain after 12 days. **(C)** Tail skin hypopigmented after 5 days of regeneration. **(D)** The same specimen as in C after 12 days of regeneration. The pigment defects remain uncovered. **(E)** *Smed-ncl* ubiquitous expression pattern throughout the body. Penetrance in: A n=1/10; B n=1/10; C n=1/10; D n=1/10. Controls Figures 3.3.2 and 3.3.5. Scale bars: (A-D) 200 µm; (E) 500 µm.

Smed-cnl has a TLC domain (TRAM LAG1 CLN8) with 5 alpha helices. Proteins containing this domain may posses multiple functions such as lipid trafficking, lipid metabolism or sensing. Neuronal ceroide lipofuscinoses (CNL) is the generic name of a family of proteins that cause neurodegenerative disorders.

They result from the accumulation of autofluorescent lipopigments (Khan et al., 2013) or two proteinases; the c subunit of mitochondrial ATPsynthase and the sphingolipid activator proteins (saposins) A and D (Winter et al., 2002). The accumulation takes place in the lysosome-derived bodies of neuronal tissue, muscle, skin, conjunctivae, and rectal mucosa (Palmer et al., 1992; Khan et al., 2013), liver, spleen, myocardium and kidneys (Haltia, 2006). In humans, the early infantile variation of NCL, called INCL or Santavuori-Haltia, begins with complete retinal blindness by the age of 2 years and ends with brain death at 4 years (Kim et al., 2006). In other variations of NCL, symptoms are retinal dystrophy followed by visual loss, cerebral atrophy, dementia, and behaviour and cognitive problems, among others (Khan et al., 2013). The relation between the mutations in the TLC domains and the accumulation of the proteins as well as the metabolic pathways involved for the survival of neurons remain to be elucidated (Haltia, 2006).

Lysosome-derived bodies of neurons, muscle and skin, could be the tissues where the mRNA of the CNL gene works in humans and animals, as Palmer suggested (Palmer et al., 1992). If the *Smed-cnl* loss-of -function also affected the eye pigmentation, accumulation could not be visually appreciated.

7.3.4 *Smed-bbs* (Bardet–Biedl syndrome)

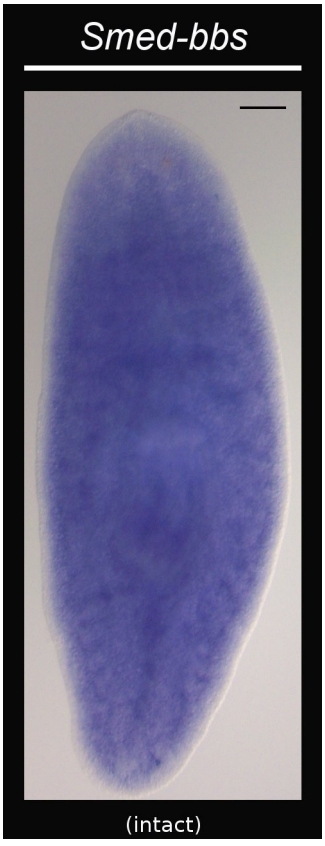

Figure 7.3.4 In situ hybridization of *Smed-bbs* (DIG-labelled antisense mRNA probe, NBT/BCIP developed). *Smed-bbs* is ubiquitously expressed in the parenchymal tissue. Controls in Figure 3.3.5. Scale bar: 500 µm.

Smed-bbs, with a tetratrico peptide repeat (TPR) motif, built in tandem arrays of 5 motifs, has been found in *S. mediterranea.* It is a transport protein across the photoreceptor-connecting cilium. Table 3.5 summarizes its full name, putative function, expression pattern, phenotype and phenotype penetrance. The mRNA of *Smed-bbs* was ubiquitously expressed throughout the body but not specifically in the photoreceptor cells (Fig.7.3.4). Some signal in Figure 7.3.4 might be background. No phenotype was observed by the injection of *Smed-bbs* mRNA (data not shown; controls Figure 3.3.2)

A clinical manifestation of the Bardet–Biedl syndrome (BBS) in humans is besides others, retinal degeneration (Chamling et al., 2013). It is characterized by atypical pigmentary retinal dystrophy of the photoreceptors with early macular involvement (Ammann, 1970; Campo et al., 1982). BBS is probably caused by a defect at the basal body of ciliated cells (Ansley et al., 2003) and disruption of intraflagellar transport (along axonemal microtubules) of proteins, such as rhodopsin and perhaps secondarily, also transducin and arrestin (Blacque et al., 2004; Kim et al., 2004; Abd-El-Barr et al., 2007). Furthermore, dysfunction of the nodal cilium in mammalian compromised protein transport across the photoreceptor-connecting cilium causing retinal dystrophy (Pazour et al., 2002; Marszalek et al., 2000). Proteins in this family, such as the human BBS 4, contain at least ten tetratricopeptide repeats (TPR) (Katsanis et al., 2001; Ansley et al., 2003). A TPR motif contains two antiparallel alpha-helices, arranged in tandem arrays of TPR motifs generating a right-handed helical structure with an amphipathic channel that might accommodate the complementary region of a target protein (Blatch et al., 1999). In addition, all available *Caenorhabditis elegans* BBS homologues are expressed exclusively in ciliated neurons. They contain regulatory elements for RFX; a transcription factor that modulates the expression of genes associated with ciliogenesis and intraflagellar transport (Ansley et al., 2003; Swoboda et al., 2000).

The human BBS 8 protein is expressed specifically in photoreceptor cells (Chamling et al., 2013). BBS 8 localizes specifically to ciliated structures, such as the connecting cilium of the retina and columnar epithelial cells in the lung (Ansley et al., 2003). In contrast, the expression of the endogenous BBS4 gene in mice includes brain, eyes, testis, heart, kidney, and adipose tissue (Chamling et al., 2013). Furthermore, many TPR-containing proteins are expected to be found in other tissues apart from the eyes. Good examples are *D. melanogaster crn* (implicated in neurogenesis), human PP5 (protein phosphatase) and *H. sapiens p67phox* (NADPH oxidase subunit) (Das et al., 1998).

The *Smed-bbs* phenotype suggests other deficiencies rather than structural defects, such as disruption of intraflagellar transport, found in BBS4 deficienci mammalian retina (Abd-El-Barr et al., 2007). Additionally, human BBS4 is able to complement the deficiency of *Bbs4* and rescue all BBS phenotypes in the *Bbs4*-null mice. Furthermore, BBS4 functionality in mice is not dose dependent (Chamling et al., 2013). Therefore, the observed weak expression of *Smed-bbs* in the eyes of *S. mediterranea* could be sufficient for its functionality.

7.3.5 *Smed-ras* (rat sarcoma)

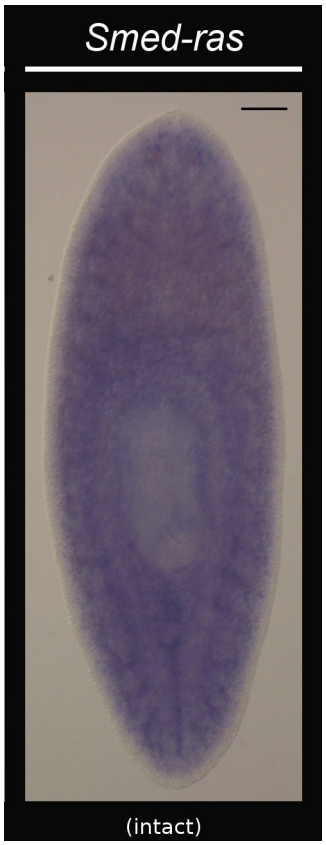

Figure 7.3.5 In situ hybridization of *Smed-ras* (DIG-labelled antisense mRNA probe, NBT/BCIP developed). *Smed-ras* mRNA is expressed in the parenchyma, around the eyes but not in the pharynx. Controls in Figure 3.3.5. Scale bar: 500 µm.

Smed-ras showed high homology with the six stranded beta sheet and 5 alpha helices of the rat sarcoma protein from the photoreceptors signal transduction. Table 3.5 summarizes its full name, putative function, expression pattern, phenotype and phenotype penetrance. *Smed-ras* RNAi animals developed as the controls did(data not shown; controls Fig. 3.3.2). *Smed-ras* was ubiquitously expressed throughout the body and the eyes were not excluded (Fig. 7.3.5).

Ras belongs to a protein family first found in rat sarcoma (Harvey, 1964; Kirsten et al., 1970). Ras is a G protein, a single-subunit small GTPase, or a guanosine-nucleotide-binding protein. All small G proteins have consensus amino acid sequences responsible for specific interactions with GDP and GTP, and for GTPase activity, which hydrolyses bound GTP to GDP and Pi (Takai et al., 2001). They function as binary signalling switches with "on" and "off" states. In the "off" state, it is bound to the nucleotide guanosine diphosphate (GDP); while in the "on" state, Ras is bound to guanosine triphosphate (GTP) (Lodish et al.,2000). Ras family members mainly regulate gene expression and signalling pathways (Takai et al., 2001; Lodish et al., 2000).

Ras contains a six-stranded beta sheet and 5 alpha helices (Vetter et al., 2001). Although Ras is attached to the cell membrane, it is ubiquitously expressed in all cell lineages and organs (Rocks et al., 2006). Ras is required for the development of all photoreceptors in the *Drosophila* eye (Simon et al., 1991). It is essential for recruitment of R1-R7 cells in *Drosophila*. R8 specification requires Ras activation; and loss of Ras perturbs the spacing and arrangement of R8 precursor cells (Yang et al., 2001).

Smed-ras might not be involved in the Ras-MAP-kinase pathway or other general barriers. Yan and Tramtrack proteins might be blocked to photoreceptor differentiation in the *S. mediterranea* rhabdomere.

7.3.6 *Smed-VATP synthase* RNAi after one round and 3 single injections

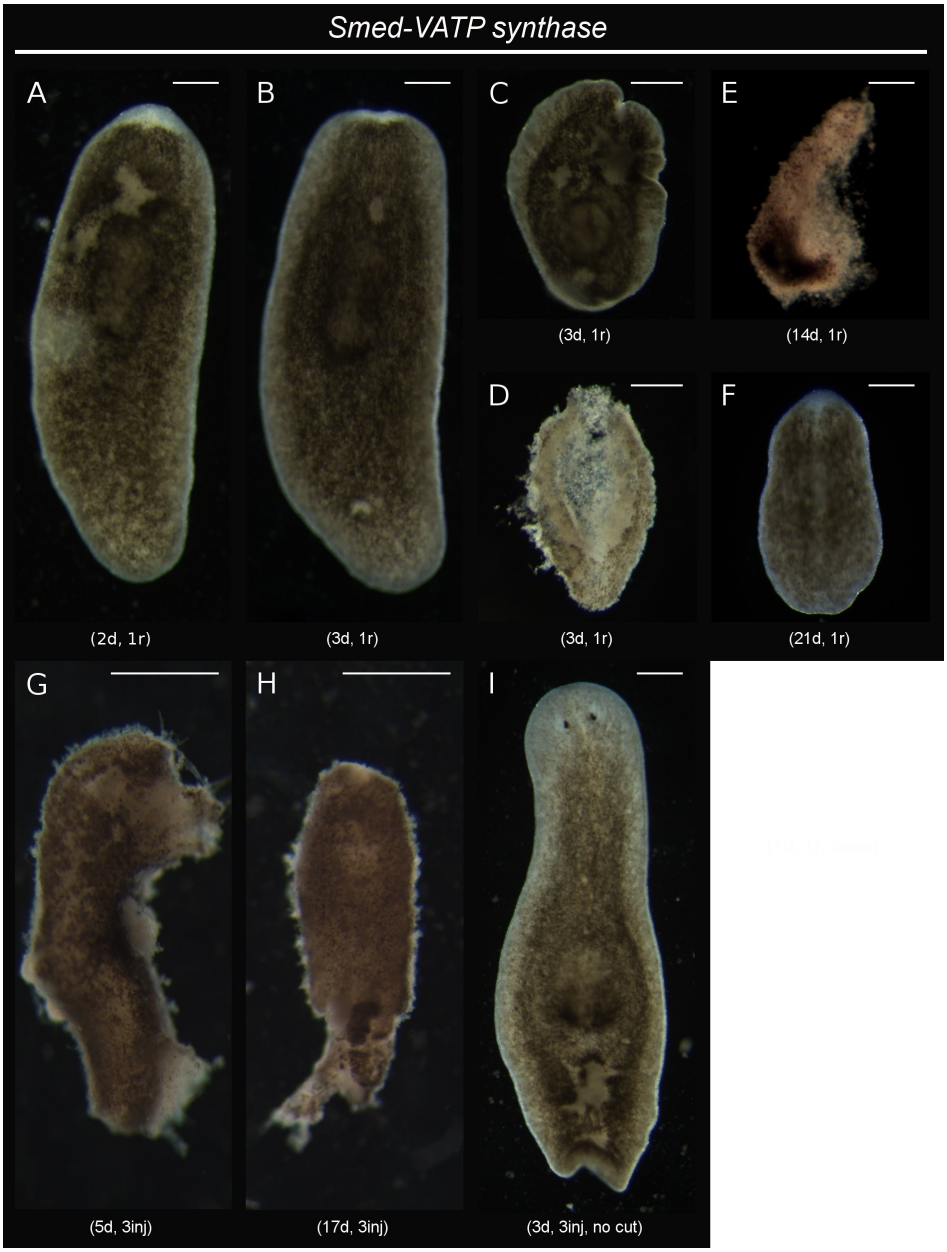

Figure 7.3.6 RNAi phenotypes of *Smed-VATP synthase*. No animal survived after one round of *Smed-VATP synthase* mRNA injections: **(A)** dorsal skin pigment defects with normal blastema; **(B)** dorsal skin pigment defects with small blastema; **(C)** regeneration failed, skin pigment defects appeared and blastema was not formed; **(D)** tissue destruction just 3 days after injection; **(E)** destroyed body 14 days after decapitation; **(F)** extreme reduction of the body size and no regeneration of the eyes after 21 days. After three consecutive injections the devastating phenotypes were the following: **(G)** regeneration failed with visible tissue destruction at five days; **(H)** body disruption after 17 days. **(I)** Injection without amputation provoked dorsal skin pigmentation failure. Penetrance in: (A) n=8/10; (B) n=7/10; (C) n=1/10; (D) n=1/10; (E) n=7/10; (F) n=1/10; (G) n=11/12; (H) n=1/12; (I) n=15/15. Controls are in the Figures 3.3.2 and 3.3.4. Scale bars: (A, B, I) 200 µm; (C-H) 100 µm.

7.3.7 *Smed-myb* (mind bomb)

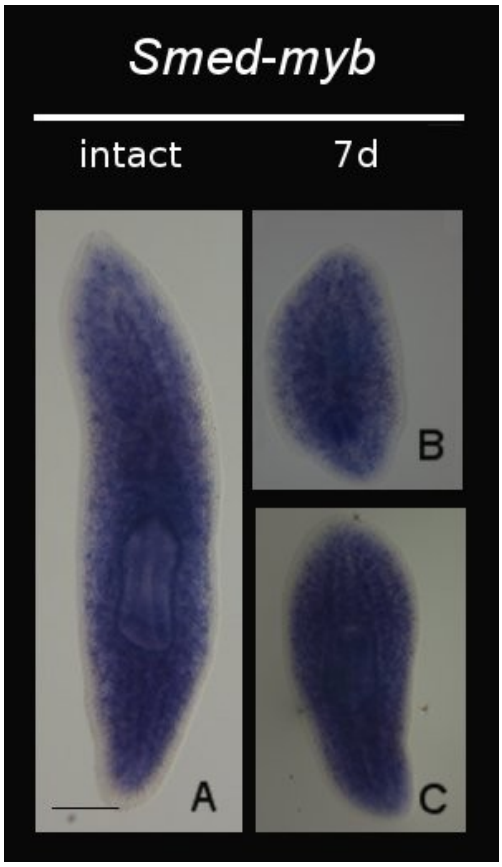

Figure 7.3.7 In situ hybridizations of DIG-labelled antisense mRNA (NBT/ BCIP development). Parenchymal and pharynx expression pattern of *Smed-myb* in intact animal **(A)** and 7-days regenerating head **(B)** and tail **(C)**. Scale bar: 1mm B-C as in A.

Smed-myb shows high homology with the zinc-finger domain of a DNA binding protein, for example a transcription factor. Table 3.6 summarizes its full name, putative function, expression pattern, phenotype and phenotype penetrance. The *Smed-myb* expression pattern, extends across the parenchymal tissue including the pharynx (Fig.7.3.7), and the *Smed-myb* RNAi flatworms regenerated as the control did (data not shown, controls Figure 3.3.2). The name *Smed-myb* was given to this sequence after a first blastx made in 2009. Nevertheless, improvement in the databases changed this result. An NCBI blastx alignment in June 2014, gave a PIEzo2 protein as a conserved domain. Moreover, a DNA sequence search of the Pfam database, resulted in no matches for this sequence. *Smed-myb* might be a Notch activator, as is the mice mind bomb (Mib1) in dendritic cells (DC)-$CD4^+$ (Jeong et al., 2012). Notch activation results in transcriptional regulation for various target genes such as *Hes* and *Hey* (Yuan et al., 2009; Kopan et al., 2009). In zebrafish, mind bomb mutants can have severe patterning defects in the hindbrain, such as a reduction of neurons number (Bingham et al., 2003). In contrast, Piezos are large transmembrane proteins conserved among various species, all having between 24 and 36 predicted transmembrane domains. Therefore, *Smed-myb* might be just a fragment of this protein type, playing a role in somatosensory neurons (Coste, et al., 2013).

7.3.8 *Smed-snap* (small nuclear RNA-activating protein complex)

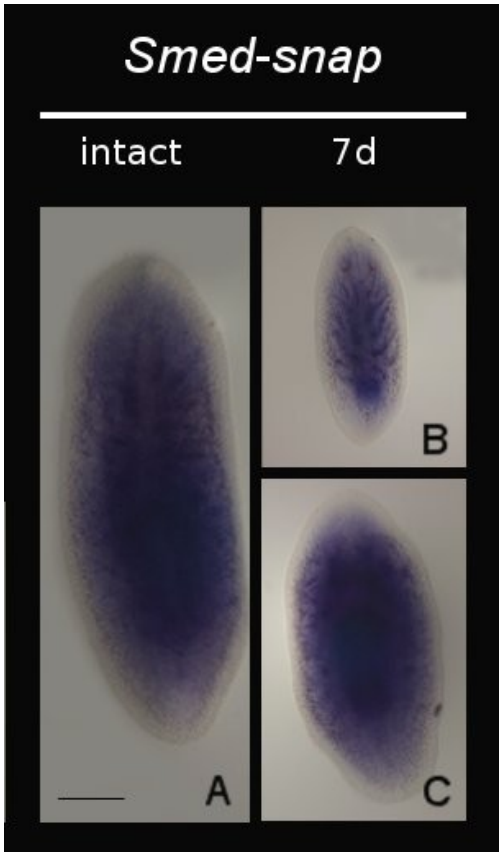

Figure 7.3.8 In situ hybridizations of DIG-labelled antisense mRNA (NBT/BCIP development). Parenchymal and pharynx expression pattern of *Smed-snap* in intact **(A)** animal and 7-day regenerating head **(B)** and tail **(C)**. Scale bar: 1 mm, B and, C as in A.

Smed-snap has a Myb-like DNA binding domain with an HTH motif, present in transcription factors. Table 3.6 summarizes its full name, putative function, expression pattern, phenotype and phenotype penetrance. *Smed-snap* mRNA was expressed in the parenchymal tissue in intact and in regenerating animals (Fig. 7.3.8). Furthermore, *Smed-snap* RNAi flatworms regenerated as the controls did (data not shown, controls Figure 3.3.2).

Myb is an acronym derived from myeloblastosis, a type of leukaemia caused by the oncogene myeloblastosis virus (Lipsick, 1996). The absence of *Drosophila Myb* induces an increase in mitotic arrest with abnormal chromosome number and aberrant spindle formation (Manak et al., 2002). Furthermore, *Dm-myb* is localized in recently replicated DNA in both mitotically cycling and endocycling cells (Beall et al., 2002).

7.3.9 *Smed-tpr2* RNAi.

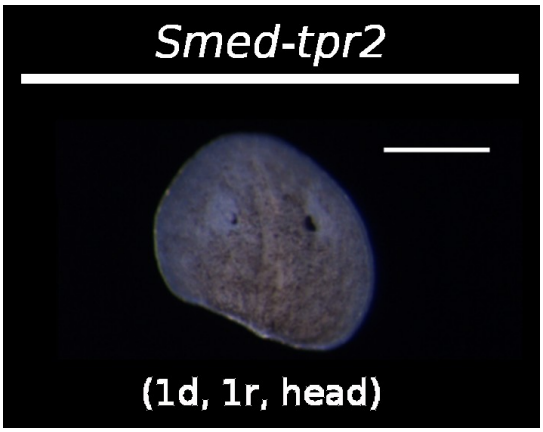

Figure 7.3.9 Phenotype of *Smed-tpr2* RNAi. Less developed eye cup in a *Smed-tpr2* RNAi decapitated head after 1 day of regeneration. Penetrance: n=1/11. Controls are in the Figure 3.3.2. Scale bar: 100 µm.

7.3.10 Electron micrograph of cilia sections located on the head of *S. mediterranea*.

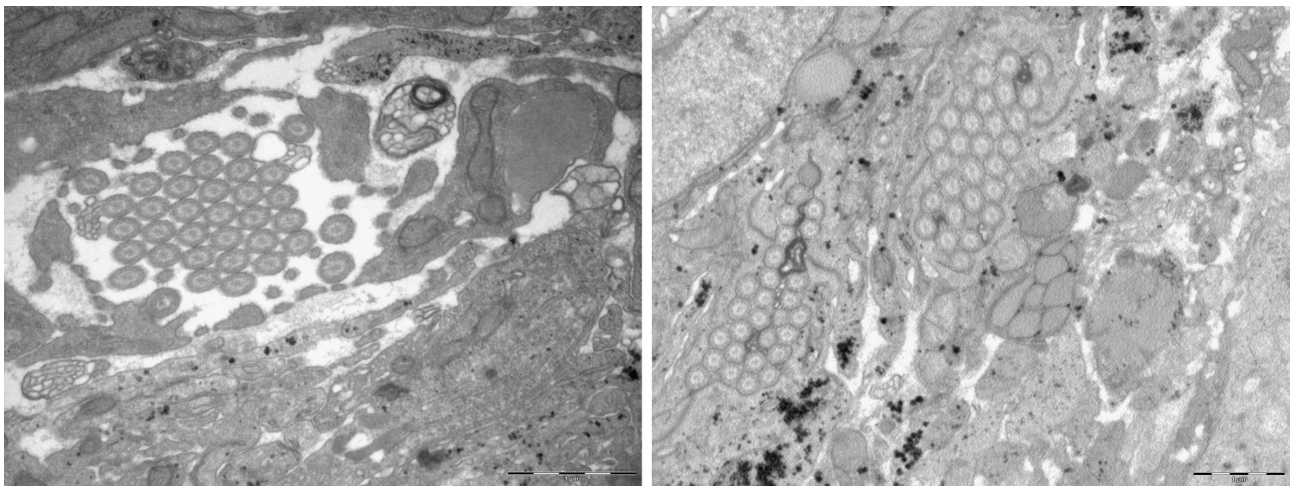

Figure 7.3.10 Electron micrograph of cilia sections. Head section performed at the eye level, perpendicular to the symmetry -axis of *S. mediterranea*. The left-hand picture shows cilia during ciliogenesis, small cilia during formation are clear to see. The right-hand picture shows two groups of cilia next to each other. These cilia might be part of a support structure of the flatworm body. *Smed-centrin* might play a role in the ciliogenesis observed here. Scale bars: 1 µm.